

GEOLOGICA ULTRAIECTINA

**Mededelingen van de
Faculteit Aardwetenschappen
Universiteit Utrecht**

No. 139

**ISOLATION AND CHEMICAL CHARACTERIZATION
OF RESISTANT MACROMOLECULAR CONSTITUENTS
IN MICROALGAE AND MARINE SEDIMENTS**

FRANÇOIS GELIN

GEOLOGICA ULTRAIECTINA

**Mededelingen van de
Faculteit Aardwetenschappen
Universiteit Utrecht**

No. 139

**ISOLATION AND CHEMICAL CHARACTERIZATION
OF RESISTANT MACROMOLECULAR CONSTITUENTS
IN MICROALGAE AND MARINE SEDIMENTS**

FRANÇOIS GELIN

CIP-GEGEVENS KONINKLIJKE BIBLIOTHEEK, DEN HAAG

Gelin, François

Isolation and chemical characterization of resistant macromolecular constituents in microalgae and marine sediments / François Gelin. - Utrecht : Faculteit Aardwetenschappen, Universiteit Utrecht. - (Geologica Ultraiectina, ISSN 0072-1026 ; no. 139)
Proefschrift Universiteit Utrecht. - Met lit. opg. - Met samenvatting in het Nederlands en Frans.
ISBN 90-71577-93-7
Trefw.: algen / mariene sedimenten / biogeochemie.

**Isolation and chemical characterization of resistant
macromolecular constituents in microalgae
and marine sediments**

**Isolatie en chemische analyse van resistente macromoleculaire
bestanddelen van microalgen en mariene sedimenten**

(met een samenvatting in het Nederlands)

**Isolation et caractérisation chimique de composants macromoléculaires
et résistants présents dans des microalgues et des sédiments marins**

(avec un résumé en français)

Proefschrift ter verkrijging van de graad van doctor
aan de Universiteit Utrecht
op gezag van de Rector Magnificus Prof. Dr. J. A. van Ginkel
ingevolge het besluit van het College van Dekanen
in het openbaar te verdedigen
op vrijdag 15 maart 1996 om 14.30 uur

door
François Gelin
geboren op 8 januari 1966 te Nantes

Promotor: Prof. Dr. J. W. de Leeuw

Contents

Summary.....	vii
1. Introduction.....	1
2. Mechanisms of flash pyrolysis of ether lipids isolated from the green microalgae <i>Botryococcus braunii</i> race A.....	9
3. Scope and limitations of flash pyrolysis-gas chromatography as revealed by the thermal behaviour of high-molecular-weight lipids derived from the green microalga <i>Botryococcus braunii</i>	21
4. The similarity of chemical structures of soluble aliphatic polyaldehyde and insoluble algaenan in the green microalga <i>Botryococcus braunii</i> race A as revealed by analytical pyrolysis.....	39
5. Novel, resistant microalgal polyethers: An important sink of organic carbon in the marine environment?.....	51
6. Resistant biomacromolecules in five marine microalgae of the classes Eustigmatophyceae and Chlorophyceae: Geochemical implications.....	59
7. Electron microscopy and pyrolysis of kerogens from the Kimmeridge Clay Formation (U.K.): Source organisms, preservation processes and origin of microcycles.....	81
8. Molecular indicators for palaeoenvironmental change in a Messinian evaporitic sequence (Vena del Gesso, Italy): III. Stratigraphic changes in the molecular structure of kerogen in a single marl bed as revealed by flash pyrolysis.....	101
9. Variations in origin and composition of kerogen constituents as revealed by analytical pyrolysis of immature kerogens before and after desulphurization.....	115

References.....	127
Acknowledgments.....	141
Samenvatting.....	143
Résumé.....	145
Curriculum Vitae.....	147

Summary

The insoluble, macromolecular fraction of sedimentary organic matter, termed kerogen, constitutes the largest reservoir of organic carbon on Earth. For this reason, it has been studied extensively over the past decades as the appropriate tools enabling its investigation were developed. However, the origin of kerogens, in particular the marine ones, is still a matter of debate. Therefore, the work described in this thesis is dedicated to this problem and an attempt was made to investigate the chemical structure of kerogen, mainly by analytical pyrolysis methods, to understand its formation. Accordingly, the first part of the investigation was focused on the understanding of mechanisms of pyrolysis of well-known high-molecular-weight compounds (chapters 2 to 4).

Ether lipids isolated from the green microalga *Botryococcus braunii* were pyrolysed (chapter 2). The pyrolysis products were identified as alkenes, alkanes and mid-chain ketones. The position of the carbonyl group in the ketones corresponded to the position of the ether bond in the ether lipids. This clearly indicated that pyrolytic cleavage of secondary ether bonds generates both mid-chain ketones and alkanes or alkenes. Moreover, cleavage of the ether bond appeared to be the initial step and triggered the formation of other pyrolysis products. Detailed mechanisms of pyrolysis were established from these studies.

Several other complex non-ether lipids isolated from *B. braunii* were also subjected to flash pyrolysis and their thermal behaviour is discussed in chapter 3. It appeared that specific lipids containing up to 64 carbon atoms and possessing long alkyl chains were not pyrolysed and simply evaporated. A significant part of the evaporated material did not transfer to the gas chromatography column coupled to the pyrolysis unit and simply condensed on the glass tube surrounding the zone of pyrolysis. This phenomenon was thought to occur also for high-molecular-weight material released from the pyrolysis of macromolecules and thus highlights a drawback of the method. However, it was shown that other lipids containing ether-bound aliphatic moieties did undergo pyrolysis. The mechanisms of pyrolysis were similar to those described in chapter 2. Based on this knowledge, the structure of the insoluble aliphatic biomacromolecule (algaenan) from *B. braunii* race L was identified as a macromolecule comprising C₄₀ isoprenoid units ether-linked mainly at the C-14 and C-15 positions.

More information concerning the pyrolysis of biomacromolecules is presented in chapter 4. A soluble biopolymer (defined as an aliphatic polyaldehyde) isolated from *B. braunii* race A was subjected to flash pyrolysis. Its very complex pyrolysate, composed of saturated and (poly)unsaturated *n*-hydrocarbons ranging from C₆ to C₃₁, *n*-alkyl cyclohexanes and *n*-alkyl benzenes, was compared with the pyrolysate of the insoluble algaenan produced by the same algal species. Detailed investigation of the two pyrolysates revealed very close structural similarities. Hence, it was concluded that the insoluble biomacromolecule, *i.e.* the algaenan, was a more condensed and/or reticulated form of the soluble aliphatic polyaldehyde.

Evidence for the occurrence of such aliphatic algaenans in the marine environment is presented in chapter 5. Five out of seven marine microalgal species investigated were found to produce the resistant biomacromolecules. The chemical structure of the algaenan biosynthesized by the eustigmatophyte *Nannochloropsis salina* was studied by solid state ¹³C NMR, chemical degradations using HI and RuO₄, and flash pyrolysis. It appeared from these investigations that the *N. salina* algaenan

was composed of C₂₈ to C₃₄ linear alkyl chains linked by ether bridges. It was concluded, based on the occurrence of similar algaenans in other marine algal species that a significant part of marine kerogens consists of selectively preserved algaenans. Therefore, these biomacromolecules are thought to be precursors of marine crude oils. Chapter 6 describes in detail the chemical nature of the isolated algaenans. A second eustigmatophyte, *Nannochloropsis* sp., was shown to biosynthesize an algaenan very similar to that produced by *N. salina*. Additional investigations of the free and ester-bound lipids of the eustigmatophytes revealed the presence of C₂₈-C₃₆ diols and C₃₀-C₃₂ alkenols. The positions of the mid-chain alcohol group and the double bonds were closely related to the position of the ether bonds in the algaenans. Thus, it was suggested that these diols and alkenols are the biosynthetic precursors and building blocks of the algaenans. No evident precursor could be established for the algaenans of the three algaenan-producing chlorophytes *Chlorella spaerckii*, *Chlorococcum* sp. and *Nannochloris* sp. These algaenans are comprised of mixtures of structurally different macromolecules, partly aliphatic for the two former algae and fully aromatic for the latter one. The geochemical implications of the occurrence of algaenan-producing species in the marine environment are also discussed.

The importance of algaenans in the marine ecosystem is discussed in chapter 7, which focuses on the nature of the heterogeneous composition of kerogens isolated from Kimmeridgian sediments (Yorkshire, U.K.). In this study, pyrolysis investigations were associated with electron microscopy observations. Close correlations were observed between the diverse morphological and chemical features of these kerogens. Three different, recognizable types of organic matter were identified: land-plant derived material, microscopically amorphous, sulfur-containing (macro)lipids and preserved algaenans. Relationships between the relative abundances of these types of organic matter and both the hydrogen index and total organic carbon contents were established.

The kerogens isolated from a more recent sediment (Vena del Gesso, Messinian, Italy) were extensively studied by flash pyrolysis (chapter 8). The nature, abundance and origin of the pyrolysis products are discussed. It appeared that the nine kerogens studied were essentially composed of homogenous macromolecular components, *i.e.* presumably algaenans, and sulfur-bound lipids incorporated into the insoluble matrix during early diagenesis. Chapter 9 describes pyrolysis of the residues after CrCl₂ and Li/EtNH₂ treatments of the same kerogens. The latter treatments removed most of the components which were (poly)sulfur-linked to the macromolecular network, leading to a fraction enriched in aliphatic macromolecules, *i.e.* algaenans. Moreover, Li/EtNH₂ treatment was shown to also reduce tetrapyrrole moieties allowing the generation of abundant alkylpyrroles in the pyrolysates of the "desulfurized" kerogens.

In summary, algaenans (non-hydrolysable macromolecules), such as those biosynthesized by contemporary marine algae, must have been produced in ancient marine environments as well and represent significant components of marine kerogens through relative enrichment via the selective preservation pathway.

Introduction

1.1 GENERAL

The recognition of novel, insoluble and non-hydrolysable macromolecular constituents in protective tissues of fresh-water algae and higher plants has had a major impact on our understanding of the origin and fate of sedimentary organic matter (OM) in terrestrial and lacustrine deposits. The investigations described in this thesis aim to explore if such macromolecules also occur in the marine environment and if so, what the consequences are for our understanding of OM in marine sediments and for the mechanisms of marine oil formation.

1.2 RESISTANT BIOMACROMOLECULES

The most abundant macromolecules in living biomass are polysaccharides and proteins. Under specific depositional conditions, traces of them can be preserved in the top layers of sediments possibly *via* sorption to the mineral matrix (*e.g.* Hedges and Keil, 1995) or *via* sulphur incorporation (Moers *et al.*, 1988; Philp *et al.*, 1992). However, mainly because they are hydrolysable, they are considered as labile substances, which are mineralized by bacteria (*e.g.* Whelan and Emeis, 1992). Hence, these polymers cannot be regarded as resistant biomolecules and, indeed, several studies have shown that their biodegradation occurs readily and almost quantitatively in depositional environments (*e.g.* Given *et al.*, 1984; Hedges *et al.*, 1985; Klok *et al.*, 1984a).

Non-hydrolysable biomacromolecules can be classified into two groups. The first group mainly comprise aromatic biomacromolecules, predominantly lignins (constituents of vascular plants), complex tannins (from higher plants), phlorotannins (in brown algae) and, partly, sporopollenins (spore and pollen wall constituents of land plants). Their predominantly polyphenolic structure, occurrence and preservation potential have been studied intensively and have recently been reviewed in some detail by de Leeuw and Largeau (1993). The second group includes non-hydrolysable aliphatic macromolecules. It is only recently that many insoluble and resistant aliphatic biomacromolecules have been isolated from organisms and sediments, and identified. These macromolecules have been encountered in cell walls of fresh-water microalgae (as algaenans, *e.g.* de Leeuw and Largeau, 1993; de Leeuw *et al.*, 1991; Derenne *et al.*, 1992a), in higher plant cuticles (as cutans, *e.g.* Nip *et al.*, 1986) and periderm tissues (as suberans, Collinson *et al.*, 1994), in inner seed coats of freshwater plants (as tegmens, van Bergen *et al.*, 1994), in spore and pollen grains (as the major part of sporopollenins, *e.g.* Hemsley *et al.*, 1993) and in resins (as polycadinenes, van Aarssen *et al.*, 1990).

The most investigated aliphatic non-hydrolysable biomacromolecules are algaenans. They essentially occur in the outer cell walls of several freshwater algal species belonging to the class Chlorophyceae, commonly named green algae. They represent *ca.* 1-5% of the dry biomass. Algaenans have been reported in common and ubiquitous microalgae such as *Tetraedron minimum*, *Scenedesmus* species, *Pediastrum* species, *Chlorella* species and *Botryococcus braunii* races A, B and L (Largeau *et al.*, 1986; Goth *et al.*, 1988; Tegelaar *et al.*, 1989c; Derenne *et al.*, 1992a). At the start of this PhD study only the chemical structure of *B. braunii* algaenans was (partly) known (Metzger *et al.*, 1991). During the period of this PhD study and apart from our investigations on the *B. braunii* races A and L and *Nannochloropsis salina* algaenans, more information about the chemical structure of other algaenans, such as that of *Tetraedron minimum*, was obtained (Largeau and de Leeuw, 1995).

1.3 KEROGEN

Kerogen is defined as the sedimentary organic matter insoluble in the usual organic solvents (Durand, 1980). Kerogens can be classified into three types based on their C, H, and O elemental compositions. Types I and II are hydrogen-rich kerogens. Type I usually derives from algae in lacustrine environments whereas most marine kerogens belong to Type II. Type III are carbon-rich kerogens, mainly deriving from higher plants, and thus, have a terrestrial origin. Sedimentary OM has been estimated to represent *ca.* 90% wt of the total OM on Earth (*ca.* 15×10^{21} g C (Berner, 1989; Hedges, 1992)). Kerogen comprises 95% wt of sedimentary OM, the remaining 5% being composed of constituents extractable by organic solvents and is termed bitumen. Hence, the understanding of the composition of kerogen, its origin and its fate is essential to estimate qualitatively and quantitatively its role in the carbon cycle.

Pathways for the formation and thermal breakdown of kerogen have been debated since petroleum and gas were thought to be generated by the thermal cracking of kerogen. It was believed that kerogen was the result of random polymerization and recondensation reactions of partly (bio)degraded polysaccharides, proteins and lipids (Tissot and Welte, 1984). The newly discovered aliphatic resistant algal biomacromolecules (see above), the evidence of their preservation in sediments and their significant contribution to OM of sediments of different ages and depositional environments (*e.g.* Goth *et al.*, 1988; Largeau *et al.*, 1984, 1986) has resulted in the proposition of an alternative pathway based on the selective preservation of such macromolecules (Fig. 1.1). It should be noted that such a pathway was first suggested by Philp and Calvin (1976) based on their studies of algal macromolecular constituents. Evidence for this pathway has accumulated in particular from lacustrine depositional environments (*e.g.* Messel Oil Shale (Goth *et al.*, 1988); Green River Shale and Rundle Oil Shale (Derenne *et al.*, 1991b); and Torbanites (Largeau *et al.*, 1986)).

Simulation experiments showed that, under relatively high temperatures and long residence times in the subsurface, these aliphatic biomacromolecules

generate *n*-alkanes (Tegelaar *et al.*, 1989b). This indicates that algae are potentially the major source of alkanes in crude oils.

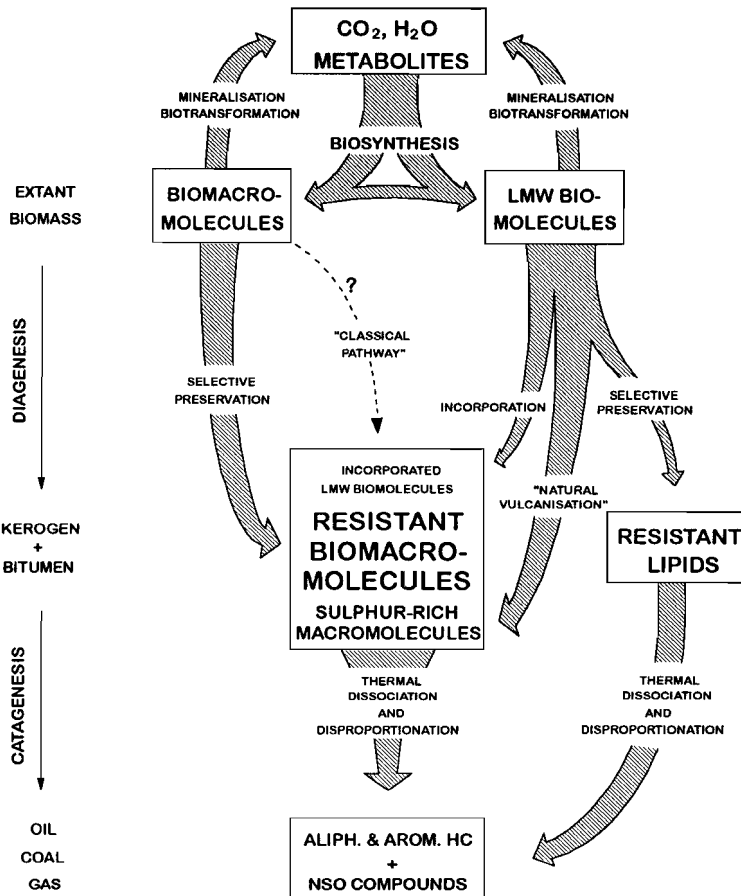


Fig. 1.1 Proposed mechanism for kerogen formation *via* the "selective preservation pathway" (after Tegelaar *et al.*, 1989c).

1.4 INSOLUBLE RESISTANT ORGANIC MATTER IN THE MARINE ENVIRONMENT

Over the last decade, it has become clear that a significant part of marine kerogen results from intermolecular reactions of inorganic sulfur species with functionalized lipids (Fig. 1.1) and/or the sulfurization of already present unaltered or partly altered biomacromolecules (*e.g.* Sinninghe Damsté *et al.*,

1989). Whether marine organisms are able to biosynthesize resistant aliphatic macromolecules was not known at the start of the research described in this thesis. Recently, circumstantial evidence has accumulated, pointing to the involvement of marine algaenans in the formation of marine kerogens. Upon flash pyrolysis of marine kerogens isolated from both Recent (Klok *et al.*, 1984; Eglinton *et al.*, 1994) and ancient (*e.g.* Derenne *et al.*, 1990c; Douglas *et al.*, 1991) sediments, homologous series of *n*-alk-1-enes and *n*-alkanes were the dominant components of the pyrolysates. Because these series usually reflect the presence of aliphatic macromolecular constituents, it was suggested that marine algaenans might have significantly contributed to the formation of these kerogens. Eglinton (1994) analysed the stable carbon isotope values of the homologous series of *n*-alk-1-enes and *n*-alkanes isolated from off-line pyrolysates of both lacustrine Type I and marine Type II kerogens. The author found that the $\delta^{13}\text{C}$ values of the individual alkenes and alkanes ranging from C_9 to C_{30} are highly similar or identical, whilst from other studies (*e.g.* Freeman *et al.*, 1990) it was clear that $\delta^{13}\text{C}$ values of extractable alkanes in the bitumens of the same sediments varied very significantly (*e.g.* from -15 to -85 ‰). The similar ^{13}C composition of the C_9 - C_{30} alkanes and alkenes released upon pyrolysis was easy to rationalize for the Type I kerogens because the alkanes and alkenes are for the greater part derived from an algaenan of one freshwater green microalga (see above). By analogy it might be assumed that the same phenomenon observed for the marine kerogens is also due to the dominant presence of one or at the most a few algaenans from specific marine algae. It is well-known that Ordovician oils predominantly derived from marine kerogens which are dominated by the microscopically recognizable extinct organism *Gloeocapsomorpha prisca* and which generate high amounts of *n*-alkenes and *n*-alkanes upon flash pyrolysis (Douglas *et al.*, 1991). Recent investigations have clearly demonstrated that the extinct marine *G. prisca* is very likely related to the algaenan-producing fresh-water green microalga *B. braunii* race A (Derenne *et al.*, 1992d). This indicates that marine green microalgae related to present-day fresh-water ones have existed in the geological past and were able to biosynthesize algaenans.

Up until now, only one marine microalga biosynthesizing an algaenan, *Nanochlorum eucaryotum*, an uncommon monospecific chlorophyte isolated from an aquarium, has been reported to biosynthesize a marine algaenan (Derenne *et al.*, 1992a). Electron microscopic studies showed that this algaenan also comprises part of the outer cell wall. After removal of all other cell components, the cell morphology was no longer preserved. However, transmission electron microscopy (TEM) revealed the presence of laminar structures, termed "ultralaminae", which are the residual forms of the outer cell walls. As most of the "amorphous" marine kerogens are, at least in part, composed of these types of "ultralaminae", the authors envisaged marine algaenans as possible precursors of these recognizable kerogen fractions (Derenne *et al.*, 1992b).

1.5 OBJECTIVES

The above findings strongly suggest that marine organisms, in particular marine (micro)algae, biosynthesize resistant non-hydrolysable macromolecules

which have the potential to be selectively preserved in sediments and may therefore play a key role in the formation of marine kerogens and in turn marine petroleum. In this respect, marine counterparts of freshwater algaenan-producing microalgae are likely candidates. To extend our understanding of the role of insoluble, resistant biomacromolecules in the global organic carbon cycle, it is also a prerequisite to study such macromolecules in sediments. Therefore, the objectives of this PhD research were to investigate non-hydrolysable macromolecular constituents of several marine microalgae, to search for them in algal-derived macromolecular OM in marine kerogens and to discuss their potential role in the genesis of marine oils.

1.6 ANALYTICAL TOOLS

Investigations and structural characterizations of macromolecular insoluble OM in sediments and organisms have been rarely undertaken in the past because of the lack of appropriate analytical tools. However, the developments of ^{13}C NMR, FT-IR and analytical pyrolysis in particular, have enabled detailed investigations of these types of macromolecules and kerogens.

Analytical Pyrolysis

Pyrolysis is defined as thermal degradation in an inert atmosphere (*i.e.* He or N_2). Typically, pyrolysis of a macromolecule generates suites of products with different molecular weights depending on the temperature of pyrolysis and on the type of chemical bonds within the macromolecular network. Excessive temperatures as well as closed chamber type pyrolysis can result in the formation of secondary pyrolysis products, and thus the formation of highly stable, less informative and mainly aromatic, low-molecular-weight (LMW) components, whereby structural information is lost. Hence, analytical pyrolysis aiming to structurally characterize macromolecular compounds is performed in an open pyrolysis system with an ultra-fast temperature rise-time (*e.g.* Boon *et al.*, 1987). The most commonly used method to identify the pyrolysis products involves the on-line coupling of a pyrolyser with a gas chromatograph-mass spectrometer system (Py-GC-MS) (Maters *et al.*, 1977; Larter, 1984; Horsfield, 1984, Boon *et al.*, 1987). The separation of the pyrolysis products by gas chromatography results in the loss of non-GC-amenable compounds, *i.e.* high-molecular-weight (HMW) and polar components. This is a major drawback of the method as only *ca.* 10% of the pyrolysed starting material can be analysed by Py-GC-MS. However, NMR and other studies have shown that the structural information which can be recovered from this small amount of identifiable material is, in most cases, representative of the bulk of the material subjected to pyrolysis (Horsfield, 1989; Larter and Horsfield, 1993; Goth *et al.*, 1988). Hence, it is likely that extrapolation of the pyrolysis data thus obtained enables an elucidation of the macromolecular structure. Resistant, insoluble OM isolated from sediments or living organisms is usually not composed of a single type of macromolecule. Even if a precise chemical structure of the macromolecules involved cannot be elucidated by Py-GC-MS, the structural elements, *i.e.* GC-

amenable pyrolysis products, can still provide information concerning the origin and biosynthesis of the kerogens and biomacromolecules, respectively. A second major drawback of flash pyrolysis is the difficulty to quantitate the pyrolysis products released. Quantitation has been attempted by the addition of a polymer standard (Larter and Senftle, 1985). This quantification method requires thorough mixing of the insoluble OM and the standard, which is generally difficult to achieve. Up until now, quantitation is usually performed in conjunction with other pyrolysis methods such as off-line pyrolysis.

Other methods

Despite the limitations of the above-mentioned approach, flash pyrolysis is still one of the most suitable tools for the analysis of kerogens and non-hydrolysable macromolecules in organisms. To complement the structural assignments obtained by pyrolysis, it is necessary to carry out other analyses or chemical degradation experiments. In particular, FT-IR and solid state ^{13}C NMR provide qualitative but also quantitative information, concerning functionalities and the nature of chemical bonds in the macromolecular system. Chemolysis such as oxidation (RuO_4), reductive desulfurization (NiB_2 , Li/EtNH_2) and ether cleavage (HI) are suitable methods for the analysis of specific moieties in HMW OM. The principal drawbacks of these chemical degradation methods and ^{13}C NMR is the requirement of relatively large amounts of material (usually a few milligrams) whereas flash pyrolysis can be carried out on less than a milligram.

1.7 FRAMEWORK OF THE THESIS

A three-step approach was followed to achieve the objectives:

1. Studies of pyrolysis mechanisms of highly aliphatic macromolecular compounds with known structures.
2. Culturing of marine microalgae, isolation of the non-hydrolysable macromolecules and structural elucidation of these biomacromolecules.
3. Studies of immature kerogens isolated from marine sediments of different depositional environments.

Most lacustrine and marine kerogens and most algaenans known so far seem to consist of long-chain alkyl units cross-linked by ether bonds. Since there is a limited knowledge concerning the mechanisms of flash pyrolysis of aliphatic polyethers, the first part of the research was dedicated to a better understanding of these mechanisms by analyses of products released after pyrolysis of structurally known (poly)ether compounds. The chemical structures of these ether lipids were determined by several analytical methods such as ^1H and ^{13}C NMR spectroscopy. Chapter 2 describes the products generated by flash pyrolysis of these types of complex ether lipids isolated from the freshwater green microalgae *Botryococcus braunii*. Mechanisms for their formation are proposed. Chapter 3 focuses on the thermal behaviour of HMW lipids isolated from the same algal species. Mechanisms of pyrolysis were established and a

detailed structure of the algaenan of *B. braunii* race L was proposed based on the data obtained. To study the mechanisms of pyrolysis of even more complex polymeric structures, a suitable soluble biomacromolecule was investigated (chapter 4). The polyaldehyde structure of this polymer had been established by ozonolysis and NMR spectroscopy. The major part of the pyrolysis products could be rationalized and the comparison of the pyrolysate of the *B. braunii* A race algaenan with that of the polyaldehyde clearly indicated that the algaenan was simply a more condensed form of the polyaldehyde and that ether bonds probably acted as cross linkages of the polyaldehyde chains.

In chapters 5 and 6, resistant biomacromolecules in marine microalgae are described. Seven microalgae, two from the class Eustigmatophyceae and five from the class Chlorophyceae, were cultured. Five of these seven algae biosynthesized algaenans representing 1-2% of the dry biomass. Their chemical structures were investigated by chemolysis and pyrolysis in combination with GC-MS. The structure of the algaenan of *Nannochloropsis salina* was fully elucidated. It consisted of aliphatic units, with chain-lengths ranging from C₂₈ to C₃₄, cross-linked by ether bonds at very specific positions in the alkyl-chains. The geochemical implications of these findings are also discussed in these chapters.

Chapter 7 describes the studies of three kerogens isolated from Kimmeridge Clay marine deposits (Upper Jurassic, Yorkshire, UK), considered as a lateral equivalent of the main source rocks of oil in the North Sea, using electron microscopy and pyrolysis methods. The important contribution of selectively preserved algaenans to these kerogens is revealed by both methods. These findings were further extended by investigations of kerogens from the Vena del Gesso formation (Miocene, Italy). Nine samples of these marine sediments representing one evaporitic cycle were analysed by flash pyrolysis as described in chapter 8. These kerogens are mainly comprised of preserved algaenans and sulfurized lipids. Chapter 9 summarizes the results obtained by pyrolysis studies performed on these nine kerogens after desulfurization with Li/EtNH₂. The aliphatic nature probably caused by major contribution of algaenans, became more evident after desulfurization.

Mechanisms of flash pyrolysis of ether lipids isolated from the green microalgae *Botryococcus braunii* race A*

François Gelin, Jean-Pierre L. A. Gatellier, Jaap S. Sinninghe Damsté, Pierre Metzger, Sylvie Derenne, Claude Largeau and Jan W. de Leeuw

2.1 ABSTRACT

Two types of ether lipids isolated from the microalga *Botryococcus braunii* have been subjected to flash-pyrolysis. The pyrolysis products were separated and analyzed by GC-MS. The nature and distribution of the pyrolysis compounds gave clues to the different mechanisms involved in the pyrolysis of ether-linked alkyl chains. The relatively abundant presence of alkenes, alkadienes, alken-9-ones and alken-10-ones with chain lengths corresponding to those of the ether-bound alkyl chains indicated that cleavage of the C-O bond is an important first step in the pyrolysis process.

2.2 INTRODUCTION

Recently, the occurrence of insoluble, non-hydrolysable highly aliphatic biomacromolecules (algaenans) has been demonstrated in outer cell walls of several species of microalgae such as *Botryococcus braunii*, *Tetraedron minimum* and *Scenedesmus* spp. (Berkaloff *et al.*, 1983; Kadouri *et al.*, 1988; Goth *et al.*, 1988; Largeau *et al.*, 1990a; Derenne *et al.*, 1989, 1992a), in protective layers of higher plants, *e.g.* cutans, suberans (Nip *et al.*, 1986; Tegelaar, 1989a), in resins (van Aarssen *et al.*, 1991) and in fossil seed walls of several water plants (van Bergen *et al.*, 1991). These resistant biomacromolecules are assumed to play an important role during the formation of some kerogens *via* a mechanism of selective preservation because good correlations were observed between various algaenans and immature kerogens (Goth *et al.*, 1988; Largeau *et al.*, 1984, 1986, 1990a,b; Dubreuil *et al.*, 1989; Tegelaar *et al.*, 1989c; de Leeuw *et al.*, 1991; Derenne *et al.*, 1991b, 1992b). Spectroscopic, chemical and pyrolysis data indicated that the algaenans consist of long *n*-alkyl chains probably linked together via ether bonds (Largeau *et al.* 1986; de Leeuw *et al.*, 1991; Metzger *et al.*, 1991). One of the most studied algaenans is that of *B. braunii*. *B. braunii* are colonial green microalgae characterized by an unusually high production of lipids. A classification of these organisms is mainly based on the nature of the

**J. Anal. Appl. Pyrolysis* 27, 155 (1993)

hydrocarbons present in the lipid fraction. The A race mainly produces linear alkadienes and alkatrienes with 27, 29 and 31 carbon atoms (Metzger *et al.*, 1986, 1991), whilst the B race is characterized by a unique production of isoprenoid hydrocarbons termed botryococcenes (Metzger *et al.*, 1985, 1991). A third race, the L race, has recently been identified on the basis of an abundant presence of a C₄₀ tetraterpenoid hydrocarbon, lycopadiene (Metzger and Casadevall, 1987; Metzger *et al.*, 1991). Pyrolysis, spectroscopy and labelling experiments demonstrated that the hydrocarbons and other simple lipids biosynthesized by races A and L can be incorporated during formation of the macromolecular structure building up the resistant biomacromolecule of these microalgae (Laureillard *et al.*, 1986, 1988; Derenne *et al.*, 1990a; Metzger *et al.*, 1991; Templier *et al.*, 1992a; Gatellier *et al.*, 1993). In the case of race B, labelling experiments have demonstrated that the botryococcenes do not participate in the formation of the algaenan (Laureillard *et al.*, 1986).

In addition to the long-chain alkadienes and alkatrienes mentioned above, a number of other "non-classical" lipids were identified in the soluble lipid fraction of *B. braunii* A race. They are reviewed in a recent paper by Metzger *et al.* (1991) and mainly consist of families of (i) botryals (even carbon numbered C₅₂-C₆₄ α -branched, α -unsaturated aldehydes), (ii) *n*-alkenylphenols, (iii) epoxides (epoxyalkanes, epoxybotryals and epoxyalkylphenols) and (iv) high-molecular-weight ether lipids derived by coupling of the epoxy-compounds (Metzger and Casadevall, 1989, 1991, 1992; Metzger *et al.*, 1991).

In the present study, two of these ether lipid types isolated from strains of *B. braunii* A race have been selected and submitted to Curie point pyrolysis-gas chromatography (Py-GC) and Curie point pyrolysis-gas chromatography-mass spectrometry (Py-GC-MS) in order to better understand the mechanisms by which pyrolysis products are generated from such structures. This study provides data enabling a better understanding of complex pyrolysis mechanisms associated with flash pyrolysis of algaenans containing macromolecular structures corresponding to alkyl groups linked together by ether bonds. Such structures have been identified in some kerogens resulting from an accumulation of *B. braunii* such as torbanites (Largeau *et al.*, 1986) or coorongites (Dubreuil *et al.*, 1989; Gatellier *et al.*, 1993) or others (Sinninghe Damsté *et al.*, 1993b).

2.3 EXPERIMENTAL

Sample description and isolation

Two types of ether lipids were recovered from different strains of *B. braunii* race A by extraction with hexane and subsequent fractionation of the hexane extract by CC, TLC and HPLC. (for details, see Metzger and Casadevall (1989)).

Type I lipids consist mainly of 10-hydroxy-heptacos-7,26-dienes with a C₂₄ or C₂₆ alkoxy group at carbon atom 9 (Fig. 2.1(A)) and were discovered in two strains of *B. braunii* race A originating from the Bolivian Lake Overjuyo and the French Lake of Coat ar Herno. The two compounds isolated accounted together for 1.1 % of the dry biomass (Metzger *et al.*, 1991).

Type II lipids consist of a mixture of series of two isomers (type IIa and type IIb) of alkenyl-alkyldimethoxyphenol ethers (Fig. 2.1(B)) which were isolated from a culture collection strain (Austin) of *B. braunii* (Metzger *et al.*, 1991). These compounds accounted together for 0.2 % of the dry biomass.

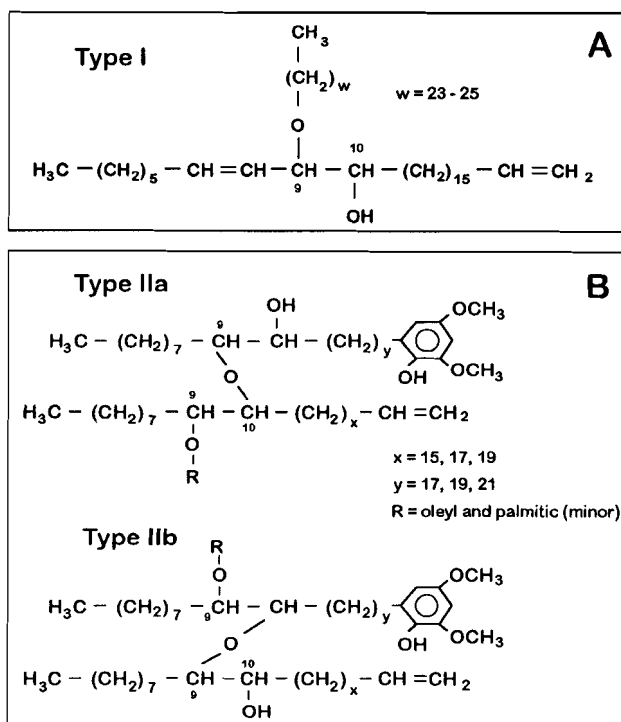


Fig. 2.1 Chemical structure of (A) type I and (B) type II ether lipids.

The elucidation of the chemical structures of these compounds is based on IR, ^1H and ^{13}C NMR spectroscopy, mass spectrometry and specific chemical derivatization reaction and has been reported elsewhere (Metzger *et al.*, 1991).

Pyrolysis methods

For Py-GC as well as Py-GC-MS, the samples were applied on to a ferromagnetic wire. On-line pyrolysis was performed by inductive heating of the ferromagnetic wires to their Curie temperature at which they were held for 10 s. The Curie temperature was 358°C for so-called thermal extraction and 770°C for pyrolysis. The gas chromatograph (Hewlett Packard HP-5890) was equipped with a cryogenic unit and programmed from 0°C (5 min) to 320°C (10 min) at a rate of 3°C/min. Separation of the products was achieved by a 25 m fused silica capillary column coated with chemically bound CP-Sil 5 (0.32 mm I.D.; film

thickness 0.45 μm). Helium was used as carrier gas. The temperature of the flame ionisation detector was 320°C.

Py-GC-MS was performed using the same pyrolysis and GC conditions. The column was coupled to the EI ion source of a VG-70s double focusing mass-spectrometer (mass range m/z 40-800; cycle time 2 s; ionisation energy 70 eV).

2.4 RESULTS AND DISCUSSION

Mechanisms of pyrolysis of type I lipids

Figure 2.2 shows the total ion current (TIC) trace of the 770°C flash pyrolysate of the type I lipids. The pyrolysate mainly consists of an homologous series of *n*-alk-1-enes ranging from C_6 to C_{26} , a series of *n*-alkanes in the C_{12} - C_{26} range and an homologous series of α,ω -alkadienes ranging from C_7 to C_{17} (alkadienes from C_{18} to C_{26} are also present but in very low amounts). Three saturated aldehydes, tetracosanal, pentacosanal and hexacosanal (the latter being the most important pyrolysis product), three saturated primary alcohols (ranging from C_{24} to C_{26}), an unsaturated aldehyde, octadecenal, and several isomers of *n*-heptacosatrienes represent the most abundant pyrolysis products (Fig. 2.2). Two other compounds have been identified as 7,26-heptacosadien-10-one and 8,26-heptacosadien-10-one.*

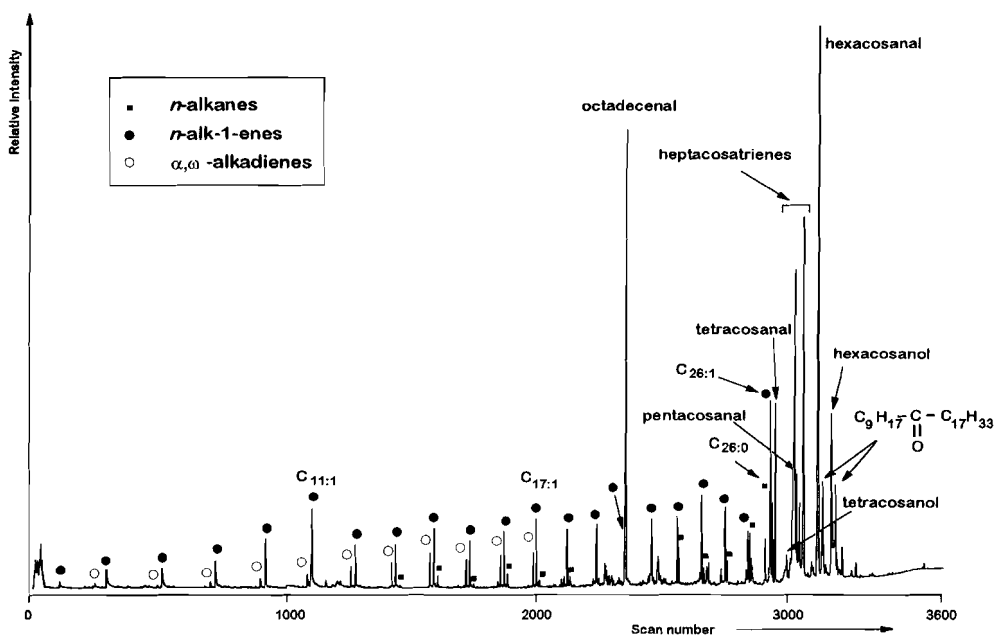


Fig. 2.2 Total ion current of the flash pyrolysate (Curie temperature 770°C) of type I ether lipids.

* For reasons of convenience the numbering of carbon atoms in these molecules is started at the terminal (non-functionalized) carbon atom.

The homologous series of *n*-alk-1-enes and *n*-alkanes can be generated by the homolytic cleavage of the relatively weak C-O bond (cleavage 1 in Fig. 2.3) generating a radical which can stabilize to C₂₄, C₂₅ and C₂₆ -alk-1-enes or C₂₄, C₂₅ and C₂₆ -alkanes by an intermolecular H-radical transfer (Fig. 2.3). It should be noted that the presence of the C₂₅ alkane and alkene indicates that the type I lipid with w=24 also occurs in the sample. This was further supported by other pyrolysis products (see later). This homologue of type I was not mentioned originally (Metzger *et al.*, 1991). A scrambling process of the primary radical leads to the formation of secondary radicals which can also stabilize *via* intermolecular H-radical transfer and random cleavage of the C-C bond resulting in homologous series of *n*-alk-1-enes (C₂ to C₂₅) and *n*-alkanes (C₁ to C₂₄). The occurrence of such "scrambling" process has already been reported in pyrolysis studies of synthetic polymers as well as in flash pyrolysis experiments performed with silicon-bound alkyl chain (Wampler and Levy, 1986; Hartgers *et al.*, 1991b). The lack of *n*-alkanes from C₆ to C₁₃ can be explained by low concentrations of H-radicals which favours the stabilization of the alkyl radicals as *n*-alk-1-enes.

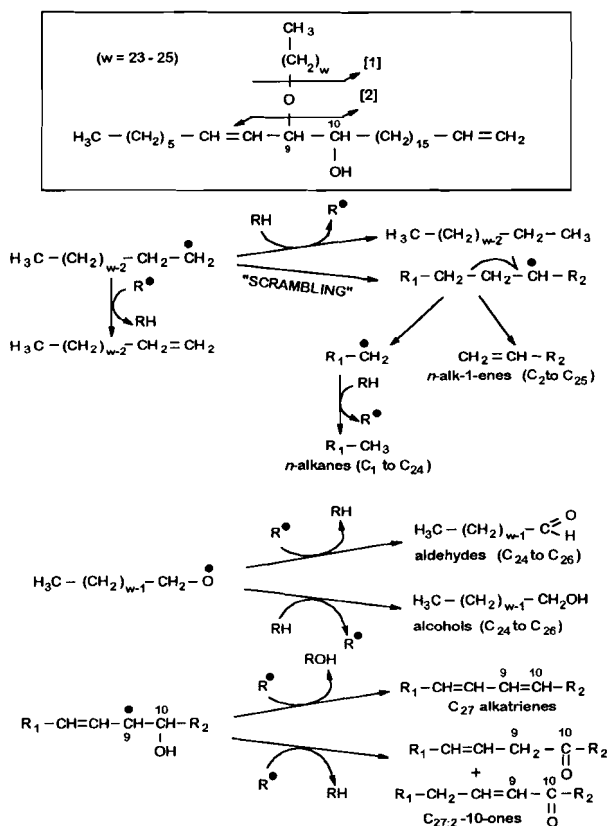


Fig. 2.3 Proposed mechanism of pyrolysis for the formation of the indicated pyrolysis products from type I ether lipids.

The occurrence of the C₂₄, C₂₅ and C₂₆-aldehydes and -alcohols can be rationalized by an "allylic" cleavage of the C-O bond (cleavage 2 in Fig. 2.3). The radical thus generated can stabilize as an aldehyde or an alcohol by intermolecular H-radical transfer reactions (Fig. 2.3). The other radical generated by cleavage of the C-O bond, can be converted *via* two different pathways yielding *n*-heptacosatriene isomers by dehydroxylation or yielding 7,26-heptacosadien-10-one and 8,26-heptacosadien-10-one by hydrogen abstraction at C-10 followed by either tautomerization of the enol intermediate or a six-membered ring rearrangement, respectively (Fig. 2.3).

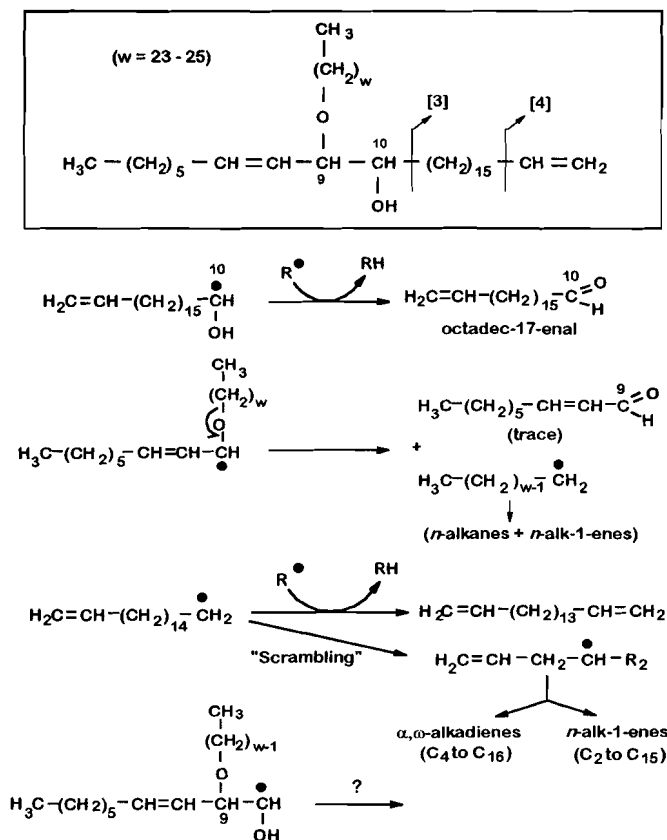


Fig. 2.4 Proposed mechanism of pyrolysis for the formation of the indicated pyrolysis products from type I ether lipids.

Octadecenal, one of the major products in the flash pyrolysate, is resulting from cleavage of the C-9-C-10 bond (cleavage 3 in Fig. 2.4). The radical generated by this cleavage can stabilize as aldehyde as shown in Fig. 2.4. The homologous series of α,ω-alkadienes is explained by a cleavage of the C-10-C-11 bond (cleavage 4 in Fig. 2.4) producing a radical transferring to α,ω-

heptadecadiene by an intermolecular H-radical transfer and a series of homologous of α,ω -alkadienes (C_4 to C_{16}) and n -alk-1-enes (C_2 to C_{15}) by a "scrambling" process as described above (Fig. 2.4). In both cases, after cleavages 3 and 4 stable compounds resulting from the other radicals corresponding to the rest of the molecule are not observed.

Small amounts of eicosenal, n -octacosatriene and α,ω -nonadecadiene suggest that among the type I lipids (Fig. 2.1(A)), the alkadienyl chain can also have a chain length corresponding to 29 carbon atoms.

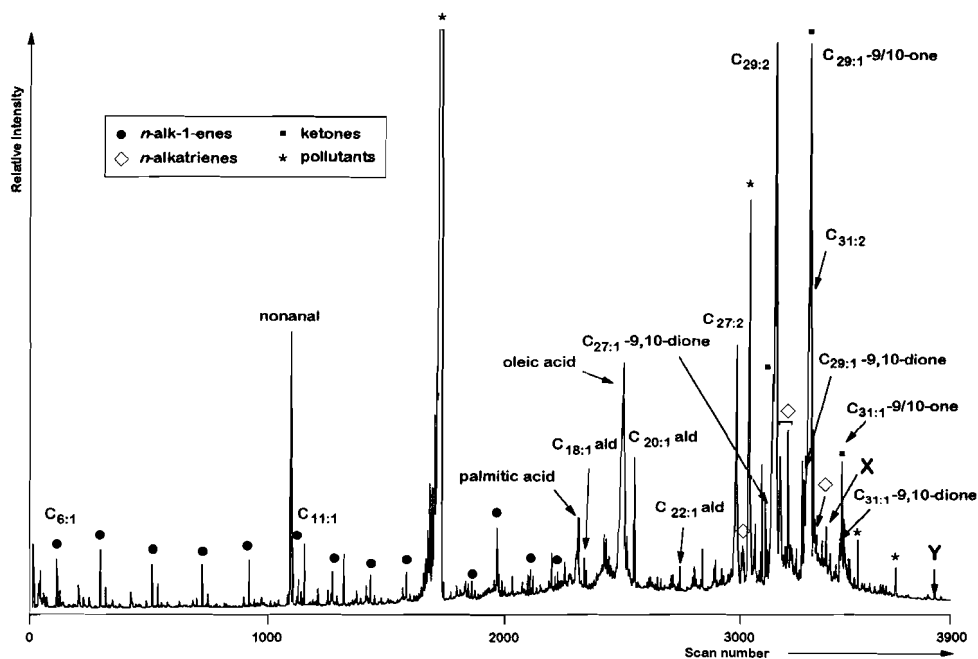


Fig. 2.5 Total ion current of the flash pyrolysate (Curie temperature 770°C) of type II ether lipids. X and Y refer to the structures shown in Fig. 2.6.

Mechanisms of pyrolysis of type II lipids

Figure 2.5 shows the TIC trace of the 770°C flash pyrolysate of the type II lipid mixture. The pyrolysate mainly consists of odd C_{27} - C_{31} n -alkadienes, n -alkatrienes and n -alken-9-ones as well as alken-10-ones. Nonanal and a series of C_{18} , C_{20} and C_{22} mono unsaturated aldehydes are also present in the pyrolysate. A small amount of palmitic acid and abundant oleic acid are observed. An homologous series of n -alk-1-enes ranging from C_6 to C_{19} is present as well. Mass chromatography of m/z 141 reveals the existence of three pyrolysis products which show mass spectra characterized by a base peak at m/z 141 and by molecular ion peaks at m/z 406, 434 and 462 corresponding to 26-heptacosen-9,10-dione, 28-nonacosen-9,10-dione and 30-hentriaconten-9,10-

dione. Two other compounds (X and Y in Fig. 2.5) have been identified as two aldehydes containing an aromatic ring. The mass spectra and related structures of these latter products are shown in Figs. 2.6(A) and 2.6(B), respectively. A number of the other peaks in the TIC trace of the flash pyrolysate originate from pollutants. They mainly consist of methyl-di-*t*-butyl-phenols, their homologous as well as their dimers (Fig. 2.5). A 358°C Curie point "pyrolysis" showed that these compounds did not originate from the lipid structure but were present in the sample as such and simply evaporated.

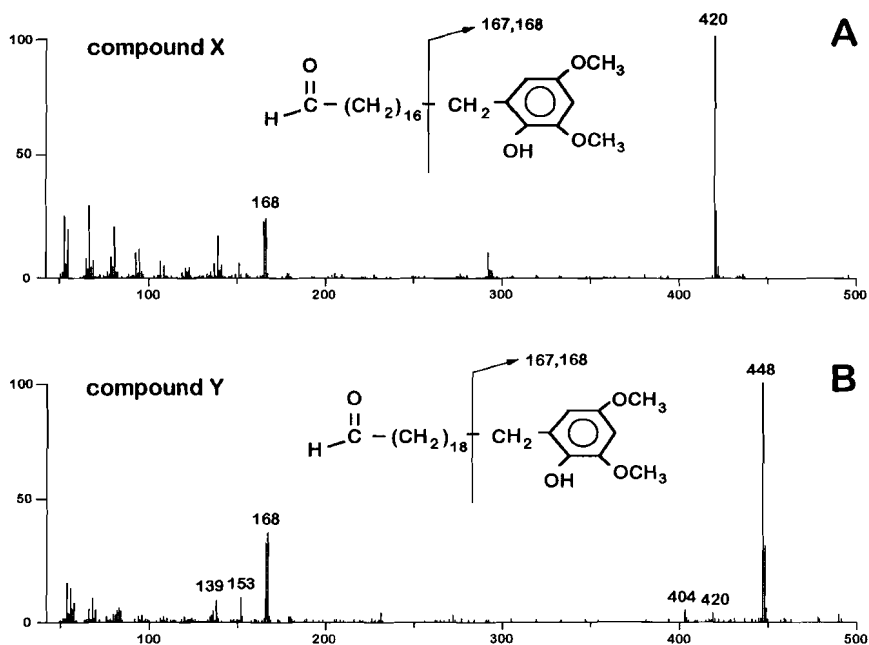


Fig. 2.6 Mass spectra, corrected for background, of (A) compound X (2,4-dimethoxy-6-octadecanalphenol) and (B) compound Y (2,4-dimethoxy-6-eisocanalphenol) detected in the flash pyrolysate of type II ether lipids.

Oleic acid and the trace amount of palmitic acid are supposed to be released from the ether lipid structure via a six-membered ring rearrangement reaction (Fig. 2.7). For the type IIa compounds, this rearrangement involves either C-10 or C-8. In the first case (Fig. 2.7(A)), it leads to the formation of the already mentioned acids and to the formation of alkadienyl-alkyl-phenols which generate, after homolytic cleavage of the C-O bond of the hydroxy-alkyl-phenol chain and an intermolecular H-radical transfer, the alken-10-ones as shown in Fig. 2.7(A). In the second case (Fig. 2.7(B)), the double bond generated at the C-8 position weakens the ether bond at C-10 and an "allylic" cleavage as described before may occur leading to the formation of the *n*-alkatrienes. It should be noted that

the six-membered ring rearrangements also occur in the type IIb compounds generating the fatty acids as well as phenol-ketones and alkadienyl-phenols. However, as observed in recent experiments (Gelin *et al.*, 1994a), 2,4-dimethoxy-6-alkenyl-phenols (the alkenyl chain lengths being C₂₇, C₂₉ and C₃₁) do not pyrolyse further under the same experimental conditions and condense on the glass wall surrounding the ferromagnetic wire in the pyrolysis unit. It is therefore believed that the alkyl-phenol and phenol-ketone compounds (having a C₂₇, C₂₉ or C₃₁ alkyl chain length), assumed to be formed from the type II ether lipids, also condense on the glass wall and are, therefore, not detected by GC or GC-MS.

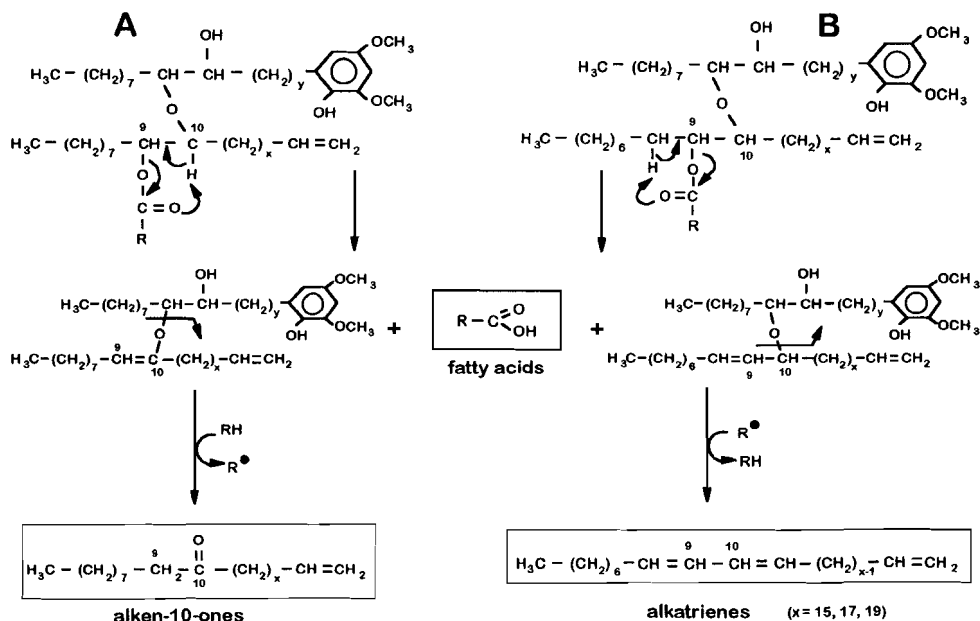


Fig. 2.7 Proposed mechanism of pyrolysis for the formation of the fatty acids, alken-10-ones and *n*-alkatrienes from type IIa ether lipids.

Formation of nonanal can be rationalized by cleavage of the C-9-C-10 bond of the alkyl-phenol chain of the type IIa compounds followed by cleavage of the C-10-O bond of the alkenyl chain (Fig. 2.8). This latter cleavage generates a radical at C-10 which stabilizes via the loss of the acyl group leading to the formation of the odd *n*-alkadienes maximizing at C₂₇-C₃₁ (Fig. 2.8). The aldehydes X and Y possessing the dimethoxyphenol structure (see mass spectra in Fig. 2.6) clearly result from the same cleavage of the C-9-C-10 bond in the alkyl-phenol chain. The relatively low abundance of these products and the

absence of the 2,4-dimethoxy-6-docosanal-phenol are probably due to the same phenomenon indicated above for the alkyl-phenol compounds.

As shown in Fig. 2.9, the nonanal can also be produced by cleavage of the C-9-C-10 bond in the alkenyl chain followed by cleavage of the C-9-O bond of the OR-alkyl-dimethoxyphenol chain from the type IIb compounds. The radical generated by the C-9-C-10 cleavage is stabilized by the loss of an H-radical and leads to the formation of the C₁₈, C₂₀ and C₂₂ monounsaturated aldehydes (Fig. 2.9).

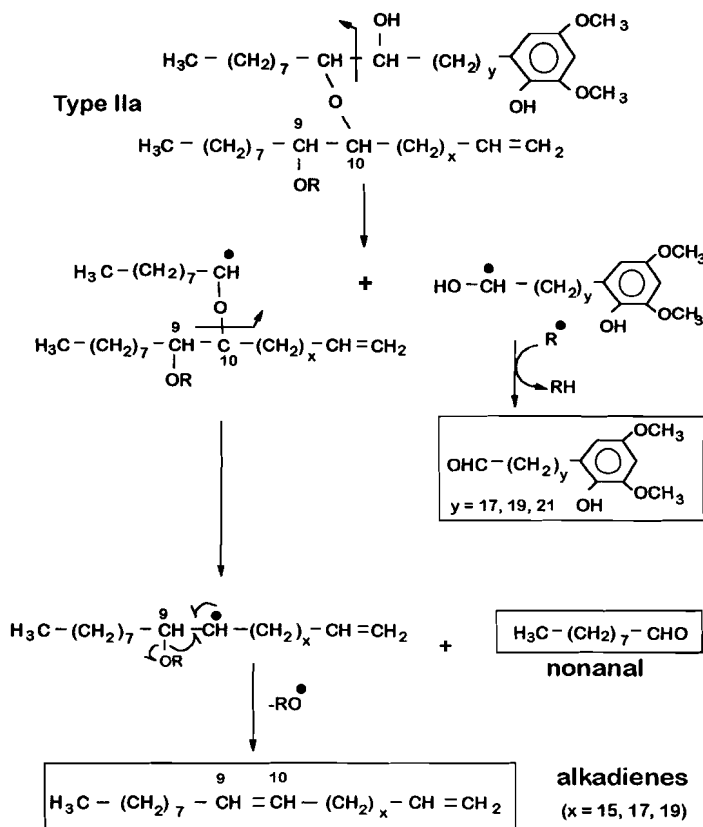


Fig. 2.8 Proposed mechanism of pyrolysis for the formation of the *n*-alkadienes, nonanal and compounds X and Y from type IIa ether lipids.

Figure 2.10 shows the pyrolysis mechanisms rationalizing the formation of both the *n*-alken-9-one and *n*-alken-9,10-dione series maximizing in the C₂₇-C₃₁ range. In both cases, the loss of an H-radical is required which triggers ketone formation *via* enol intermediates. It should be noted that these products can be generated from the type IIb ether lipids only.

The predominance of the eicosenal among the unsaturated aldehydes and of the C₂₉ isomers for the *n*-alkadienes, *n*-alkatrienes, *n*-alken-9-ones, *n*-alken-10-ones and diketones suggests that the chain length of the alkenyl chain is preferentially composed of 29 carbon atoms ($x = 17$; Fig. 2.1(B)).

It is interesting to note that the presence of an ether bond in a molecule can generate significantly different suites of pyrolysis products depending on the position of this ether bond: In the type I lipids the ether bond links a "mid-chain" carbon of an alkadienyl chain to an end-chain carbon atom of an alkyl chain whilst in the type II lipids the ether bonds link two "mid-chain" carbon atoms of alkyl chains.

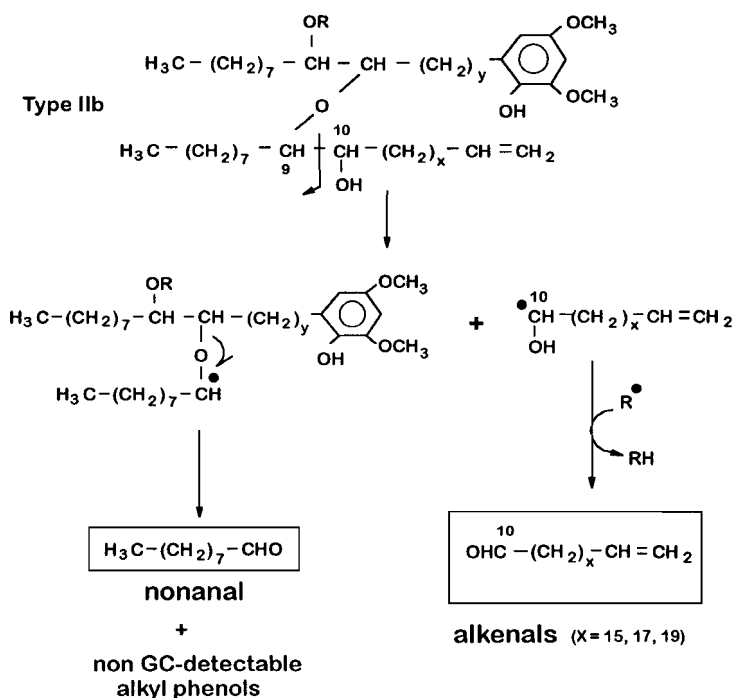


Fig. 2.9 Proposed mechanism of pyrolysis for the formation of nonanal and the C₁₈, C₂₀ and C₂₂ alkenals from type IIa ether lipids.

The pyrolysis products described above are also important pyrolysis products obtained by flash pyrolysis of sediments consisting of an accumulation of *B. braunii* A race deposited under oxic conditions corresponding to a coorongite-type deposit (Gatellier *et al.*, 1993) and under anoxic conditions (Sinninghe Damsté *et al.*, 1993b). In particular the mid-chain alken-9-ones and alken-10-ones with 27 and 29 carbon atoms are highly specific pyrolysis

Scope and limitations of flash pyrolysis-gas chromatography-mass spectrometry as revealed by the thermal behaviour of high-molecular-weight lipids derived from the green microalga *Botryococcus braunii* *

François Gelin, Jan W. de Leeuw, Jaap S. Sinninghe Damsté, Sylvie Derenne, Claude Largeau and Pierre Metzger

3.1 ABSTRACT

Curie point pyrolysis-gas chromatography-mass spectrometry studies of four types of high-molecular-weight (HMW) lipids isolated from the green microalga *Botryococcus braunii* race A were performed to determine the thermal behavior of these lipids and to propose mechanisms of pyrolysis for these types of compounds. Although two types of lipids induced detectable pyrolysis products upon heating of the ferromagnetic wires at Curie temperature of 610 and 770°C, transfer problems from the pyrolysis unit to the GC column were observed. Therefore, further analysis of the pyrolysis residues is suggested. Furthermore, two types of lipids presenting long alkyl chains (up to C₆₄) did not pyrolyse under the experimental conditions but were thermally extracted from the wire at any tested temperatures. Some of these HMW lipids could, however, be analysed by high temperature gas chromatography (temperature up to 375°C). Mechanisms of pyrolysis, partly based on previous studies, were proposed for the two types of ether lipids. These mechanisms allowed the structural reconstruction of the main biopolymer that composes the cell outer walls of the microalga *B. braunii* race L. This biomacromolecule was found to be comprised of C₄₀ isoprenoid (lycopene) units ether linked at the C(14) and C(15) positions.

3.2 INTRODUCTION

Flash pyrolysis-gas chromatography (Py-GC) and flash pyrolysis-gas chromatography-mass spectrometry (Py-GC-MS) have been used successfully in organic geochemistry and petroleum geochemistry to structurally characterise macromolecular organic substances in source rocks, kerogens, crude oils, coals and soils (van de Meent *et al.*, 1980; Larter *et al.*, 1984). Recently, Py-GC-MS analyses of these materials have resulted in a major reappraisal of the formation

* *J. Anal. Appl. Pyrolysis* **28**, 183 (1994)

of "geopolymers" and have contributed to our understanding of crude oil formation (Tegelaar *et al.*, 1989b,c). It has become clear that resistant highly aliphatic biomacromolecules derived from algal cell walls, plant cuticles, seeds and periderm plant tissues are sometimes significant constituents of "geopolymers". Reversibly, pyrolysis data of kerogens have contributed significantly to the recognition of these resistant aliphatic macromolecules in organisms (Goth *et al.*, 1988; Derenne *et al.*, 1991b).

To further increase our understanding of kerogen, coal and crude oil formation, it is a prerequisite to understand better mechanisms of pyrolysis of these aliphatic macromolecules. Since the highly aliphatic biopolymers in cell walls of several races of the microalga *Botryococcus braunii* contribute significantly to many kerogens in source rocks (sometimes the kerogens consist mainly of these materials, *e.g.* Torbanites (Largeau *et al.*, 1986; Derenne *et al.*, 1988), Coorongites (Dubreuil *et al.*, 1989; Gatellier *et al.*, 1993) and Ribesalbes oil shale (Sinninghe Damsté *et al.*, 1993b)), detailed pyrolysis studies of isolated and purified biopolymers and related high-molecular-weight (HMW) lipids of *B. braunii* have been performed recently (Gatellier *et al.*, 1993; Gelin *et al.*, 1993, 1994b). These studies also helped to clarify mechanisms of pyrolysis since the structures of high-molecular-weight lipids isolated from these algae are well characterized (Metzger *et al.*, 1991).

During the initial stages of the work described here erroneous results were observed upon Py-GC-MS studies of a new series of complex lipids isolated from *B. braunii* race A. Therefore a more detailed study was undertaken to understand better pitfalls and limitations of Py-GC-MS analyses of these materials.

Furthermore, thanks to this and earlier studies concerning mechanisms of pyrolysis of ether lipids isolated from *B. braunii*, it was possible to reconstruct the detailed macromolecular structure of the insoluble aliphatic cell wall biopolymer of *B. braunii* race L.

3.3 EXPERIMENTAL

Origin and isolation of high-molecular-weight lipids

The four series of compounds investigated were recovered from different strains of *B. braunii* race A by hexane extraction. Silica gel column chromatography, TLC and HPLC of this hexane extract allowed for the isolation of series of related and individual compounds (Metzger and Casadevall, 1989, 1991, 1992).

6-*n*-Alkenyl-2,4-dimethoxyphenols (**1**; Fig. 3.1) and botryals (**2**; Fig. 3.1) have both been detected in almost all strains of *B. braunii* race A investigated so far. Compounds **1** were isolated from a collection strain from Austin (Texas) and accounted for *ca.* 1.5% of dry algal biomass (Metzger and Casadevall, 1989). Compounds **2** were isolated from the Austin strain and accounted for 9.9 % of dry biomass (Metzger and Casadevall, 1989).

The alkatrienyl-alkadienyl ether (**3**; Fig. 3.1) was found in two strains of the race A originating from the Bolivian Lake Overjuyo and the French Lake Coat ar Herno (Metzger and Casadevall, 1991). Compounds **3** accounted for up to 26%

Isolation of the PRB of B. braunii race L

Lyophilized *B. braunii* race L material was ultrasonically extracted twice with MeOH, five times with MeOH/CH₂Cl₂ (1/1) and twice with hexane. The residue recovered after these extractions was saponified with 2N KOH in MeOH and extracted. The residue thus obtained was hydrolysed with HCl according to a previously reported procedure (Goossens *et al.*, 1989). The residue was washed several times with water to remove salts and then dried under vacuum. The highly resistant material isolated, termed PRB L* , accounted for about 25 % of the dry biomass.

Pyrolysis methods

In case of the soluble lipids, samples were directly applied to ferromagnetic wires and the solvent was allowed to evaporate at elevated temperatures using an infrared lamp under a nitrogen atmosphere. The algaenan sample from the race L was pressed onto a flattened ferromagnetic wire. The samples were heated by inductive heating of the ferromagnetic wires (Curie temperatures 610°C or 770°C for pyrolysis and 358°C for thermal extraction) for 10 s using a Curie point high frequency generator (Fischer 9425). The glass tube in which the ferromagnetic wire is positioned was surrounded by a ceramic tube which was independently heated at 250°C. The gas chromatograph (Hewlett Packard HP-5890) was equipped with a cryogenic unit and programmed from 0°C (5 min) to 320°C (10 min) at a rate of 3°C/min. Separation of the products was achieved by a 25 m fused silica capillary column coated with chemically bound CP-Sil 5 (0.32 mm I.D.; film thickness 0.45 µm). Helium was used as carrier gas and the temperature of the flame ionisation detector (FID) was 320°C.

Py-GC-MS was performed using the same pyrolysis and GC-conditions. The column was coupled to the EI ion source of a VG-70S double focusing mass-spectrometer (mass range *m/z* 40-800; cycle time 1.8 s; ionisation energy 70 eV).

Gas chromatography

GC was performed with a Carlo Erba 4160 instrument equipped with an FID and an on-column injector. A fused silica capillary column (25 m x 0.32 mm) coated with CP Sil-5 (film thickness 0.45 µm) was used with helium as carrier gas. The oven was programmed from 70°C to 320°C at 4°C/min.

High temperature GC (HT-GC) was performed with the same instrument. The samples were directly injected into a 10 m fused silica capillary column coated with chemically bound CP-Sil 5 (0.32 mm I.D.; film thickness 0.45 µm). Helium was used as carrier gas and the oven was programmed from 75°C to 200°C at 20°C/min and then at a rate of 6°C/min to 375°C, at which temperature it was held for 10 min.

* The term PRB L was previously attributed to material isolated from the race L following a procedure that was only different for the acid treatment; concentrated phosphoric acid was used instead of hydrochloric acid in the present study.

Gas chromatography-mass spectrometry and probe-mass spectrometry

GC-MS and HT-GC-MS analyses were performed using the same conditions as described for GC and HT-GC, respectively, using a Hewlett Packard gas chromatograph (HP-5890). The column was directly inserted into the ion source of a VG -70S mass spectrometer (mass range m/z 40-800 for GC-MS and m/z 50-1000 for HT-GC-MS; cycle time 1.8 s; ionisation energy 70 eV).

Probe-MS analyses were performed using a direct probe inlet and the same mass spectrometer using a mass range m/z 40-1000 with a cycle time of 1.8 s. and an ionisation energy of 70 eV. The probe was heated gradually at a rate of 200°C/min.

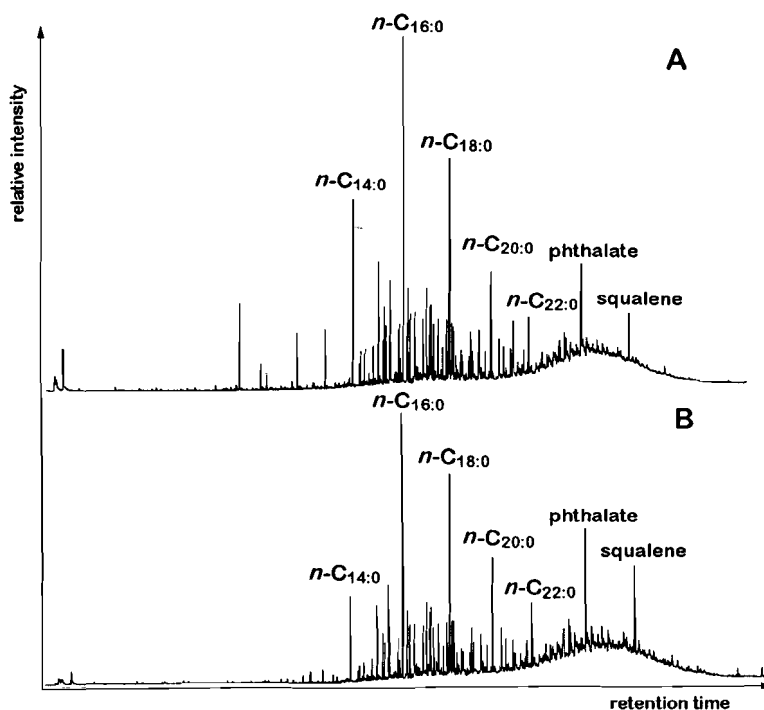


Fig. 3.2 Gas Chromatograms of compounds encountered after subjecting compounds 1 to pyrolysis conditions at (A) 770°C and to evaporation at (B) 358°C. $n-C_{x:0}$ indicate n -alkanes, x being the carbon number.

3.4 RESULTS AND DISCUSSION

Alkenyl-phenols

Fig. 3.2(A) shows the chromatogram of the compounds derived from the alkenyl-phenols 1 using a Curie temperature of 770°C. Identification of these

compounds by mass spectrometry after Py-GC-MS analysis indicated the presence of *n*-alkanes ranging from C₁₂ to C₂₂, C₉ to C₁₃ alkyl-substituted benzenes (alkylbenzenes occurring as contaminants in linear alkylbenzenes sulphonates (LAS) (Harvey *et al.*, 1985)), phthalate and squalene. Based on previous studies (Gelin *et al.*, 1993) it was clear that none of these compounds could have been generated by pyrolysis of **1**. Moreover, expected pyrolysis products of **1**, such as compounds containing a dimethoxyphenol moiety, were not found. Therefore, these results strongly suggest that pyrolysis of **1** had not occurred or that the pyrolysis products were not transferred to the GC-column.

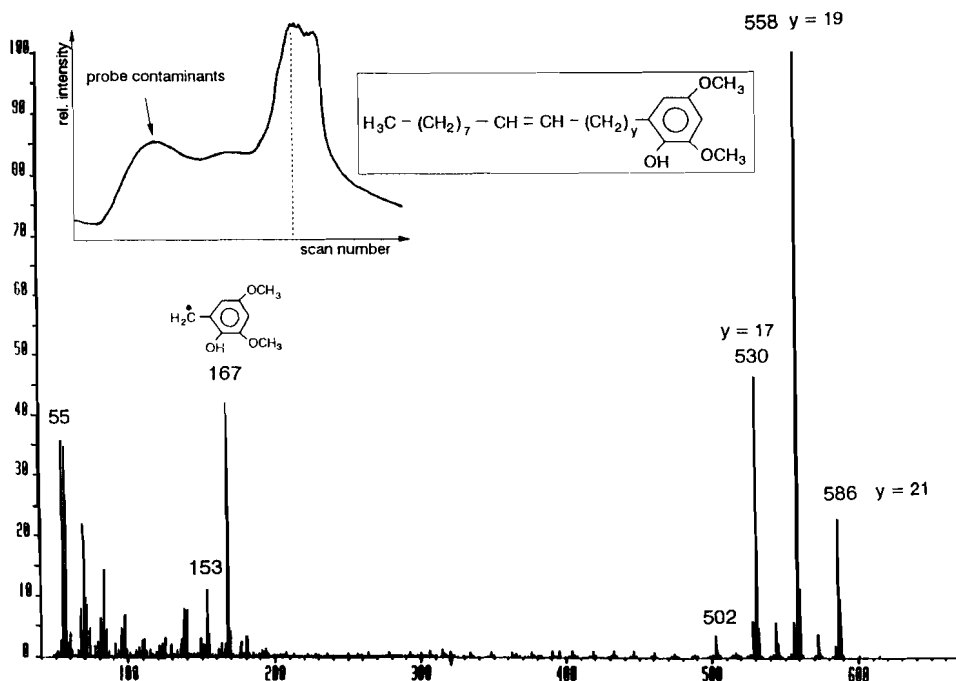


Fig. 3.3 Probe-mass spectrum of the residue obtained by rinsing the glass tube after subjecting compounds **1** to pyrolysis conditions at 770°C. The curve shown in the upper left part of the figure indicates the total ion current trace and the dashed line indicates the scan selected for the mass spectrum.

The *n*-alkanes, alkylbenzenes, phthalate and squalene were thus ascribed to minor compounds present as such in the samples which thermally evaporated upon heating. This interpretation was substantiated by the results of subsequent GC-analyses using ferromagnetic wires with a Curie temperature of 358°C as injector device (Fig. 3.2(B)); essentially the same distributions of *n*-alkanes, alkylbenzenes, phthalate and squalene were observed.

To explore the possibility that compounds **1** were not pyrolysed but had evaporated and condensed on the inside of the glass tube, the glass wall

surrounding the ferromagnetic wire in the pyrolysis unit was rinsed with dichloromethane to recover any condensed residue. Probe mass spectrometry of this material clearly indicated that compounds **1** indeed had evaporated and that no pyrolysis had taken place (Fig. 3.3); the mass spectra revealed the molecular ions expected and were similar to those previously reported for these compounds (Metzger and Casadevall, 1989).

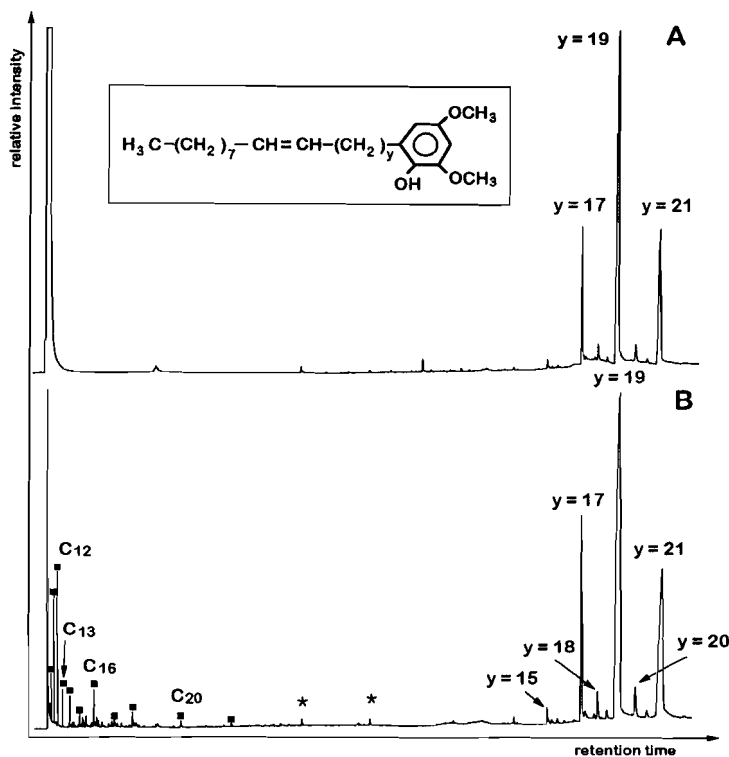


Fig. 3.4 Gas chromatograms of (A) the condensed residue and (B) compounds **1**: (■) *n*-alkanes, (*) phthalate and squalene.

Straightforward GC-analyses of the condensed residue further confirmed these probe mass spectrometry results (Fig. 3.4(A)). GC analysis of compounds **1** revealed that *n*-alkanes, alkylbenzenes, phthalate and squalene only represent a very small amount of the sample (Fig. 3.4(B)). The absence of high-volatile compounds (C₉-C₁₃) in the compound mixtures obtained in the experiments using the ferromagnetic wires is likely due to their pre-evaporation during the gentle heating of the wires before they are introduced into the pyrolysis unit.

We have to conclude that compounds **1** cannot be analysed either as pyrolysate or as evaporate because of their condensation onto the relatively cold glass wall (250°C) after evaporation from the wire; they were not transferred to the GC column.

Botryals

The C₅₂-C₆₄ botryals represent complex lipids with a long straight chain containing a conjugated aldehyde function in the middle (compounds 2 in Fig. 3.1).

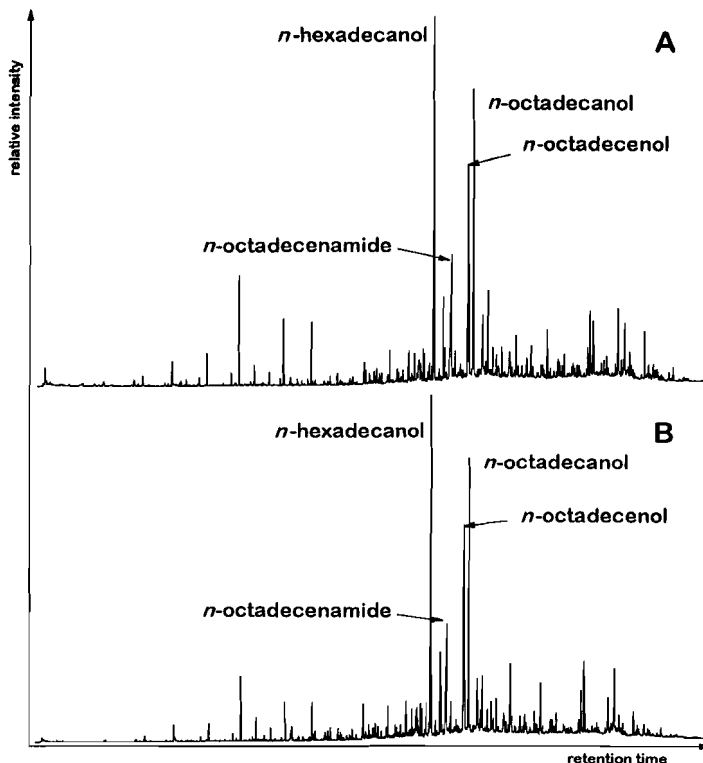


Fig. 3.5 Gas chromatograms of compound encountered after subjecting compounds 2 to (A) pyrolysis conditions at 610°C and (B) evaporation at 358°C.

Fig. 3.5(A) shows the compounds obtained after Py-GC at 610°C. The three major compounds were identified as C_{16:0}, C_{18:1} and C_{18:0} primary alcohols. The other components represented by this chromatogram were mainly series of *n*-alkanes, octadecenamide and phthalates. Since the alcohols and the other compounds observed are difficult to explain by pyrolysis of the botryals, an identical behavior as observed for compounds 1 seemed likely. Using a wire with a Curie temperature of 358°C (Fig. 3.5(B)) showed indeed very similar distributions of the compounds found in the experiment at 610°C, indicating that these compounds represent small amounts of evaporated lipids not related to the botryals. It is assumed that the alcohols and octadecenamide originate from the alga itself and were not separated from the botryals during the isolation process.

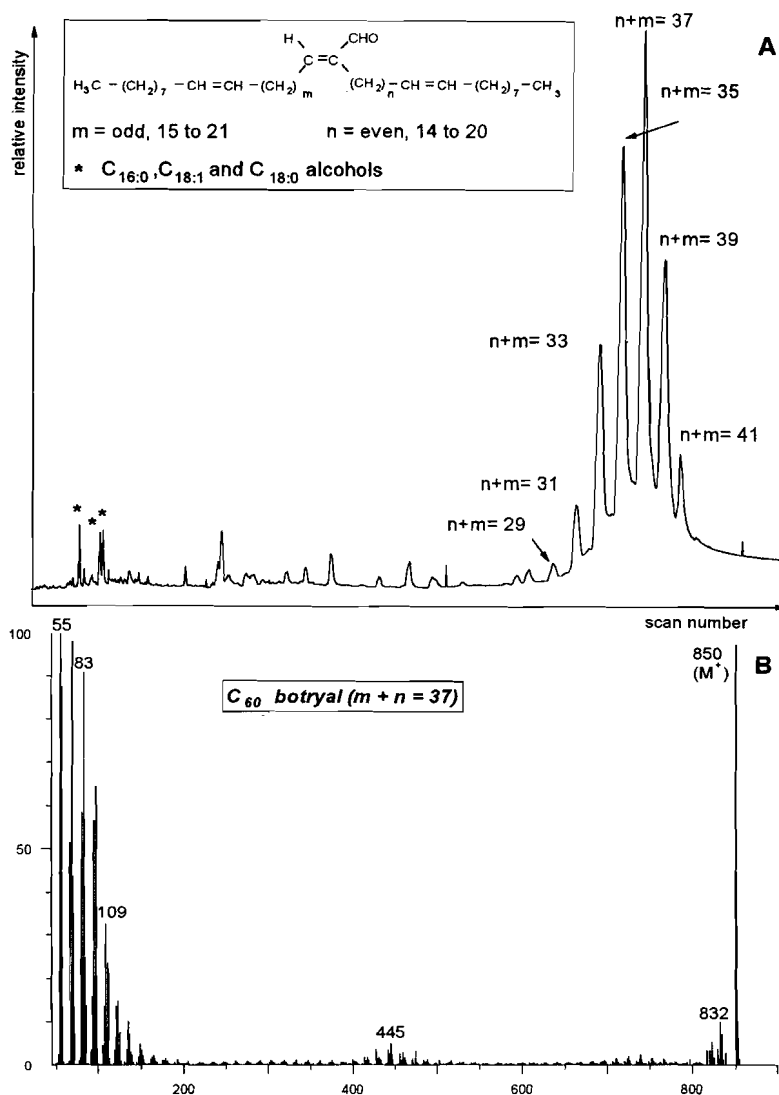


Fig. 3.6 (A) TIC trace of compounds 2 obtained through HT-GC; (*) $\text{C}_{16:0}$, $\text{C}_{18:1}$, $\text{C}_{18:0}$ alcohols. (B) Mass spectrum of the C_{60} botryals obtained by HT-GC-MS of the residue condensed in the glass tube after treatment of compounds 1 at 610°C .

The glass tube was rinsed after the 610°C experiment and the condensed residue recovered was analysed by high temperature-gas chromatography (HT-GC). This analysis revealed the almost exclusive presence of compounds 2. To determine the relative abundance of the impurities in the sample of compounds 2, HT-GC-MS analysis was performed on both the condensed residue and the unheated sample. In the TIC trace of the latter, most of the impurities dominantly present in the Py-GC analysis were found in trace quantities only (Fig. 3.6(A)).

Fig. 3.6(B) shows a typical mass spectrum of the C_{60} botryals obtained by HT-GC-MS. The molecular ion peak at m/z 850 is very intense indicating the intact structure of the C_{60} botryals.

Despite their long chain-length, the high molecular weight and the presence of functional groups, the botryals, like the alkenyl-phenols **1**, evaporated before pyrolysis could take place but their transfer to the GC column was hampered by condensation on the relatively cold glass tube.

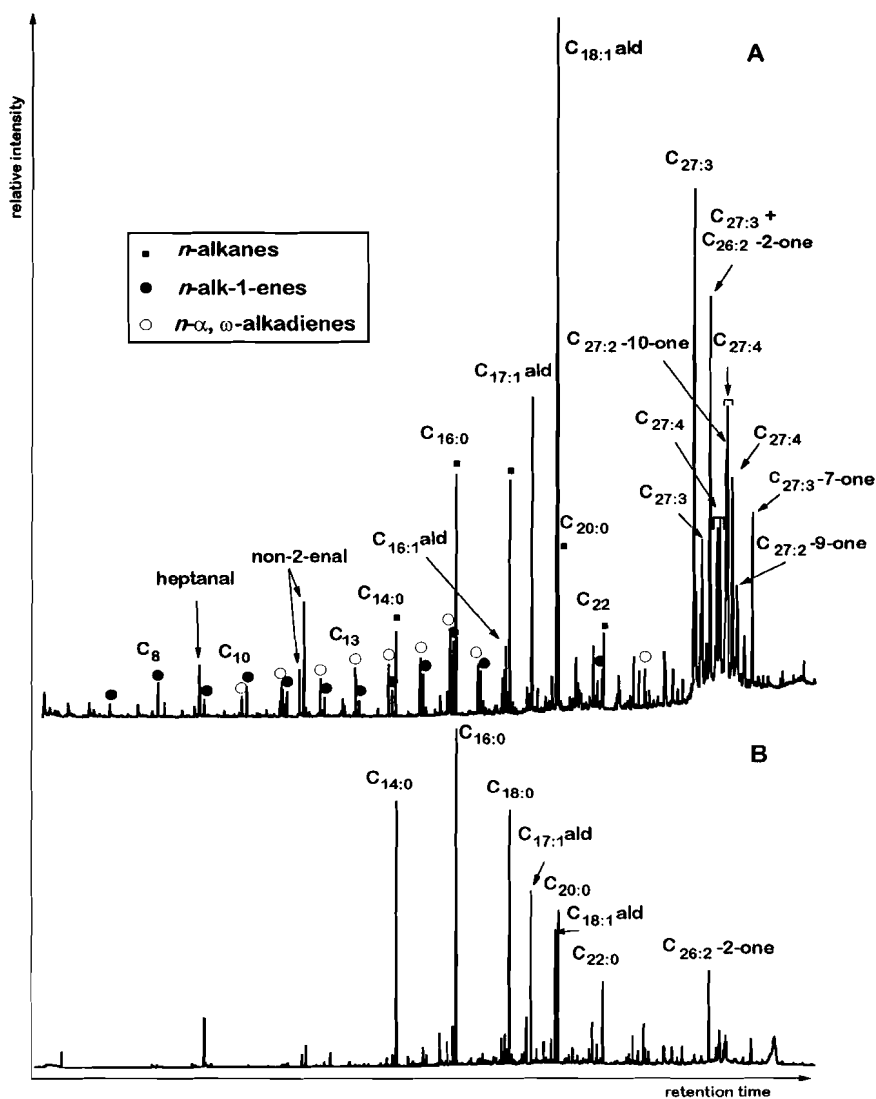


Fig. 3.7 TIC trace of the compound encountered after subjecting compounds **3** to (A) pyrolysis conditions at 770°C and (B) evaporation at 358°C.

Alkatrienyl-alkadienyl ether lipids

The pyrolysis behavior of long-chain alkylethers related to the alkatrienyl-alkadienyl ether lipids indicated in Fig. 3.1 (compounds **3**) has recently been discussed (Gelin *et al.*, 1993). The cleavage of the C-O ether bond was considered as an important first step in the pyrolysis process.

The TIC trace of the flash pyrolysate of compounds **3** at 770°C (Fig. 3.7(A)) reveals the presence of C₇, C₉, C₁₆, C₁₇ and C₁₈ aldehydes, C₂₇ linear hydrocarbons and ketones, series of alk-1-enes and α,ω -alkadienes and a series of even carbon numbered *n*-alkanes.

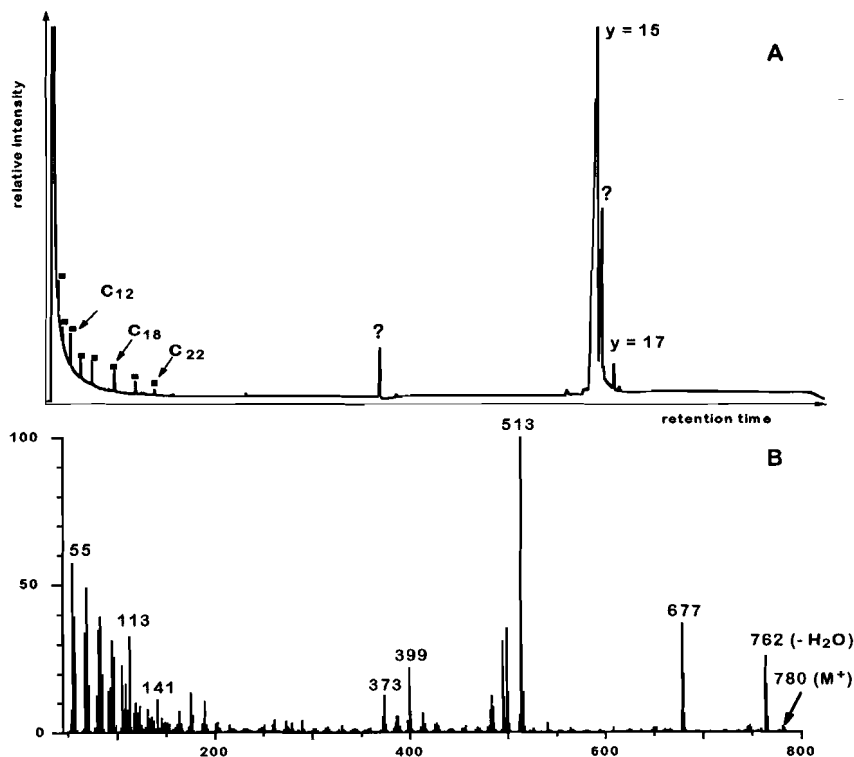


Fig. 3.8 High-temperature gas chromatogram of compounds **3**; (■) series of *n*-alkanes. (B) Mass spectrum of compound **3** ($y = 15$) obtained by HT-GC-MS.

Most of these compounds are pyrolysis products of compounds **3** because thermal evaporation at 358°C of compounds **3** mainly revealed the series of *n*-alkanes (Fig. 3.7(B)). As previously observed for compounds **1** and **2**, these alkanes probably represent impurities in the sample which evaporate. The HT-GC-FID trace revealed that the alkanes were indeed present in low amount. A large difference in the relative abundances of the alkanes was revealed by the Py-GC

and the HT-GC traces (cf. Fig. 3.7(A) and 3.8(A)). This suggests that compounds **3** are only pyrolysed for a small part resulting in an overestimation of the alkanes impurities reflected by the Py-GC trace. HT-GC analysis clearly indicates that the residue recovered from the glass tube is composed almost exclusively of compounds **3**. This observation proved that a substantial part of these ether lipids did not pyrolyse but evaporated and condensed before transfer to the GC column.

The integral structure of ether lipid **3** ($y=15$) was confirmed by the mass spectrum obtained through HT-GC-MS analysis (Fig. 3.8(B)). The base peak at m/z 513 results from cleavage of the bond between the oxygen-bearing carbon atoms. Two other major fragmentations are due to the loss of H_2O (m/z 762) and the loss of H_2O followed by loss of C_6H_{13} (m/z 677).

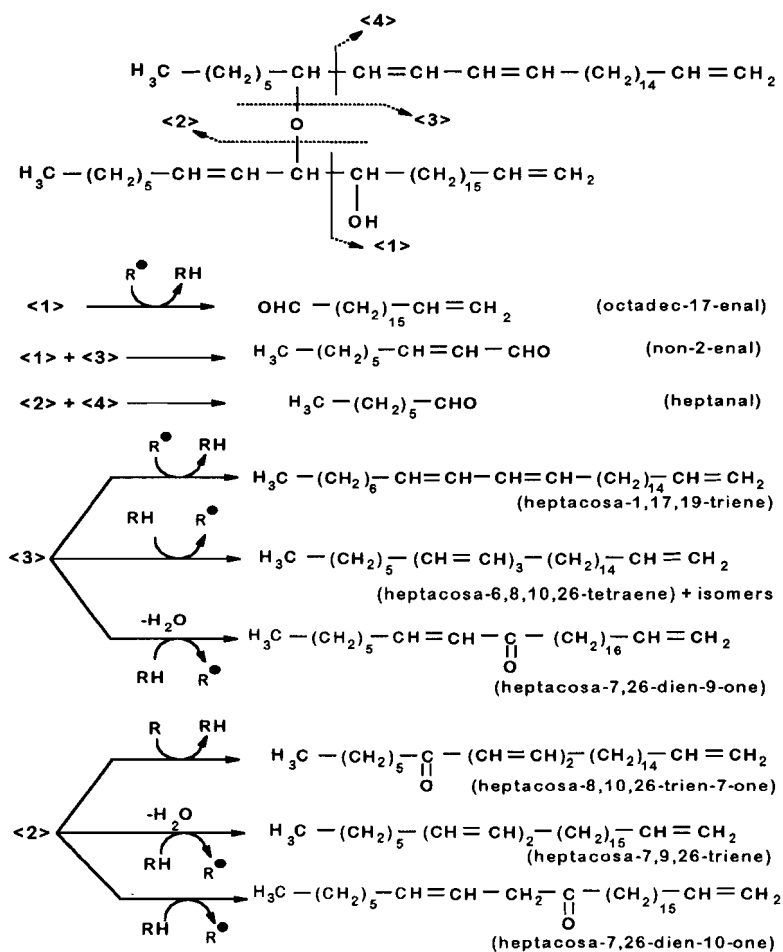


Fig. 3.9 Proposed mechanisms of pyrolysis for the formation of the major products found in the pyrolysate of compound **3**.

Apart from the alkanes, most of the other compounds encountered after pyrolysis of compounds **3** are true pyrolysis products. Fig. 3.9 rationalizes the formation of most of these pyrolysis products by assuming four major cleavages. The presence of the major product, octadec-17-enal is probably triggered by cleavage <1>. The radical formed can be stabilized as the aldehyde by an intermolecular H radical transfer. Non-2-enal and heptanal are produced by two successive bond cleavages: <1> + <3> and <2> + <4> generate non-2-enal and heptanal, respectively. Cleavages <2> and <3> lead to the formation of various C₂₇ compounds, most of them present in the pyrolysates. The introduction of unsaturations in the structures of these products induces the formation of various isomers of heptacosatriene and heptacosatetraene. Those represented in Fig. 3.9 are the products generated upon cleavage and H radical transfer sometimes in combination with loss of H₂O.

The mid-chain ketones indicated in Fig. 3.9 were identified by their relative retention times and their characteristic mass spectra. Their formation is rationalized by C-O cleavage <2> followed by a hydrogen abstraction and by C-O cleavage <3> followed by dehydration and H-radical addition. It should be noted that the position of the keto groups are in full agreement with the location of the ether linkages in compounds <3>.

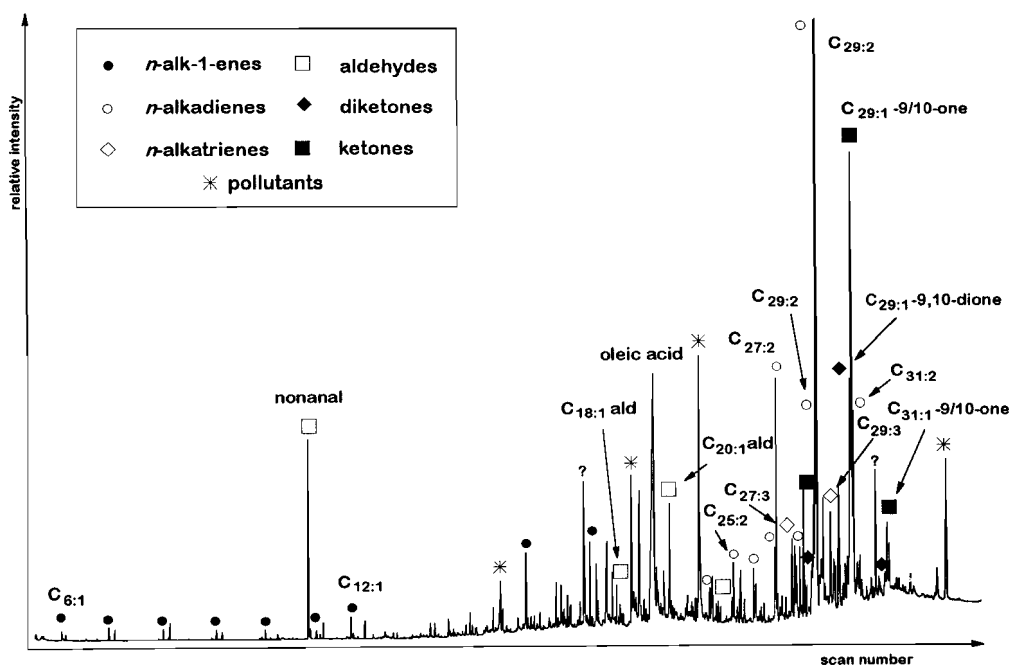


Fig. 3.10 Total ion current trace of the flash pyrolysate of compound **4** (Curie temp. 610°C).

Alkenyl-botryal ether lipids

The alkenyl-botryal ethers (compounds **4** in Fig. 3.1) were not amenable by HT-GC(MS) analyses due to their high molecular weight (> 1400 D) and probe-MS analyses failed to produce the molecular ion peaks (Metzger *et al.*, 1991). Therefore, studies of the condensed residue obtained after Py-GC experiments did not give any information concerning the efficiency of the pyrolysis. Although the probe mass spectrum of the condensed residue showed high abundances of peaks in the mass area of the botryal molecular ion peaks, it was not possible to establish if these peaks represented molecular ions of "botryal-like" compounds produced by pyrolysis of **4** or if they were fragment ions of the ether lipids **4** which were partly evaporated and condensed. Fig. 3.10 shows the TIC trace of the pyrolysate of compounds **4**.

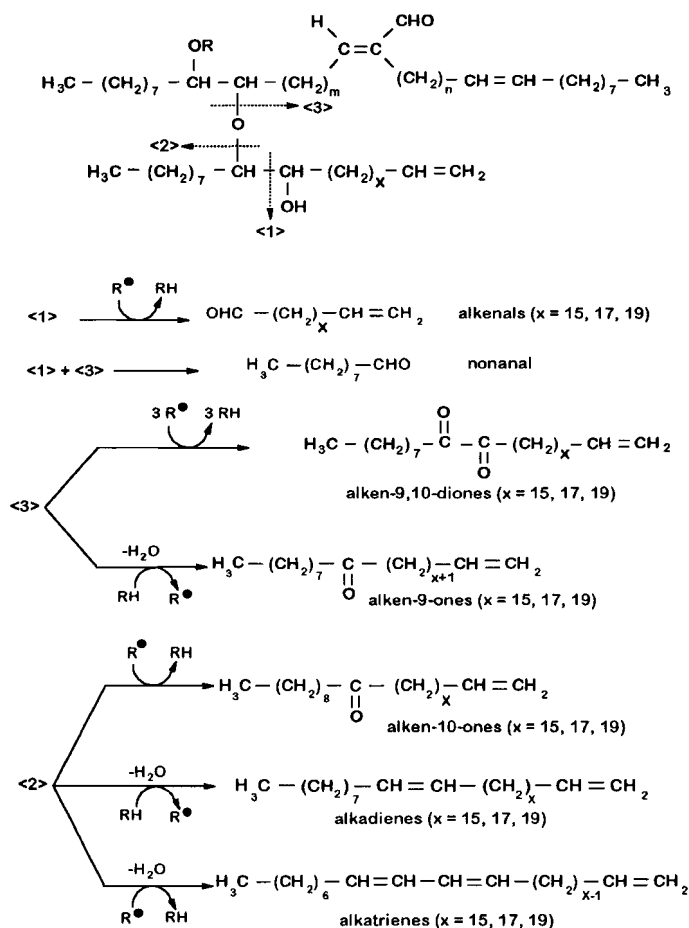


Fig. 3.11 proposed mechanisms of pyrolysis for the formation of some of the major products found in the pyrolysate of compounds **4**.

Oleic and palmitic acids, as discussed previously are thought to derive from a six-membered ring rearrangement triggered by the ester functionality (Gelin *et al.*, 1993). Expected cleavages near the ether bond obviously occurred and result in the formation of C_{27} , C_{29} and C_{31} compounds. However, based on the absence of even carbon numbered carbon compounds, it seems that no further pyrolysis of the botryal moieties occurred: almost all the compounds present in the pyrolysates represent the C_{27} , C_{29} and C_{31} alkyl moieties. The three cleavages leading to the formation of most of the pyrolysis products are shown in Fig. 3.11. Cleavage <1> followed by a H radical transfer explains the formation of the C_{18} , C_{20} , C_{22} ω -aldehydes and cleavages <1> + <3> may explain the genesis of nonanal. The formation of the alkadienes was probably induced by cleavage <3> followed by H radical transfers. The C_{27} , C_{29} and C_{31} alken-9-ones are generated *via* cleavage <3> followed by dehydration and an H-radical transfer. The major component in the pyrolysate, nonacosadiene, is probably produced by cleavage <2> and subsequent dehydration. This reaction sequence also explains the formation of C_{27} , C_{29} and C_{31} alken-10-ones and alkatrienes.

More detailed mechanisms of pyrolysis for the formation of these types of compounds and identifications of ketones and diketones are reported by Gelin *et al.* (1993).

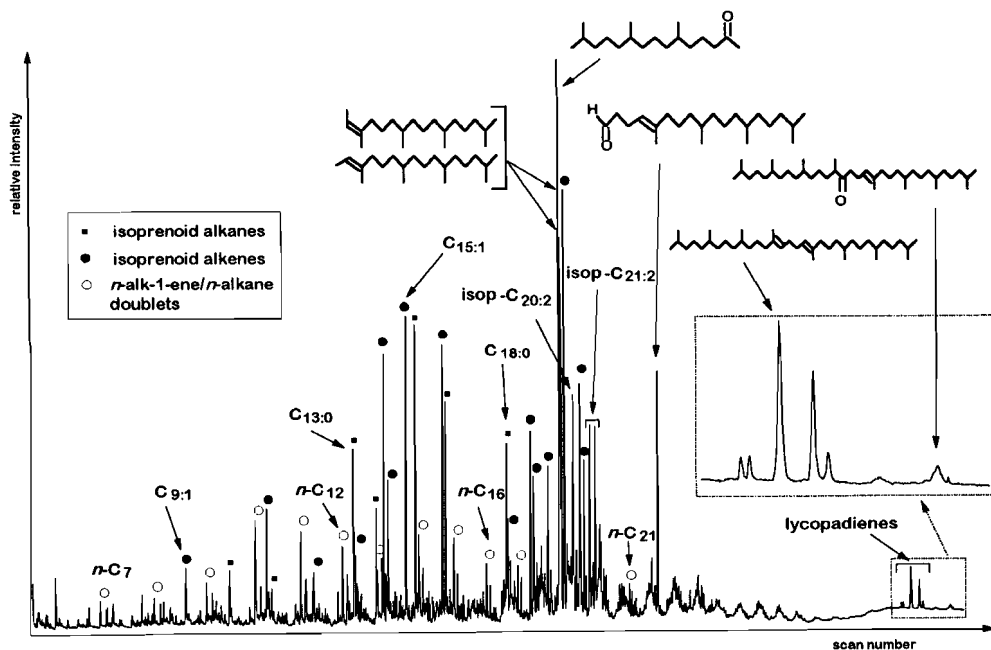


Fig. 3.12 TIC trace of the flash pyrolysate of PRB L (Curie temperature 610°C).

PRB L

The resistant biopolymer of *B. braunii* race L has been studied previously by spectroscopic methods and off-line pyrolysis experiments (Derenne *et al.*, 1989, 1990a). It was demonstrated that the structure of this macromolecule is mainly composed of C₄₀ isoprenoid units with the isoprenoid lycopane skeleton linked *via* ether bridges. However, a precise structure could not be proposed based on the results of these experiments.

The TIC trace of the flash pyrolysate of the PRB L showed several series of alkanes and alkenes (Fig. 3.12). *n*-Alkanes and *n*-alk-1-enes were present in relatively low amounts and ranged from C₇ to C₂₁. The occurrence of these two series seems to indicate that at least a small part of the PRB L consists of long, linear methylene chains similar to those found in the PRB of races A and B of *B. braunii*. The two major series of pyrolysis products are isoprenoid alkenes ranging from C₉ to C₂₁ and alkanes ranging from C₁₀ to C₁₈. Apart from these series, phyt-2-enes were found in relatively large amounts. The mass spectrum of the major product of the pyrolysate was indicative of 6,10,14-trimethylpentadecan-2-one. An other important carbonyl compound was the C₂₂ aldehyde whose spectrum showed a major fragment ion at *m/z* 98 (Fig. 3.13(A)). Similar fragmentations for γ -unsaturated aldehydes can be explained by a six-membered ring rearrangement involving the carbonyl. Fragmentations at M⁺-18, M⁺-43 and M⁺-44 confirmed the presence of the aldehyde moiety. Among the

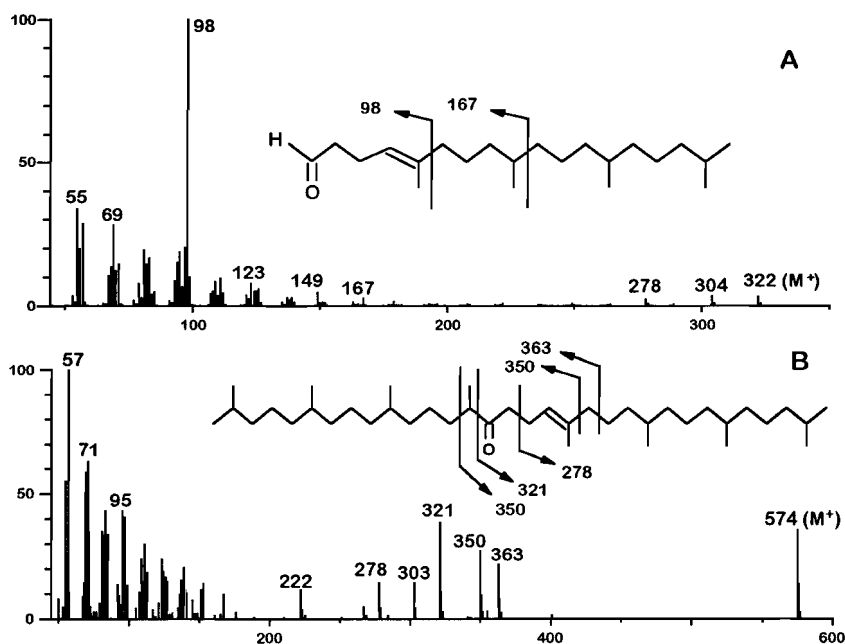


Fig. 3.13 Mass spectra of (A) 5,9,13,17-tetramethyloctadec-4-enal and (B) 2,6,10,14,19,23,27,31-octamethyldotriacont-14-en-18-one.

HMW pyrolysis products (Fig. 3.12, insert), alkadienes and unsaturated ketones with 40 carbons were identified. The structure of one of the C_{40} alkadienes indicated in Fig. 3.12 was determined in previous studies (Metzger and Casadevall., 1987). The positions of the double bonds in the other lycopadienes could not be determined by mass spectrometry. It should be noted that *B. braunii* race L produces only one hydrocarbon, a C_{40} isoprenoid lycopadiene which was identified as 2,6(R),10(R),14,19,23(R),27(R), 31-octamethyldotriaconta-14(E),18(E)-diene (Metzger and Casadevall, 1987). The C_{40} ketone identified was present in small amounts; Fig. 3.13(B) shows its mass spectrum. The structure indicated was determined by specific mass spectrometric fragment ions most likely derived from 2,6,10,14,19,23,27,31-octamethyldotriacont-14-en-18-one (Fig. 3.13(B)).

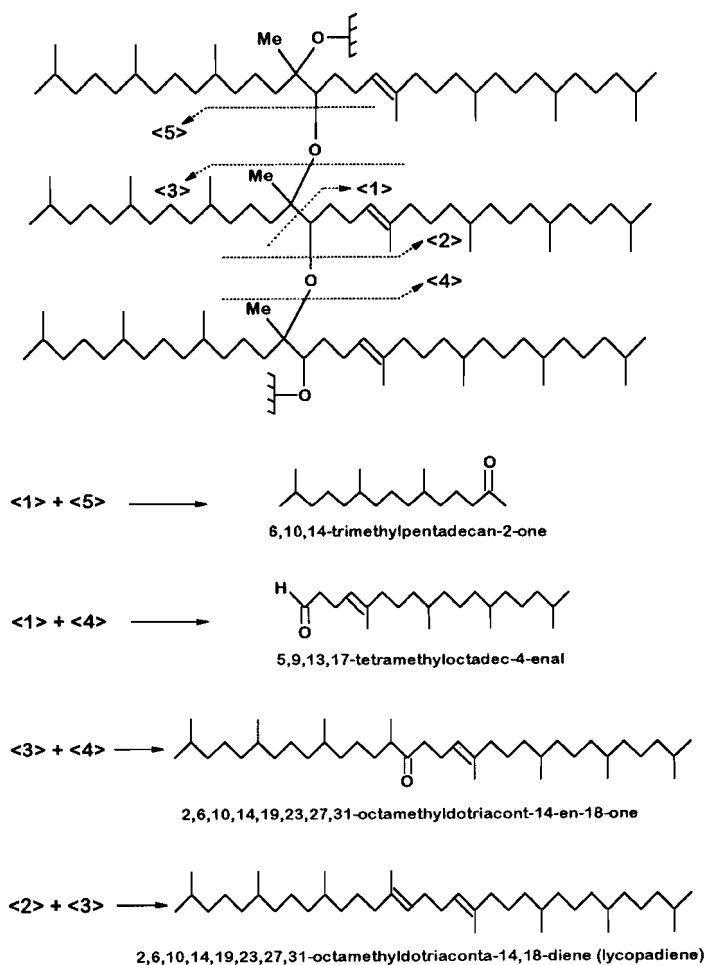


Fig. 3.14 Proposed structure for the major biopolymer of PRB L; dashed arrows indicate some major cleavages occurring upon pyrolysis leading to the formation of the indicated compounds.

The presence of the three oxygen-containing compounds and of lycopadienes described above strongly indicate that similar cleavages as those observed during pyrolysis of the ether lipids studied in this paper also occurred in PRB L. The positions of the ether bonds at C(14) and C(15) as indicated in Fig. 3.14 are supported by the generation of both the C₁₈ alkan-2-one and C₄₀ alken-15-one and the production of the C₂₂ aldehyde. A partial structure of the polymer composing the major part of the PRB L is proposed in Fig. 3.14. The five cleavages indicated nicely rationalize the formation of the four compounds already discussed. The clue to the reconstruction of the polymer structure proposed was the formation of the C₂₂ aldehyde *via* a pathway similar to that described for the formation of nonanal during the pyrolysis of compounds 4. The hypothetical formation of the C₄₀ alcohol with the hydroxyl group at the C(14) position would probably be followed by a dehydration, thus generating the lycopadienes.

It should be noted that the structure of PRB L proposed here and essentially based on mechanisms of Curie point pyrolysis of ether lipids is in full agreement with data obtained in other pyrolysis studies aiming to study changes of these type of polymers during burial in the earth under various temperature and time conditions (Behar *et al.*, 1995).

3.5 CONCLUSIONS

- 1) To interpret Py-GC and Py-GC-MS data of HMW lipids, it is a prerequisite to analyze constituents left behind in the pyrolysis unit to check on evaporation versus pyrolysis and to be alert on transfer problems from the pyrolysis chamber to the GC column.
- 2) HT-GC and HT-GC-MS are powerful methods of analyses of HMW lipids which appear to be thermostable.
- 3) Detailed investigations of pyrolysis mechanisms of well selected model compounds are needed to optimally benefit from pyrolytic analysis methods.
- 4) A detailed structure was proposed for a natural algal biopolymer partly based on flash Py-GC-MS analysis. To the best of our knowledge, it is the first time that a precise structure could be determined by this analytical method.

The similarity of chemical structures of soluble aliphatic polyaldehyde and insoluble algaenan in the green microalga *Botryococcus braunii* race A as revealed by analytical pyrolysis*

François Gelin, Jan W. de Leeuw, Jaap S. Sinninghe Damsté, Sylvie Derenne, Claude Largeau and Pierre Metzger

4.1 ABSTRACT

Curie point pyrolysis-gas chromatography-mass spectrometry studies of recently isolated CHCl_3 soluble aliphatic polyaldehyde and of an insoluble biopolymer, termed Bb(A) algaenan of the green microalga *Botryococcus braunii* (race A) were performed to determine the structural relationships between these two polymers. Comparisons of specific mass chromatograms and of the composition of three clusters of pyrolysis products with different chain lengths of pyrolysates of both materials clearly show major similarities in their chemical structures. According to these results, the molecular structure of Bb(A) algaenan is probably a more condensed and/or a reticulated form of the soluble aliphatic polyaldehyde. Furthermore, the results confirm that kerogens derived from these algae consist of mixtures of algaenan and polyaldehydes which have become insoluble due to oxygen cross-linking.

4.2 INTRODUCTION

The green microalga *Botryococcus braunii* race A biosynthesises high amounts of various types of specific lipids such as alkadienes, alkenylphenols, C_{52} - C_{64} aldehydes (botryals), epoxides and ether lipids (for a review, see Metzger *et al.*, 1991). The bulk of these lipids is located in its outer walls. These outer walls were thought to consist mainly of a highly aliphatic, insoluble and chemically resistant (non-hydrolysable) biopolymer termed PRB A (Berkaloff *et al.*, 1983; Largeau *et al.*, 1986). The term PRB A referred to the material isolated from *B. braunii* race A after subsequent extractions with hexane and methanol-chloroform (MeOH-CHCl_3) and chemical treatment of the extracted biomass to eliminate all hydrolysable constituents. Recently, it was observed, however, that further extraction with CHCl_3 alone allows further recovery of an additional

**Org. Geochem.* 21, 423 (1994)

soluble fraction. This fraction was shown to be almost entirely composed of a new class of macromolecular lipids, aliphatic polyaldehydes (Metzger *et al.*, 1993). The structure of the soluble aliphatic polyaldehyde (Fig. 4.1) was determined by IR and ^1H - and ^{13}C -NMR spectroscopy and *via* ozonolysis (Metzger *et al.*, 1993). It was also noted that as soon as these aliphatic polyaldehydes are subjected to air they cannot be redissolved in organic solvents. PRB A as isolated and examined in previous studies, thus comprised two fractions: (i) a native, insoluble macromolecular fraction and (ii) a soluble aliphatic polyaldehyde which became insoluble during biomass processing. Comparison of the molecular structures of these fractions is the subject of the present investigation.

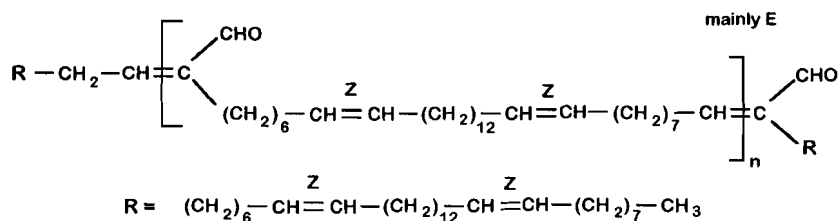


Fig. 4.1 Proposed structure of the aliphatic polyaldehyde (from Metzger *et al.*, 1993).

To avoid any confusion for the reader we will refer to the initially soluble fraction as "aliphatic polyaldehyde" and to the native insoluble fraction as *B. braunii* race A algaenan (Bb(A) algaenan). It should be noted that the general term algaenan is used for the non-hydrolysable, highly aliphatic insoluble biomacromolecules present in microalgal cell walls (Tegelaar *et al.*, 1989c, de Leeuw and Largeau, 1993).

To determine the origin of these two types of macromolecules, various feeding experiments with labelled oleic acid were performed recently. Experiments with $[1-^{14}\text{C}]$ and $[10-^{14}\text{C}]$ oleic acid suggested a biosynthesis of the aliphatic polyaldehyde by elongation followed by ω -oxidation of oleic acid forming a C_{32} diunsaturated α - ω -dialdehyde (Metzger *et al.*, 1993). *Via* a condensation pathway, this dialdehyde is further polymerised. Labelling experiments to establish the biosynthesis of PRB A also indicated that oleic acid plays a major role in the formation of Bb(A) algaenan (Laureillard *et al.*, 1988). It should be noted however that these experiments were performed without the CHCl_3 -extraction so that no firm conclusion can be drawn for the biosynthesis of the Bb(A) algaenan *sensu stricto*. Furthermore, other labelling experiments showed that oleic acid is also a major building block of most of the lipids present in the outer walls (Templier *et al.*, 1992a, 1993).

From a geochemical point of view, investigations of the structure of Bb(A) algaenan are important to better understand the molecular composition of kerogens derived from *B. braunii* alga. Recently, a study of a Coorongite sample (recent material formed by drying of algal biomass on the shorelines of lake Balkash, Russia) showed that this Coorongite was derived almost entirely from *B. braunii* A race deposits but that the selective preservation of Bb(A) algaenan was

not the only important mechanism involved in the formation of the kerogen (Gatellier *et al.*, 1993). High abundances of very specific pyrolysis products like C_{27} , C_{29} and C_{31} *n*-alk-1-en- ω^9 -ones and *n*-alk-1-en- ω^{10} -ones indicated that oxidative cross-linking of *B. braunii* lipids during the deposition under oxic conditions was an important process of Coorongite formation as well. Pyrolysis studies of ether lipids present in *B. braunii* outer walls also generated these specific compounds (Gelin *et al.*, 1993). As a result, the soluble high-molecular-weight lipids present in the living algae should be taken into account since their contribution to kerogens may be important.

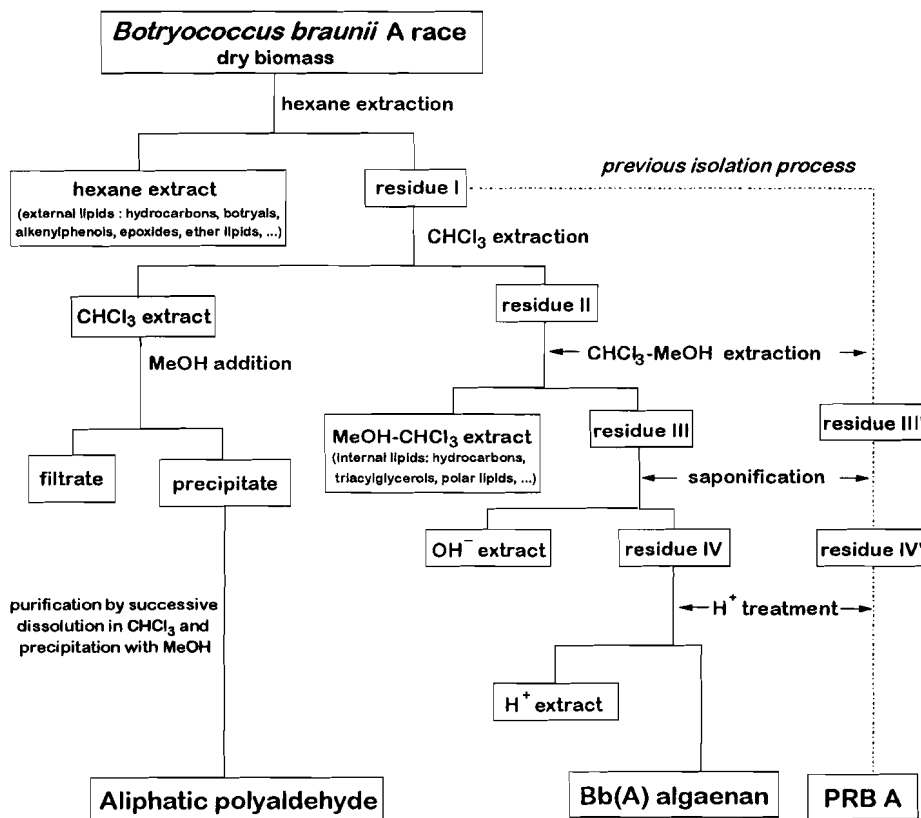


Fig. 4.2 Analytical flow diagram illustrating the isolation of the soluble aliphatic polyaldehyde and the insoluble Bb(A) algaenan. PRB A indicates the final residue (resistant biopolymer) previously reported (Berkaloff *et al.*, 1983; Largeau *et al.*, 1986), obtained without the $CHCl_3$ extraction.

To explore whether structural relationships existed between the aliphatic polyaldehyde and Bb(A) algaenan and to provide insight into the molecular structure of Bb(A) algaenan, a detailed comparison of the aliphatic polyaldehyde and of Bb(A) algaenan was performed by Curie point-pyrolysis-gas chromatography-mass spectrometry (Py-GC-MS).

4.3 EXPERIMENTAL

The aliphatic polyaldehyde and Bb(A) algaenan were obtained from a strain of *B. braunii* race A (culture collection of the University of Texas at Austin). The alga was grown under air lift conditions with air-enriched by 1% CO₂ (Metzger *et al.*, 1985). The procedure for the isolations of the aliphatic polyaldehyde and of Bb(A) algaenan is described in Fig. 4.2. Extraction and purification of the aliphatic polyaldehyde were carried out as recently described (Metzger *et al.*, 1993). Bb(A) algaenan was obtained after saponification (KOH/MeOH) and acid treatment with concentrated H₃PO₄ (Berkaloff *et al.*, 1983). Precautions were taken to prevent the oxidative transformation of the aliphatic polyaldehyde, since it has been observed that these macromolecules are very sensitive to exposure to air and/or light (Gelin *et al.*, 1994a). The two macromolecular fractions each accounted for *ca.* 5% of dry algal biomass.

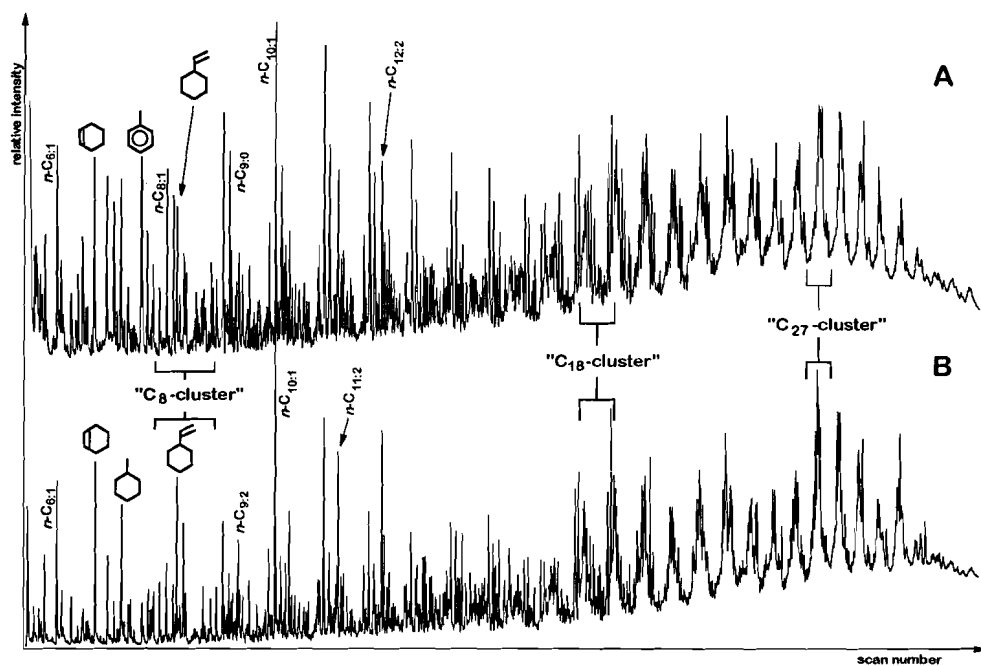


Fig. 4.3 Total ion current trace of the flash pyrolysate (Curie temperature 610°C) of (A) Bb(A) algaenan and (B) the aliphatic polyaldehyde. The structures of some of major compounds are indicated. The square brackets indicate the areas expanded in Fig. 4.4.

Py-GC-MS was performed on both samples. The Bb(A) algaenan sample was pressed on to flattened ferromagnetic wire. The aliphatic polyaldehyde sample, dissolved in CHCl₃, was directly applied to the wire and the CHCl₃ was allowed to evaporate under a N₂ atmosphere. The samples were pyrolysed by inductive heating of the ferromagnetic wires (Curie temperature 610°C for pyrolysis and

358°C for thermal extraction) for 10 s. The gas chromatograph (Hewlett Packard HP-5890) was equipped with a cryogenic unit and programmed from 0°C (5 min) to 320°C (10 min) at a rate of 3°C/min. Separation of the products was achieved by a 25 m fused silica capillary column coated with chemically bound CP-Sil 5 (0.32 mm I.D.; film thickness 0.45 µm). Helium was used as carrier gas and the temperature of the flame ionisation detector was 320°C. The column was coupled to the EI ion source of a VG-70s double focusing mass-spectrometer (mass range m/z 40-800; cycle time 1.8 s; ionisation energy 70 eV).

4.4 RESULTS

Py-GC-MS was performed with both biopolymers isolated following the procedure described in Fig. 4.2. The total ion current (TIC) traces of the pyrolysates (Fig. 4.3) are similar and show very complex mixtures of compounds. Most pyrolysis products are linear alkanes and alkenes. Oxygen-containing compounds are only present in low relative abundances. Pyrolysis products were identified based on their retention times and mass spectra. In some cases, comparisons were made with compounds identified earlier in these types of pyrolysates (Gatellier *et al.*, 1993, Hartgers *et al.*, 1992).

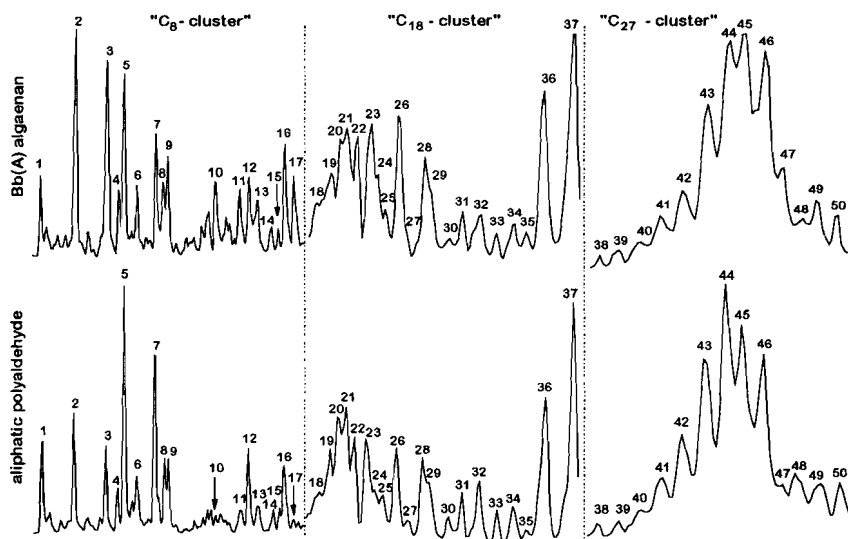


Fig. 4.4 Partial TIC traces of the flash pyrolysates of (A) Bb(A) algaenan and (B) the aliphatic polyaldehyde. " $C_{\#}$ -cluster" indicates the chain length of most of the products present in that cluster. Numbers refer to compounds listed in Table 4.1.

To compare both pyrolysates several clusters of pyrolysis products with different chain-lengths were investigated in detail (Fig. 4.4). Peak assignments

are given in Table 4.1. The relative intensities of the components identified in the corresponding clusters of both polymers are similar. Significant differences in the abundances of *n*-alkane, *n*-alk-1-ene and aromatic compounds are only observed between the C₈-clusters: a higher relative contribution of these compounds was observed in the Bb(A) algaenan pyrolysate. These differences were not observed in the C₁₈- and C₂₇-clusters which showed remarkable similarities. Several peaks in the C₁₈-cluster and all peaks in the C₂₇-cluster represent coeluting compounds. Consequently, not all compounds in these clusters could be identified unambiguously. It should be noted, however, that a very detailed comparison of the two biopolymers was nevertheless possible by comparison of the mass spectra corresponding to similar multicomponent peaks in both pyrolysates.

Table 4.1 Major compounds identified in "clusters" of the flash pyrolysates*

<i>C₈ cluster</i>	
1	<i>n</i> -octa-1,7-diene
2	<i>n</i> -oct-1-ene
3	<i>n</i> -octane
4	<i>n</i> -octene
5	ethenylcyclohexane
6	unknown components
7	<i>n</i> -octa-1,3-diene
8	ethylcyclohexane
9	<i>n</i> -propylcyclopropane
10	ethylbenzene
11	<i>m</i> - and <i>p</i> -xylene
12	ethylidene cyclohexane
13	1-ethylcyclohexane
14+15	ethenyl-methylcyclohexane
16	styrene
17	<i>o</i> -xylene + trace of <i>n</i> -heptan-2-one
<i>C₁₈ cluster</i>	
18	<i>n</i> -undecylbenzene
19-21	<i>n</i> -octadecadiene or cyclic C ₁₈ monounsaturated hydrocarbon
22	<i>n</i> -octadecene + <i>n</i> -octadecadiene
23+24	<i>n</i> -octadecene + trace of <i>n</i> -hexadecan-2-one
25	<i>n</i> -octadecadiene or cyclic C ₁₈ monounsaturated hydrocarbon
26	<i>n</i> -octadec-1-ene
27	<i>n</i> -octadecadiene or cyclic C ₁₈ monounsaturated hydrocarbon
28	<i>n</i> -octadecane
29	<i>n</i> -octadecene + <i>n</i> -octadecadiene
30	C ₁₈ :3 hydrocarbon
31	C ₁₈ :2 hydrocarbon
32	<i>n</i> -octadecadiene + phthalate
33	C ₁₈ :3 + C ₁₈ :2 hydrocarbons
34	C ₁₈ :3 hydrocarbon
35	C ₁₈ :3 + C ₁₈ :2 hydrocarbons
36	<i>n</i> -dodecenylcyclohexane + C ₁₉ :2 hydrocarbon
37	<i>n</i> -dodecylcyclohexane + <i>n</i> -tridecycyclopentane + C ₁₉ :2 hydrocarbon
<i>C₂₇ cluster</i>	
38-41	mixture of C ₂₆ and C ₂₇ hydrocarbons
42	C ₂₆ :2 + C ₂₆ :3 + C ₂₇ :3 hydrocarbons
43	C ₂₇ :2 hydrocarbons + unknown components
44	C ₂₆ :2 + C ₂₇ :2 + C ₂₇ :3 hydrocarbons
45	C ₂₇ :2 hydrocarbons + unknown components
46	C ₂₆ :2 + C ₂₇ :1 + C ₂₇ :2 hydrocarbons
47+48	mixture of C ₂₆ and C ₂₇ hydrocarbons
49	<i>n</i> -heptacos-1-ene + C ₂₇ :3 + C ₂₇ :4 hydrocarbons
50	<i>n</i> -heptacosane + C ₂₇ :2 + C ₂₇ :3 hydrocarbons

*numbers refer to Fig. 4.4

To further substantiate the similarities between the pyrolysates, mass chromatograms reflecting several homologous series of pyrolysis compounds were generated. Homologous series of *n*-alkanes and *n*-alk-1-enes are revealed by mass chromatograms of m/z 57 (Fig. 4.5). Both pyrolysates show similar chain-lengths distributions and both series extend up to C_{31} and dominate the pyrolysates up to C_{16} for the algaenan and in the C_{10} - C_{12} range for the aliphatic polyaldehyde. Two major differences can be observed: (i) The relative intensities of the *n*-alkanes and *n*-alk-1-enes ranging from C_{15} to C_{31} vary with respect to the other pyrolysis products and (ii) the relative intensities of the C_{16} , C_{18} and C_{20} *n*-alkanes are higher in the pyrolysate of the aliphatic polyaldehyde. The latter observation is explained by a thermal evaporation experiment using a wire with a Curie point temperature of 358°C which proved that these compounds were partially present in the CHCl_3 -extract as such.

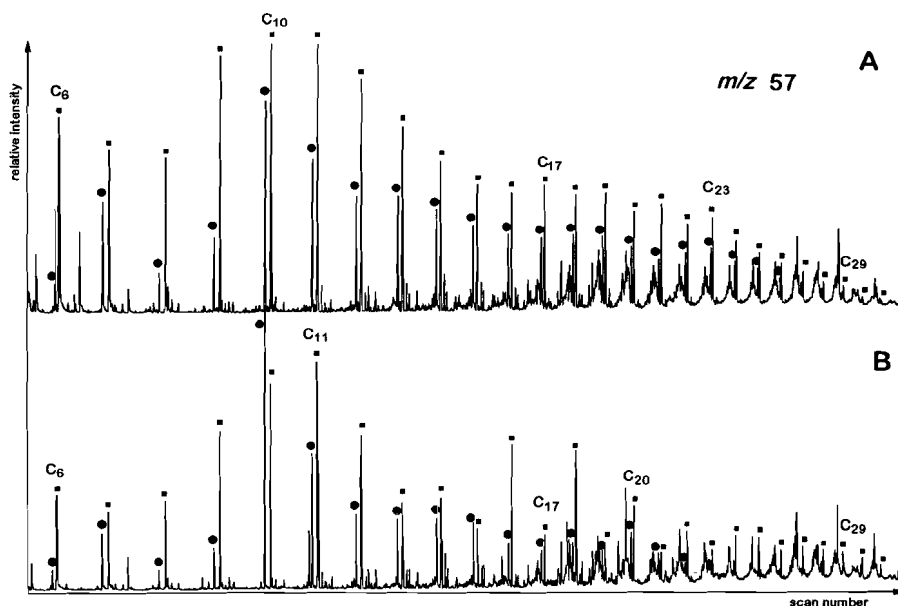


Fig. 4.5 Mass chromatogram of m/z 57 revealing the distribution of *n*-alkanes (■) and *n*-alk-1-enes (●) in the flash pyrolysates of (A) Bb(A) algaenan and (B) the aliphatic polyaldehyde.

Two homologous series of linear alkadienes were also present. *n*-Alka-1,3-dienes were identified based on reference mass spectra and are characterised by a base peak at m/z 54. Mass chromatograms of m/z 54 reveal a series ranging from C_7 to C_{20} and maximising at C_8 (Fig. 4.6). The two traces demonstrate once again the similar composition of both pyrolysates. Linear α - ω -alkadienes, also maximising at C_8 and eluting before the *n*-alk-1-enes, are also present in similar relative abundances and distributions in both pyrolysates.

Fig. 4.7 shows *n*-alkylcyclohexane and *n*-alkene distributions by means of mass chromatograms of m/z 83. The distribution of these compounds is similar in

both pyrolysates and range from C₆ to C₂₀ maximising at C₁₈ in case of the *n*-alkylcyclohexane series.

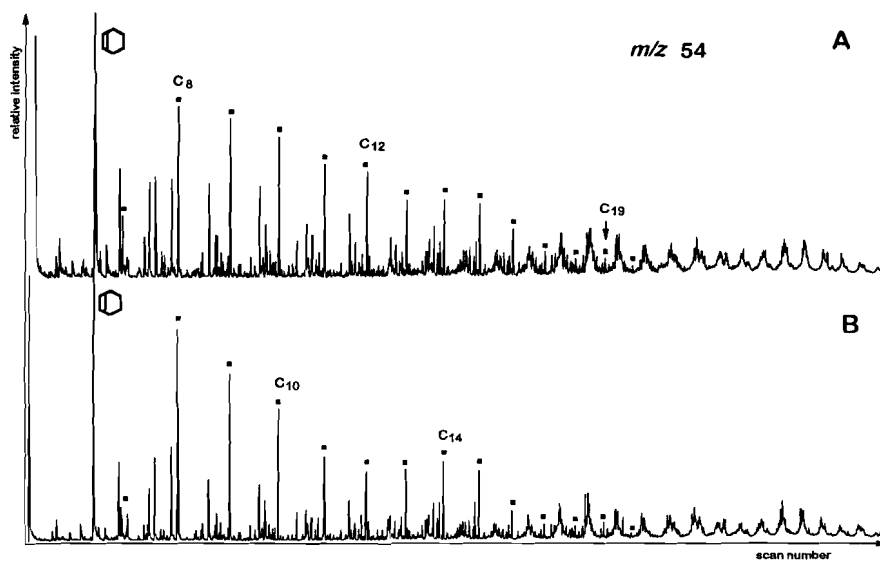


Fig. 4.6 Mass chromatogram of m/z 54 revealing the distribution of *n*-alka-1,3-dienes (■) in the flash pyrolysates of (A) Bb(A) algaenan and (B) the aliphatic polyaldehyde.

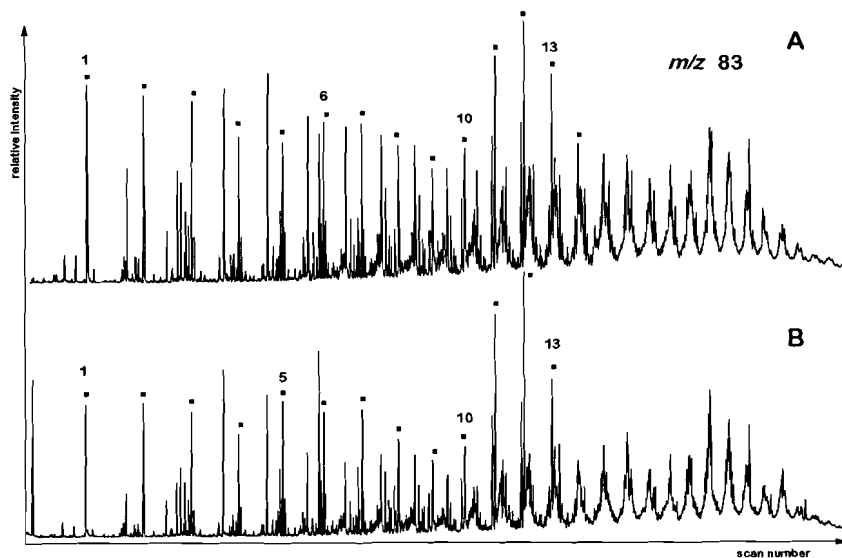


Fig. 4.7 Mass chromatogram of m/z 83 revealing the distribution of *n*-alkylcyclohexane (■) in the flash pyrolysates of (A) Bb(A) algaenan and (B) the aliphatic polyaldehyde. Numbers indicate the length of the alkyl chains.

The relative abundances of alkylated benzenes are different in the two pyrolysates. These compounds are trace components in the aliphatic polyaldehyde pyrolysate and significant components in the C_7 - C_{18} range of the Bb(A) algaenan pyrolysate. They are dominated by *n*-alkylbenzenes and *ortho-n*-alkyltoluenes as revealed by the summed mass chromatogram of m/z 78+91+92+105+106+119+120 (Fig. 4.8), both related to linear precursors, which is consistent with earlier findings (Douglas *et al.*, 1991; Derenne *et al.*, 1990b).

Examination of the oxygen-containing pyrolysis products indicates the presence of series of linear alkan-2-ones with decreasing relative intensities ranging from C_3 to C_{24} , saturated carboxylic acids ranging from C_2 to C_{18} and maximising at C_{16} and oleic acid in very low abundances in the Bb(A) algaenan pyrolysate and in trace amounts in the aliphatic polyaldehyde pyrolysate. *n*-Heptan-2-one and *n*-hexadecan-2-one are reported in trace amount in the C_8 - and C_{18} -clusters, respectively (Table 4.1). Mid-chain ketones are only present at C_{27} and C_{29} as *n*-alk-1-en- ω^9 -ones and *n*-alk-1-en- ω^{10} -ones in similar (low) relative intensities in both pyrolysates. The latter compounds are identified based on previously reported mass spectra and retention times (Gatellier *et al.*, 1993).

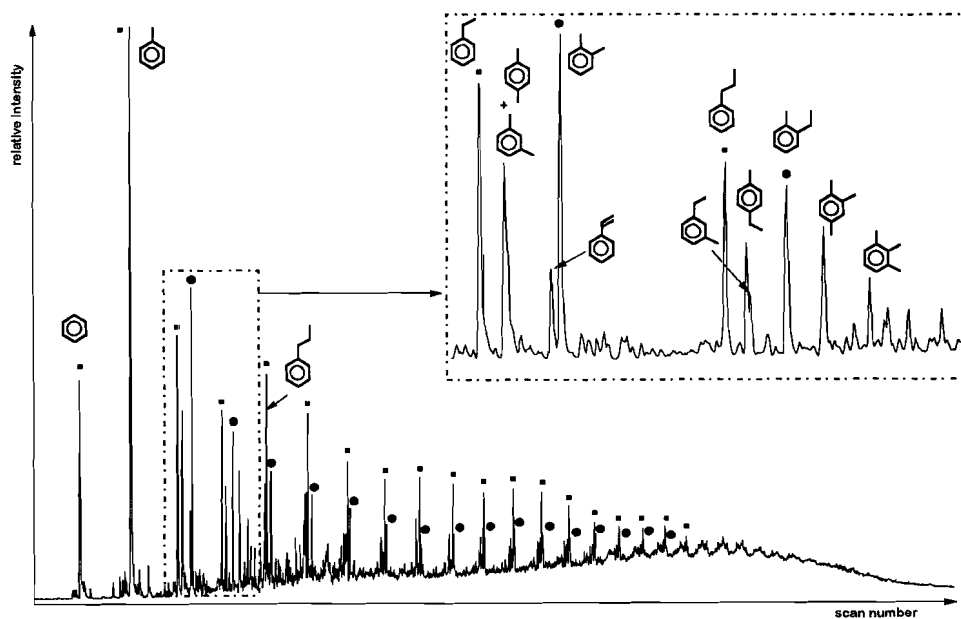


Fig. 4.8 Mass chromatogram of m/z 78+91+92+105+106+119+120+133+134 revealing the distribution of *n*-alkylbenzenes (■) and *ortho-n*-alkyltoluenes (●) in the flash pyrolysate Bb(A) algaenan. The insert shows the distribution of the C_2 - C_3 alkylated benzenes.

4.5 DISCUSSION

No pyrolysis products containing the aldehyde moiety of the aliphatic polyaldehyde were detected in either pyrolysates. However, such products were also absent in pyrolysates of botryals and alkenyl-*O*-botryal ether-lipids which contain similar aldehyde moieties (Gelin *et al.*, 1994a). Furthermore, a pyrolysis study of a Coorongite sample which revealed the presence of cross-linked lipids of *B. braunii* race A did not reveal the presence of aldehyde moieties (Gatellier *et al.*, 1993).

The formation of several series of pyrolysis products can be rationalised based on the structure proposed for the aliphatic polyaldehyde. The abundance of cyclic products found in the C₈-cluster and in general among the low-molecular-weight compounds can be explained by rearrangements of linear alkyl radicals generated upon pyrolysis. *n*-Decane, a predominant *n*-alkane of both pyrolysates, can be rationalised by allylic cleavages of the central polymethylene chain as indicated in the structure shown in Fig. 4.1. However, the presence of C₁₀₊ *n*-alkanes is difficult to explain in view of the structure proposed and suggests a small contribution of compounds with longer saturated polymethylene chains.

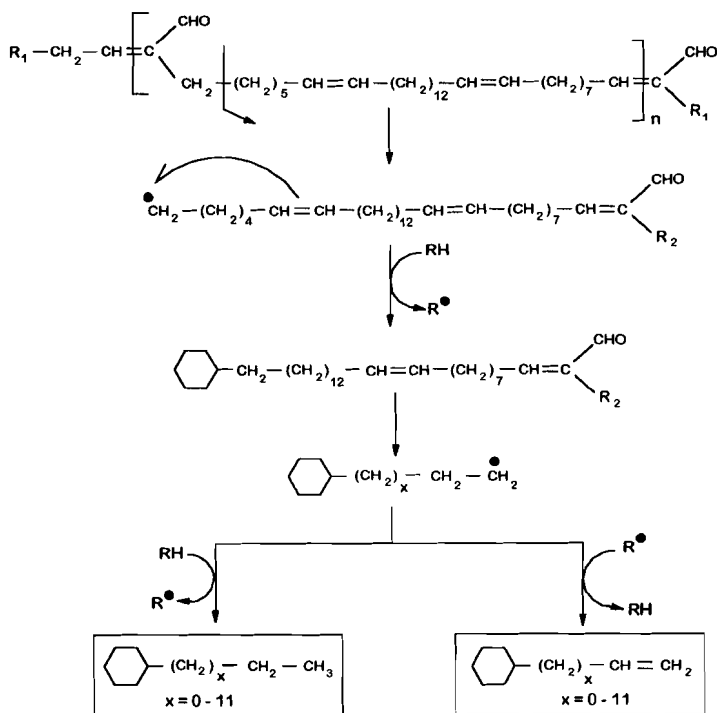


Fig. 4.9 Proposed mechanism of pyrolysis for the formation of *n*-alkylcyclohexanes and *n*-alkenylcyclohexanes from the proposed structure of the aliphatic polyaldehyde (Fig. 4.1).

The presence of *n*-alkylcyclohexanes can be rationalised by allylic cleavage followed by cyclisation during pyrolysis of the aliphatic polyaldehyde. A mechanism of pyrolysis for the formation of *n*-alkylcyclohexanes up to C₁₉ is proposed in Fig. 4.9. Their unsaturated counterparts are tentatively identified as well (Table 4.1, peak 36 for the dodecenylcyclohexane). *n*-Alkylcyclohexanes have been commonly observed in crude oils and sediments (Dong *et al.*, 1993) and in pyrolysates of Torbanites (Allan *et al.*, 1980, Largeau *et al.*, 1986) and Kukersites (Derenne *et al.*, 1990b). It has been suggested that the cyclohexyl units were already present as such in the unheated kerogens (Dong *et al.*, 1993). However, according to the similarities observed in the *m/z* 83 mass chromatograms of both pyrolysates, and assuming the formation of these cyclohexyl compounds as described above, these moieties are probably absent as such in the molecular structure of Bb(A) algaenan.

The relatively higher abundance of aromatic compounds in the Bb(A) algaenan pyrolysate can be explained either by their presence as such in the native algaenan or by the drastic chemical treatments applied on the extracted residue preceding its isolation, which could cause the genesis of some aromatic units. However, the similar distributions and relative abundances of aromatic compounds in the pyrolysates of the residue obtained with and without (res IV in Fig. 4.2) acid treatments rules out the latter explanation. It should be noted that the aromatic compounds, except for toluene and styrene, are only minor products in both these pyrolysates.

The striking similarities observed can only be explained by assuming the presence of identical moieties in both polymeric structures. The presence of C₂₇ and C₂₉ *n*-alk-1-en- ω ⁹-ones and *n*-alk-1-en- ω ¹⁰-ones in both pyrolysates indicates that a small amount of other lipids is cross-linked to both macromolecules. The alkan-2-ones are also thought to reflect thermal cleavage of ether bridges (Largeau *et al.*, 1986, Gatellier *et al.*, 1993). The fatty acids present in the pyrolysates are probably due to the presence of ester moieties which are not saponified due to a steric protection in the three-dimensional network.

In conclusion we may speculate that the aliphatic polyaldehyde and Bb(A) algaenan essentially contain the same building blocks but differ only by the degree of cross-linking and/or the degree of condensation.

Previous studies on PRB A, *i.e.* the insoluble non-hydrolysable material obtained without prior elimination of aliphatic polyaldehydes, have led to substantial overestimations (a factor 2) of the level of algaenan in *B. braunii* race A. Due to the chemical similarities observed between aliphatic polyaldehydes and Bb(A) algaenan, we feel that PRB A analyses have provided, however, relevant informations on the chemical structure of the native algaenan. The present observations are also consistent with the tight chemical correlations previously noted between PRB A and immature Torbanite (Largeau *et al.*, 1986). Indeed the latter kerogen can now be viewed as chiefly derived from the selective preservation of two macromolecular constituents: (i) native insoluble algaenan and (ii) insoluble material diagenetically derived from soluble aliphatic polyaldehydes.

4.6 CONCLUSIONS

Comparison of two biopolymeric fractions of *B. braunii* race A, *i.e.* Bb(A) algaenan and aliphatic polyaldehydes by flash pyrolysis, shows that the chemical structure of the insoluble Bb(A) algaenan is similar to the structure of the soluble aliphatic polyaldehydes. These results also confirm that the previously substance termed PRB A, which was thought to be a highly resistant biomacromolecule derived from *B. braunii* and selectively preserved in sediments, is actually composed of Bb(A) algaenan and slightly transformed aliphatic polyaldehydes. The latter become insoluble after exposure to air and chemical treatments. Consequently, this study yields new information concerning the chemical structure of kerogens predominantly derived from *B. braunii* algae.

Novel, resistant microalgal polyethers: An important sink of organic carbon in the marine environment?*

François Gelin, Ilco Boogers, Anna A. M. Noordeloos, Jaap S. Sinninghe Damsté, Patrick G. Hatcher and Jan W. de Leeuw

5.1 ABSTRACT

Five out of seven marine microalgal species investigated were found to biosynthesize non-hydrolysable, mainly aliphatic, biomacromolecules (algaenans). The molecular structure of the algaenan isolated from the microalgae *Nannochloropsis salina* of the class Eustigmatophyceae was determined by solid state ^{13}C NMR spectroscopy, Curie point pyrolysis-gas chromatography-mass spectrometry and chemical degradations with HI and RuO_4 . The structure is predominantly composed of C_{28} - C_{34} linear chains linked by ether bridges. The algaenan isolated from a second eustigmatophyte (*Nannochloropsis* sp.) was structurally similar. Algaenans isolated from two chlorophytes also possess a strongly aliphatic nature, as revealed by the dominance of alkenes/alkanes in their pyrolysates. Accordingly, we propose that the aliphatic character of numerous Recent and ancient marine kerogens reflects selectively preserved algaenans and that these algaenans may act as a source of *n*-alkanes in marine crude oils.

5.2 INTRODUCTION

A wide variety of novel, insoluble, non-hydrolysable aliphatic biomacromolecules has recently been isolated from several lacustrine and terrestrial primary producers. These macromolecules have been recognised as algaenans in common, ubiquitous fresh-water green microalgae (Philp and Calvin, 1976; Berkaloﬀ *et al.*, 1983; de Leeuw *et al.*, 1991; Derenne *et al.*, 1992b; de Leeuw and Largeau, 1993), as cutans and suberans in higher plant cuticles (Nip *et al.*, 1986; Tegelaar *et al.*, 1989a) and periderm tissue (Collinson *et al.*, 1994), respectively, as tegmens in inner seed coats of fresh-water plants (van Bergen *et al.*, 1994), as sporopollenins in spores and pollen grains (Guilford *et al.*; 1988; Hemsley *et al.*, 1993) and as polycadinenes in resins (van Aarssen *et al.*, 1990). Because of their chemical stability and their resistance against bacterial decay,

* Accepted in *Geochim. Cosmochim. Acta*

these macromolecules are selectively preserved (Zeliber *et al.*, 1988; Nip *et al.*, 1989) and make up a significant part of organic carbon in non-marine sediments ranging in age from Recent to over 300 million years. They eventually can act as the source of high-wax crude oils upon burial and thermal cracking (Tegelaar *et al.*, 1989b). Similarly, it has been proposed that the bulk of *marine* sedimentary organic matter (OM) derives from marine algaenans (Tegelaar *et al.*, 1989c), but evidence for that has been rather circumstantial (Hatcher *et al.*, 1983; Derenne *et al.*; 1992c) and the existence of a marine algaenan was only shown for an uncommon monospecific chlorophyte (Derenne *et al.*, 1992a). Accordingly, the possible occurrence of algaenans in five common marine green microalgae (Chlorophyceae) and two marine microalgae of the class Eustigmatophyceae has now been investigated.

5.3 EXPERIMENTAL

Culture conditions - All strains were obtained from the Culture Collection of the Natural Environment Research Council (U.K.). Algae were grown in batch cultures [in a medium described in Veldhuis and Admiraal (1987)] in a light/dark cycle of 16/8 h at 15°C. Cultures were kept axenic. Algaenans were isolated from the dry algal biomass by ultrasonic extraction with different organic solvents and by successive hydrolyses with KOH, HCl and H₂SO₄. Extracts, saponified extracts and organic fractions isolated after the KOH and HCl hydrolyses of the extracted algal biomass were analysed by GC and GC-MS.

Solid state ¹³C NMR - The NMR spectrum was obtained at a ¹³C frequency of 25.2 MHz using cross polarization with magic-angle spinning. Pertinent experimental parameters are the following: contact time = 1 ms, pulse delay = 1 sec, acquisition length = 0.5 K and line broadening = 30 Hz. The chemical shift scale is referred to tetramethylsilane at 0 ppm.

Curie point pyrolysis-gas chromatography-mass spectrometry - Samples were pyrolysed using a FOM-4LX Curie point pyrolysis unit directly coupled to a Hewlett Packard 5890 series II gas chromatograph fitted with a 25 m x 0.32 mm CP-Sil 5 (film thickness 0.12 µm) fused silica capillary column, temperature programmed from 0°C to 320°C (hold time 10 min) at a rate of 3°C/min. Structural assignments were made based on MS and retention time data. MS conditions: VG Autospec Ultima instrument, ionization energy 70 eV, mass range 40-800, cycle time 1.8 s.

Chemical degradations - Oxidation with RuO₄ followed the procedure described by Boucher *et al.* (1990). The acid products were derivatized with diazomethane to form methylester derivatives.

Treatment with hydroiodic acid (HI) followed the procedure described by Panganamala *et al.* (1971). Iodide was displaced with sodium methyl thiolate in methanol for 18 h at room temperature to obtain thiomethyl ethers. The thiomethylether derivatives show a highly characteristic fragmentation pattern upon GC-MS analyses (Carlson *et al.*, 1989).

Table 5.1. Summary of the presence and nature of algaenans in the microalgae investigated.

Name	Algaenan*	Main series of pyrolysis products of algaenan †				Chemical nature
		alk-1-enes/ alkanes	alkan-2-ones, mid- chain ketones II	alkyl- benzenes	alkyl- phenols	
<i>Brachiomonas submarina</i>	-- ‡		--			--
<i>Chlorella spaerckii</i>	1.2	C ₇ -C ₄₁ (C ₁₄)	C ₇ -C ₂₂ (C ₁₉)	C ₆ -C ₁₀ (C ₇)	C ₆ -C ₉ (C ₇)	aliphatic/ aromatic
<i>Chlorococcum</i> sp.	1.0	C ₇ -C ₃₄ (C ₂₆)	C ₇ -C ₂₆ (C ₁₉)	C ₆ -C ₁₀ (C ₇)	C ₆ -C ₉ (C ₇)	aliphatic/ aromatic
<i>Nannochloris</i> sp.	~1	--	--	C ₆ -C ₁₀ (C ₇)	C ₆ -C ₉ (C ₇)	aromatic
<i>Stichococcus bacillaris</i>	-- ‡		--			--
<i>Nannochloropsis salina</i>	1-2 ‡	C ₇ -C ₃₆ (C ₁₆ , C ₂₈)	C ₇ -C ₂₂ (C ₁₈ , C ₁₉) C ₂₀ -C ₃₄ (C ₂₈)	C ₆ -C ₂₂ (C ₇)	--	aliphatic
<i>Nannochloropsis</i> sp.	1.5	C ₇ -C ₃₃ (C ₁₆ , C ₂₆)	C ₇ -C ₂₆ (C ₁₉) C ₂₂ -C ₃₂ (C ₂₆)	C ₆ -C ₂₂ (C ₇)	--	aliphatic

* In % of the dry algal biomass. † Carbon number range of the indicated series of the algaenans pyrolysis products. The maxima are indicated in brackets. ‡ The entire biomass was dissolved after HCl hydrolysis. § The range indicated reflect 3 different batch cultures of this alga. II Series of mid-chain *n*-alkanones (only present in the pyrolysates of the *Nannochloropsis* algaenans) are indicated below the series of *n*-alkan-2-ones.

5.4 RESULTS AND DISCUSSION

Freeze-dried algal cells, obtained from axenically grown batch cultures, were extracted and the residues were treated with base (KOH) and acids (HCl and H₂SO₄) to remove free lipids, ester-bound lipids, proteins and carbohydrates, respectively. These treatments afforded 1-2% of an insoluble residue, *i.e.* algaenan, in the case of three chlorophytes, *Chlorella spaerckii*, *Chlorococcum* sp. and *Nannochloris* sp., and the eustigmatophytes *Nannochloropsis* sp. and *Nannochloropsis salina* (Table 5.1). The algaenan of the latter alga was analysed by solid state ¹³C NMR (Fig. 5.1). The chemical shift maximizing at 33 ppm indicates the highly aliphatic nature of this algaenan since at least 95 % of the NMR response is represented by this chemical shift of CH₂ moieties.

The results of pyrolysis-gas chromatography-mass spectrometry (Py-GC-MS) of this algaenan are in full agreement with the NMR data. The pyrolysate of *N. salina* algaenan (Fig. 5.2A) is strongly dominated by homologous series of C₇ to C₃₆ *n*-alkanes and *n*-alk-1-enes maximizing at C₁₆ and C₂₈, revealing the presence of long polymethylenic moieties in its algaenan. Series of ketones identified as coeluting *n*-alkan-17-ones* and *n*-alkane-18-ones with up to 34 carbon atoms (Fig. 5.2B) indicate the presence of oxygen functionalities mainly at the C-17 and C-18 positions and the maximum carbon chain length, *i.e.* 34 carbon atoms, of the building blocks of the macromolecules. The presence of such oxygen functionalities was confirmed by the highly specific distribution patterns of *n*-alkan-2-ones which maximize at C₁₈ and C₁₉ (Fig. 5.2B). The additional occurrence of mono-unsaturated mid-chain ketones with the unsaturation located

* The nomenclature used for the mid-chain ketones is purposely not correct and should be, for example, C₃₀ alkan-13- and alkan-14-ones. The reason for using such numbering is due to the common, specific positions of the keto group for all the mid-chain ketones.

in the shortest alkyl chain suggests the presence of another functionality, probably located at the first carbon atom. Based on earlier pyrolysis studies with model compounds and algaenans derived from fresh-water microalgae, it is concluded that both functionalities represent ether linkages (Gelin *et al.*, 1993,1994a). This is confirmed by the presence of a small but recognizable peak for alkyl-O carbons in the ^{13}C NMR spectrum at approximately 70 ppm (Fig. 5.1).

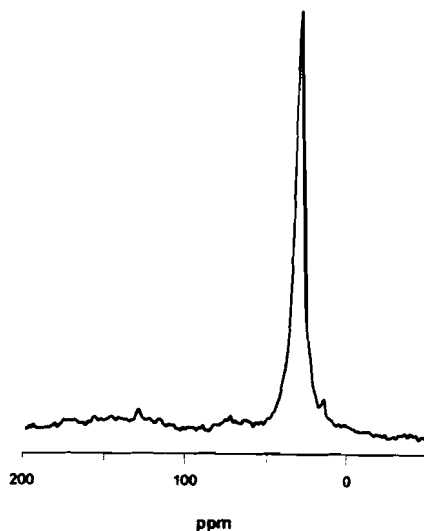


Fig. 5.1 Solid state ^{13}C NMR spectrum of *N. salina* algaenan. The large peak at 33 ppm is assigned to long-chain polymethylenic structures, the peak at 15 ppm to methyl groups, the broad region between 50 and 90 ppm is due to O-bound alkyl carbons, the region between 100 and 160 ppm corresponds to sp^2 carbons, and the broad resonance between 160 and 180 ppm is assigned to carbonyl or amide carbons.

Chemical degradation of the *N. salina* algaenan with ruthenium tetroxide (RuO_4) further supports the presence of ether bonds at the ω -17 or ω -18 positions and likely indicates ether bonds at the C-1 position as indicated by the generation of C_{24} - C_{34} ω -17- and ω -18-keto-alkanoic acids (Fig. 5.3A). A series of C_{24} - C_{34} ω -17,18 -diketo-alkanoic acids was also produced by RuO_4 oxidation of this algaenan and reveals the presence of three ether linkages located at the C-1, ω -17 and ω -18 positions of the polymethylenic carbon chains (Fig. 5.3B). The third functionality is probably involved in cross-linking so that a three-dimensional

network is built up, helping to explain the insolubility of the algaenan. The C₈-C₁₈ *n*-alkanedioic and C₁₂-C₁₈ *n*-alkanoic acids which represent the major products of the RuO₄ degradation result from mid-chain oxidations at the vicinal ether positions (Figs. 5.3C,D). The long-chain fatty acids, maximizing at C₂₉, probably result from the oxidation of ether-linked alkyl moieties. The prevalence of ether-linked long-chain alkyl units in the *N. salina* algaenan structure was further demonstrated by the release of, predominantly, 1,ω-17- and 1,ω-18-C₂₈-C₃₆ diiodo-alkanes after hydroiodic acid treatment, known to selectively cleave ether bonds (Panganamala *et al.*, 1971).

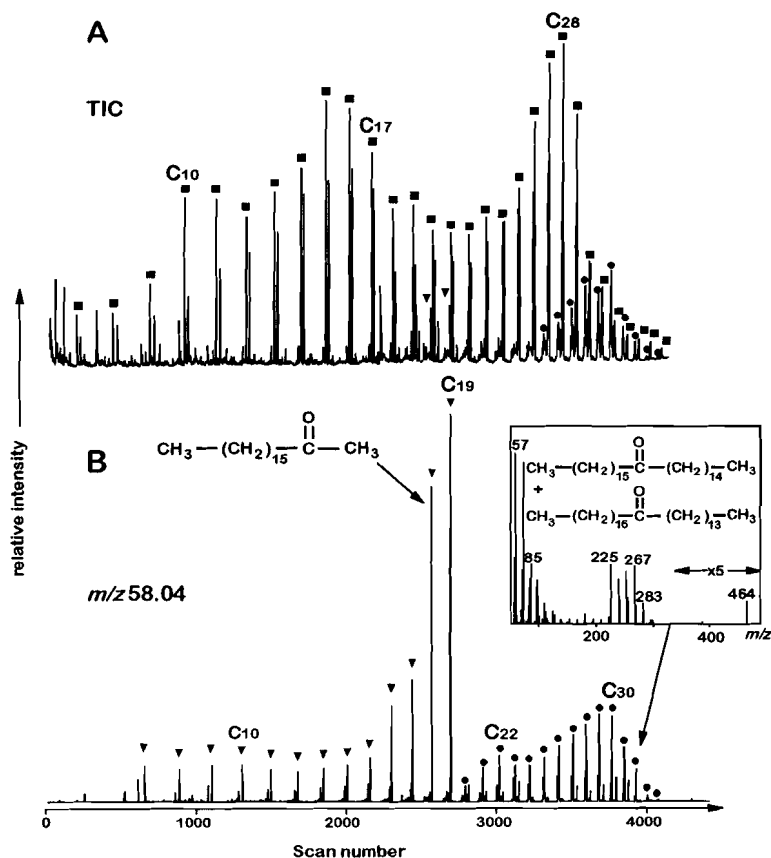


Fig. 5.2 Analysis of *N. salina* algaenan by Curie-point pyrolysis-gas chromatography-mass spectrometry; (A) total ion current trace (TIC) and (B) mass chromatograms of *m/z* 58.04 revealing the distribution of ketones. Filled squares indicate the *n*-alk-1-ene/*n*-alkane doublets, filled triangles indicate the *n*-alkan-2-ones and filled circles indicate the mid-chain ketones. Numbers indicate the total numbers of carbon atoms. The insert in the bottom figure shows the mass spectrum of the coeluting C₃₂ alkan-15- and -16-ones, identified based on MS data from previous studies (de Leeuw *et al.*, 1981; Gatellier *et al.*, 1993).

Pyrolysis of the algaenan of *Nannochloropsis* sp. showed very similar distributions of alkenes, alkanes and alkanones in its pyrolysate, indicating that both eustigmatophytes biosynthesize structurally related algaenans (Table 5.1).

Analyses of the extracts of the two eustigmatophytes revealed the presence of free and ester-bound C₃₀-C₃₂ alken-1-ols and C₃₀-C₃₆ *n*-alkadiols with alcohol groups at ω-17 or ω-18 and C-1. These findings are in agreement with those of a previous study of the lipids of *N. salina* and other *Nannochloropsis* species (Volkman *et al.*, 1992). The structural similarity of these lipids with units in the algaenan strongly indicates that the specific C₃₀-C₃₄ diols are the main building blocks of the *Nannochloropsis* algaenan. Since their identification in Black Sea sediments (de Leeuw *et al.*, 1981), C₃₀-C₃₂ diols have shown to be ubiquitous in marine sediments in relatively high abundances (*e.g.* Smith *et al.*, 1983; ten Haven *et al.*, 1987a-c, 1992; Morris and Brassell, 1988; McCaffrey *et al.*, 1991; Hoefs *et al.*, 1995a) implying that their macromolecular counterparts can be important contributors to the OM of marine sediments.

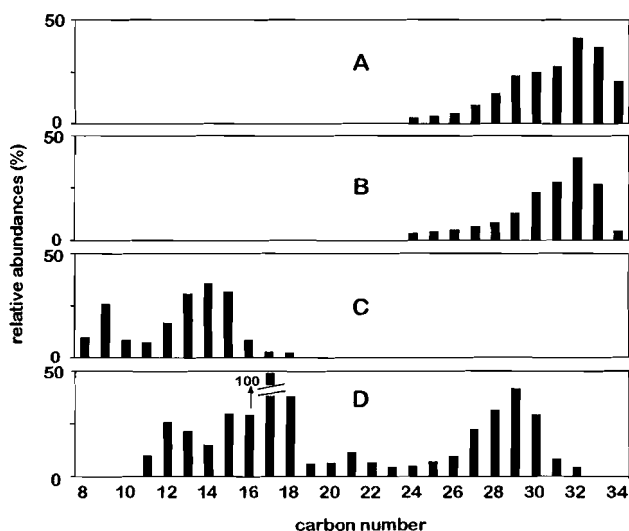


Fig. 5.3 Histograms displaying the major series of oxidation products derived from RuO₄ degradation of *N. salina* algaenan; (A) coeluting *n*-ω¹⁷- and *n*-ω¹⁸-keto-alkanoic acids, (B) *n*-ω^{17,18}-diketo-alkanoic acids, (C) *n*-alkanedioic acids and (D) *n*-alkanoic acids.

The abundant alkene/alkane patterns noticed in the pyrolysates of the eustigmatophyte algaenans were also observed, though with different distributions, in the pyrolysates of algaenans of the marine chlorophytes, *C. spaeckii* and *Chlorococcum* sp. (Table 5.1). Because homologous series of

alkenes and alkanes often dominate pyrolysates of marine kerogens isolated from both Recent (Klok *et al.*, 1984; Eglinton *et al.*, 1994) and ancient (Derenne *et al.*, 1990b; Douglas *et al.*, 1991) sediments, it is concluded that a common source, which could be algaenans, although not necessarily derived from the four microalgae investigated here, are probably important contributors to marine sedimentary OM. Further support of this comes from stable carbon isotope studies of alkenes and alkanes isolated from pyrolysates of marine kerogens. Their $\delta^{13}\text{C}$ values are rather uniform and thus seem to indicate a common source, *i.e.* algaenan (Eglinton, 1994; Collister *et al.*, 1994; Hoefs *et al.*, 1995b). However, very specific alkene/alkane distribution patterns, such as those found in the pyrolysates of the *Nannochloropsis* algaenans, have not been found so far in the pyrolysates of marine kerogens. This is readily explained by assuming that a suite of structurally diverse algaenans derived from different algae make up these kerogens. Although these different algaenans may be isotopically distinct, they all produce a full range of *n*-alkanes upon pyrolysis. This will lead to averaged carbon isotopic compositions for all *n*-alkanes which will not differ much from each other. These considerations indicate that the contribution of algaenan-producing microalgae to marine OM should be traced *via* specific biomarkers, *i.e.* diols in eustigmatophytes, rather than through specific pyrolysis patterns of their algaenans.

Aromatic and phenolic compounds were significantly present in the pyrolysates of the two chlorophyte algaenans already mentioned and were predominant in that of *Nannochloris* sp. (Table 5.1). The origin of the aromatic moieties observed in algaenan pyrolysates is still unclear, whereas the phenols are likely generated by the thermal cleavage of polyphenolic macromolecules such as phlorotannin (van Heemst *et al.*, 1995).

Our results strongly indicate that specific marine eustigmatophyte and chlorophyte microalgae biosynthesize algaenans. These biomacromolecules, due to their highly resistant nature, are thought to escape from mineralization and become selectively preserved in marine sediments, as it has been observed previously for algaenans of fresh-water microalgae in lacustrine environments (Goth *et al.*, 1988; Tegelaar *et al.*, 1989c; Derenne *et al.*, 1991b; Sinninghe Damsté *et al.*, 1993b). Therefore, we regard marine algaenans as a major sink of organic carbon in marine sediments. Upon burial in the Earth crust these materials may act as an important source of *n*-alkanes in marine petroleum.

Acknowledgements - We thank Prof. J. M. Hayes, Dr T. I. Eglinton and a number of anonymous referees for helpful comments on earlier drafts of this paper.

Resistant biomacromolecules in five marine microalgae of the classes Eustigmatophyceae and Chlorophyceae: Geochemical implications*

François Gelin, Ilco Boogers, Anna A. M. Noordeloos, Jaap S. Sinninghe Damsté, Roel Riegman and Jan W. de Leeuw

6.1 ABSTRACT

Non-hydrolysable macromolecular constituents (*i.e.* algaenans) were isolated from five out of seven marine microalgae investigated. *Nannochloropsis salina* and *Nannochloropsis* sp. from the class of Eustigmatophyceae produce highly aliphatic algaenans. Flash pyrolysis and chemical degradations with HI and RuO₄ allowed for the identification of their chemical structure which is mainly composed of polyether-linked long-chain (up to C₃₆) *n*-alkyl units. The building blocks of this polymer were also recognized in lipid fractions. Three other algaenans were encountered in green microalgae (Chlorophyceae). *Chlorella spaerckii* and *Chlorococcum* sp. both biosynthesize algaenans comprising a predominant aliphatic moiety and a polyphenolic one. The latter was also present in the algaenan of the green microalga *Nannochloris* sp. which was dominated by aromatic constituents. Similar to algaenans from fresh water green microalgae, these algaenans are likely to be selectively preserved in depositional environments and the aliphatic algaenans might ultimately serve as source rock organic matter of marine crude oils. Furthermore they may play an important role in the carbon cycling.

6.2 INTRODUCTION

The far greater part of organic matter (OM) in the subsurface consists of kerogen, a high-molecular-weight material insoluble in water and common organic solvents. Because kerogens act as the source of petroleum under appropriate conditions, knowledge of the formation and molecular structure of kerogen is of paramount importance to understand the mechanisms of oil genesis and to predict oil quality. Moreover, kerogen represents a long-term sink of resistant organic carbon and its quantity and composition therefore has an important impact on the global carbon cycle through time.

* Submitted to *Org. Geochem.*

Until a decade ago, kerogen was thought to be formed by random condensation and polymerization of sugars, amino acids and lipids which, in their turn, were produced through bacterially mediated enzymatically-induced depolymerizations of the most important constituents of biomass, polysaccharides, proteins and complex lipids (Tissot and Welte, 1984). This concept of the molecular structure of kerogen and its formation has, however, altered drastically (Philp and Calvin, 1976; Hatcher *et al.*, 1983; Largeau *et al.*, 1984; Goth *et al.*, 1988; Zelibor *et al.*, 1988; Tegelaar *et al.*, 1989c; Derenne *et al.*, 1991; Gatellier *et al.*, 1993; Sinninghe Damsté *et al.*, 1993b). The recognition of insoluble, non-hydrolysable highly aliphatic biomacromolecules in protective tissues of freshwater green microalgae (*i.e.* algaenans in their cell walls) and higher plants (*i.e.* cutans in the cuticles, suberans in the periderm tissues and tegmen in the inner seed coats) shed new light on the formation of kerogen and its structure. It was postulated that these types of aliphatic biomacromolecules consisting mainly of *n*-alkyl units linked *via* ether bonds are selectively preserved and consequently enriched in sedimentary organic matter during burial, despite their relatively small concentrations in the original biomass (Tegelaar *et al.*, 1989c; de Leeuw *et al.*, 1991; de Leeuw and Largeau, 1993). *Via* simulation experiments, it has become clear that under appropriate conditions in the subsurface, *i.e.* relatively high temperatures and long residence times, these aliphatic biomacromolecules produce *n*-alkanes which can make up the bulk of "high-wax" crude oils upon accumulation in reservoir rocks (Tegelaar *et al.*, 1989b).

Complementary data obtained by electron microscopy, spectroscopy (^{13}C NMR and FT-IR) and flash pyrolysis in combination with GC-MS and irm-GC-MS of sedimentary organic matter deposited in lacustrine palaeoenvironments has shown the validity of the above mentioned selective preservation pathway of kerogen formation. The so-called type I kerogens, characterized by their high H/C ratios and excellent source rock potential and their mostly lacustrine origin, consist almost exclusively of algaenans of one or several fresh-water green micro-algae such as *Botryococcus braunii* (races A, B and L), *Pediastrum* spp., *Tetraedron minimum*, *Scenedesmus* spp. or their related ancestors such as *Gloeocapsomorpha prisca* in the Ordovician (for a review, see de Leeuw and Largeau, 1993; Eglinton, 1994; Boreham *et al.*, 1994).

Because of these findings it has been indicated that a similar situation may exist with regard to the formation and molecular structure of kerogens in marine depositional environments assuming that marine counterparts of the freshwater algae mentioned above exist, that their algaenans are also selectively preserved and that ultimately these algaenans are the major source of alkanes in marine crude oils (Tegelaar *et al.*, 1989b).

Circumstantial evidence pointing to the existence of such aliphatic macromolecules in marine (micro)algae stems from pyrolysis studies of marine kerogens from Recent (*e.g.* Klok *et al.*, 1984; Eglinton *et al.*, 1994) to ancient (*e.g.* Douglas *et al.*, 1991; Derenne *et al.*, 1990b) sediments. For example, Fig. 6.1a shows the pyrolysate of a kerogen isolated from an oil producing Kimmeridgian sediment (Boussafir *et al.*, 1995). This pyrolysate clearly indicates the predominant presence of *n*-alkyl moieties in the source rock kerogen as revealed by the abundance of the alkene/alkane doublets. A large fraction of

marine kerogens is often composed of sulphur-containing units due to the reaction of (macro)lipids with inorganic sulphur species at the early stages of diagenesis (Sinninghe Damsté and de Leeuw, 1990; Sinninghe Damsté *et al.*, 1993b). Desulphurization by Li/EtNH₂ treatment of the organic sulphur-rich Messinian kerogens from the Vena del Gesso formation (Hofmann *et al.*, 1992; Gelin *et al.*, 1996b) resulted, as shown by flash pyrolysis (Fig. 6.1b), in an enrichment of alkene/alkane producing kerogen moieties. Thus, the basic matrix of these kerogens was assumed to be built up from aliphatic biomacromolecules,

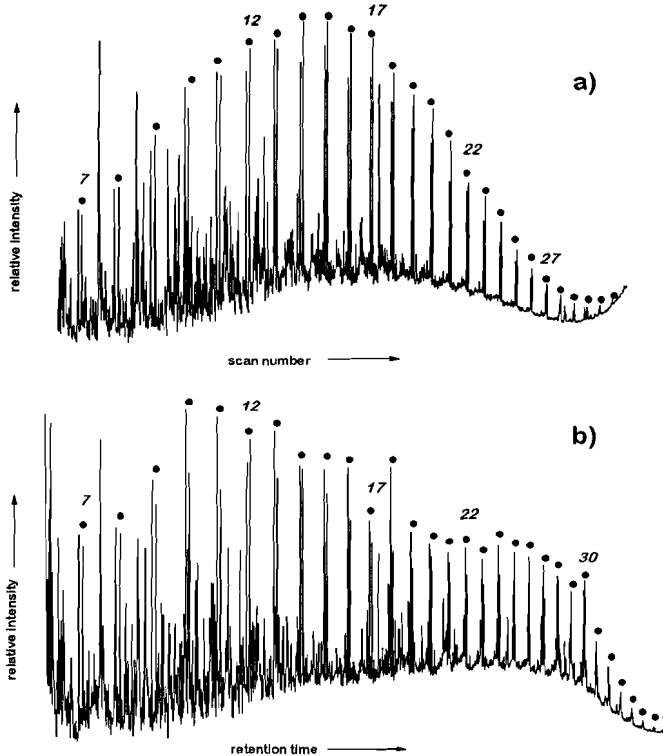


Fig. 6.1 (a) Total ion current trace of a kerogen pyrolysate from Kimmeridgian (Marton, Yorkshire) sediments and (b) Gas chromatogram of a pyrolysate of a desulphurized (Li/EtNH₂ treated) kerogen from Miocene (Vena del Gesso, Italy) sediment. *n*-Alk-1-ene/*n*-alkane doublets are indicated (●) and italic numbers indicate their carbon-chain length.

possibly algaenans. Furthermore, it is well known that Ordovician oils are predominantly derived from marine kerogens which are dominated by the microscopically recognizable extinct organism *Goeocapsomorpha prisca* and which generate high amounts of *n*-alkenes and *n*-alkanes upon flash pyrolysis (Douglas *et al.*, 1991). It was clearly demonstrated that this extinct marine

microalga *G. prisca* is very likely related to the fresh water green microalga *Botryococcus braunii* race A (Derenne *et al.*, 1992d), an alga which biosynthesizes relatively high amount of a well-characterized algaenan (Metzger *et al.*, 1991). This indicates that marine green microalgae related to present-day fresh water ones have existed in the geological past and were able to biosynthesize algaenans. Stable carbon isotope studies of marine kerogens further supported the occurrence of resistant aliphatic algaenans in some marine organisms (Eglinton, 1994; Collister *et al.*, 1994). $\delta^{13}\text{C}$ values of the *n*-alk-1-enes and *n*-alkanes isolated from pyrolysates of several marine kerogens were highly uniform, thus implying a common macromolecular source.

So far only one report on the occurrence of an aliphatic algaenan in a marine (micro)alga exists (Derenne *et al.*, 1992a). Based on spectroscopic, microscopic and pyrolytic data, they reported the presence of non-hydrolysable macromolecular constituents with large amounts of long (up to C_{30}) polymethylenic chains (1.5 % of the biomass) in the trilaminar outer wall of a recently discovered marine chlorophyte, *Nanochlorum eucaryotum*. The electron microscopic observations of the isolated *N. eucaryotum* algaenan revealed the presence of the so-called ultralaminae which were also observed in several marine kerogens. Accordingly, the authors suggested that algaenans from marine green microalgae could significantly contribute to the OM of marine sediments *via* the selective preservation pathway (Derenne *et al.*, 1992c).

In order to corroborate these suppositions, we decided to investigate several, more common marine microalgae. Lipids and macrolipids of seven marine microalgae including the eustigmatophytes *Nannochloropsis salina* and *Nannochloropsis* sp. and the chlorophytes *Brachiomonas submarina*, *Chlorella spaerckii*, *Chlorococcum* sp., *Nannochloris* sp. and *Stichococcus bacillaris* were analysed.

6.3 EXPERIMENTAL

Culture conditions - Axenic strains of *Nannochloropsis salina*, *Nannochloropsis* sp., *Brachiomonas submarina*, *Chlorella. spaerckii*, *Chlorococcum* sp. and *Stichococcus bacillaris* were obtained from the Culture Collection of the Natural Environment Research Council (U.K.). Strain designations and sources are given in Table 6.1. Algae were grown in batch cultures using a medium based on aged North Sea water which contained very low concentrations of nutrients. Prior to sterilisation of the sea water, 2 mL.L⁻¹ of 1.2 N HCl solution was added to prevent precipitation of calcium and magnesium salts. After sterilisation, sterile nutrient solutions were added aseptically, resulting in the following concentrations: 2667 μM NaHCO_3 , 25 μM NaH_2PO_3 , 150 μM NaNO_3 , 150 μM NH_4Cl , trace metals and vitamins according to Veldhuis and Admiraal (1987). The pH was adjusted to 8.0 ± 0.1 with a sterile 1.2 N HCl solution or 1.2 N NaOH solution. The algae were cultured in 10L polycarbonate Nalgene bottles at 15°C. Light was supplied by TLD tubes (colour 54) at an average intensity of 150 $\mu\text{Einst.m}^{-2}\text{s}^{-1}$ in a light/dark cycle of 16/8 h. The monoalgal cultures were kept axenic and were occasionally controlled for bacteria using the Acridine Orange method (Hobbie *et al.*, 1976).

Isolation process - Algaenans were isolated from the freeze dried algal biomass according to the scheme shown in Fig. 6.2. The successive ultrasonic extractions of the algal biomass were carried out with methanol (x2), methanol/dichloromethane (50/50; x5) and hexane (x2). The extracted residues were saponified with 1N KOH in MeOH (reflux for 1 h) and hydrolysed with 4N HCl at 100°C for 6 h. Experimental conditions and work-up of the H₂SO₄ hydrolysis are previously described (Moers *et al.*, 1990). Extracts I were hydrolysed with KOH and HCl under similar experimental conditions to those used for residues I and II. Extracts obtained after each step were derivatized and analysed by GC and GC-MS. Each residue was washed several times with H₂O, MeOH, MeOH/DCM and DCM. The final residues were then dried over N₂ and analysed by flash pyrolysis.

Table 6.1. Strain designations and sources of the microalgae investigated

Name	Class	Strain number	Place of collection
<i>Brachiomonas submarina</i>	Chlorophyceae	CCAP 7/2B	Supralittoral rock pool, Scotland, U.K.
<i>Chlorella spaerckii</i>	Chlorophyceae	CCAP 211/29A	Shell Fish tanks, North Wales, U.K.
<i>Chlorococcum</i> sp.	Chlorophyceae	CCAP 11/62	Inshore sea water, Nova Scotia, Canada
<i>Nannochloris</i> sp.	Chlorophyceae	CCAP 251/2	Rock pool, Guernsey, U.K.
<i>Stichococcus bacillaris</i>	Chlorophyceae	CCAP 379/32	Mangroves, US Virgin Islands
<i>Nannochloropsis salina</i>	Eustigmatophyceae	CCAP 849/4	Supralittoral rock pool, Scotland, U.K.
<i>Nannochloropsis</i> sp.	Eustigmatophyceae	CCAP 849/7	Lake of Tunis (Mediterranean), Tunisia

RuO₄ oxidation - This treatment was carried out after the procedure reported by Sharpless *et al.* (1981) with some modifications. Ca. 10 mg of algaenan was transferred into a round-bottom flask and 500 mg of NaIO₄, 10 mg of RuCl₃.xH₂O, 8 mL of a CHCl₃/CH₃CN mixture (1:1 v/v) and 1 mL of bidistilled water were added. The reaction mixture was stirred in an ultrasonic bath for 1 h and then under normal conditions for 4 h. The reaction mixture was filtered and extracted twice with DCM. The DCM-layer was dried over MgSO₄. The reaction products were methylated using diazomethane prior to gas chromatographic analyses.

HI Treatment - This treatment was carried out according to the description by Panganamala *et al.* (1971). Ca. 6 mg of *N. salina* algaenan was placed in a centrifuge tube and 3-4 mL of a 56% HI solution was added. The reaction mixture was stirred and refluxed for 1 h. After cooling the solution was transferred to a separatory funnel. The centrifuge tube was washed with bidistilled water and hexane. The washings were added to the separatory funnel which then contained two layers. The water layer was discarded and the hexane layer was successively washed with bidistilled water, 5% sodium thiosulphate (Na₂S₂O₃) and bidistilled water (2x). The hexane layer was then dried over Na₂SO₄ and chromatographed using an Al₂O₃ pipette column with DCM as the eluent. Iodides were derivatized with sodium thiomethoxide (NaSMe) to substitute the iodine by thiomethyl group: To this end, the products from the HI treatment were dissolved in MeOH and 100 mg of NaSMe were added. The

reaction mixture was stirred at room temperature for 18 h. After addition of DCM, the solution was washed with bidistilled water and dried over MgSO_4 .

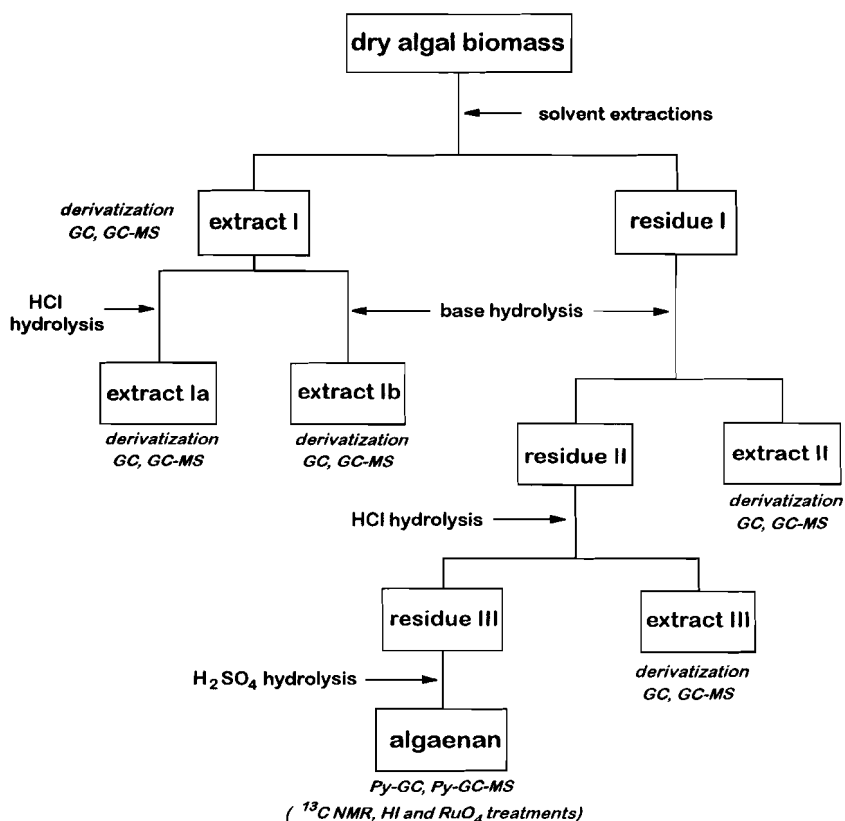


Fig. 6.2 Algaenan isolation process, also indicating the fractions investigated and the analyses carried out.

DMDS Derivatizations - Following the procedure described by Vincenti *et al.* (1987), *ca.* 5 mg of an extract were dissolved in 250 mL hexane and reacted with 250 mL dimethyl disulfide (DMDS) and 125 mL of an iodine solution (60 mg of iodine in 1 mL diethyl ether). The reaction mixture was held at 50 °C for 24 h and then diluted with hexane. The reaction was quenched with 2 mL of 5% $\text{Na}_2\text{S}_2\text{O}_3$ and the hexane layer was pipetted off. The solution was extracted twice with 2 mL hexane. The hexane fractions were combined, dried over anhydrous MgSO_4 and the solvent was evaporated.

Flash pyrolysis - Pyrolysis was performed using a FOM-4LX Curie point pyrolysis unit directly coupled to a Hewlett Packard 5890 series II gas chromatograph

fitted with a 25 m x 0.32 mm CP-Sil 5 (film thickness 0.12 μm) fused silica capillary column. Samples were pressed on to a flattened ferromagnetic wire and heated by inductive heating (Curie temperature 610 $^{\circ}\text{C}$) for 10 s using a Curie point high frequency generator (Fischer 9425). The gas chromatograph was equipped with a cryogenic unit and programmed from 0 $^{\circ}\text{C}$ (5 min) to 320 $^{\circ}\text{C}$ (hold time 10 min) at a rate of 3 $^{\circ}\text{C}/\text{min}$. Separation of the products was achieved by a 25 m fused silica capillary column coated with CP-Sil 5 (0.32 mm I.D.; film thickness 0.45 μm). Helium was used as carrier gas and the temperature of the flame ionisation detector (FID) was 320 $^{\circ}\text{C}$. Identification of the pyrolysis products was performed by Curie point pyrolysis-gas chromatography-mass spectrometry (Py-GC-MS) using the same pyrolysis and GC-conditions as described above. The column was coupled to the electron impact ion source of a VG Autospec Ultima mass spectrometer (mass range m/z 40-800 at a resolution of 1000); cycle time 1.8 s; ionisation energy 70 eV).

Gas chromatography - GC was performed with a Carlo Erba 4160 instrument equipped with an FID and an on-column injector. A 25 m fused silica capillary column coated with CP-Sil 5 (0.32 mm I.D.; film thickness 0.45 μm). Helium was used as carrier gas and the temperature of the flame ionisation detector (FID) was 320 $^{\circ}\text{C}$. The oven was programmed from 70 to 130 $^{\circ}\text{C}$ at 20 $^{\circ}\text{C}/\text{min}$, then to 320 $^{\circ}\text{C}$ at 4 $^{\circ}\text{C}/\text{min}$ and held at this temperature for 10 min. GC-MS was performed using the same gas chromatograph and mass spectrometer as used for Py-GC-MS.

6.4 RESULTS AND DISCUSSION

Seven microalga belonging to the classes Eustigmatophyceae and Chlorophyceae were analysed for the presence of free and bound lipids as well as for non-hydrolysable macromolecular constituents, *i.e.* algaenans, following the scheme shown in Fig. 6.2. Five out of the seven microalgae investigated biosynthesize 1-2% of algaenans. The bulk data of some of the fractions obtained during the algaenan isolation process are indicated in Table 6.2.

Eustigmatophytes

Structural studies of the algaenans

Solid state ^{13}C NMR analysis of the *N. salina* algaenan revealed that it is composed of >95% of methylenic carbon (Gelin *et al.*, 1996a). Investigation of the second eustigmatophyte, *Nannochloropsis* sp., showed that this alga also produces algaenan (*ca.* 1.5 % of the dry algal biomass). Comparison of the flash pyrolysates of these two eustigmatophycean algaenans clearly reveals that both algae biosynthesize structurally similar algaenans (Fig. 6.3). Both pyrolysates are characterized by a strong predominance of the *n*-alk-1-enes and *n*-alkanes with two maxima at $\text{C}_{15}\text{-C}_{17}$ and $\text{C}_{26}\text{-C}_{28}$. The second maximum in the *n*-alkenes and *n*-alkanes series is at C_{28} in the case of *N. salina* and C_{26} in the case of *Nannochloropsis* sp. Series of mid-chain ketones, indicated by filled circles in Fig. 6.3 are relatively more abundant in the pyrolysate of *N. salina*. In both

pyrolysates the keto group is mainly at the ω^{17} or ω^{18} positions. Their mono-unsaturated counterparts, also ranging from C_{20} to C_{34} and maximizing around C_{28} - C_{30} , are also present as revealed by the TIC traces of the pyrolysates and elute just before the saturated ones. Mass spectrometric fragmentations at the α or β position of the carbonyl group indicate that the double bond is always located in the longer carbon chain relative to the mid-chain keto group, presumably at the ω^1 position. Flash pyrolysis data obtained for standard ether compounds have revealed that ketones result from pyrolytic cleavage of secondary ether bonds (Gelin *et al.*, 1993, 1994a). Hence, the mid-chain ketones encountered in both pyrolysates probably reveal ether linkages at the ω^{17} and ω^{18} positions of long-chain *n*-alkyl units. The presence of both saturated and unsaturated ketones may indicate a second functionality also linking these alkyl units together. Beside small amounts of prist-1-ene and toluene, only traces of aromatic, isoprenoid and branched hydrocarbons are present in both pyrolysates. These pyrolysis data are in good agreement with the ^{13}C NMR data of *N. salina* and clearly indicate the virtually exclusive contribution of long-chain *n*-alkyl units to the chemical structure of the two eustigmatophycean algaenans. These alkyl units are probably cross-linked by ether bridges as revealed by the presence of the series of ketones.

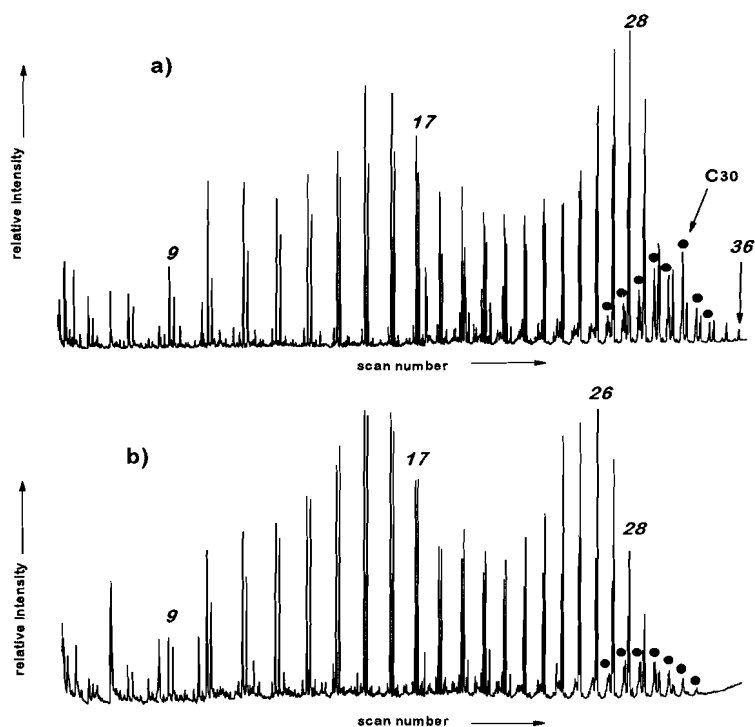


Fig. 6.3 Total ion current trace of the pyrolysates of the algaenans isolated from (a) *Nannochloropsis salina* and (b) *Nannochloropsis* sp. Mid-chain ketones (●) are indicated. Italic numbers indicate the carbon chain length of the *n*-alk-1-ene/*n*-alkane doublets.

To further establish the chemical structure of these algaenans, chemical degradation studies were performed with both eustigmatophyte algaenans. RuO₄ oxidation has been shown to oxidize both ether and ester bonds and also forms acids from alkylbenzenes and is thus capable of decomposing macromolecular substances to a large extent (Boucher *et al.*, 1990). Indeed, RuO₄ treatment oxidized and solubilized the algaenan and produced degradation products which were characterized by GC(MS) analyses (Fig. 6.4). Four major series of oxidation

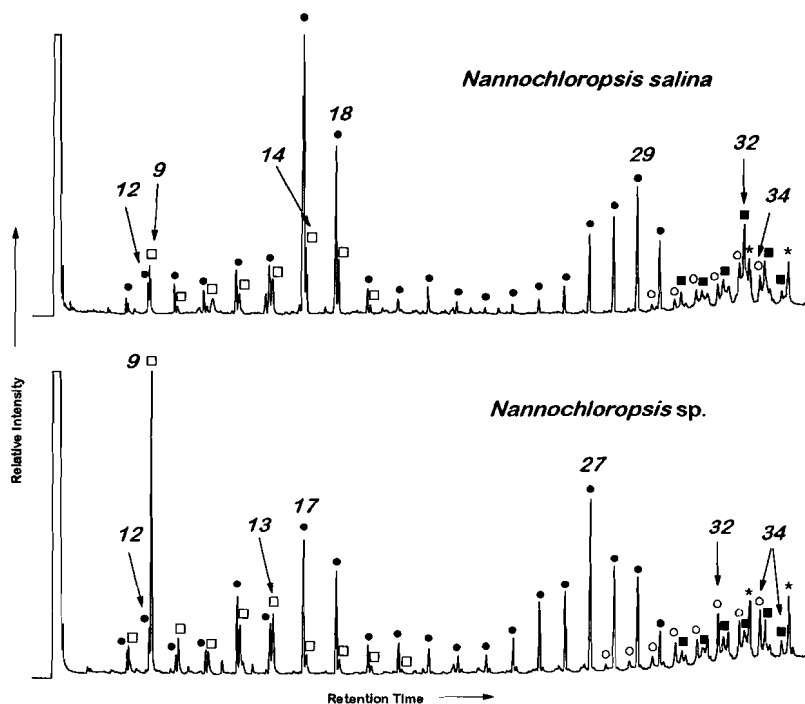


Fig. 6.4 GC-FID trace of the derivatized reaction mixture after the RuO₄ oxidation of *N. salina* and *Nannochloropsis sp.* algaenans. *n*-Alkanoic acids (●), α,ω -alkanedioc acids (□), midchain-keto-alkanoic acids (○) (the keto groups are predominantly at the ω^{17} and ω^{18} positions) and diketo-alkanoic acids (■) (the keto groups are predominantly at the ω^{17} and ω^{18} positions), are indicated. Italic numbers indicate the carbon chain lengths.

products were encountered in the reaction mixtures. Series of *n*-alkanoic acids range from C₁₂ to C₃₂. These series are characterized by two maxima, at C₁₇ for both algae and at C₂₉ for *N. salina* and at C₂₇ for *Nannochloropsis sp.* The heptadecanoic and octadecanoic acids are the major RuO₄ oxidation products observed for *N. salina* algaenan. It is likely that these products were generated by oxidation of the ether bonds that produced the ω^{17} and ω^{18} mid-chain ketones upon pyrolysis. A series of α,ω -alkanedioc acids ranging from C₈ to C₁₇ was also

abundant for both algaenans and maximized at C_{14}/C_{15} for *N. salina* and C_9 for *Nannochloropsis* sp. It is noteworthy that the nonadioic acid is the major oxidation product of the *Nannochloropsis* sp. algaenan, indicating a slightly different structure, *i.e.* more functionalities or double bonds. Series of C_{28} to C_{34} mid-chain keto- and diketo-acids dominated the HMW components, maximizing at C_{30} and C_{32} . The mid-chain keto groups in these acids were predominantly at the

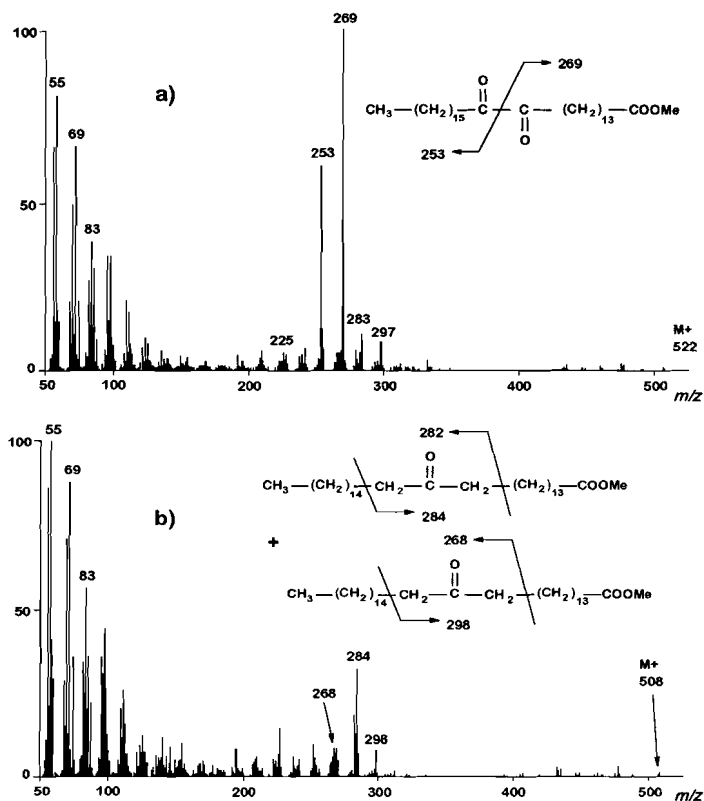


Fig. 6.5 Mass spectra of (a) isomers of diketo-ditriacontanoic acid and (b) isomers of keto-ditriacontanoic acid.

ω^{17} and ω^{18} positions, confirming the flash pyrolysis data. All diketo-acids possess keto groups at vicinal positions as revealed by very intense fragments in their mass spectra. As seen for the C_{32} diketoacids, the $\omega^{17,18}$ diketo-acid is by far the major isomer (Fig. 6.5a). The mass spectra of the monoketo-acids reveal intense fragment ions corresponding to McLafferty rearrangements involving the mid-chain keto group. The mass spectrum of the C_{32} keto-acid mainly comprise ω^{17} and ω^{18} isomers (Fig. 6.5b), indicating a common origin for the series of diketo- and keto-acids. Each of these four series of oxidation products reveals the nature and position of functionalities in the original algaenans. The maximum carbon number of the long-chain *n*-alkanoic acids differ by two units between the

two algal species, supporting a similar difference observed for the long-chain alkene/alkanes distributions in the pyrolysates. This probably indicates a common origin for these long-chain compounds, which derived from moieties linked to the macromolecular matrix by a single bond, presumably an ether bond. The vicinal positions of the keto groups in the diketo-acids revealed the occurrence of two vicinal ether bonds serving as cross-links in the three-dimensional network as it was previously observed for the *B. braunii* L race algaenan structure (Gelin *et al.*, 1994a).

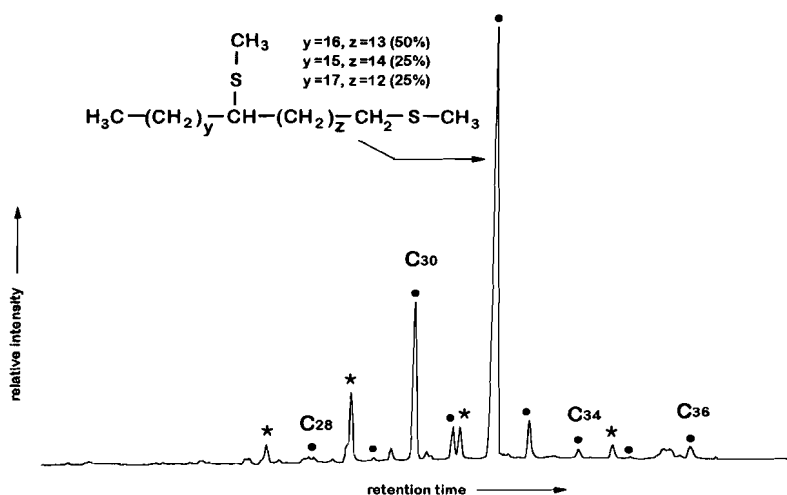


Fig. 6.6 Partial GC-FID trace of the products (derivatized with NaSMe) obtained after HI treatment of *N. salina* algaenan. 1,x-(MeS)₂-alkanes (x = 13-17) (●) and contaminants (*), are indicated.

Because of the assumed presence of ether linkages in the macromolecular network, as indicated in by the RuO₄ oxidation and pyrolysis, it was decided to use HI as a specific reagent capable of cleaving ether bonds (Panganamala *et al.*, 1971; Bhatt and Kulkarni, 1983). Although only *ca.* 15 % of the starting material from *N. salina* algaenan could be dissolved, flash pyrolysis of the residue after HI treatment indicated marked changes in the composition of the insoluble material. Ketones showed a lower relative abundance and no strong maxima could be observed in the distribution of the *n*-alk-1-ene/*n*-alkane doublets anymore. To determine the position of the ether bonds in the alkyl units the alkyl iodides resulting from the HI treatment of *N. salina* algaenan were derivatized with sodium thiomethoxide (NaSMe) allowing the substitution of the iodide groups with methylthio (SMe) groups. The structural identification of the resulting compounds was based on specific mass fragments in their mass spectra. The major compounds are comprised of mixtures of isomers of bis(methylthio) *n*-alkanes ranging from C₂₈ to C₃₆ (Fig. 6.6). A high *m/z* 61 fragment ion indicates that one of the thiomethyl groups is positioned at the terminal carbon atom. As

revealed by the main fragment ions (fragmentations a to mid-chain C-SMe moiety), the second thiomethyl group occurs at various mid-chain positions, mainly ω^{16} , ω^{17} and ω^{18} . Inspection of the relative intensities of these fragment ions reveals the relative abundances of these isomers as indicated for the C₃₂ compounds (Fig. 6.6). These HI/NaSMe treatments confirm the structural information concerning the *Nannochloropsis algaenans* based on pyrolysis and RuO₄ oxidation, *i.e.* *n*-alkyl units, with carbon chain lengths predominantly ranging from C28-C34, linked with ether bonds at one or two mid-chain and one terminal position.

Based on the combined data above and on previous studies of flash pyrolysis mechanisms of aliphatic polyethers (Gelin *et al.*, 1994a), a partial structure for the *N. salina* algaenan is proposed (Fig. 6.7). As indicated, most of the major pyrolysis, HI and RuO₄ oxidation products can be rationalized based on this structure. However, some compounds expected to be released from such a macromolecular structure were not encountered. For example, vicinal diketones supposed to result from pyrolysis of the vicinal ether bonds (Gelin *et al.*, 1993) are absent. This is probably due to pyrolysis cleavages excluding the oxygen atom as demonstrated by cleavages (2)+(3)+(5) which produce the monoketones only. To explain the absence of mono- and tri-(methylthio) *n*-alkanes after HI/MeSNa treatments whereas monoacids and diketacids were formed upon RuO₄ oxidation, it is necessary to compare the two degradation methods for polyether units. A typical alkyl unit linked via two ether linkages would lead to bis(methylthio) alkanes and keto-alkanoic acids when treated with HI/MeSNa and RuO₄, respectively (Fig. 6.7). However, the presence of two vicinal ether bonds might create steric hindrance which would prevent HI from attacking both ether bonds. Hence, a complete cleavage could not occur and the attacked alkyl moiety is likely to stay bound to the insoluble residue. However, oxidation with RuO₄ either only oxidizes the C-O bonds and leads to the formation of keto or acid groups for secondary and primary carbons, respectively, or cleaves the C-C bond at the vicinal ether bonds, thus forming alkanolic acids and diacids.

Building blocks of the eustigmatophycean algaenans

Recent studies of the freshwater green microalgae *Botryococcus braunii* races A and L showed that structural relationships exist between the algaenans and several extractable lipids (for a review, see Metzger *et al.*, 1991). *B. braunii* race A biosynthesizes abundant C₂₇, C₂₉ and C₃₁ *n*-alkadienes and *n*-alkatrienes, C₅₂-C₆₄ aldehydes (botryals), long-chain polyaldehydes ("rubber") and ether lipids. All these lipids are thought to contribute to the formation of the algaenan composing the outer wall of that alga, essentially *via* ether bridges (Metzger *et al.*, 1991; Gelin *et al.*, 1994b). Likewise, *B. braunii* race L biosynthesizes lycopadiene (a C₄₀ isoprenoid hydrocarbon) which was shown to be the building blocks of the algaenan of this alga (Metzger *et al.*, 1991; Gelin *et al.*, 1994a; Behar *et al.*, 1995). Furthermore studies of several freshwater Chlorophyceae synthesizing algaenan, *i.e.* *Scenedesmus*, *Tetraedron*, *Pediastrum*, showed that close relationships exist between the algaenan monomeric units and specific lipids (Schouten *et al.*, 1996). Accordingly, the analysis of the lipids of the two eustigmatophytes was undertaken to search for possible building block lipids.

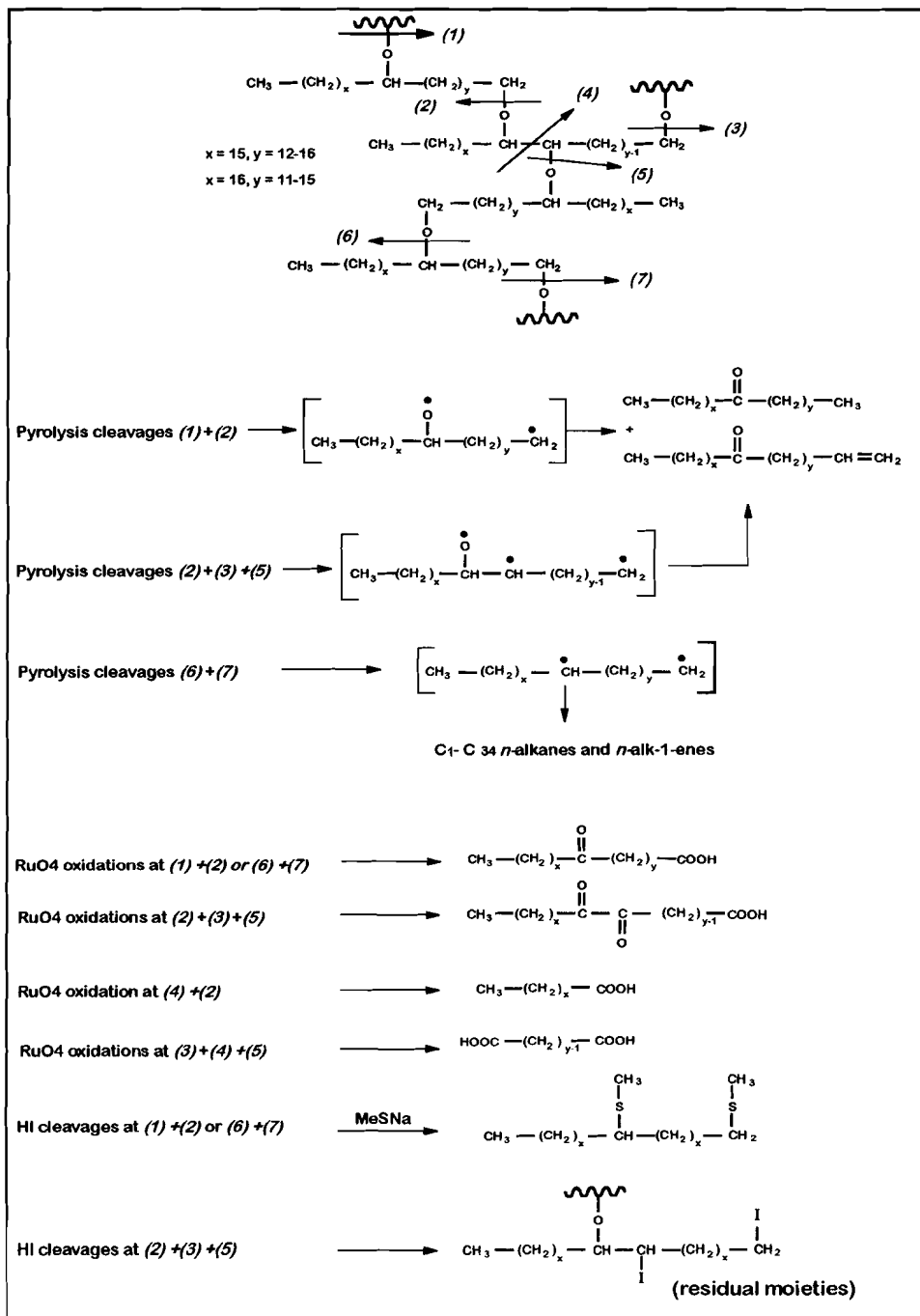


Fig. 6.7 Proposed partial structure of *N. salina* algaenan and rationalization of most of the products obtained by pyrolysis and by RuO₄ and HI treatments.

The occurrence, after acid and/or base hydrolysis of the extractable material, of C₃₀-C₃₂ diols and alkenols in three different *Nannochloropsis* species was recently reported by Volkman *et al.* (1992). Our results reveal that long-chain diols and alkenols are also present as free lipids (in extract I) and as extractable (in extracts Ia and Ib) and non-extractable (in extracts II and III) ester- and amide-bound constituents in our *Nannochloropsis* species. As observed in the extract Ia (Fig. 6.8), the alkanediols range from C₂₉ to C₃₆ and maximize at C₃₀ and C₃₂. These diols consist of 1,ω¹⁷- and 1,ω¹⁸-*n*-alkanediols for the odd and even carbon-numbered diols, respectively. The only exception is the 1,ω¹⁶-C_{30:0} diol that coelutes with the 1,ω¹⁸-C_{30:0} diol. Unsaturated C₃₀ and C₃₂ alcohols were also abundant in these extracts. To establish the position of the double bonds in these unsaturated long-chain alcohols, extract III from *N. salina* was treated with dimethyl disulfide (DMDS) (Vincenti *et al.*, 1987). The double bond positions in the C₃₀ and C₃₂ alken-1-ols were determined from the mass spectra of their corresponding DMDS derivatives (Fig. 6.9). Both spectra reflect several isomers derived from the alken-1-ols with the double bonds predominantly at ω¹⁷ and ω¹⁸, as determined by the fragments formed by cleavage between the carbons bearing the thioether groups. These ω¹⁷ and ω¹⁸ positions correspond well with the positions of the mid-chain alcohol groups in the diols and the mid-chain functionalities of the products generated upon thermal and chemical degradations of the algaenans, *i.e.* the mid-chain ketone pyrolysis products, the keto acids from the RuO₄ experiments and the alkyl iodides from the HI treatment. Consequently, the chain lengths, the location of the alcohol groups in the diols and the double bond position in the alkenols clearly indicate close biochemical relationships between these lipids and the *Nannochloropsis* algaenans.

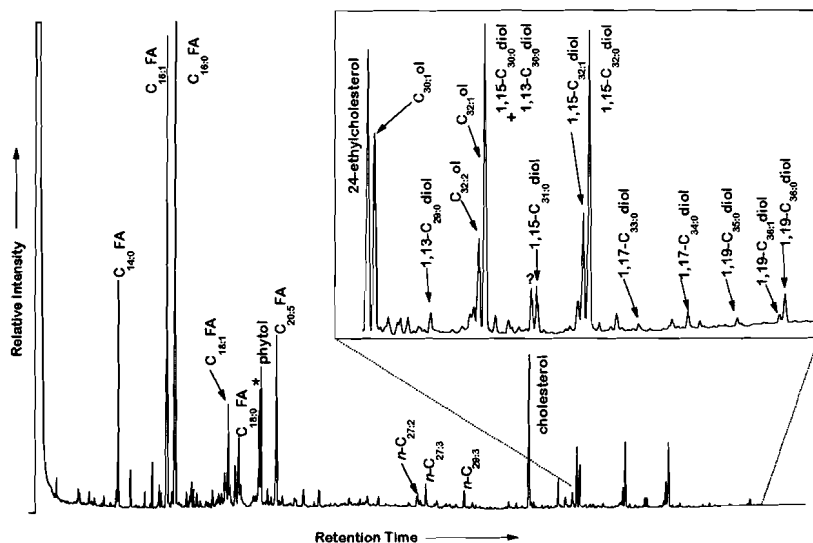


Fig. 6.8 GC-FID trace of the lipids of Extract Ib (released after hydrolysis with HCl of Extract I) from *N. salina*. Fatty acids (FA) are identified as methyl esters and alcohol groups are converted to trimethylsiloxy groups.

Free hydrocarbons were also encountered in extract I of the two eustigmatophytes investigated. The hydrocarbons were separated from the other compounds in extract I by column chromatography over silica with hexane as the eluent. Saturated and (poly)unsaturated (up to 4 unsaturations) hydrocarbons ranging from C_{14} to C_{31} were recovered. The odd-over-even carbon number predominance is very strong for both algal species and the major compounds are the C_{25} , C_{27} and C_{29} hydrocarbons. Catalytic reduction of these hydrocarbon fractions with H_2/Pd afforded n -alkanes with distributions represented in Fig. 6.10. It is noteworthy that these marine microalgae can biosynthesize odd long-chain n -alkenes since their presence in sedimentary OM are commonly believed to be indicators of higher plant contributions (Eglinton *et al.*, 1962). Moreover, it should be noted that the C_{25} hydrocarbons are predominant (45% of the total fraction) in *Nannochloropsis* sp., whereas almost 60% of the hydrocarbons of *N. salina* possess 27 carbon atoms. DMDS treatment of the two fractions and subsequent GC-MS analyses revealed the double bond positions in the long-chain

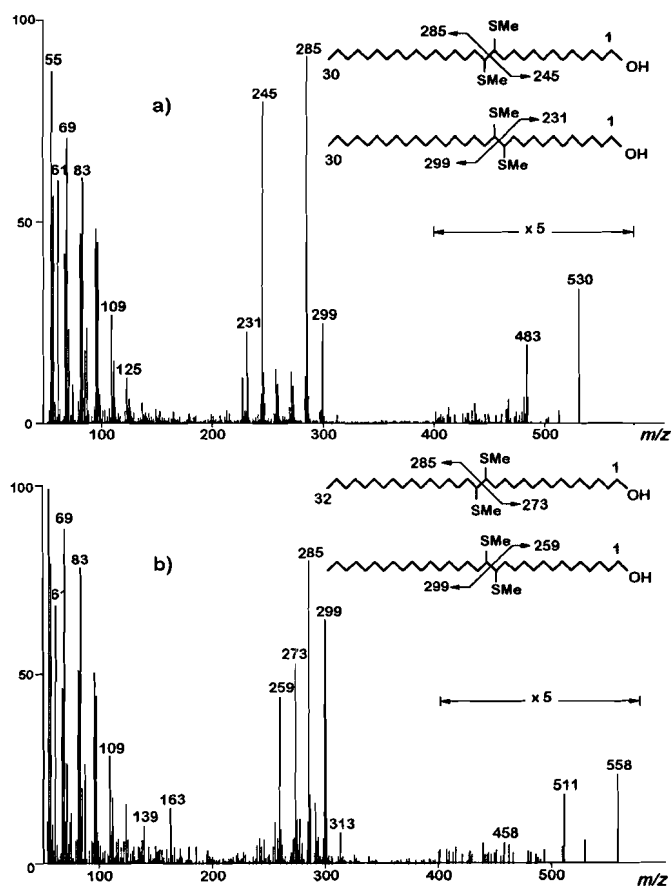


Fig. 6.9 Mass spectra of (a) 13,14- and 12,13-bis(methylthio)triacontan-1-ol and (b) 15,16- and 14,15-bis(methylthio)ditriacontan-1-ol.

n-alkenes. In the monoenes, the double bond is at the terminal position and in the dienes, they are predominantly at the terminal and ω^{17} positions. The differences observed in the distributions of the hydrocarbons between these two eustigmatophytes are consistent with those noted in the distributions of the alk-1-enes and alkanes in their algaenan pyrolysates as well as those observed in the distributions of the long-chain alkanolic acids in the RuO₄ oxidations reaction mixture. These findings probably indicate a further relationship between the biosynthesis of the hydrocarbons and the occurrence of alkyl-chains in the algaenans. A possible biosynthetic pathway might involve, as suggested for *B. braunii* race A (Templier *et al.*, 1992a), the epoxidation of the double bonds of long-chain *n*-alkadienes or *n*-alkatrienes followed by dimerization and further polymerization ultimately leading to the highly aliphatic algaenans.

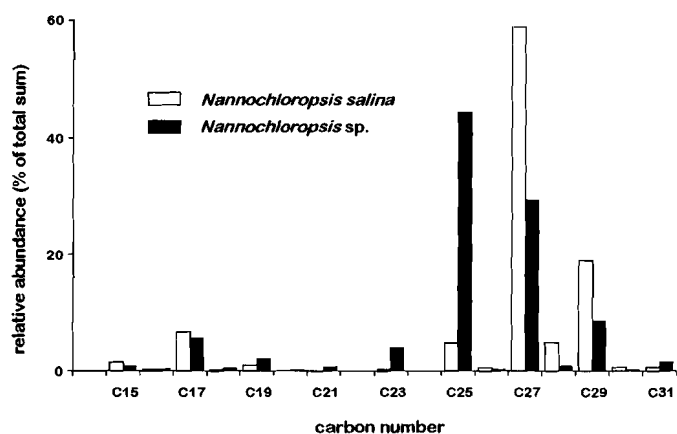


Fig. 6.10 Histogram showing the relative distributions of the free hydrocarbons of *Nannochloropsis salina* and *Nannochloropsis sp.*

Chlorophytes

Three of the five chlorophytes investigated biosynthesize non-hydrolysable insoluble macromolecules (Table 6. 2). *Chlorella spaerckii* and *Chlorococcum sp.* produce 1.2% and 1%, respectively, of resistant final residues which were characterized by flash pyrolysis (Fig. 6.11a,b). The pyrolysates of these two algaenans show similar series of products dominated by series of *n*-alk-1-ene/*n*-alkane doublets and low-molecular-weight (LMW) aromatic compounds such as benzenes, phenols, pyrroles and indoles. The two pyrolysates differ mainly in the distributions of the alkene/alkane doublets. They range up to C₄₁ without a clear maximum in the pyrolysate of *Chlorella spaerckii* algaenan, whereas they maximize at C₂₇-C₂₉ and range up to C₃₄ in the pyrolysate of *Chlorococcum sp.* algaenan. The presence of abundant LMW phenolic pyrolysis products has already been reported in the pyrolysates of residues of several marine

macroalgae and one marine microalga (van Heemst *et al.*, 1995). The authors suggested that these alkylphenols derive from the thermal cleavage of phlorotannin-type macromolecules. Hence, they show in agreement with our results, that phenols in pyrolysates of marine sediments cannot be used as specific indicators of terrestrial contributions. N-Containing compounds, *i.e.* methylpyrroles and indoles, are relatively abundant in the pyrolysate of the *Chlorella* algaenan (Fig. 6.11a). The two possible sources of nitrogen in such organisms are proteins and tetrapyrroles pigments. However, it is unlikely that proteins would survive the acid hydrolyses whereas tetrapyrroles are shown to be too stable to generate N-containing products upon flash pyrolysis analysis (Sinninghe Damsté *et al.*, 1992). Hence, nitrogen-containing pyrolysis products

Table 6.2. Bulk data of isolated fractions and chemical nature of the algaenans

Name	biomass extract (extract I) ^a	Residue before acid hydrolyses (residue II) ^a	Final residue (algaenan) ^a	Nature of the algaenan
<i>Brachiomonas submarina</i>	11	27	-- ^b	--
<i>Chlorella spaerckii</i>	7	77	1.2	mainly aliphatic partly aromatic
<i>Chlorococcum</i> sp.	19	39	1.0	mainly aliphatic partly aromatic
<i>Nannochloris</i> sp.	15	<i>n.d.</i>	~1	mainly aromatic non-aliphatic
<i>Stichococcus bacillaris</i>	27	52	-- ^b	--
<i>Nannochloropsis salina</i> ^c	18-22	32-43	1-2	> 95% aliphatic
<i>Nannochloropsis</i> sp.	18	52	1.5	> 95% aliphatic

^a In % of the dry algal biomass. ^b The entire biomass was dissolved after HCl hydrolysis.

^c The ranges indicated reflect 3 different batch cultures of this alga. *n.d.* Not determined.

are probably generated by non-labile constituents of unknown origin. It should also be noted that pyrolysis of *Chlorococcum* sp. algaenan produces a substantial amount of tetramethylbenzene (TMB), a pyrolysis product previously associated with macromolecularly-bound isorenieratene (Hartgers *et al.*, 1994a). This carotenoid is however specific for green sulphur bacteria (Liaaen-Jensen, 1978). The presence of TMB in the *Chlorococcum* sp. algaenan pyrolysate as well as pyrolysates of resistant residues of several other marine planktonic species indicates that an alternative source for TMB exist (Hoefs *et al.*, 1995b). Based on these pyrolysis data, these two algaenans seem to be composed of several macromolecular constituents, although the main one comprises long chain *n*-alkyl units that give the *Chlorococcum* sp. and *Chlorella spaerckii* algaenans a strong aliphatic character.

The third algaenan-producing Chlorophyceae is *Nannochloris* sp. The pyrolysate of its algaenan essentially consists of series of alkylbenzenes and phenols and, unlike the pyrolysates of the other algae, does not comprise *n*-alk-

1-ene/*n*-alkane doublets (Fig. 6.11c). The aromatic nature of an algaenan was recently reported for another marine Chlorophyceae, *Chlorella marina* (Derenne *et al.*, 1995). In the latter case, the authors showed that polyaromatic compounds were also present in the algaenan pyrolysate. *Nannochloris* sp. algaenan has undoubtedly a different structure as reflected by the absence of these polyaromatics and by the presence of oxygen-containing products such as phenols in its pyrolysate. Hence, the algaenan might comprise at least two types of biomacromolecules, *i.e.* polyphenolic macromolecules as suggested for the two other Chlorophyceae and aromatic macromolecules. Both macromolecular types have a highly resistant character.

The lipids of these chlorophytes were also investigated. Besides the commonly found C₁₆, C₁₈ and C₂₀ (with various degrees of unsaturation) fatty acids, phytol and C₂₇-C₂₉ sterols, less commonly encountered C₂₂-C₂₆ saturated and mono-unsaturated α -hydroxy-fatty acids were the major components in the extracts III (Fig. 6.2) in all three algaenan-producing chlorophytes. Accordingly, in sharp contrast with the observations of the *Nannochloropsis* species, no direct relationships were found between these lipids and the pyrolysis-based chemical nature of the corresponding algaenans.

Geochemical implications

How important is the recognition of algaenan-producing marine microalgae in terms of OM preservation in the marine environment and what is their impact on the organic carbon cycle? The Chlorophyceae represent a class of algae which is widespread in the marine environment although their unicellular and planktonic forms are essentially present in coastal zones (Chrétiennot-Dinet, 1990). Reports on the occurrence and abundance of eustigmatophytes are not numerous, mainly because of their recent recognition (Hibberd, 1979, 1981) and their small size (<5 μ m) requiring electron microscopy for identification. However, eustigmatophytes are thought to be the only species capable of producing long-chain alkyl diols. Since their identification in Black Sea sediments (de Leeuw *et al.*, 1981), these diols have been found in relatively high abundances in many other marine sediments (Smith *et al.*, 1983; Morris and Brassell, 1988; ten Haven *et al.*, 1987a-c, 1992; McCaffrey *et al.*, 1991; Hoefs *et al.*, 1995a). Taking into account both the ubiquity of these sedimentary long-chain alkyl diols and the resistance and aliphatic nature of the *Nannochloropsis* algaenans, it is likely that the latter macromolecules may contribute significantly to marine sedimentary OM. Moreover, the resistant nature of such aliphatic macromolecules would lead to their enrichment upon diagenesis. The highly aliphatic nature of the *Nannochloropsis* and other algaenans make them suitable candidates for *n*-alkane production during catagenesis. Therefore, they may act as important precursors of *n*-alkanes of marine oils in analogy with their fresh water counterparts (Tegelaar *et al.*, 1989b,c).

Long-chain diols were not only found in marine sediments. Several authors reported high abundances of these compounds in the extracts of lacustrine Quaternary sediments (Robinson *et al.*, 1987; Cranwell *et al.*, 1987) and of the Eocene Messel Oil Shale (Zeng *et al.*, 1988). These diols are also the dominant components in total lipid fractions from Late Miocene Mediterranean lacustrine

deposits (Bosch, unpublished data). Investigation of the kerogens of the latter sediments by flash pyrolysis revealed the presence of mainly *n*-alk-1-ene/*n*-alkane

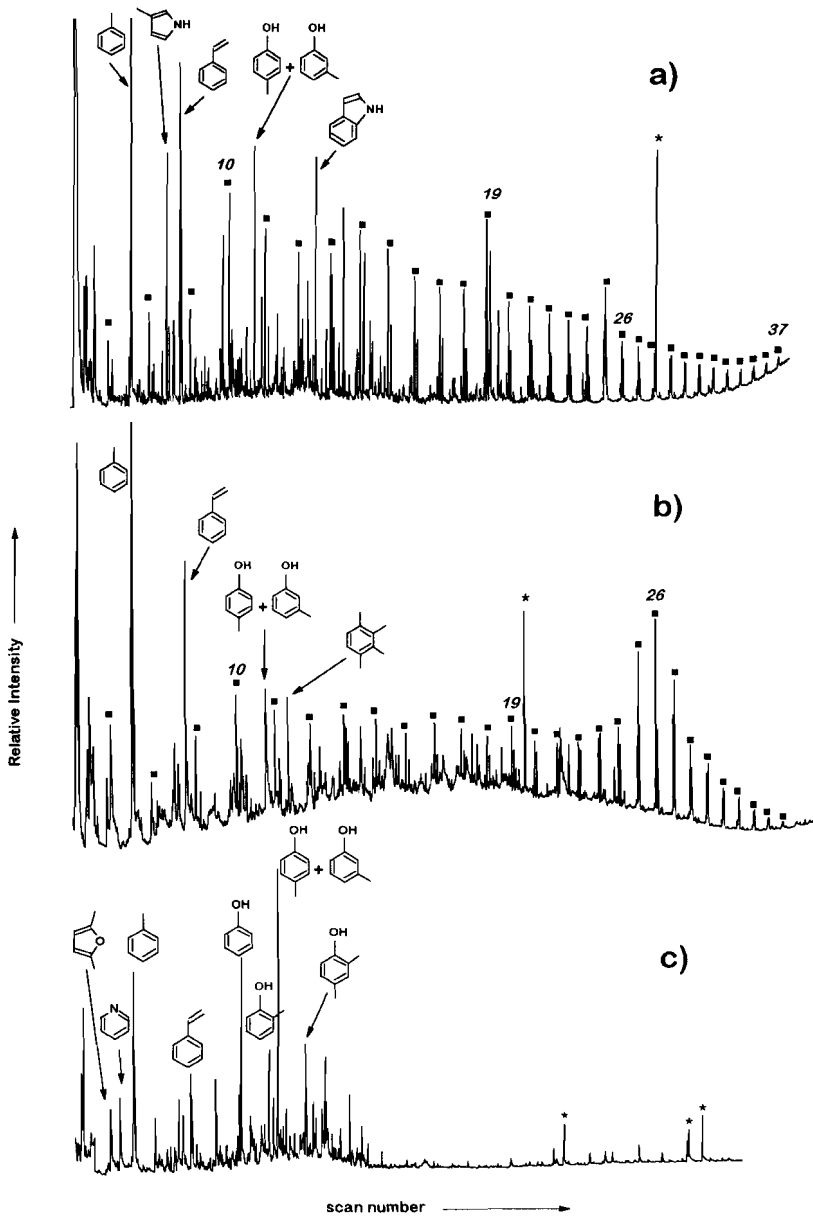


Fig. 6.11 Total ion current traces of the pyrolysates of (a) *Chlorella spærckii* algaenan, (b) *Chlorococcum* sp. algaenan and (c) *Nannochloris* sp. algaenan. Carbon-chain length of *n*-alk-1-en/*n*-alkane doublets (■) are indicated with italic numbers. Stars indicate contaminants.

doublets and mid-chain ketones with similar structures as those found in the pyrolysates of the *Nannochloropsis* algaenans. Furthermore, it has been reported recently (Horsfield *et al.*, 1994) that pyrolysis experiments on kerogens from Eocene alkaline lacustrine sediments generate similar *n*-alkenes/*n*-alkanes distribution patterns, *i.e.* two maxima at C₁₇ and in the C₂₈ range, as those in the pyrolysates of the *Nannochloropsis* algaenans. These findings indicate that (i) freshwater counterparts of the *Nannochloropsis* species investigated in this paper exist and that (ii) the eustigmatophycean algaenans can be traced in both lacustrine and marine sediments and that they may significantly contribute to sedimentary OM.

The *n*-alk-1-ene/*n*-alkane distributions in the pyrolysates of the four aliphatic algaenans described in this paper are unique. Therefore, it might be possible to trace the contribution of these different algae to sedimentary OM via their macromolecular biomarkers when using pyrolysis as the analytical tool for kerogen investigations. However, use of algaenans as biomarkers should be taken cautiously since their recognition in sediments can be strongly affected by two factors. The presence of several algaenan-producing species in the depositional environment implies that the kerogen pyrolysate reflects a combination of all these macromolecules, thereby complicating the issue. Sulphurization process of the OM during the very early stages of diagenesis is the second factor influencing the chemical structure of (marine) kerogens. It increases the contribution of LMW compounds to the kerogen *via* sulphur-bound incorporation and probably leads to intramolecular sulphurization (vulcanization) of the macromolecular lipids (François, 1987). These diagenetic phenomena are thought to have occurred in the Vena del Gesso sediments (Gelin *et al.*, 1995; Schaeffer *et al.*, 1995). Contribution of eustigmatophytes to these Messinian sediments was suggested by the presence of sulphurized C₃₀-C₃₂ alkyl moieties in the polar fraction (Kenig *et al.*, 1995) and the occurrence of C₃₀-C₃₂ thiophenes with the sulphur atom predominantly attached at position C-15 of the carbon skeleton after artificial maturation of the samples (Koopmans *et al.*, 1995). Although flash pyrolysis of the Vena del Gesso kerogens did not reveal the alkene/alkane doublets pattern observed for the *Nannochloropsis* algaenans, detailed analysis of the pyrolysis products of some of these kerogens showed clear indications for the specific ketone functionalities at ω^{17} and ω^{18} in long chain alkyl unit thus reflecting the presence of these algaenans (Gelin *et al.*, 1995). Because of diagenetic processes, a quantitative estimation of the relative contribution of algaenans to the total sedimentary OM is difficult. This contribution is, however, highly dependent on the primary productivity whereas contribution of incorporated LMW constituents depends more on conditions in the depositional environment such as anoxicity and the abundance of reduced inorganic sulphur species.

6.5 CONCLUSIONS

- 1) Various marine microalgae from the classes Chlorophyceae and Eustigmatophyceae biosynthesize algaenans. Those from the two eustigmatophytes, *N. salina* and *Nannochloropsis* sp., are almost exclusively

aliphatic and comprise 1-2% of the dry biomass. The *Nannochloropsis* algaenans are composed of long-chain *n*-alkyl units linked by up to three ether bridges. *Chlorella spaerckii* and *Chlorococcum* sp. biosynthesize ca. 1% of algaenan of a similar nature though with different distributions of alkene/alkane doublets in their pyrolysates. The chemical composition of these algaenans consists of a mixture of predominant aliphatic and phlorotannin-type macromolecules, whereas the *Nannochloris* sp. algaenan essentially comprises aromatic constituents. The two chlorophytes *Brachiomonas submarina* and *Stichococcus bacillaris* do not biosynthesize non-hydrolysable macromolecules.

- 2) Biosynthetic precursors of the eustigmatophycean algaenans are probably C₂₈-C₃₆ diols and C₃₀-C₃₂ alkenols, found as free or ester-bound lipids as well as C₂₅, C₂₇ and C₂₉ (poly)unsaturated free hydrocarbons. The long-chain diols, biomarkers of the *Nannochloropsis* species, are ubiquitous in marine sediments. As a consequence, the corresponding *Nannochloropsis* algaenans may contribute substantially to the OM of these sediments.
- 3) The potential of preservation of the algaenans implies their enrichment with depth in sediments. Hence, the productivity of algaenan-containing microalgae can highly influence the TOC content of marine sediments. Consequently, one can assume that marine algaenans may play an important role in the marine OM record.
- 4) The strong aliphatic nature of most of these algaenans makes them suitable as *n*-alkanes producers upon catagenesis. As *n*-alkanes are the major components of marine crude oils, we hypothesize that the aliphatic algaenans are significant contributors to marine oil and gas.

Acknowledgements - L. Megens assisted in the isolation and analysis of *Nannochloris* sp. algaenan. This work was partly supported by a PIONIER grant to JSSD by the Netherlands Organisation for Scientific Research (NWO).

Electron microscopy and pyrolysis of kerogens from the Kimmeridge Clay Formation (U.K.): Source organisms, preservation processes and origin of microcycles*

Mohammed Boussafir, François Gelin, Elisabeth Lallier-Vergès, Sylvie Derenne, Philippe Bertrand and Claude Largeau

7.1 ABSTRACT

Recent studies revealed short-term cyclic variations (microcycles) in total organic carbon (TOC) and the hydrogen index (HI) in the Kimmeridge Clay Formation, an organic-rich deposit considered to be a lateral equivalent of the main source rocks of the North Sea. In addition, three different types of organic matter, that all appear amorphous when observed by light microscopy (AOM), were recognized. Together these AOM types account for over 80% of total kerogen and their relative abundances show large variations along each microcycle. In the present work, transmission electron microscopy (TEM) observations were carried out on samples (whole kerogens, kerogen subfractions only comprising a single type of AOM, selected rock fragments) corresponding to typical points within a microcycle and obtained via high resolution sampling. The nature and the relative abundances of the products generated by Curie-point Py-GC-MS and off-line pyrolyses of isolated kerogens were also determined for two selected samples corresponding to the beginning and the top of the microcycle. Combination of such ultrastructural observations, including some semi-quantitative studies, and of analyses of pyrolysis products allowed (i) determination of the ultrastructural features of the three AOM types thus providing what we believe to be the first example of correlations between light microscopy (palynofacies, in situ maceral analysis) and TEM observations on "amorphous" fossil materials; (ii) identification of the source organisms and elucidation of the mode of formation of the different AOM types in the Kimmeridge Clay; (iii) explanation of the variations in their relative abundances taking place along a microcycle and establishment of tight correlations with TOC and HI changes; (iv) explanation of the origin of the microcyclic variations in kerogen quantity (TOC) and quality (HI) occurring in the Kimmeridge Clay Formation. Interrelationships between primary productivity, sulphate reduction intensity and lipid "vulcanization" likely played a major role in the control of such variations.

*After *Geochim. Cosmochim. Acta* **59**,3731 (1995)

7.2 INTRODUCTION

The aim of this work was to gain information on kerogen genesis and source organisms in the Kimmeridge Clay and on the origin of the short term cyclic variations, in both kerogen quantity and quality, occurring in this formation. Kimmeridge Clay is a marine deposit, with alternating organic-rich shales and marls, considered as a lateral equivalent of the main source rocks of the North Sea. This Upper Jurassic formation, up to five hundred meters thick, outcrops in Britain as a belt stretching from Dorset to Yorkshire (Williams and Douglas, 1980). It is generally considered that the Kimmeridge Clay was deposited below wave base under a shallow shelf regime (Tyson *et al.*, 1979) during a period of maximum eustatic rise and transgression (Gallois, 1976). Depositional conditions were mainly controlled by the topography of the basin and sedimentation and subsidence rates. The onshore basin topography led to the sedimentation of organic matter-rich mudstones and to anoxic conditions in restricted areas only (Tribovillard *et al.*, 1994). Previous studies on the bulk chemical features of Kimmeridge Clay kerogens, chiefly based on elemental analyses and pyrolyses (Williams and Douglas, 1980, 1983; Farrimond *et al.*, 1984; Pfendt, 1984; Eglinton *et al.*, 1986, 1988a,b), showed a type II material with a low degree of maturity, consistent with a maximal burial depth around 1,500 m (Williams, 1986). In addition, a recent bitumen examination pointed to an important contribution of algae along with a minor contribution of land-derived organic material (Ramanampisoa and Disnar, 1994).

Recently, high resolution measurements of total organic carbon (TOC) on Kimmeridge Clay cores from three boreholes in the Cleveland basin (Yorkshire, UK) revealed a conspicuous feature (Herbin *et al.*, 1991, 1993). Pronounced, short term, cyclic variations in TOC were observed with each microcycle corresponding to about 30,000 years. Moreover, it was noted (Ramanampisoa *et al.*, 1992) that hydrogen index (HI) also exhibits substantial cyclic variation along with TOC. As a result of such parallel, wave-shaped, changes in TOC and HI, the oil potential of the Kimmeridge Clay formation shows a sharp maximum at the top of each cycle.

The first petrographic observations carried out on Kimmeridge Clay kerogens, by light and UV fluorescence microscopy (Tyson *et al.*, 1979; Williams and Douglas, 1980; Smith, 1984) indicated a marked predominance of a seemingly structureless matter with bituminite as the main maceral according to Williams and Douglas (1980). A low contribution of recognizable elements, mainly of a terrestrial origin (humic material), was also noted (Bertrand *et al.*, 1990; Huc *et al.*, 1992). Examinations by transmitted and reflected light microscopy were recently carried out on kerogens obtained via high resolution sampling of a microcycle, from one of the three boreholes previously studied by Herbin *et al.* (1991, 1993): Cleveland basin, Marton 87 well (Ramanampisoa *et al.*, 1992; Pradier and Bertrand, 1992). The palynofacies study (transmitted light microscopy) revealed that the dominant "amorphous" organic material (AOM, over 80% of total organic matter) is in fact comprised of three distinct types of particles that can be characterized by differences in texture and color: orange homogeneous flakes with sharp edges (orange AOM); brown heterogeneous flocks with fuzzy outlines (brown AOM); opaque aggregates (black AOM). It was

observed that important differences in the relative abundances of the three above types take place along the cycle. Moreover, Ramanampisoa *et al.* (1992) noted a strong parallel between the variations in TOC and HI values, on the one hand, and the abundance of orange AOM, on the other hand. The beginning and the end of the cycle are thus characterized by a predominance of the black and brown AOMs associated with land-derived debris, whereas the peak (or top) of the cycle, where maximum TOC and HI occur, shows a major contribution of orange AOM.

The purposes of the present study were therefore to derive information on (i) the ultrastructural and chemical features, the source organisms and the mode of formation of these different types of so-called "amorphous organic matter", (ii) the origin of the substantial variations in AOM relative abundances occurring along the microcycle, (iii) the relationships between such variations and TOC and HI changes and (iv) the cause(s) of the cyclic variations observed in the Kimmeridge Clay. The conclusions obtained from the study may also aid in understanding the factors that control organic matter quantity (TOC) and quality (HI) in marine sediments in general. To this end, transmission electron microscopy observations (TEM) and pyrolytic studies were carried out on isolated kerogens, corresponding to typical points from the above Kimmeridge Clay microcycle. Bulk kerogens and kerogen subfractions, obtained by micromanipulation and only comprising a single type of AOM particles, were both examined by TEM. Additionally, *in situ* TEM observations were also directly performed on untreated rock fragments.

7.3 EXPERIMENTAL

Samples

The studied microcycle (90 cm thick, corresponding to about 30,000 years, depth in the core 128.2 to 129.1 m) was sampled in the Eudoxus zone of the Marton 87 borehole, Pickering Vale, Cleveland Basin, Yorkshire, UK (Herbin *et al.*, 1991). The corresponding geologic section is discussed in Herbin *et al.* (1991, 1993), Tribouvillard *et al.* (1994) and Desprairies *et al.* (1995). TOC values range from ca 2% (beginning and end of the microcycle) to 9.5% at the top of the microcycle and HI from ca. 250 to ca. 780 mg of hydrocarbons/g of organic carbon (Ramanampisoa *et al.*, 1992). The microfacies observed by light microscopy (reflected light and UV excitation on polished sections) is laminated throughout the cycle and no bioturbation features are observed. The distribution of the organic matter appears to be relatively heterogeneous. In samples with relatively low TOC values, the organic matter is comprised predominantly of small irregular or angular particles, from 5 to 20 μm in size, identified as inertinite. For samples with TOC values >4%, the microfacies are characterized by an increase in size and abundance of more or less continuous elongated organic particles (up to 500 μm) which are largely predominant at the peak of the cycle; when studied by reflected light they appear as bituminite maceral (Pradier and Bertrand, 1992). For the highest TOC values, the organic matter tends to form thick laminations and to occur within the mineral matrix in greater amounts.

The eight samples examined were selected on the basis of previous light microscopy and Rock-Eval high resolution studies (centimetric scale) carried out by Ramanampisoa *et al.* (1992). These samples correspond to the beginning of the cycle (128.23 m), the section encompassing the increasing TOC values (128.62 and 128.67 m), the top of the cycle (128.74 and 128.75 m), the section covering decreasing TOC values (128.79 m) and the end of the cycle (129.09 and 129.1 m). In agreement with the previously stated occurrence of low maturity type II material in the Kimmeridge Clay, elemental analysis indicated atomic H/C ratios of 1.1 to 1.2 for the selected kerogens.

Kerogens used for petrographic and pyrolytic studies were isolated from these different rock samples via the classical HF/HCl treatment. Direct TEM observations were then carried out on whole kerogens and on hand-picked kerogen subfractions comprising only a single type of AOM. The subfractions were obtained by picking out AOM particles under a stereomicroscope, with a microsyringe coupled to a micromanipulator, from aqueous suspensions of whole isolated kerogens (Boussafir *et al.*, 1994a). Fragments of untreated rocks dominated by a single type of maceral (*e.g.* bituminite), or by the organo-mineral matrix, were also selected by light microscopy, from polished sections, for in situ TEM observations.

All the above materials (whole kerogens, kerogen subfractions and selected rock fragments) were fixed in osmium tetroxide, embedded in resin, cut with an ultramicrotome and stained as described in Boussafir *et al.* (1994b) prior to TEM examination using a STEM Jeol 100 CX.

Pyrolyses

"Off-line" pyrolyses and identification of pyrolysis products were performed according to Largeau *et al.* (1986). Briefly, kerogens are firstly heated at 300°C for 20 min so as to eliminate adsorbed compounds by thermovaporization and, after extraction with CHCl₃/MeOH (2/1), the insoluble residue is pyrolysed at 400°C for 2 hr under an Helium flow. The released products are trapped in CHCl₃ at -5°C, separated by column chromatography on activity 2 alumina into three fractions of increasing polarity by eluting with hexane, toluene and methanol, respectively. The hexane-eluted, low polarity, products are further separated into three subfractions by TLC on SiO₂-AgNO₃ (10%). The various pyrolysate fractions thus obtained were analysed by GC-MS (DB1 capillary column, 60 m x 0.25 mm i.d., oven heated from 120 to 260°C at 4°C/min). Curie point pyrolysis-gas chromatography-mass spectrometry (Py-GC-MS) was performed as described in Derenne *et al.* (1992d) using a Curie point pyrolyser (FOM3-LX) and a ferromagnetic wire with a Curie temperature of 610°C.

7.4 RESULTS AND DISCUSSION

Electron microscopy

A first series of TEM observations on whole isolated kerogens, corresponding to typical points of the microcycle, revealed the presence of various ultrastructures in the eight samples examined: a massive, gel-like,

amorphous material; very thin lamellae; small ligneous debris; a granular material and a diffuse amorphous material. The above ultrastructures were shown to occur all along the microcycle but sharp differences in their relative abundances were noted. A semi-quantitative study was therefore carried out by examining, for each kerogen sample, 60 to 75 ultrathin sections. The gel-like material was thus shown to exhibit large changes in relative abundances that parallel TOC and HI variations (and hence variations in orange AOM relative contribution). This structureless material is only a minor constituent at the end and the beginning of the cycle (about 5 to 10% of total AOM) but markedly predominates at the top (up to 75%). Reverse changes in relative abundances were noted, along the microcycle, for other types of ultrastructures (lamellae, ligneous debris) and the latter are only abundant at the end and the beginning of the cycle. The above semi-quantitative features suggested that tight correlations may occur between the three types of AOM, previously detected by transmitted light microscopy (palynofacies), and the different ultrastructures identified at higher magnification in the present TEM study. The occurrence of such correlations was fully confirmed by TEM examination of kerogen subfractions, composed of a single type of AOM, obtained by picking out particles under the light microscope.

In fact, when taken together, the above TEM observations indicate the following:

- 1) The orange AOM corresponds to the massive gel-like material. This material is characterized by a completely homogeneous texture without any apparent biological structures and it appears truly amorphous, even at a very high magnification (up to $\times 80,000$). That this material is a discrete entity is suggested by well-defined, distinct edges. The orange AOM can therefore be defined as a "nanoscopically amorphous organic matter". Such a material is often associated with pyrite crystals and framboids. In addition, Electron Energy Loss Spectrometry (EELS) pin-point analyses (Boussafir *et al.*, 1995a) showed that the orange AOM contains substantial amounts of organic sulphur (atomic S/C ratios of 0.9 to 1.1).
- 2) The brown AOM corresponds to very thin lamellae with a regular thickness ranging from 50 to 400 nm. Similar structures, with thickness up to 60 nm, were previously observed, by TEM, in a number of kerogens isolated from source rocks and oil shales (Raynaud *et al.*, 1988; Largeau *et al.*, 1990a,b; Lugardon *et al.*, 1991; Derenne *et al.*, 1991b, 1993) and termed ultralaminae (Largeau *et al.*, 1990a). No pyrite and no organic sulphur were detected in the brown AOM.
- 3) The black AOM corresponds to a mixture dominated by minute ligneous debris and also comprises a diffuse nanoscopically amorphous material; low amounts of granular organic matter are also detected. The amorphous diffuse material was closely associated with mineral constituents in the untreated rock and built an organic network within the mineral groundmass. This network is well preserved following mineral elimination by chemical leaching. Such a preservation reveals the occurrence of a continuous organic network exhibiting a high degree of cohesion.

The above TEM observations thus revealed major ultrastructural differences between the three types of AOM identified by transmitted light microscopy. The

orange AOM is truly amorphous whereas the brown and black forms of AOM comprise well-defined structures that could not be detected by light microscopy. The combination of TEM examination on whole kerogens and on kerogen subfractions obtained by micromanipulation thus provided what we believe to be the first example of correlations between "amorphous" organic materials identified in palynofacies studies and ultrastructures observed by TEM. Moreover, close relationships can be noted between the relative abundances of these different ultrastructures and TOC and HI values (Fig. 7.1).

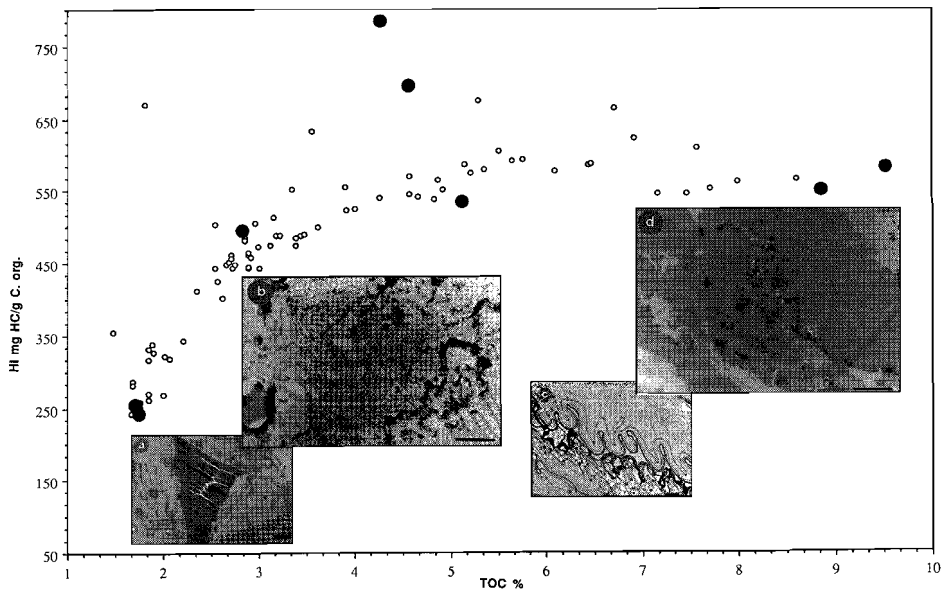


Fig. 7.1 Main ultrastructures identified by TEM in Kimmeridge Clay isolated kerogens and relationships with TOC and HI variations along the microcycle (after Lallier-Vergès *et al.*, 1993a). Filled circles represent the samples studied by TEM. Ultralaminar (b, c) and minute ligneous debris (a) dominate in samples with relatively low TOC values while the massive amorphous matter (d) is predominant in kerogens with higher TOC.

Finally, in-situ TEM observations were carried out on rock fragments selected by light microscopy from polished sections. The purpose of these observations was to (i) attempt a correlation between the main ultrastructures identified above by TEM in isolated kerogens (and hence the AOM types observed in palynofacies studies) and the macerals identified by light microscopy from polished sections of untreated rock samples and (ii) examine the association

of these macerals with the mineral constituents. Selected bituminite particles, when observed by TEM, show a massive nanoscopically amorphous gel-like organic matter embedding clay particles and pyrite framboids. In addition, previous analyses performed by X-ray mapping (Lallier-Vergès *et al.*, 1993a) revealed a specific enrichment in organic sulphur within bituminite particles from the Kimmeridge Clay. Bituminite and the orange AOM therefore exhibit the same lack of ultrastructure, the same close association with sulphur and the same variability in relative abundances along the microcycle. The bituminite maceral thus appears to correspond to the orange AOM observed in palynofacies studies. In sharp contrast, the ultralaminar structures (and hence the brown AOM) do not correspond to any recognizable macerals. They are thought to be dispersed in the organo-mineral matrix and thus difficult to be identified by light microscopy from polished sections. The ligneous debris observed in the black AOM present the same morphology at high magnification and the same ultrastructural features as inertinite macerals. Because of their small size (about 1 μm), these debris were not detected by light microscopy.

Further studies were carried out, by pyrolysis, so as to examine the chemical features, the source organisms and the mode of formation of the different constituents identified above in Kimmeridge Clay AOM's.

Pyrolyses

On the basis of the above petrographic results, two samples termed B (128.23 m) and I (128.75 m) were selected for pyrolytic studies; they correspond to the beginning and the top of the microcycle, respectively. Sample B is thus characterized by lower values for TOC and HI (1.8% and 255 mg HC/g C_{org}) when compared to I (9.5% and 582 mg HC/g C_{org}).

Curie-point Py/GC/MS of isolated kerogens

GC/MS analysis of the 610°C flash pyrolysates revealed complex mixtures of products dominated by doublets corresponding to *n*-alkanes and *n*-alk-1-enes from C₇ to C₃₀ (Fig. 7.2). These two dominant series show maxima around C₁₅, no significant difference in their distributions and relative intensities was noted between kerogens B and I. These observations indicate an abundant contribution of long polymethylenic chains in both samples. The GC-MS traces also show the presence of a large number of compounds eluting between the alkane/alkene doublets. These compounds correspond, as indicated for some of them on Fig. 7.2, to series of alkylated thiophenes, alkylated phenols, alkylated benzenes and to additional series of linear/branched, (un)saturated hydrocarbons. The major difference between B and I flash pyrolysates is to be found in the higher relative abundance of thiophenic compounds for I. This difference can be assessed from the thiophene index: $\text{ThI} = [2,3\text{-dimethylthiophene}] / ([\text{non-1-ene}] + [1,2\text{-dimethylbenzene}])$. This ratio is known to provide a convenient way for a rapid estimation of organic sulphur content in kerogens (Eglinton *et al.*, 1990). A significantly higher ratio is indeed noted (0.22 instead of 0.12) from I pyrolysate when compared to B, thus indicating a larger contribution of sulphur-containing moieties in the former sample. Such a difference is also supported by bulk elemental analyses and the atomic S_{org}/C ratio is about twice as high for I.

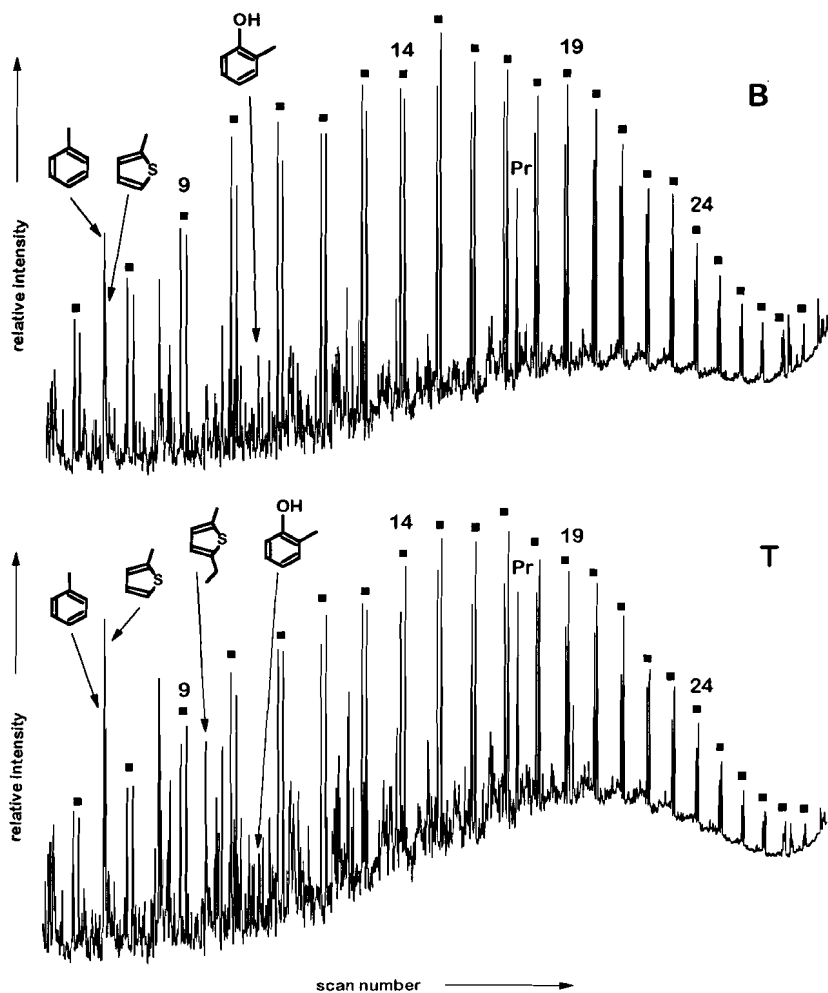


Fig. 7.2 Total ion current (TIC) traces of the flash pyrolysates of kerogens **B** and **T**. Filled squares indicate the homologous series of *n*-alk-1-enes and *n*-alkanes. Numbers indicate their chain length. The structure of some major compounds is indicated and Pr designates prist-1-ene.

Off-line pyrolyses of isolated kerogens

Due to the very high complexity of the effluents produced upon thermal degradation of kerogens **B** and **T**, "off-line" pyrolyses were also carried out so as to obtain further information on the generated products. Prior to GC/MS analyses the crude pyrolysate was separated by column chromatography into three fractions (low polarity products, medium polarity products and polar products) accounting for about 35, 25 and 40% of the total pyrolysates, respectively. Thereafter the low polarity, hexane-eluted, fraction was further separated by TLC

on $\text{SiO}_2\text{-AgNO}_3$ and the polar methanol-eluted fraction was separated by extraction into acid and non-acid compounds.

Table 7.1. Nature and relative abundances of the homologous series of low polarity compounds identified in the 400°C pyrolysates of kerogens **B** and **I**^a

	B		I	
	constituents	r.a.	constituents	r.a.
<i>n</i> -alkanes	C ₁₄ -C ₃₁ (C ₁₇)	1	C ₁₂ -C ₃₀ (C ₁₅)	1
isoprenoid alkanes	C ₁₅ -C ₂₀ (C ₁₈)	0.16	C ₁₅ -C ₂₀ (C ₁₈)	0.23
dimethylalkanes I ^b	C ₁₇ -C ₃₁ (C ₂₅)	0.08	n.d.	—
dimethylalkanes II ^b	C ₁₅ -C ₃₁ (C ₂₁)	0.05	n.d.	—
3-methylalkanes	C ₁₄ -C ₃₀ (C ₂₀)	0.10	C ₁₃ -C ₂₂ (C ₁₅)	0.04
<i>n</i> -alkylcyclopentanes	C ₁₄ -C ₂₆ (C ₂₀)	0.27	n.d.	—
<i>n</i> -alkylcyclohexanes	C ₁₄ -C ₂₅ (C ₁₉)	0.05	C ₁₂ -C ₂₃ (C ₁₄)	0.13
<i>n</i> -alkenes (E)	C ₁₄ -C ₂₆ (C ₁₇)	1	C ₁₃ -C ₂₅ (C ₁₅)	1
<i>n</i> -alkadienes ^c	C ₁₄ -C ₂₄ (C ₁₇)	0.52	C ₁₂ -C ₂₂ (C ₁₅)	0.62
<i>n</i> -alkylbenzenes	C ₁₄ -C ₂₂ (C ₁₆)	0.16	C ₁₂ -C ₁₈ (C ₁₄)	0.35
<i>n</i> -alkyltoluenes	C ₁₄ -C ₂₃ (C ₁₆)	0.18	C ₁₂ -C ₂₁ (C ₁₅)	0.28
<i>n</i> -alkyldimethylbenzenes	C ₁₄ -C ₂₀ (C ₁₆)	0.16	C ₁₂ -C ₁₈ (C ₁₄)	0.33
2- <i>n</i> -alkylthiophenes	C ₁₂ -C ₂₄ (C ₁₄)	0.15	C ₁₀ -C ₂₄ (C ₁₂)	0.65
2- <i>n</i> -alkyl,5-methylthiophenes	C ₁₂ -C ₂₄ (C ₁₄)	0.33	C ₁₀ -C ₂₀ (C ₁₂)	0.86
<i>n</i> -alkyl, dimethylthiophenes	C ₁₂ -C ₂₄ (C ₁₅)	0.06	C ₁₀ -C ₂₀ (C ₁₂)	0.28
<i>n</i> -alk-1-enes	C ₁₄ -C ₂₈ (C ₁₈)	1	C ₁₂ -C ₂₈ (C ₁₅)	1
<i>n</i> -alkenes (Z)	C ₁₄ -C ₂₅ (C ₁₈)	0.09	n.d.	—
<i>n</i> -alkadienes ^c	C ₁₄ -C ₂₂ (C ₁₈)	0.08	C ₁₂ -C ₁₈ (C ₁₄)	0.11
<i>n</i> -alkylbenzothiophenes	C ₈ -C ₁₂	trace	C ₈ -C ₁₂ (C ₁₁)	0.40
<i>n</i> -alkylnaphthalenes	C ₁₀ -C ₁₄	trace	C ₁₀ -C ₁₄ (C ₁₂)	0.15

^a Identifications were carried out following further separation of the hexane-eluted compounds into three fractions by TLC. r.a.: relative abundances of the homologous series calculated with respect to the predominant series of each fraction (ratios of maxima); the bracketed values correspond to the maximum of the series. ^b Based on their mass spectra, these compounds correspond either to 3,7-dimethylalkanes or to 3,ω-7-dimethylalkanes (series I) and either to 3,5-dimethylalkanes or to 3,ω-5-dimethylalkanes (series II). ^c Double bond positions could not be determined. The alkadienes series of the second and third fractions exhibit different retention times and do not correspond to α,ω-alkadienes. n.d.: not detected.

Low polarity products

The different series of compounds identified in the low polarity fractions are reported in Table 7.1, along with their distributions and relative abundances. In addition to the already mentioned *n*-alkanes and *n*-alk-1-enes series, a number of other homologous series were identified. They comprise various types of branched alkanes, normal unsaturated hydrocarbons, and compounds with long

normal alkyl chains associated with a cyclopentyl, a cyclohexyl, a benzene, a thiophene, a benzothiophene or a naphthalene ring (in addition the benzene and thiophene rings can be substituted by one or two methyl groups). Despite the occurrence of these different types of cyclic units, the identification of the low polarity pyrolysis products confirms the important contribution of long $(\text{CH}_2)_n$ chains to both B and I kerogens. Indeed it can be noted that (i) each fraction is dominated by a series corresponding to normal compounds and that other series of acyclic unbranched products also occur in substantial amounts, (ii) the cyclic structures are always associated with long normal alkyl chains, (iii) the abundant series of alkylmethylthiophenes corresponds to the isomer (2-alkyl,5-methyl) with a "normal carbon skeleton", *i.e.* to compounds derived from sulphur incorporation in unbranched precursors (Sinninghe Damsté *et al.*, 1989; Sinninghe Damsté and de Leeuw, 1990). This major contribution of long polymethylenic chains was confirmed, as shown thereafter, by analysis of the toluene- and methanol-eluted fraction of B and I pyrolysates; it is also consistent with previous studies on Kimmeridge Clay kerogens, from the Dorset area, using solid state ^{13}C NMR spectrometry and RuO_4 oxidation (Boucher *et al.*, 1990).

As discussed below, the abundance and the nature of the organic sulphur compounds (OSC) generated from samples B and I provide important information. As shown in Table 7.1, although the same series with similar distributions are observed in both cases, much larger relative amounts of OSC are always obtained from I. In agreement with flash pyrolyses, the latter kerogen therefore comprises a markedly higher contribution of sulphur-containing moieties. This difference can be also illustrated by comparison of the two mass chromatograms of m/z 111 of the total pyrolysates of B and I (Fig. 7.3), highlighting the series of 2-*n*-alkyl, 5-methylthiophenes and *n*-alk-1-enes.

It is well documented that a rapid incorporation of sulphur into various functionalized lipids takes place during early diagenesis in the presence of reduced sulphur species (reviewed in Sinninghe Damsté and De Leeuw, 1990). Such an incorporation occurs in lipids comprising carbon-carbon double bonds but also, as recently demonstrated, in ketones and aldehydes (Schouten *et al.*, 1993; Krein and Aizenshtat, 1994). Due to this "natural vulcanization", the above lipids can become tightly associated, *via* covalent bonds, within insoluble macromolecular structures. As a result such lipids are likely to be protected against microbial mineralization and thus to efficiently contribute to kerogen formation (Sinninghe Damsté *et al.*, 1989). The main outcome of sulphur incorporation may therefore be to strongly reduce the degradation that would take place if these lipids remained in a free state. Regarding morphological features, the "vulcanization" process should lead to amorphous kerogen fractions. As already emphasized, the orange AOM that occurs in Kimmeridge Clay kerogens appears truly amorphous when examined by TEM; it is often associated with pyrite and pin-point analyses indicated a substantial content of organic sulphur. In addition, its relative abundance sharply increases with TOC and is at a maximum at the top of the cycle, what is to say for sample I. Moreover, as just discussed, the level of organic sulphur-containing moieties is higher in kerogen I when compared to B. Finally, it is noted that the different series of OSC generated both from B and I are commonly found in the pyrolysates of kerogens which formed *via* sulphur incorporation into lipids. Taken

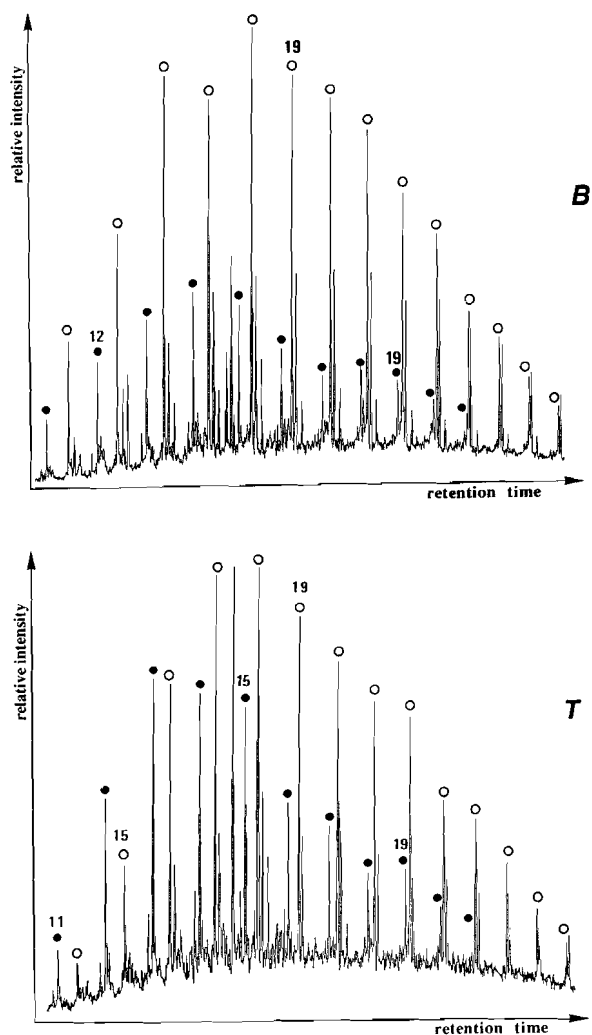


Fig. 7.3 Mass chromatograms of m/z 111 revealing the homologous series of 2- n -alkyl, 5-methylthiophenes (filled circles) and n -alk-1-enes (empty circles) in the total "off-line" pyrolysates of kerogens **T** and **B**. Numbers indicate the length of the alkyl chains.

together, the morphological and chemical features described above therefore strongly point to the formation of the orange AOM occurring in Kimmeridge Clay kerogens *via* lipid "vulcanization". The nature of the OSC generated upon pyrolysis indicate that such lipids were dominated by products comprising long polymethylenic chains as commonly noted, for example, in the total lipid fraction of most microalgae. This formation pathway for the orange AOM is also

consistent with previous observations on T_{\max} obtained by Rock-Eval pyrolyses (Ramanampisoa and Disnar, 1994) which indicated a slight but regular increase in T_{\max} when TOC decreases in the microcycle (422°C for sample I and 427°C for B). Differences in maturity could not be responsible for T_{\max} variations over this short term cycle since no hydrothermal or volcanic alterations occurred and the above differences were considered as reflecting changes in the degree of organic sulphur content. In fact, it is well documented that sulphur-sulphur and sulphur-carbon bonds are much weaker than carbon-carbon bonds (Orr, 1986) thus facilitating thermal degradation. Indeed, it was previously reported that samples with the highest ThI also show the lowest T_{\max} values (Eglinton *et al.*, 1989). A higher content of orange AOM thus likely accounts for the lower T_{\max} observed in kerogen I when compared to B.

Medium polarity products

The compound series occurring in the toluene-eluted fraction of B and I pyrolysates are reported in Table 7.2. In both cases the fraction is dominated by a series of *n*-alkan-2-ones. This type of ketone was observed in the pyrolysates of all the algaenans so far examined and, also, of all the kerogens known to be derived from the selective preservation of these resistant biomacromolecules (*e.g.* Largeau *et al.*, 1986; Flaviano *et al.*, 1994). The thermal cleavage of the ether bridges linking some of the hydrocarbon chains building up the macromolecular skeleton of algaenans accounts for the formation of the ketones (Gelin *et al.*, 1993). Substantial amounts of aromatic, N-containing products, corresponding to series of substituted indoles and quinolines, are also formed from B and I. However, these compounds have not been so far related to a specific type of source organism and biomolecules, thus the significance of their abundant presence in both pyrolysates has yet to be established.

Normal alkylnitriles are also generated in substantial amounts from kerogen B where they account for *ca* 6% of the total pyrolysate; in sharp contrast, these compounds are not clearly detected in the case of sample I. It is now well documented that such nitriles are specific pyrolysis products of the algaenans building up the thin resistant outer walls of numerous species of green microalgae (Derenne *et al.*, 1991b, 1992a). Unlike the *n*-alkan-2-ones mentioned above, these *n*-alkylnitriles are not produced from all types of algaenan and a complete absence of such compounds was previously noted in the case of species (*Botryococcus braunii* and *Tetraedron minimum*) exhibiting thick resistant outer walls. These nitriles were also systematically detected in the pyrolysates of ultralaminae-containing kerogens. Indeed as previously shown, the latter structures, which can only be identified by electron microscopy, originate from the selective preservation of thin resistant outer walls of microalgae (Derenne *et al.*, 1991b, 1992b). It was also observed that important differences in *n*-alkylnitrile distribution occur depending whether the examined samples, *i.e.* algaenan-composed thin outer walls from extant green microalgae and ultralaminae-containing kerogens, are of a marine or lacustrine origin (Derenne *et al.*, 1992c). With regard to Kimmeridge Clay kerogens, light microscopy and TEM observations revealed a major contribution of brown AOM in kerogen B and the bulk of this brown material appears to be composed of lamellar structures reminiscent of ultralaminae. The nature and the origin of these lamellar structures

was ascertained, from the pyrolysis experiments, by (i) the relatively abundant presence of *n*-alkylnitriles in sample **B** pyrolysate and (ii) the identical distribution of these nitriles when compared to those generated from ultralaminae-containing marine kerogens and from thin algaenan-composed outer walls of extant marine microalgae. These morphological and chemical features observed from kerogen **B** therefore clearly indicate that the brown AOM of the Kimmeridge Clay was formed via the selective preservation of thin resistant microalgal walls. The difficulty of clearly establishing the presence of *n*-alkylnitriles in **I** pyrolysate reflects the relatively low level of brown AOM in this kerogen.

Table 7.2. Nature and relative abundances of the homologous series of medium polarity compounds identified in the 400°C pyrolysates of kerogens **B** and **I**^a

	B		I	
	constituents	r.a.	constituents	r.a.
<i>n</i> -alkan-2-ones	C ₁₄ -C ₃₁ (C ₁₇)	1	C ₁₀ -C ₂₃ (C ₁₃)	1
branched alkyl, methylketones ^b	n.d.	—	C ₁₁ -C ₂₁ (C ₁₃)	0.3
<i>n</i> -alkyl, ethylketones	n.d.	—	C ₁₀ -C ₂₅ (C ₁₃)	0.2
<i>n</i> -alkylnitriles	C ₁₁ -C ₂₁ (C ₁₄)	0.8	trace	—
alkylated indoles	C ₉ -C ₁₂	0.9	C ₉ -C ₁₁	0.1
alkylated quinolines	C ₁₀ -C ₁₂	0.15	C ₁₀ -C ₁₃	0.3

^a Toluene-eluted compounds. r.a.: relative abundance of the homologous series calculated with respect to the predominant series (ratios of maxima). n.d.: not detected. The bracketed values correspond to the maximum of each series. ^b The methyl branch is not on carbon 3, but its precise location was not established.

Insoluble and non-hydrolysable macromolecular constituents have been recently shown to also occur in some species of bacteria (Le Berre *et al.*, 1991; Flaviano *et al.*, 1994). As observed for algaenans, the so-called bacterans are located in cell walls. However the skeleton of the cell wall of these bacteria is chiefly composed of hydrolysable macromolecules like peptidoglycans. Accordingly bacterans, when isolated after drastic base and acid hydrolyses, appear as amorphous materials. Similarly, the selective preservation of bacterans results in the formation of amorphous kerogen fractions. Indeed, close chemical relationships have been established between some bacterans and kerogens dominated by nanoscopically amorphous organic matter, as shown by TEM observations (Flaviano *et al.*, 1994). As discussed above, sample **I** is characterized by a low contribution of selectively preserved algal material whereas such constituents played a major role in kerogen **B** formation. Pyrolysis results also point to a substantial contribution of bacteran selective preservation in the genesis of the latter kerogen. Thus, the low polarity fraction of **B** pyrolysate is characterized by the presence of significant amounts of dimethylalkanes (series I) and 3-methylalkanes (Table 7.1). These two series were previously detected, with similar relative abundances and distributions (odd-

carbon-numbered dimethylalkanes and even-carbon-numbered 3-methylalkanes), in pyrolysates of bacterans and derived kerogens (Flaviano *et al.*, 1994). Sample B constituents originating from the selective preservation of bacterans should appear as an amorphous material. Accordingly, such constituents are likely to be associated with the amorphous matrix occurring in the black and/or in the brown organic matter and embedding ligneous debris or minerals and ultralaminae, respectively. In agreement with the low contribution of black and brown matter in kerogen I, bacteran-related products are not detected, or in much lower amounts, in the pyrolysate of this sample (Table 7.1).

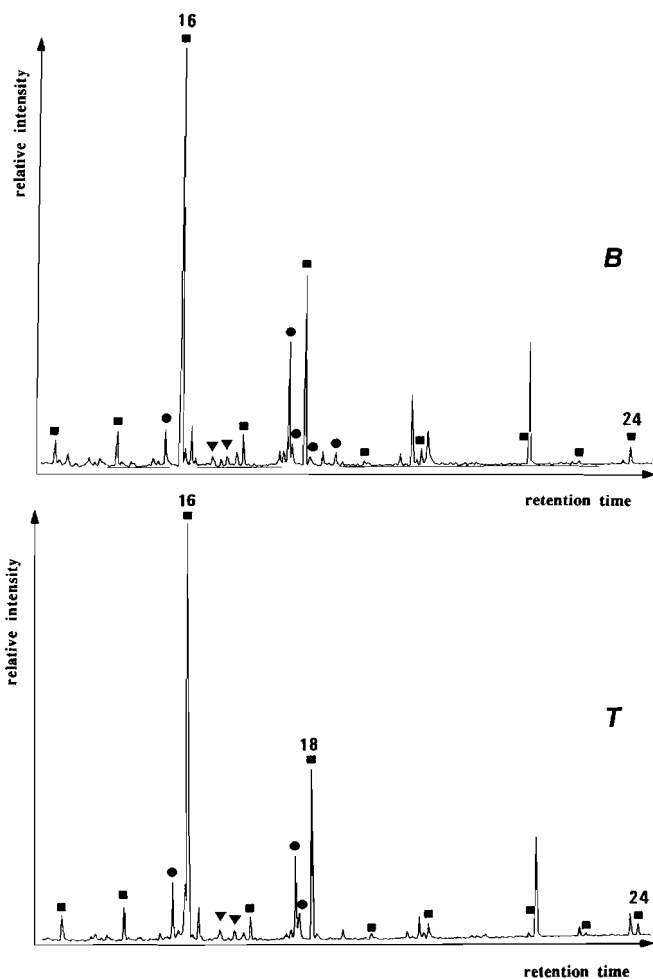


Fig. 7.4 TIC traces of the acid fractions from "off-line" pyrolysates of samples B and T. Filled squares and circles indicate saturated and unsaturated fatty acids, respectively; filled triangles indicate branched saturated acids.

Polar products

Fatty acids. The nature and the relative abundances of the fatty acids generated upon pyrolysis of kerogens B and I are illustrated in Fig. 7.4. In both cases the acid fraction is dominated by palmitic acid and also comprises substantial levels of stearic and *n*-C₂₂ saturated acid. The main series in these fractions thus corresponds to C₁₄-C₂₄ normal saturated acids that are characterized by a very strong predominance of the even-carbon-numbered compounds, with Carbon Preference Indexes (CPI)* of 0.12 and 0.10 from samples B and I, respectively. Substantial amounts of normal monounsaturated C₁₆ and C₁₈ acid are also observed, along with low levels of diunsaturated C₁₈ acids including the ω(9) cis, ω(12) cis isomer (linoleic acid). A very low contribution of branched, iso and anteiso, saturated C₁₇ compounds is also noted. Comparison of B and I (Fig. 7.4) reveals almost identical compositions regarding both their nature and their relative abundances, for the acids released upon pyrolysis.

Fatty acids from extant microalgae and higher plants are generally characterized by a marked predominance of even normal fatty acids, comprising substantial amounts of unsaturated compounds along with saturated acids. However, it is well documented that fatty acids, especially the unsaturated ones, are highly sensitive to microbial degradation. Accordingly, both fatty acids esterified into lipid structures and occurring in a free form are markedly altered during early diagenesis, as reflected by a sharp decrease in the predominance of the even compounds and a nearly complete disappearance of the unsaturated acids. Nevertheless, it has been recently shown that fatty acids can escape to diagenetic degradations when they are included, as esters, in insoluble and non-hydrolysable macromolecules like algaenans (Largeau *et al.*, 1986; Kawamura *et al.*, 1986; Fukushima and Ishiwatari, 1988; Derenne *et al.*, 1991b). Such "tightly bound" fatty acids can only be released by a thermal stress and the corresponding ester moieties remain nearly unaffected following diagenesis owing to the very efficient protection provided by the macromolecular network. As a result, the fatty acid fractions generated by pyrolysis of kerogens derived from algaenan selective preservation are characterized by a very low level of alteration.

Fatty acids may also be protected from diagenetic degradation *via* a second way, based on sulphur incorporation. As already stressed, if "vulcanization" reactions take place during early diagenesis, various lipids can be involved in the formation of insoluble macromolecular structures. Such lipids, including their fatty acid moieties, are then efficiently protected and, owing to this acquired resistance, they will only undergo negligible alterations after the "vulcanization" step.

The presence in kerogen pyrolysates of fatty acids which distribution reveals a low level of alteration should therefore reflect a contribution of the selective preservation of algaenans and/or the occurrence of a fast "vulcanization" during early diagenesis. In fact, these two mechanisms of fatty acid protection appear to be important in B and I kerogens, respectively. The very low level of alteration observed in the acid fractions of their pyrolysates is

*Calculated according to Bray and Evans (1961).

thus consistent with (i) the formation of the brown AOM, that predominates in B, *via* algaenan selective preservation and (ii) the formation of the orange AOM, accounting for the bulk of I, *via* lipid "vulcanization".

Non-acid compounds. GC-MS analysis of the non-acid polar fractions only indicated the presence of phenolic compounds. Their distribution is illustrated in Fig. 7.5 in the case of kerogen B. A similar distribution is also observed from sample I although the relative abundance of these phenols is substantially lower (1.5-2 times), as shown by comparison of the GC traces of the crude pyrolysates. A number of phenols, including series of alkyl-substituted compounds, are generated upon pyrolysis of both B and I. However, the subfractions are dominated by mono- and dimethyl products. The latter phenols are well known as typical pyrolysis products of diagenetically-altered lignins (Nip *et al.*, 1987). As already discussed, electron microscopy observations on picked out particles showed the prevalence of minute ligneous debris in the black AOM. In addition, the latter material is relatively more abundant in sample B than in I. Such features, added to the above results on the nature and abundance of phenols in pyrolysates, indicate that a part of the black AOM of Kimmeridge Clay kerogens is of a terrestrial origin and is derived from lignins.

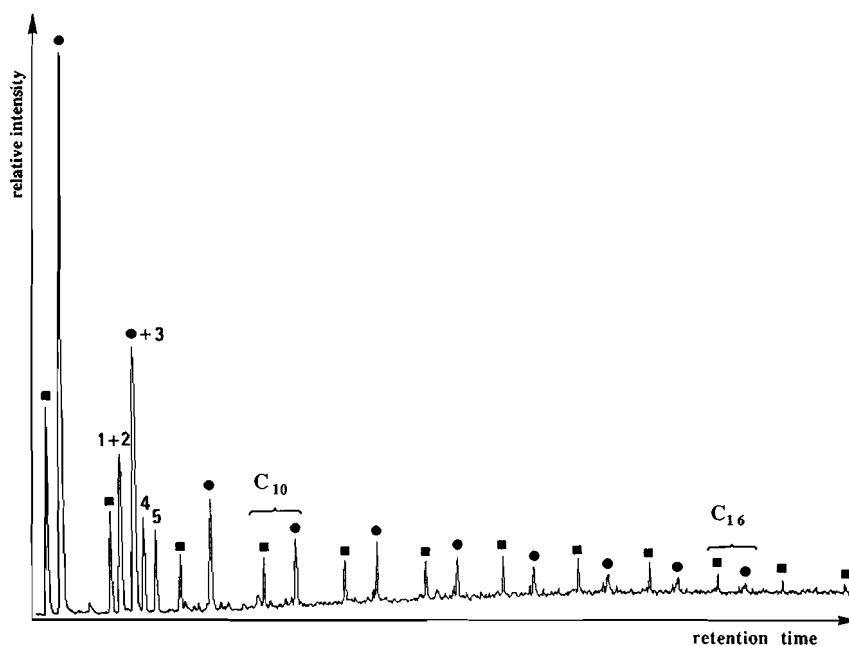


Fig. 7.5 Summed mass chromatogram of m/z 107+108 revealing the distribution of *n*-alkylphenols in the total "off-line" pyrolysate of sample B. Filled squares indicate the homologous series of *ortho-n*-alkylphenols and filled circles indicate the homologous series of the coeluting *meta*- and *para-n*-alkylphenols. Numbers correspond to the following dimethylphenols: 1 = 2,4-dimethylphenol, 2 = 2,5-dimethylphenol, 3 = 3,5-dimethylphenol, 4 = 2,3-dimethylphenol, 5 = 3,4-dimethylphenol. A similar mass chromatogram was obtained for kerogen I

The information obtained from the electron microscopy and pyrolytic studies, on the ultrastructure, the source organisms and the mechanism of formation of the different types of AOM in the Kimmeridge Clay are summarized in Table 7.3. Based on these results, and on the variations in AOM relative abundances, a general scheme accounting for the occurrence of TOC and HI microcycles in the Kimmeridge Clay Formation can be established.

Table 7.3. Relationships between the ultrastructural features, the typical pyrolysis products and the origin of the different types of AOM occurring in Kimmeridge Clay kerogens

Ultrastructure and AOM type	Typical pyrolysis products *	Process of formation
Massive nanoscopically amorphous orange AOM	Organic sulphur compounds	Lipid "vulcanization"
Ultralaminae of brown AOM	Alkyl nitriles	Algaenan selective preservation
Minute ligneous debris of black AOM	Alkylphenols	Altered lignin preservation
Nanoscopically amorphous matrix of brown and/or black AOM	Branched alkanes	Contribution of bacteran selective preservation

* Fatty acids cannot be related with a given AOM type; they can be associated with any fraction described in this Table except the lignin-derived debris in the black AOM.

Origin of TOC and HI cycles

Previous studies indicated that cyclic variations in the Kimmeridge Clay can result neither from changes in redox conditions (because bottom water remained continuously anoxic during deposition, as shown by the lack of bioturbation and the analysis of inorganic trace elements), nor from changes in the extent of organic matter dilution by detrital and/or biogenic minerals (Tribovillard *et al.* 1992, 1994; Bertrand and Lallier-Vergès, 1993). Accordingly, the typical cycles occurring in the Kimmeridge Clay probably reflect changes in the primary productivity of phytoplanktonic species without mineral tests (Bertrand and Lallier-Vergès, 1993; Bertrand *et al.*, 1994). In addition, examination of kaolinite distribution, also carried out on Kimmeridge Clay samples from the Marton 87 borehole, pointed to a climatic origin for the above changes in primary productivity (Desprairies *et al.*, 1995).

It is well documented that increasing phytoplankton productivity is associated with faster sinking rates (Wefer, 1989). The resultant higher export to deep water is due to the formation of aggregates and flakes (Jackson, 1990). As a result, a larger proportion of the degradable constituents of the primary microalgal biomass can escape mineralization in the upper part of the water column and thus reach the oxic-anoxic interface. This increasing supply of metabolizable organic matter to anoxic bottom water should promote a prolific

growth of sulphate-reducing bacteria (an ubiquitous group of micro-organisms in anoxic environments containing both sulphate and organic matter sources, Widdel, 1988; Trudinger, 1992; Elsgaard *et al.*, 1994) hence an intense production of hydrogen sulphide. The latter will rapidly react with available iron to generate iron sulphides; however a part may react with various lipids according to the already mentioned "vulcanization" process. Lipidic compounds that, otherwise, would be heavily degraded may escape mineralization *via* this process. Owing to such an acquired resistance, the above lipids will contribute to kerogen formation and a large increase in TOC in the corresponding sediments is thus achieved. (This is also supported by a recent study (Lallier-Vergès *et al.*, 1994) concerned with sulphur content in the Kimmeridge Clay (total S, organic S, pyrite) and suggesting an important role for sulphate reduction intensity in controlling organic matter accumulation). All these interrelationships between primary productivity, sinking rates and sulphate-reduction intensity, and the resulting control on TOC values, as illustrated in Fig. 7.6, are fully consistent with the present morphological and chemical results. Thus an increasing "vulcanization" should be reflected by the formation of high TOC sediments with an abundant content of orange AOM, as observed at the top of the cycle. Moreover, the morphology of the orange AOM particles and their close association with sulphate-reduction markers (iron sulphides) and clays indicate that such a material was probably generated very early as flocks or mats.

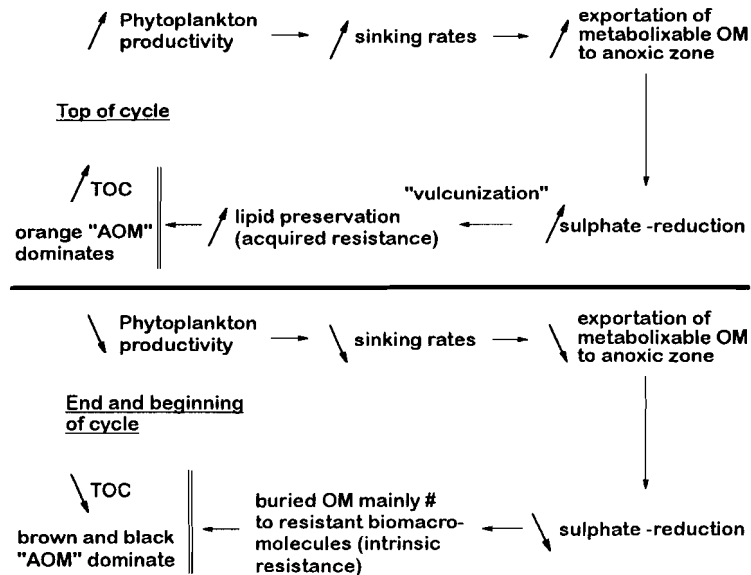


Fig. 7.6 Postulated relationships between primary productivity, sulphate reduction intensity, TOC and HI microcyclic variations, and the dominant type(s) of AOM in Kimmeridge Clay kerogens.

As shown in Fig. 7.6, decreasing primary productivity will result in lower sinking rates. Extensive mineralization of the degradable constituents of microalgae will therefore take place in the oxic part of the water column. Accordingly, only a weak sulphate reduction intensity will develop in anoxic bottom water. Under these conditions the amount of buried organic matter will be relatively low and chiefly comprised of biomacromolecules exhibiting a high intrinsic resistance to diagenetic degradations such as the refractory constituents of algal cell-walls and (to a lesser extent) lignins. Indeed, the kerogen samples corresponding to relatively low TOC's, *i.e.* at the beginning and the end of the cycle, exhibit a low content of orange AOM and are dominated by the brown and black AOM's.

The interrelationships illustrated in Fig. 7.6 can also account for the cyclic changes in HI occurring, along with TOC variations, in the Kimmeridge Clay Formation. Thus, the high HI values observed at the top of the TOC cycle result from the marked predominance of the orange AOM. The latter, being derived from sulphur incorporation into long chain lipids, should be characterized by a high oil generation potential. Resistant biomacromolecules from algal cell walls are known to be highly aliphatic. As a result, the relatively abundant presence of brown, ultralaminae-composed, AOM in kerogen samples with lower TOC, corresponding to the beginning and the end of the cycle, will favour high values for HI. In sharp contrast the black AOM, mainly derived from lignins, shall be characterized by extremely low HI. The substantial contribution of this material in the samples with lower TOC account for their relatively low HI. Moreover, in such samples with TOC values around 2%, a mineral matrix effect (Espitalié *et al.*, 1980; Katz, 1983) may also contribute to HI lowering.

7.5 CONCLUSIONS

The combination of high resolution sampling of a Kimmeridge Clay microcycle, of transmission electron microscopy observations on total isolated kerogens, on hand-picked kerogen particles and on untreated rock fragments, along with flash and off-line pyrolytic studies allowed:

- 1) Precise information to be derived on the morphological features of the three types of so-called "amorphous" organic matter previously defined by light microscopy in the Kimmeridge Clay. The orange AOM is truly amorphous whereas the brown AOM is chiefly composed of ultralaminae and the black AOM of minute ligneous debris embedded within a diffuse nanoscopically amorphous matrix. It was also shown that the maceral bituminite, observed *in situ* from polished sections, corresponds to the orange AOM identified in palynofacies studies.
- 2) Elucidation of the sources and modes of formation of the three above types of organic matter. The orange AOM originates from sulphur incorporation into lipids, whereas the brown AOM is derived from the selective preservation of algaenan-composed thin outer walls of microalgae. The black AOM is likely to be highly heterogeneous and it was shown to comprise contributions from altered lignins and selectively preserved bacterans.

- 3) Explanation of (i) the large changes in the relative abundances of the three types of AOM occurring, in Kimmeridge Clay kerogens, along a *ca* 30,000 years microcycle and (ii) the origin of the parallel, cyclic, wave-shaped variations in kerogen quantity (TOC) and quality (HI) typical of the Kimmeridge Clay Formation. Such variations stemmed from modifications in primary productivity rate. However, the production of microalgal biomass did not exert a direct and simple control on TOC and HI. In fact, the extent of lipid "vulcanization" was probably a major parameter that strongly amplified the effects of primary productivity variations originating from global environmental changes. The values of TOC and HI and the relative abundances of the different types of AOM in the Kimmeridge Clay appear therefore to be controlled by a balance between a number of interrelated processes concerned both with the nature of the deposited biomass and deposition conditions : (i) the extent of terrestrial material contribution (minute ligneous debris of the black material), (ii) the level of resistant biomacromolecules in the source micro-organisms (algaenans and bacterans forming, *via* selective preservation, the bulk of the brown material (ultralaminiae) and a part of the amorphous matrix of the black and/or brown AOM's, respectively) (iii) the intensity of lipid "vulcanization" leading to the orange material. This intensity being controlled by several factors including the amount of metabolizable organic matter reaching the oxic-anoxic interface, the occurrence of suitable conditions, in anoxic bottom water, allowing for a prolific growth of sulphate-reducers and a somewhat limited supply of iron so that the produced H₂S is not entirely trapped as pyrite. Finally, the first of the above parameters is determined, in turn, by the depth of the oxic part of the water column and by primary productivity-controlled sinking rates. The OM accumulated in the Kimmeridge Clay thus chiefly originates from the contributions of both macromolecular compounds with a high intrinsic resistance to diagenetic degradations, like algaenans, bacterans and lignins, and lipidic components that acquired a resistant nature *via* "vulcanization". Kerogen quality (HI) reflects the balance between these different contributions, high HI values being promoted by large levels of "vulcanized" lipids and/or selectively preserved algaenans.

Acknowledgements - Financial support was provided by the Research Group GdR 942 (CNRS, IFP, Total, Elf Aquitaine, Universités d'Orléans et de Paris-Sud). A special thank is devoted to all the scientists of this Research Group. We are also indebted to D. Jalabert from the "Service central de microscopie électronique de l'Université d'Orléans" for its technical assistance. We are grateful to the reviewers, Drs. T. I. Eglinton, B. Horsfield and S. W. Imbus and the Associate Editor for constructive comments.

Molecular indicators for palaeoenvironmental change in a Messinian evaporitic sequence (Vena del Gesso, Italy): III. Stratigraphic changes in the molecular structure of kerogen in a single marl bed as revealed by flash pyrolysis*

François Gelin, Jaap S. Sinninghe Damsté, Wayne N. Harrison, James R. Maxwell and Jan W. de Leeuw

8.1 ABSTRACT

Kerogens of nine samples from a single marl bed of the Gessoso-solfifera Formation in the Vena del Gesso basin (Messinian, Italy) were qualitatively and quantitatively studied by analytical pyrolysis. Relationships between the nature of the pyrolysis products and the source organisms were determined. The high abundance of (i) algal-derived components (*n*-alkanes and *n*-alk-1-enes) and (ii) sulphur-containing and sulphur-bound products signifying a high degree of early diagenetic sulphurization were observed. Presence of photic zone anoxia during the deposition of these sediments was discussed *via* the presence of 1,2,3,4-tetramethylbenzene in the pyrolysates. Unusual distributions were found for three series of pyrolysis products (*i.e.* C₁₃ and C₁₄ *n*-alkylated thiophenes and thiolanes and C₁₂ and C₁₃ *n*-1,3-alkadienes were by far the major products of these series) in the pyrolysates of two samples corresponding to the middle of the cycle (samples 3 and 5) which also have the highest $\delta^{13}\text{C}_{\text{TOC}}$ values and the highest pyrolysis yields. Therefore, the contribution of organisms biosynthesizing resistant algal biopolymer was considered as much more important during the deposition of the sediments associated with samples 3 and 5. We finally proposed partial structural elements from which the specific low molecular weight compounds of samples 3 and 5 can be derived upon pyrolysis.

8.2 INTRODUCTION

Free and sulphur-bound lipids, and free pigments, present in the extracts of ten samples from marl bed IV of the Vena del Gesso basin have been examined by Kenig *et al.* (1995) and Keely *et al.* (1995), respectively. Differences in component concentrations implying changes in the major source organisms and in degree of sulphurization of organic matter and changes in depositional setting

**Org. Geochem.* 23, 555 (1995)

were observed. However, the extracts represent only *ca.* 5% of the organic matter (OM). Hence, qualitative and quantitative investigations of components which can be released from the kerogens are necessary in order to extend the geochemical informations which can be obtained about the source organisms, depositional conditions and degree of sulphurization. The products released from the kerogens by Li/EtNH₂ treatment have been examined and were found to contain in particular compounds of algal origin (Schaeffer *et al.*, 1995). Flash pyrolysis is considered one of the most powerful analytical tools for exploring the chemical structure of kerogens (*e.g.* van de Meent *et al.*, 1980; Larter, 1984; Nip *et al.*, 1988). Hence, we have used this approach, employing a method that permits quantification of the GC-amenable products obtained by Curie point pyrolysis-gas chromatography.

8.3 EXPERIMENTAL

Samples - Cycle IV of the Messinian evaporitic sequence from the Vena del Gesso sediments (see Vai and Ricci Lucchi, 1977 and Sinninghe Damsté *et al.*, 1995 for geological background) consists of a 1.3 m. thick marl layer deposited under slow sedimentation rates and overlaid by a stromatolitic bed and a thick gypsum bed. The marl layer was split in ten samples, each representing a thickness of *ca.* 13 cm. and are numbered 1 to 10 from base to top. Together they cover the entire marl bed of cycle IV. Sample 9 was not analysed in the present study.

Kerogen isolation by treatment with HCl and HF/HCl is described in Schaeffer *et al.* (1995). Determination of the total organic carbon content (TOC) of the kerogen concentrates was performed by flash combustion using a Carlo Erba NA-1500 analyser (Verardo *et al.*, 1990).

Pyrolysis methods - The kerogen samples were crushed as finely as possible using a pestle and a mortar. A standard, 2,3-dimethyl-5-(1',1'-d₂-hexadecyl)thiophene, was added and each sample was ultrasonicated in dichloromethane under a nitrogen flow. About 20 µg of standard was generally used for *ca.* 20 mg of kerogen. The kerogen samples were pressed on to a flattened ferromagnetic wire and heated by inductive heating (Curie temperature 610°C) for 10 s using a Curie point high frequency generator (Fischer 9425). The gas chromatograph (Hewlett Packard HP-5890) was equipped with a cryogenic unit and programmed from 0°C (5 min) to 320°C (10 min) at a rate of 3°C/min. Separation of the products was achieved by a 25 m fused silica capillary column coated with CP-Sil 5 (0.32 mm I.D.; film thickness 0.45 µm). Helium was used as carrier gas and the temperature of the flame ionisation detector (FID) was 320°C. Identification of the pyrolysis products was performed by Curie point pyrolysis-gas-chromatography-mass spectrometry (Py-GC-MS) using the same pyrolysis and GC-conditions as described above. The column was coupled to the electron impact ion source of a VG Autospec Ultima mass spectrometer (mass range *m/z* 40-800 at a resolution of 1000); cycle time 1.8 s; ionisation energy 70 eV). The concentrations of the pyrolysis products which showed no evidence of coelution were determined by integration of the peak

areas in the FID traces. Integration of peak areas in specific mass chromatograms of selected compounds classes, in combination with the quantified FID data, were used for quantitation. It was assumed that the MS response factors do not vary significantly within each class.

To test the validity of the quantitative pyrolysis method, ten analyses of sample 4 were carried out at two different standard concentrations (0.92 and 2.49 mg/g kerogen). A selection of 16 peaks scanning the almost entire FID trace were quantified. The relative standard deviations of the 10 measurements for the 16 peaks varied from 17 to 31%, the latter corresponding to the less intense peak, thus causing larger integration errors.

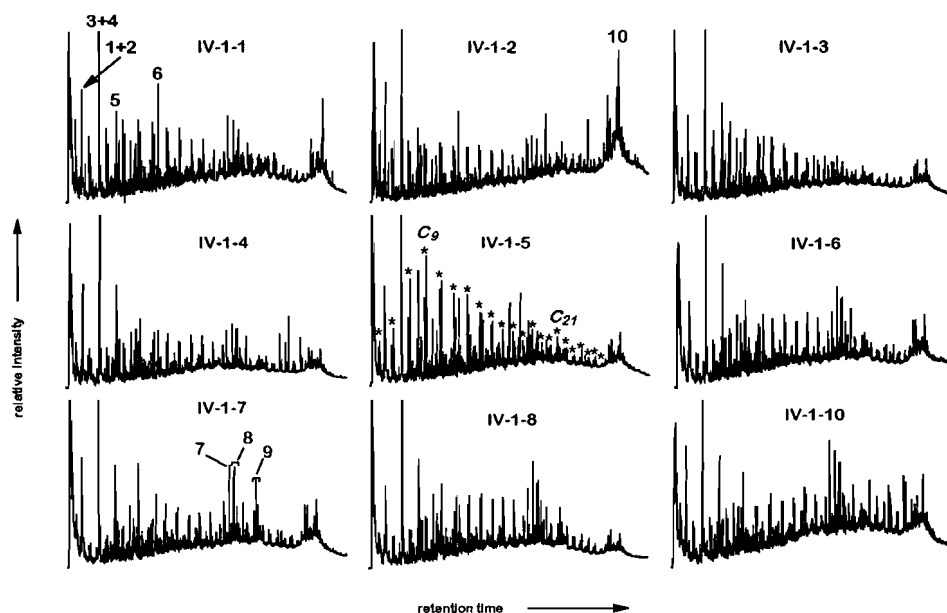


Fig. 8.1 FID trace of the flash pyrolysates of kerogens 1-8 and 10. Stars indicate (only shown for sample 5) the doublets of *n*-alkanes/*n*-alk-1-enes, the italic numbers indicating the carbon numbers. Peak numbers identify the indicated pyrolysis products as (1) benzene, (2) thiophene, (3) toluene, (4) 2-methylthiophene, (5) *m*-xylene + *p*-xylene, (6) 1,2,3,4-tetramethylbenzene, (7) prist-1-ene, (8) phytene, (9) thiophenes with a phytanyl skeleton (10) C_{29:1} sterene. Note that these chromatograms reflect analyses without internal standard.

8.4 RESULTS AND DISCUSSION

Identification and significance of pyrolysis products

The gas chromatograms of the flash pyrolysates of the nine isolated kerogens revealed contributions from several series of compounds (Fig. 8.1). Series of *n*-alkanes, *n*-alk-1-enes, alkylated benzenes, alkylated thiophenes,

steranes, sterenes, C_{20} isoprenoid thiophenes, phytanes, alkan-2-ones and fatty acids dominate the pyrolysates of all the samples. Although all the samples released the same series of products, the relative abundances vary significantly. For instance, sterenes are very abundant in the pyrolysate of sample 2, whereas they are present in relatively low abundance in the other samples.

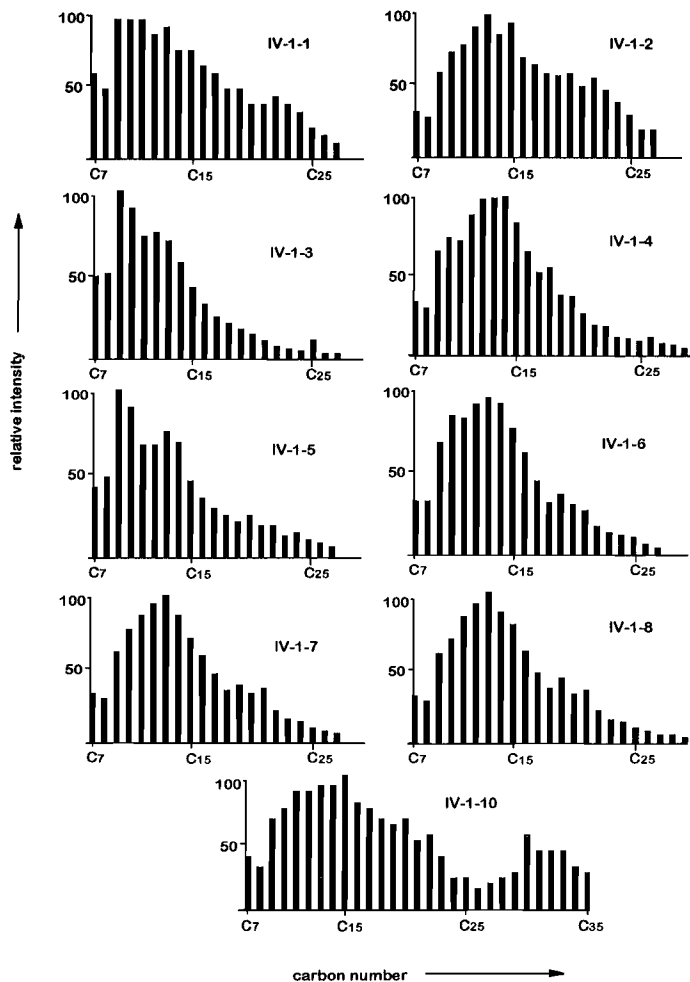


Fig. 8.2 Distribution of *n*-alkanes, determined from mass chromatograms (m/z 57) of the pyrolysates of kerogens 1-8 and 10.

Series of *n*-alkanes and *n*-alk-1-enes in pyrolysates typically reflect the presence of long polymethylenic chains, as shown by studies on the mechanism of pyrolysis of polyolefins (*e.g.* Lattimer, 1994). It is now well known that certain microalgae, especially Chlorophyceae, can produce non-hydrolysable and highly

aliphatic macromolecules, termed "algaenan", which comprise the outer cell walls (Largeau *et al.*, 1984; Goth *et al.*, 1988; Derenne *et al.*, 1992a; de Leeuw and Largeau, 1994). The ability of these macromolecules to resist the bacterial and chemical degradation that takes place during early diagenesis has also been demonstrated. Their potential for preservation is therefore responsible for their presence in many sediments. Furthermore, Eglinton (1994) showed for several different kerogens that the $\delta^{13}\text{C}$ values of *n*-alkanes released by pyrolysis were almost identical for a given kerogen with respect to the carbon number. In most cases the values were close to the $\delta^{13}\text{C}_{\text{TOC}}$ values, demonstrating the importance of the aliphatic macromolecules in kerogens. As shown in Fig. 8.2, the distributions of the *n*-alkanes in the pyrolysates are very similar for samples 4 and 6-8, with a maximum at C_{13} , and for samples 3 and 5, with a maximum at C_9 , respectively. The distribution for sample 10 is different, showing a distribution up to C_{35} . Such long-chain *n*-alkanes are usually found only in the pyrolysates of lacustrine kerogens and of some algaenans derived from freshwater algae (*e.g.* Largeau *et al.*, 1986). It should be noted that desulphurization of sample 10 (and 9) by Li/EtNH_2 treatment released HMW *n*-alkanes up to C_{38} maximizing at C_{30} indicating that the products originate from sulphur-bound lipids which have an unknown source (Schaeffer *et al.*, 1995). In support of this, the desulphurized kerogen (treated with CrCl_2 and Li/EtNH_2) of sample 10 does not release such long-chain *n*-alkanes, upon flash pyrolysis (Gelin *et al.*, 1996b). Desulphurization of the other kerogens also released large amounts of *n*-alkanes (Schaeffer *et al.*, 1995). Desulphurization experiments thus show that a significant part of the linear hydrocarbons in pyrolysates can result from the cleavage of sulphur-containing bonds. These findings are supported by quantitative pyrolyses of the desulphurized kerogens 1-10, which revealed a decrease in the quantity of thermally released *n*-alk-1-enes and *n*-alkanes with respect to the non-treated kerogens (Gelin *et al.*, 1996b). Therefore, the abundance of the alkene/alkane series in the pyrolysates of all the samples is probably due to the presence of selectively preserved algaenans, although a fraction of these hydrocarbons might derive from diagenetically incorporated lipids.

Alkan-2-ones are commonly found in pyrolysates of algaenans and of kerogens known to be composed primarily of algaenans (*e.g.* Largeau *et al.*, 1986). Pyrolytic studies have shown that ketones can be formed by homolytic cleavage of ether bonds (Gelin *et al.*, 1993, 1994a), which participate in the macromolecular network of many algaenans (Gatellier *et al.*, 1993; Derenne *et al.*, 1989; Gelin *et al.*, 1996a). Fig. 8.3 shows the distributions of the alkan-2-ones in the pyrolysates, which slightly differ, although the distributions for samples 3 and 5 are almost identical.

Aromatic components are abundant products and show a dominance of the short-chain alkylated benzenes. The summed mass chromatograms of m/z 78+91+92+105+106+119+120+133+134, revealing the distribution of benzene and C_1 - C_4 alkylated benzenes, differ mainly with respect to the relative abundance of 1,2,3,4-tetramethylbenzene (TMB). This is shown in Fig. 8.4 for three representative samples (2, 5 and 10). The presence of TMB in pyrolysates is attributed to pyrolysis of macromolecularly bound aromatic carotenoids (Hartgers *et al.*, 1991a; Douglas *et al.*, 1991; Requejo *et al.*, 1992). Hartgers *et al.*

al. (1994a,b) demonstrated that TMB in the kerogen pyrolysate of the Devonian Duvernay Formation is derived from macromolecularly-bound isorenieratene and an as yet undiscovered diaromatic carotenoid with a 2,3,6- and 3,4,5- methyl substitution pattern (Hartgers *et al.*, 1993). The occurrence of this latter carotenoid seems, however, to be restricted to the Mesozoic and Paleozoic and so may not have contributed to the Vena del Gesso sediments. The absence of its carbon skeleton in the extracts after desulphurization of the polar and kerogen fractions is in line with this idea (Kenig *et al.*, 1995; Schaeffer *et al.*, 1995). Since isorenieratene is a specific carotenoid of photosynthetic green sulphur bacteria (Liaaen-Jensen, 1978), the presence of TMB in the kerogen pyrolysates suggests the presence of green sulphur bacteria in the palaeoenvironment. Further evidence comes from the presence of isorenieratane in the products from desulphurization of the polar and asphaltene fractions of the extracts (Kenig *et al.*, 1995) and the kerogens (Schaeffer *et al.*, 1995), as well as its ^{13}C content. In addition, the intact carotenoid precursor occurs in the extracts (Keely *et al.*, 1995). Since the occurrence of green sulphur bacteria require the presence of both light and hydrogen sulphide, they indicate photic zone anoxia (*cf.* Sinninghe Damsté *et al.*, 1993a).

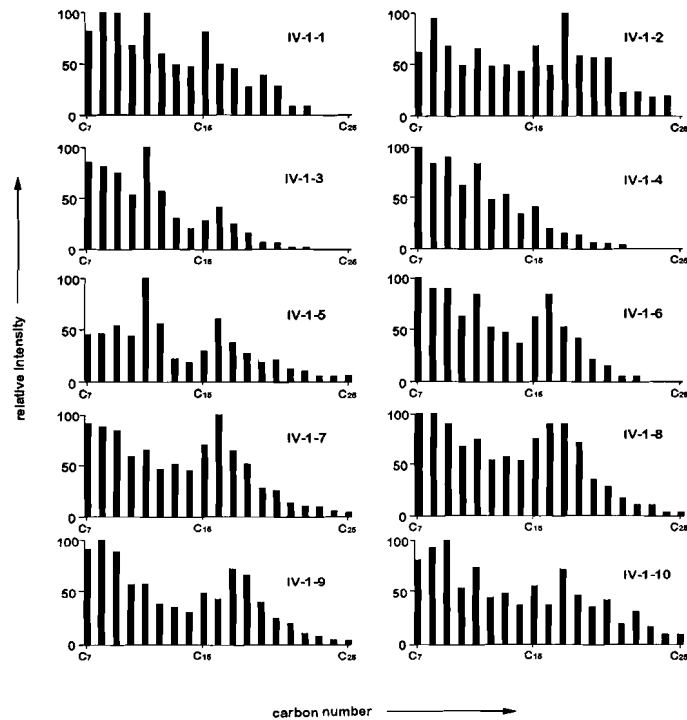


Fig. 8.3 Distribution of *n*-alkan-2-ones, determined from mass chromatograms (m/z 58) of the pyrolysates of kerogens 1-8 and 10.

Sulphur-containing components are abundant in all the pyrolysates indicating a high abundance of organic sulphur compounds in the kerogens (cf. Eglinton *et al.*, 1990). Series of thiophenes and thiolanes are dominated by compounds with linear carbon skeletons (*i.e.* 2-alkylthiophenes and 2-alkyl-5-methylthiophenes). It has been shown that incorporation of inorganic sulphur species into aliphatic macromolecules forms thiophenes, thiolanes and benzothiophenes with linear carbon skeletons (Douglas *et al.*, 1991). Thiophenes with a phytanyl carbon skeleton are also abundant and result mainly from the pyrolysis of (poly)sulphur-bound isoprenoid C₂₀ compounds derived from phytol (*e.g.* Sinninghe Damsté *et al.*, 1987; Schouten *et al.*, 1993). Phytanes, the predominant pyrolysis products in the carbon number range C₁₇ to C₂₅ are also likely to derive from such moieties. Pyrolysis of ester-bound phytol produces preferentially phytadienes (van de Meent *et al.*, 1980), which are in low abundance in the pyrolysates, suggesting that most of the phytanyl moieties are probably sulphur-linked to the matrix.

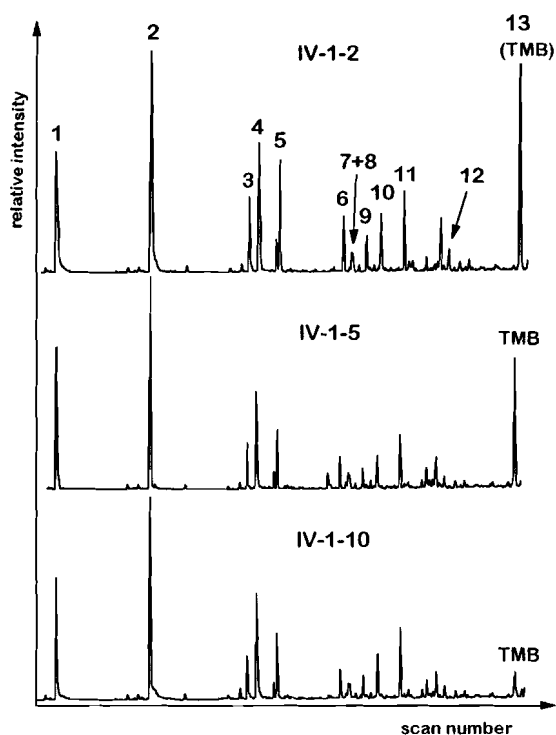


Fig. 8.4 Partial summed mass chromatograms of m/z 78+91+92+105+106+ 119+120+133+134 revealing the distributions of benzene and C₁-C₄ alkylated benzenes (identified according to Hartgers *et al.*, 1991) in the flash pyrolysates of the indicated kerogens. Key: 1 = benzene, 2 = toluene, 3 = ethylbenzene, 4 = *m*-xylene + *p*-xylene, 5 = *o*-xylene, 6 = propylbenzene, 7 = 1-ethyl-3-methylbenzene, 8 = 1-ethyl-4-methylbenzene, 9 = 1-ethyl-2-methylbenzene, 10 = 1,2,3-trimethylbenzene, 11 = 1,2,4-trimethylbenzene, 12 = butylbenzene, 13 = 1,2,3,4-tetramethylbenzene (TMB).

A high abundance of steranes in the desulphurized polar and asphaltene (Kenig *et al.*, 1995) and kerogen (Schaeffer *et al.*, 1995) fractions has been reported, indicating a significant extent of sulphurization of the precursor steroids. It is therefore not surprising to find these compounds in the pyrolysates. The main products were assigned as C₂₇ and C₂₉ steranes and sterenes. Furthermore, as reported by Kohnen *et al.* (1993), the flash pyrolysate of the polar fraction of another Vena del Gesso marl, the C₂₇ steranes comprise a mixture of cholest-2-enes, cholest-3-enes, cholest-4-ene and cholest-5-ene, which indicates the presence of sulphur-linkages at C-2, C-3, C-4 and C-5 positions of the steranes. The high relative abundance of these pyrolysis products is probably in part the consequence of significant sulphurization of organic matter during early diagenesis. Ester-bound steroid hydrocarbons are also present in the kerogen as revealed by the Li/EtNH₂ treatment, which yielded high abundance of sterols (Schaeffer *et al.*, 1995). Therefore, the presence of steroid hydrocarbons in the pyrolysates probably reflects both sulphur- and ester-bound moieties.

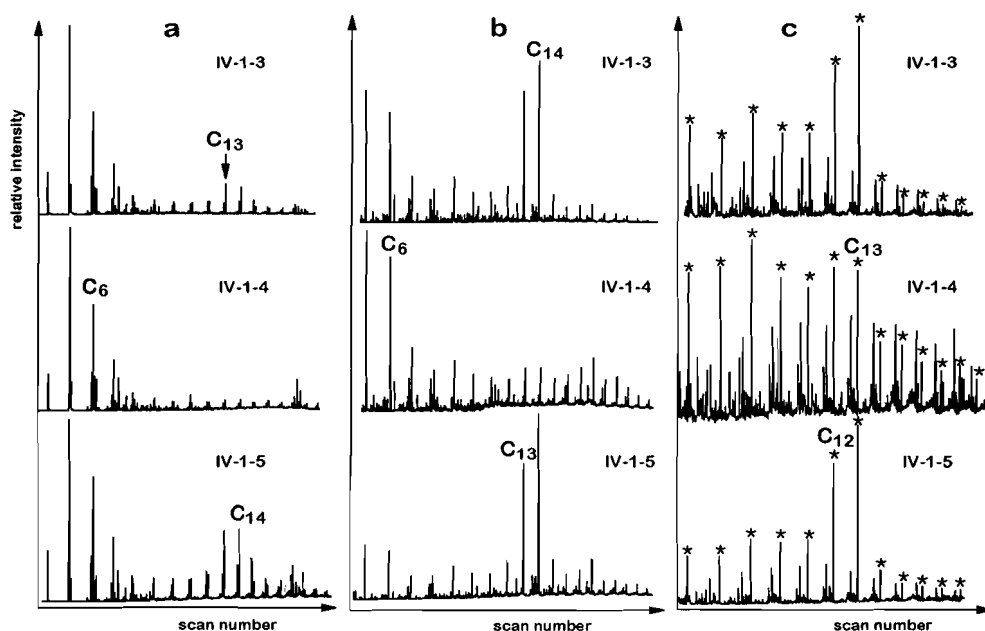


Fig. 8.5 (a) Partial summed mass chromatograms of m/z 84+97+98+111+112+125+126+139+140 revealing the distributions of thiophene and alkylated thiophenes in the flash pyrolysates of the indicated kerogens, (b) partial, accurate mass chromatograms of m/z 87.02 revealing the distributions of the C₅-C₂₃ thiolanes in the flash pyrolysates of the indicated kerogens and (c) accurate mass chromatograms of m/z 54.03 revealing the distributions of the *n*-1,3-alkadienes (indicated by the stars) in the flash pyrolysates of the indicated kerogens.

Three series of compounds differ significantly from the rest in the pyrolysates of kerogens 3 and 5. In these cases, series of alkylthiophenes, alkylthiolanes and 1,3-alkadienes have distributions with two dominant compounds, the C₁₃ and C₁₄ *n*-alkylthiolanes and -thiophenes and the C₁₂ and C₁₃ 1,3-alkadienes (Figs. 8.5(a-c)). These Figs. display only the mass chromatograms of samples 3 and 5 together with sample 4 which generated similar mass chromatograms as the six other kerogen pyrolysates. It is also noteworthy that for the three series this phenomenon is more pronounced in sample 5 than sample 3, revealing that these pyrolysis products are certainly correlated with each other.

Quantitative pyrolysis

The concentrations of the pyrolysis products were normalised to total organic carbon (TOC) content of the kerogens. The TOC values range from 10.1 % for sample 4 to 27.7 % for sample 8. The relatively low content in organic carbon is probably due to the high abundance of inorganic sulphur species occurring as pyrite and gypsum. Indeed, removal of pyrite using CrCl₂ from the HF/HCl-treated sediments increased significantly the TOC contents (Schaeffer *et al.*, 1995).

Fig. 8.6(a) shows the concentrations of all the selected pyrolysis products, which comprise *n*-alkanes, *n*-alk-1-enes, benzene and C₇-C₁₀ alkylated benzenes, thiophene and C₅-C₉ alkylated thiophenes, C₂₇ hopene, C₂₇+C₂₉ steranes and sterenes, prist-1-ene, naphthalene and C₁₁-C₁₂ alkylated naphthalenes, benzothiophene and C₉-C₁₀ benzothiophenes, phytanes, thiophenes with a phytanyl carbon skeleton, *n*-alkanoic acids and *n*-alkan-2-ones. It is remarkable that flash pyrolysis of the kerogens of samples 3 and 5 gave a much higher yield (more than 300 mg/g TOC for the selected products only) than the pyrolysates of the kerogens isolated from the other sediments of this marl (from 32 mg/g TOC for samples 4 and 10 to 167 mg/g TOC for sample 1).

As expected, the series of *n*-alkanes, *n*-alk-1-enes, and the alkylated benzenes and thiophenes, which represent the bulk of the pyrolysates, follow a trend similar to the total yield (*cf.* Figs. 8.6(b) and 8.6(c) with 8.6(a)). It is also not surprising that the depth profile of the *n*-alkanones (Fig. 8.6(d)) also follows that of the *n*-alkanes and *n*-alkenes, since these three series are believed to derive from pyrolysis of algal aliphatic macromolecules (Largeau *et al.*, 1986). The depth profile of prist-1-ene, which originates from the pyrolysis of bound tocopherol units (Goossens *et al.*, 1984), is also similar to the previous ones (Fig. 8.6(e)). It is surprising, however, that the TMB depth profile (Fig. 8.6(f)) also follows the same trend, since the source of this compound is green sulphur bacteria and not algae. Indeed only three classes of pyrolysis products do not follow the *n*-alkane trend; these are thiophenes with a phytanyl skeleton, phytanes and sterenes (Figs. 6(g,h)). These three classes are all generated, at least in part, from S-bound moieties in the kerogens. Phytanes and sterenes are probably formed from a direct elimination of a (poly)sulphide linkage. However, sterenes may to some extent also derive from a direct elimination of ester-bound sterols (Schaeffer *et al.*, 1995). Thiophenes with a phytanyl skeleton are probably formed by pyrolysis of polysulphide-bound phytanyl moieties

(Koopmans *et al.*, 1995). In contrast, *n*-alkanes and *n*-alk-1-enes derive from the pyrolytic cleavage of long polymethylene chain as a result of a radical-chain mechanism pathway (see Poutsma, 1990 for a review).

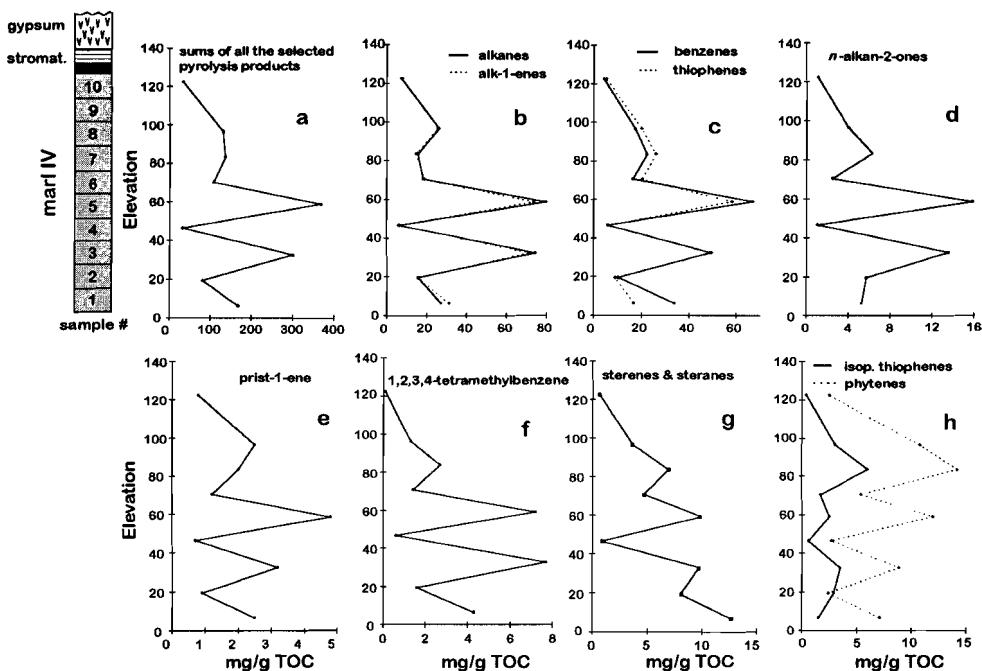


Fig. 8.6 Depth profiles of the concentration of products in the flash pyrolysates. (a) Sum of all selected (main) pyrolysis products; (b) *n*-alkanes and *n*-alk-1-enes; (c) C_0 - C_4 alkylated benzenes and C_0 - C_5 alkylated thiophenes; (d) *n*-alkan-2-ones; (e) prist-1-ene; (f) 1,2,3,4-tetramethylbenzene; (g) $C_{27} + C_{29}$ steranes and sterenes; (h) phytanes and thiophenes with a phytanyl skeleton. A lithological column is indicated for reference.

The difference between mechanisms for the formation of phytanes, sterenes and isoprenoid thiophenes on the one hand and the rest of the pyrolysis products on the other hand could explain the different yields. Indeed, the free radical pathway which dominates in the thermal dissociation of C-C bonds leads to the formation of very unstable radicals which will "catalyse" the pyrolysis of the rest of the organic matrix by their need to stabilise by hydrogen transfer. This phenomenon could explain why the yield of pyrolysis products from different sources (*e.g.* alkanes vs. TMB) and structures (*e.g.* benzenes vs. thiophenes) can follow a similar trend. The depth profile of the phytanes, isoprenoid thiophenes and sterenes, which are probably formed by elimination independent from the free radical pathway is therefore different from the main trend.

The comparison of Figs. 8.6(f) and 8.3 clearly demonstrates the necessity to quantify the kerogen pyrolysates. The absolute concentration of TMB in the pyrolysate of sample 5 is much higher than that in sample 2 whilst the relative intensity of TMB is higher in the mass chromatogram of sample 2 (Fig. 8.3). However, a stronger contribution of TMB to the pyrolysates does not necessarily indicate a higher abundance of aromatic carotenoid-derived moieties since the concentration of TMB depends on the degree of sulphurization of organic matter and on the degree of catalysis during pyrolysis (see above). The relatively high contribution of TMB in most of the pyrolysates can only be interpreted as an indication for photic zone anoxia but does not tell about the importance of the latter. However, the absence of TMB in the pyrolysate of the kerogen from the top layer of this marl (sample 10) confirms the absence of photic zone anoxia during deposition of that sediment as also revealed by studies of the extracts (Kenig *et al.*, 1995; Keely *et al.*, 1995) and the kerogens (Schaeffer *et al.*, 1995).

Origin and structure of the main component of kerogen from samples 3 and 5.

As reported by Kenig *et al.* (1995), $\delta^{13}\text{C}_{\text{TOC}}$ values for samples 3 and 5 are more enriched than those of other samples. These excursions in δ -values are followed by C_{16} , C_{31} and C_{32} *n*-alkanes released by desulphurization of the polar fractions of the extracts (Kenig *et al.*, 1995), indicating that organisms which are the precursor for these S-bound alkanes are probably also major contributors of kerogen in sample 3 and 5. Koopmans *et al.* (1995), in artificial maturation experiments with the same marl, showed the presence of long-chain thiophenes with the sulphur atom predominantly attached at position 15 of the linear carbon skeleton and attributed this to sulphurization of C_{30} - C_{32} 1,15-alkyl diols and alkyl-15-one-1-ols or their diagenetic derivatives. It is well documented that saturated and mono-unsaturated C_{30} - C_{32} 1,15-alkyl diols are present as bound lipids in marine microalgae of the class Eustigmatophyceae (Volkman *et al.*, 1992; Gelin *et al.*, 1996a). These diols and C_{28} - C_{32} alkan-15-one-1-ols were found in many recent marine sediments (*e.g.* de Leeuw *et al.*, 1981; Morris and Brassell, 1988). Furthermore, it was recently demonstrated that the marine eustigmatophyte *Nannochloropsis salina* biosynthesizes highly aliphatic algaenans probably composed of ether-linked C_{30} - C_{32} units (Gelin *et al.*, 1996a). Although fossil eustigmatophytes are still unknown, Hibberd (1979) suggested that this group of algae might resemble a common ancestor of other important groups of algae, *i.e.* Xanthophyta and Chrysophyta. These findings suggest that a significant part of the kerogens of samples 3 and 5 derives from a similar origin which may be algaenan derived from Eustigmatophyceae microalgae or is formed by sulphurization of diols or keto-ols from Eustigmatophyceae.

The results obtained by flash pyrolysis of the kerogens strongly support this hypothesis. The kerogens from sample 3 and 5 are completely different from the kerogen of the other samples because of (i) their much higher pyrolysis yields and (ii) the characteristic distribution of the *n*-alkanes, alkan-2-ones, alkylated thiophenes, alkylated thiolanes and 1,3-alkadienes (Figs. 8.2, 8.4 and 8.5(a-c), respectively). Both observations can be linked to the presence of algaenan derived from eustigmatophytes or sulphurized diols or keto-ols from these algae.

This conclusion can be corroborated by proposing a schematic mechanism that shows the formation of 1,3-dodecadiene, 1,3-tridecadiene, 2-nonylthiolane, 2-decylthiolane, 2-nonylthiophene and 2-decylthiophene and hexadecan-2-one, as significant products in their respective compound classes, from the pyrolysis of geomacromolecules derived from unsaturated C_{30} alkyl-1,15-diol or alkyl-15-one-1-ol precursors (Fig. 8.7). Structure I, a hypothetical macromolecular entity based on the above considerations, could be diagenetically altered at its point of unsaturation, forming structure IIa with a S-bond at C-20 and structure IIb with a S-bond at C-21. During early diagenesis and upon pyrolysis, structures IIa and IIb could cyclize and aromatize with a C-C cleavage between positions 16 and 17 for IIa and positions 17 and 18 for IIb. As shown in Fig. 8.7, these transformations could lead to the formation of 2-decylthiolane, 2-decylthiophene and also hexadecan-2-one on the one hand and of 2-nonylthiolane and 2-nonylthiophene on the other hand. Elimination of the S-bound moieties of IIa and IIb could create unsaturations at three different positions which could lead, after allylic cleavages and hydrogen transfer, to the formation of C_{11} , C_{12} and C_{13} n -1,3-alkadienes. However, the absence of abundant C_{11} 1,3-alkadienes in the pyrolysates of samples 3 and 5 is not explained with this mechanism.

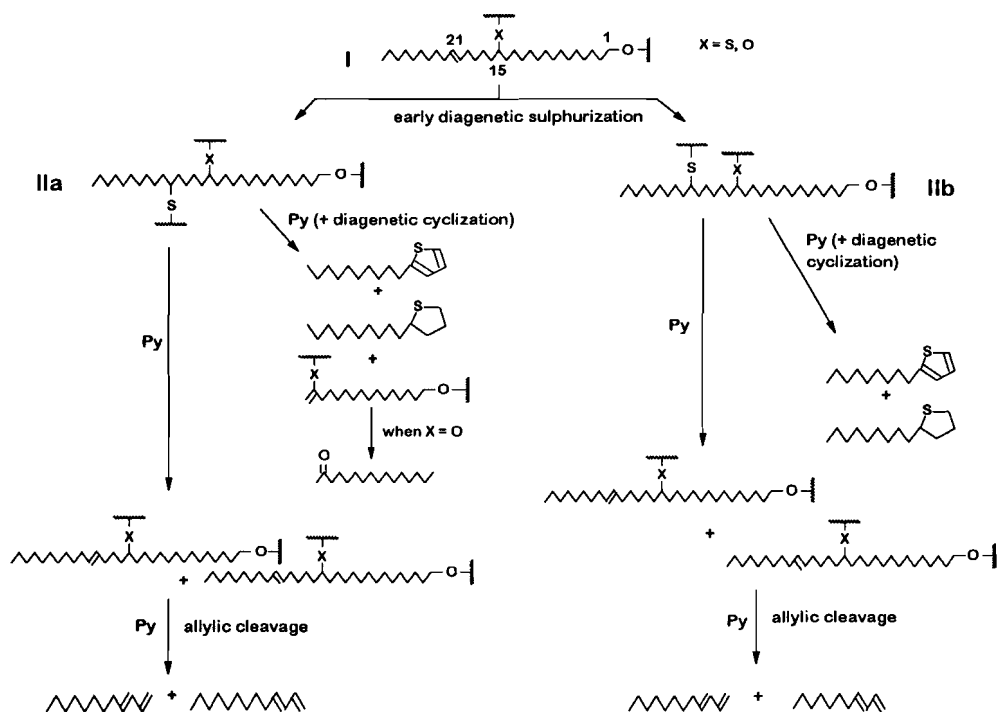


Fig. 8.7 Proposed mechanism of pyrolysis for the formation of C_{13} and C_{14} thiolanes and thiophenes, C_{12} and C_{13} 1,3-alkadienes and hexadecan-2-one from a macromolecular aliphatic matrix.

8.5 CONCLUSIONS

- 1) Quantitative analytical pyrolysis allowed for the determination of a large part of the insoluble organic matter (up to *ca.* 400 mg/gTOC). This method revealed that kerogens of samples 3 and 5 produced a much higher yield upon pyrolysis than the other samples. This also holds for the major pyrolysis products (*n*-alkanes, *n*-alk-1-enes, alkylbenzenes and alkylthiophenes).
- 2) The depth profile of three series of pyrolysis products (phytenes, sterenes and thiophenes with a phytanyl skeleton) do not follow the general trend described above. A different pyrolysis mechanism may be responsible for this difference since the formation of these three series of pyrolysis products is probably due to elimination of (poly)sulphide or ester bonds whilst the major pyrolysis products involve C-C cleavage *via* a free radical pathway.
- 3) Flash pyrolysis revealed that the major contributors to these kerogens were biomacromolecules from microalgae. This contribution is much higher for two samples in the bottom middle of the marl bed (samples 3 and 5) as revealed by the $\delta^{13}\text{C}_{\text{TOC}}$ values, the yields of pyrolysis and the very specific distribution patterns for 2-alkylthiophenes and -thiolanes, methylketones and 1,3-alkadienes. These specific distributions are thought to be related to the presence of an algaenan with 1,15-diols as major building blocks derived from algae of the class Eustigmatophyceae or/and incorporation of 1,15-diols or keto-ols in the kerogen through natural sulphurization.
- 4) 1,2,3,4-Tetramethylbenzene, which is the pyrolysis product revealing the contribution of photosynthetic sulphur bacteria to the OM, is abundantly present in pyrolysates of samples 1-8. This confirms the occurrence of photic zone anoxia during the almost entire marl deposition excepting of as shown by investigations on desulphurized extracts (Kenig *et al.*, 1995; Keely *et al.*, 1995) and kerogens (Schaeffer *et al.*, 1995).

Acknowledgments - This work was performed under the auspices of ENOG (European Network of Organic Geochemists) and has benefited from scientific discussions within the group. ENOG comprises Laboratoire de Géochemie, IFP, Rueil-Malmaison, France; Institute of Petroleum and Organic Geochemistry, KFA, Jülich, Germany; Laboratoire de Chimie Organique des Substances Naturelles associé au CNRS, Université Louis Pasteur, Strasbourg, France; Netherlands Institute for Sea Research, Department of Marine Biogeochemistry, Texel, the Netherlands; Department of Environmental Chemistry, CID-CSIC, Barcelona, Spain; Organic Geochemistry Unit, University of Bristol, UK and receives funding from the European Community (EC contract #ERBSC1*CT91-0736). This work was partly supported by a PIONIER grant to JSSD from the Netherlands Organization for Scientific Research (NWO). We thank Gian Batissta Vai, B.C. Schreiber, Brendan Keely, Peter Hofmann, Jan Ebbing, Stefan Schouten, other members of the ENOG group and the management of the gypsum mine for advice and assistance during sampling. We acknowledge R. Kloosterhuis (NIOZ) for elemental analysis of the isolated kerogens. We also thank W. Pool and M. Dekker (NIOZ) for MS analyses. Drs. B. Horsfield and W. Michaelis provided constructive reviews on an earlier draft of this manuscript

Variations in origin and composition of kerogen constituents as revealed by analytical pyrolysis of immature kerogens before and after desulphurization*

François Gelin, Jaap S. Sinninghe Damsté, Wayne N. Harrison, Christine Reiss, James R. Maxwell and Jan W. de Leeuw

9.1 ABSTRACT

Kerogens isolated from nine samples from of a single marl bed of the Gessoso-solfifera formation in the Vena del Gesso basin (Upper Miocene, Italy) were treated with CrCl_2 and Li/EtNH_2 to remove inorganic and organic sulphur, respectively. The "untreated" and "desulphurized" kerogens were qualitatively and quantitatively analysed by flash pyrolysis-gas chromatography-mass spectrometry. Typically, significant variations in the relative contributions and abundances of *n*-alk-1-enes/*n*-alkanes, alkylated pyrroles, thiophenes and supposedly S-bound moieties released as phytene and sterene were observed. The first series of products contributed relatively more to the pyrolysates of the "desulphurized" kerogens, indicating an enrichment of microalgal-derived aliphatic macromolecules. These marine micro-organisms are thought to belong in part to the class of Eustigmatophyceae. Alkylated pyrroles were hardly detectable in the 'untreated' kerogen pyrolysates, whereas they contributed significantly to those from the Li/EtNH_2 -treated kerogens. Similar treatment of an authentic porphyrin, octaethylporphyrin, revealed that alkylporphyrins are thermally too stable to be cleaved upon pyrolysis. However, Li/EtNH_2 treatment reduced the porphyrin standard, such that it could generate mainly monopyrroles upon pyrolysis. It is concluded that Li/EtNH_2 treatment reduced tetrapyrrole moieties which remained bound to the "desulphurized" kerogen network.

9.2 INTRODUCTION

In marine evaporitic systems, sulphate is often abundant and, under anaerobic conditions, the development of sulphate reducing bacteria in the top layer of the sediments is favoured. These bacteria are thought to affect significantly the preservation of organic matter (OM) by way of two opposite processes. Bacterial reworking and mineralization of the OM generates reduced inorganic sulphur species (H_2S , polysulphides), that may subsequently react with

* Submitted to *Org. Geochem.*

lipids to form low- and high-molecular-weight organic constituents which have a much higher potential of preservation since they are thought to be resistant to further biodegradation. Consequently, kerogens from marine evaporitic environments often contain significant amounts of sulphur-bound organic moieties (for a review see Sinninghe Damsté and de Leeuw, 1990).

To determine the importance and nature of the organic sulphur in such kerogens, to estimate the degree of sulphurization and to identify contributions from source organisms, qualitative and quantitative analyses of the products released by flash pyrolysis of kerogens before and after desulphurization have been performed on nine sub-samples from a marl bed from the Vena del Gesso evaporitic basin (Italy). This study is part of a wider investigation which aims to understand better the processes of kerogen formation and to reconstruct the depositional environment of this particular Miocene marl bed (Schaeffer *et al.*, 1995; Gelin *et al.*, 1995; Kenig *et al.*, 1995). Studies concerning the free lipids and the lipids released after desulphurization of the polar, asphaltene and kerogen fractions have resulted in the palaeoreconstruction of the depositional environment of these sediments to some extent (Kenig *et al.*, 1995; Schaeffer *et al.*, 1995). The aim of the present study is to discriminate diagenetically incorporated kerogen constituents from the preserved biomacromolecules and to estimate the contribution of these two processes during the depositional period in question.

9.3 EXPERIMENTAL

Sample descriptions

Cycle IV of the Messinian evaporitic sequence from the Vena del Gesso sediments (see Vai and Ricci Lucchi, 1977 and Sinninghe Damsté *et al.*, 1995 for geological background) consists of a 1.3 m thick marl layer deposited under slow sedimentation rates and overlaid by a stromatolitic bed and a thick gypsum bed. The marl layer was split in ten samples, each representing a thickness of *ca.* 13 cm and are which numbered 1 to 10 from base to top. Together they cover the entire marl bed of cycle IV. Sample 9 was not analysed in the present study.

Isolation and desulphurization of kerogens

Detailed procedures for the isolation and desulphurization processes have been previously described in detail (Schaeffer *et al.*, 1995). In summary, the samples were Soxhlet-extracted and the residues were sequentially treated with HCl, HCl/HF and KOH. The residues were extracted and dried. The kerogens thus obtained were treated with chromous chloride (CrCl₂) to remove inorganic sulphur, *i.e.* pyrite, following the method of Cranfield *et al.* (1986). The resulting residues were then treated with lithium/ethylamine (Li/EtNH₂) following the method of Hofmann *et al.* (1992).

Flash pyrolyses

The nine samples were analysed by Curie point pyrolysis. The pyrolysis products were identified by Curie-point pyrolysis-gas chromatography (Py-GC) and Curie-point pyrolysis-gas chromatography-mass spectrometry (Py-GC-MS).

The samples were pressed on to a flattened ferromagnetic wire and heated by inductive heating (Curie temperature 610°C) for 10 s using a Curie point high frequency generator (Fischer 9425). The gas chromatograph (Hewlett Packard HP-5890) was equipped with a cryogenic unit and programmed from 0°C (5 min) to 320°C (10 min) at a rate of 3°C/min. Separation was achieved using a 25 m fused silica capillary column coated with CP-Sil 5 (0.32 mm I.D.; film thickness 0.45 µm). Helium was used as carrier gas and the temperature of the flame ionisation detector (FID) was 320°C. Py-GC-MS was performed using the same pyrolysis and GC-conditions as described above. The column was coupled to the electron impact ion source of a VG Autospec Ultima mass spectrometer (mass range m/z 40-800 at a resolution of 1000; cycle time 1.8 s; ionisation energy 70 eV). To the weighted aliquots (*ca.* 20 mg) of "untreated" and "desulphurized" kerogens, 20.6 µg of an internal standard (2,3-dimethyl-5-(1',1'-d₂-hexadecyl)thiophene) was added to allow quantitation of the pyrolysis products. The determination of the concentrations and the validity of this quantitation method has been discussed previously (Gelin *et al.*, 1995). The authors indicated that the relative standard deviation of 10 measurements of 16 peaks in the FID trace varied from 17 to 31%. Such deviation has been taken into account in the discussion of the results presented here.

9.4 RESULTS AND DISCUSSION

As shown for sample 7, flash pyrolysates from the "untreated and "desulphurized" kerogens contain complex mixtures of products, including homologous series of components (Fig. 9.1). Like all the pyrolysates of the "untreated" kerogens, the pyrolysate of this sample is dominated by C₁-C₂ alkylated benzenes and thiophenes (Fig. 9.1a); *n*-alk-1-enes and *n*-alkanes are also abundant and range over the entire TIC trace. Isoprenoid hydrocarbons, *i.e.* prist-1-ene, phytene and thiophenes with a phytanyl carbon skeleton, are major products, though in different relative abundances depending on the sample. Polycyclic compounds, mainly steranes, sterenes and hopenes, are the most abundant HMW pyrolysis products and can be the dominant components, as seen in the pyrolysates of samples 1 and 2.

As determined for sample 2, the flash pyrolysate of the residue after CrCl₂ treatment was very similar to the pyrolysate of the "untreated" kerogen. Although CrCl₂ treatment released up to 60 mg/g_{TOC} (45 mg/g_{TOC} for sample 2) of organic products (Schaeffer *et al.*, 1995), this does not seem to affect the relative composition of the pyrolysate. Significantly, however, relative contributions of the main series of pyrolysis products changed dramatically after Li/EtNH₂ treatment. Whereas aromatic, isoprenoid and steroid products dominate the pyrolysate of the "untreated" kerogens, the series of *n*-alk-1-enes and *n*-alkanes become by far the most dominant products in the "desulphurized" kerogen pyrolysate, as shown for sample 7 (Fig. 9.1b). Hence, if we assume that the GC-amenable pyrolysis products are representative of the whole kerogen (Horsfield; 1989; Larter and Horsfield, 1993), it appears that it becomes much more aliphatic in nature after Li/EtNH₂ treatment and, as suggested by the flash pyrolysis, its structure is dominantly composed of polymethylene units linked by

C-C or C-O bonds (Lattimer, 1994). Also, alkylated pyrroles are observed in high abundance in most of the "desulphurized" kerogen pyrolysates, while they are minor in, or absent from, the "untreated" ones.

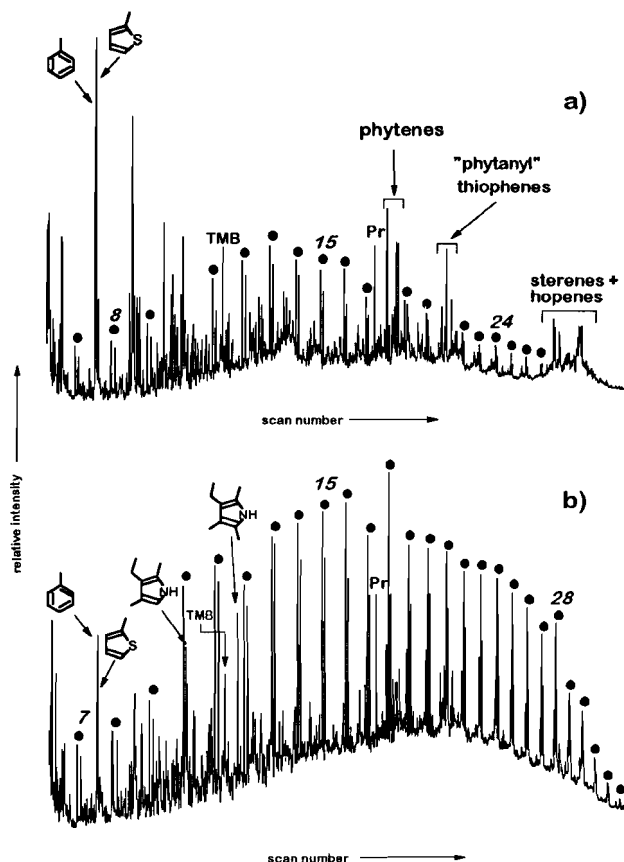


Fig. 9.1 Total ion current chromatograms of the pyrolysates of (a) "untreated" VdG-IV-7 kerogen and (b) "desulphurized" VdG-IV-7 kerogen. Italic numbers indicate the carbon chain length of the *n*-alk-1-ene/*n*-alkane doublets, indicated by filled circles. TMB and Pr represent 1,2,3,4-tetramethylbenzene and prist-1-ene, respectively.

Variations in abundance of organic sulphur components

The organic sulphur content can be estimated by pyrolysis-gas chromatography by using the ratio $[1,2\text{-dimethylthiophene}]/([1,2\text{-dimethylbenzene}] + [n\text{-non-1-ene}])$, termed the thiophene ratio (*TR*) (Eglinton *et al.*, 1990). The authors showed that this ratio correlates with atomic S_{org}/C ratios for most of the bitumens, asphaltenes and kerogens investigated. Hence, *TR* values were used here to obtain information on both the efficiency of the

Li/EtNH₂ treatment, *i.e.* the relative amount of sulphur-bound constituents left in the "desulphurized" kerogens, and the degree of sulphurization. Elemental analyses of a representative sample of the marl layer of cycle IV allowed calculation of the atomic S_{org}/C ratio of this kerogen (Koopmans *et al.*, 1995). The value obtained (0.08) corresponds to a Type II-S kerogen (Orr, 1986). The *TR* calculated from the pyrolysate of the "untreated" VdG kerogens ranges from 0.19 to 0.40, with no particular depth trend (Fig. 9.2). These values are consistent with those of most Type II immature marine kerogens (Eglinton *et al.*, 1990). The discrepancy noted between the S_{org}/C and *TR* ratios may be explained by the presence of unusually high contribution of intermolecular rather than intramolecular S-bonds. Cleavage of the former linkages lead to the formation of *n*-alk-1-ene/*n*-alkanes whereas the latter are presumed to generate mainly alkylthiophenes upon pyrolysis.

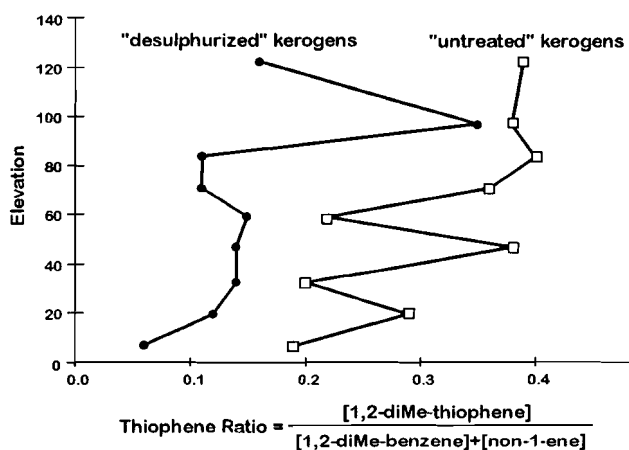


Fig. 9.2 Depth profiles of the thiophene ratio calculated from the pyrolysates of the "untreated" (□) and "desulphurized" (●) kerogens.

After desulphurization, with the exception of VdG-8, the *TR* values are around 0.1 which corresponds to Type I kerogens (Eglinton *et al.*, 1990). Therefore, according to these *TR* values, Li/EtNH₂ treatment of the kerogens released a significant part of the S-bound lipids, *i.e.* those intermolecularly incorporated. Indeed, yields of the extracts obtained after Li/EtNH₂ treatment revealed that up to 30 wt% of the kerogen could be released, though some of the released material may have resulted from ester bond cleavage (Schaeffer *et al.*, 1995).

Relative distributions of pyrolysis products

Whereas the relative contributions of the pyrolysis products vary significantly with respect to the different series of components, there are no

major differences in the "internal" distributions within these series for the untreated and treated kerogens (Fig. 9.3). The *n*-alkan-2-one distribution, revealed by the *m/z* 58 chromatogram, of the "desulphurized" kerogen pyrolysate is virtually identical to that of the untreated kerogen, ranging from C₆ to C₂₆ with a maximum at C₁₆. Likewise, the distributions of benzenes in the two sample pyrolysates are very similar and consist mainly of benzene itself and C₁-C₄ alkylated benzenes. Only the relative intensity of the 1,2,3,4-tetramethylbenzene (TMB) is slightly higher in the pyrolysate of the "desulphurized" sample. TMB is thought to be a specific pyrolysis product of macromolecularly-bound isorenieratene derivatives (Hartgers *et al.*, 1991a, 1994a; Douglas *et al.*, 1991; Requejo *et al.*, 1992). Isorenieratene holds several

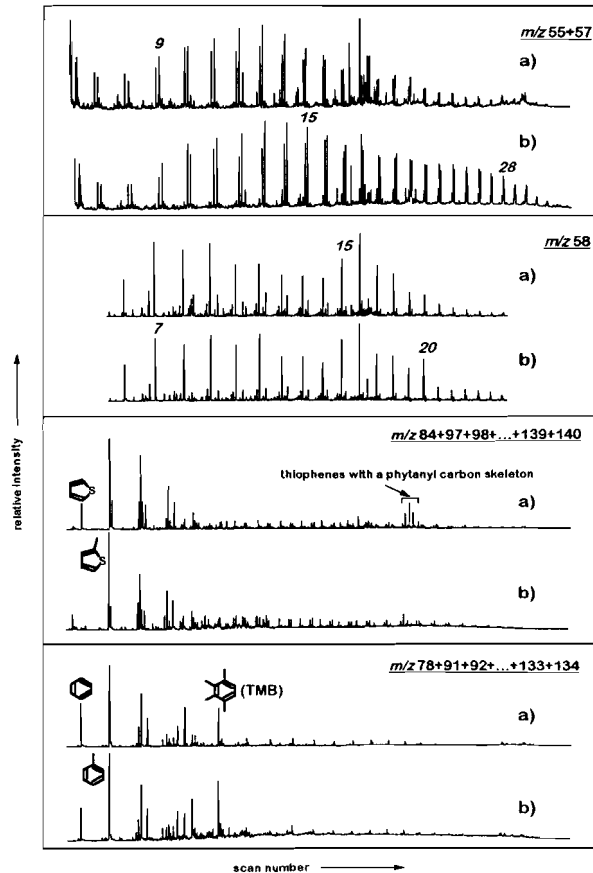


Fig. 9.3 Mass chromatograms of the pyrolysates of (a) "untreated" VdG-IV-7 kerogen and (b) "desulphurized" VdG-IV-7 kerogen. Mass chromatograms of *m/z* 55 + 57, 58, 84 + 97 + 98 + 111 + 112 + 125 + 126 + 139 + 140 and 78 + 91 + 92 + 105 + 106 + 119 + 120 + 133 + 134 reveal the distributions of *n*-alk-1-ene/*n*-alkanes, *n*-alkan-2-ones, alkylthiophenes and alkylbenzenes, respectively, italic numbers indicate carbon chain lengths.

sites for sulphurization or oxygenation and a fraction of this compound is probably more strongly linked to the kerogen network than the other aromatic moieties. Very similar distributions are also observed for the alkylthiophenes. The only difference is the presence of relatively abundant thiophenes with a phytanyl carbon skeleton exclusively in the "untreated" kerogen pyrolysate. These thiophenes are thought to be generated by pyrolysis of poly-S-bound phytanyl moieties (Koopmans *et al.*, 1995) which were probably released by the CrCl_2 and Li/EtNH_2 treatments. The *n*-alk-1-enes and *n*-alkanes, as revealed by the m/z 55+57 chromatogram, range from C_6 to C_{33} and maximize at $\text{C}_{13}/\text{C}_{14}$ in both pyrolysates. However, as also observed for most of the other samples, the *n*-alk-1-enes and *n*-alkanes with chain length over 14 carbons are relatively more abundant in the "desulphurized" kerogen pyrolysate. This phenomenon may be partly explained by the fact that the S-incorporated lipids possess *n*-alkyl units with fewer than 15 carbons .

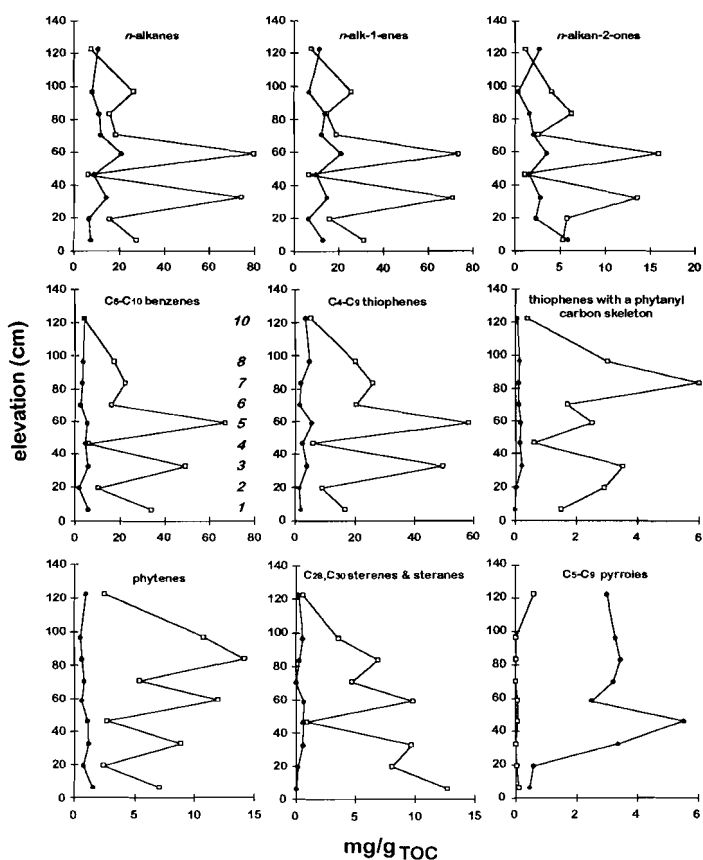


Fig. 9.4 Depth profiles of the concentration of the main products in the flash pyrolysates of the "untreated" (□) and "desulphurized" (●) kerogens; italic numbers indicate samples VdG-IV-1 to VdG-IV-10.

Quantitative variations in pyrolysis products

Fig. 9.4 indicates the depth concentration profiles of the main compounds or series of compounds in the pyrolysates of the "untreated" and "desulphurized" kerogens. The "untreated" kerogens of samples 3 and 5 released by far the highest amounts of *n*-alkanes, *n*-alk-1-enes (from 70 to 80 mg/g_{TOC}) (Gelin *et al.*, 1995). However, no such significant trend was observed in the pyrolysates of the desulphurized samples. Consequently, a large decrease (75%) in *n*-alk-1-enes/*n*-alkanes is observed. Moreover, the amount of released material after Li/EtNH₂ treatment (and column chromatography) was not higher for these two samples (Schaeffer *et al.*, 1995). We assume, therefore, that desulphurization of samples 3 and 5 released abundant extractable aliphatic macromolecules which were originally attached to the kerogen via S-bond(s). Soluble macromolecules have been shown to occur as polyaldehydes in the green microalga *Botryococcus braunii* A race and account for ca 5% of the dry algal biomass (Metzger *et al.*, 1993). Conversely, the amount of released *n*-alk-1-enes/*n*-alkanes in the pyrolysates of samples 4 and 10 increased after desulphurization. This can be explained either by the 30% error estimated for quantitative flash pyrolysis analyses or by an increase in thermal energy leading to more extensive cleavage of aliphatic macromolecules upon pyrolysis of these desulphurized samples. The yields of GC-amenable phytanes, steranes, thiophenes with a phytanyl carbon skeleton and thiophenes are strongly decreased in the pyrolysates of all the desulphurized samples. This is probably due to the high degree of sulphur and possibly ester linkages by which they are bound to the matrix. The phytane concentrations in the apolar fraction of the extracts released after Li/EtNH₂ treatment range from 0.1 to 1.1 mg/g_{TOC} (Schaeffer *et al.*, 1995), whereas the differences of phytanes concentrations between the pyrolysates of the "untreated" and "desulphurized" kerogens range from 14 to 1 mg/g_{TOC}. Hence, it is likely that a significant proportion of the phytanes in the flash pyrolysates of the "untreated" kerogens derives from the cleavage of O-bound phytanyl moieties or S-bound dihydrophytol. Therefore, these phytanyl moieties were probably present in the polar fraction after Li/EtNH₂ treatment. Similar observations and explanations can be made for the concentrations of steranes (and sterenes). In the pyrolysates of the "desulphurized" kerogens of samples 1, 6 and 10, the small concentration of these steroids was below the detection limit for a suitable quantitation.

Algaenan contribution

The pyrolysates of the "desulphurized" kerogens contain predominantly compounds derived from resistant aliphatic biomacromolecules, indicating that the desulphurization leads to a selective enrichment of these macromolecules in the kerogens. In particulate, *n*-alk-1-enes and *n*-alkanes are highly predominant in the pyrolysates of the "desulphurized" kerogens. Recently, it has been established that marine micro-algae, *i.e.* eustigmatophytes and some chlorophytes, biosynthesize highly aliphatic macromolecules, termed algaenans and which are probably located in the outer algal cell walls (Derenne *et al.*, 1992a; Gelin *et al.*, 1996a). Upon pyrolysis, these biomacromolecules release

essentially *n*-alk-1-enes and *n*-alkanes. Thus, the polymethylenic moieties are much less affected by the LiEtNH₂ treatment than the other macromolecularly-bound moieties (except for samples 3 and 5), *i.e.* aromatic, thiophenic, steroid and isoprenoid species. Circumstantial evidence for a major contribution of these aliphatic macromolecules came from the presence in the polar and asphaltene fractions of C₃₀-C₃₂ *n*-alkyl units which were S-bound, mainly at the C-15 position (Kenig *et al.*, 1995; Koopmans *et al.*, 1995). These long-chain S-linked alkyl units are thought to be derived diagenetically from the sulphurization of C₃₀-C₃₂ 1,15-diols which are produced by microalgal *Nannochloropsis* species from the class Eustigmatophyceae (Volkman *et al.*, 1992; Gelin *et al.*, 1996a). These diols and their diagenetic derivatives have also been found as such in many marine sediments (*e.g.* de Leeuw *et al.*, 1981; Morris and Brassell, 1988). Consequently, a significant part of the kerogens from the Vena del Gesso marl sediments is composed of selectively preserved algaenans originating from marine nanophytoplankton such as the eustigmatophytes. It is also likely that these algaenans favour the preservation of free lipids through their incorporation into the algaenan matrix as a result of sulphurization.

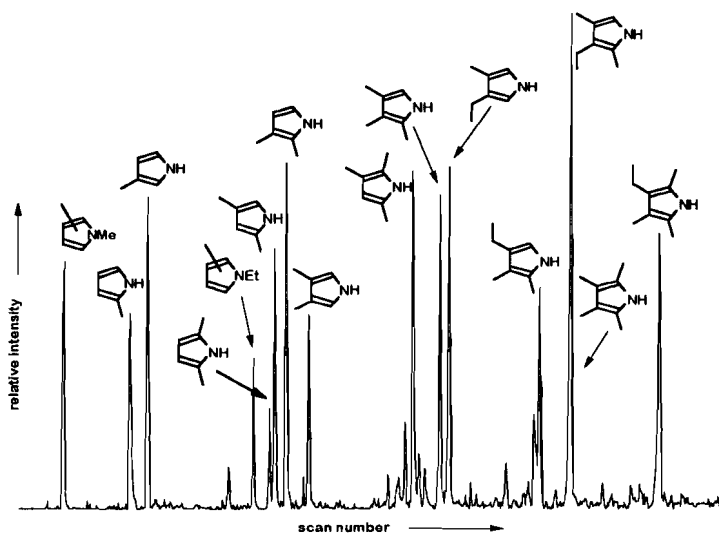


Fig. 9.5 Partial, accurate summed mass chromatogram of m/z 80.06 + 81.06 + 94.08 + 95.08 + 108.1 + 109.1 + 122.11 + 123.11 + 136.13 + 13.13 (mass window 0.02 Da) revealing the distribution of the C₁-C₅ alkylated pyrroles in the flash pyrolysates of VdG-IV-4 "desulphurized" kerogen.

Alkylpyrroles

Alkylpyrroles were also relatively abundant components in all the "desulphurized" kerogen pyrolysates (up to 6 mg/g_{TOC} for sample 4), whereas

they were present in trace amounts (0 to 0.6 mg/g_{TOC}) in the "untreated" kerogen pyrolysates (Fig. 9.4). Alkylpyrroles in kerogen flash pyrolysates have only been reported twice, *i.e.* in kerogen pyrolysates of sulphur-rich sediments from the Miocene Monterey Formation (Sinninghe Damsté *et al.*, 1992) and in a kerogen pyrolysate of Recent diatomaceous ooze from the Namibian Shelf (Klok *et al.*, 1984). The alkylpyrrole distributions in the flash pyrolysates of these two sediments are very similar to those in the pyrolysates of the Vena del Gesso kerogens after desulphurization as shown in Figure 9.5 for sample 4, the main products being C₁-C₅ alkylated pyrroles. The major components are 2,3-dimethylpyrrole, 3-ethyl-4-methylpyrrole and 2,4-dimethyl-3-ethylpyrrole. The distribution pattern of the alkylpyrroles found in the Monterey, the Namibian shelf and the "desulphurized" VdG kerogens indicates that these products originate from tetrapyrrole pigments ultimately derived from chlorophylls, as suggested

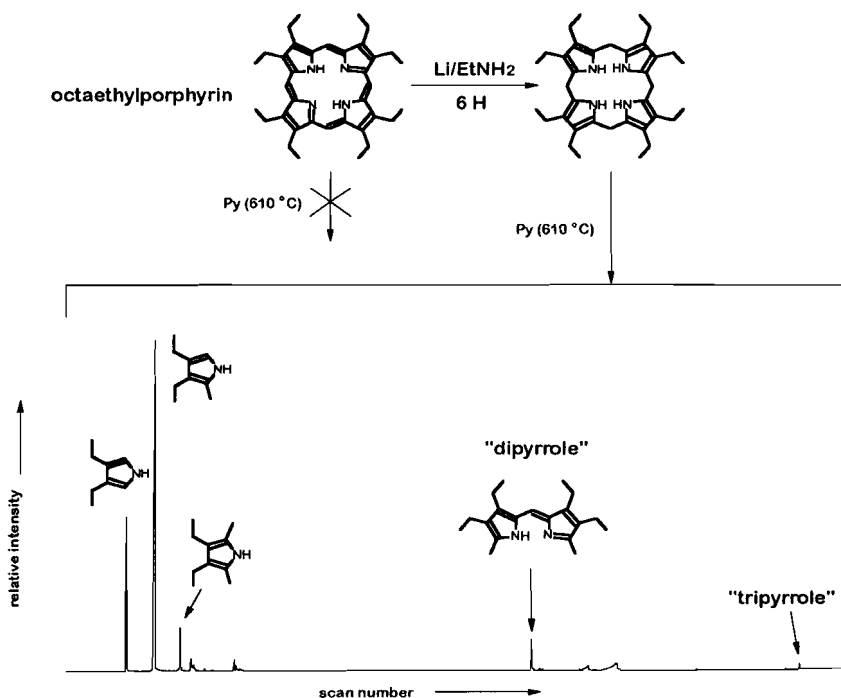


Fig. 9.6 Total ion current of the pyrolysates of the products obtained after Li/EtNH₂ treatment of octaethylporphyrin. The structure of the reduced porphyrin that generated these products is tentative.

previously (Sinninghe Damsté *et al.*, 1992). Also, their presence in high abundance in the pyrolysates of the "desulphurized" kerogens suggest that tetrapyrrole units were preserved in the sediments by incorporation into

macromolecules *via* S-bond(s), the presence of S-bound porphyrins in other sulphur-rich sediments corroborating this hypothesis (*e.g.* Schaeffer *et al.*, 1993). Given the absence of alkylpyrroles in the pyrolysis products from the "untreated" kerogens, it can also be envisaged that Li/EtNH₂ might reduce double bonds in the cyclic tetrapyrrole system, decreasing their aromaticity and allowing the formation of alkylpyrroles by pyrolysis. To investigate this hypothesis, a standard porphyrin, octaethylporphyrin, was subjected to Li/EtNH₂ treatment under the same conditions as applied for the desulphurization method. The starting porphyrin and the reduction product were pyrolysed at 610°C. Only the reduction product released GC-amenable compounds upon pyrolysis (Fig. 9.6). The main products were alkylpyrroles with ethyl substituents at the 3 and 4 positions of the pyrrole ring, in good agreement with the substitution pattern in the starting material. Di- and tripyrroles were also detected in the pyrolysate but in much lower abundance. The absence of alkylated pyrroles in the flash pyrolysate of the octaethylporphyrin is consistent with the findings of Meuzelaar *et al.* (1982) and Sinninghe Damsté *et al.* (1992) who performed Py-MS on tetraethyltetramethylporphyrin and Py-GC(MS) on metallo and free base octaethylporphyrins, respectively. This indicates that porphyrins are too stable to generate pyrolysis products which can be observed under our experimental conditions. Hence, the octaethylporphyrin probably simply evaporated as such, so we can consider that bound porphyrins in kerogens or asphaltenes are probably released as intact tetrapyrroles upon pyrolysis. This is confirmed by studies of ETIO- and DPEP vanadylporphyrins released after pyrolysis of Woodford and New Albany Shale kerogens (Sundararaman *et al.*, 1988).

Our results show that Li/EtNH₂ treatment affects the thermal stability of octaethylporphyrin. Probe mass spectra of the Li/EtNH₂-treated porphyrin suggested the presence of reduced products including one with a molecular ion at *m/z* 540 (the molecular mass of octaethylporphyrin is 534 Da). Although the exact nature of these products was not examined, it is suggested that double bonds, presumably at the bridgehead carbons, were reduced, forming less stable cyclic products which were more readily cleaved upon flash pyrolysis.

9.5 CONCLUSIONS

The combined results of kerogen desulphurization and flash pyrolysis studies allowed the following conclusions:

- 1) The amount and nature of originally low-molecular-weight compounds, *i.e.* C₂₀ isoprenoids, steroids and hopanoids, which have been incorporated into the kerogen *via* sulphurization, vary significantly over cycle IV as judged from the differences in the compositions of pyrolysis products before and after desulphurization.
- 2) Removal of a significant part of sulphur-bond lipids by Li/EtNH₂ treatment of the kerogens results in an enrichment of algaenan-derived organic matter in the "desulphurized" kerogens as revealed by the predominance of *n*-alk-1-enes and *n*-alkanes in the pyrolysates of the latter.
- 3) Series of C₅-C₉ alkylpyrroles in the pyrolysates of the "desulphurized" kerogens revealed the significant presence of bound tetrapyrroles. The

absence of these alkylpyrroles in the pyrolysates of the “untreated” kerogens indicate that the Li/EtNH₂ treatment reduced double bonds, thereby facilitating the generation of alkylpyrroles upon pyrolysis.

Acknowledgements - This work was performed under the auspices of ENOG (European Network of Organic Geochemists) and has benefited from scientific discussions within the group. ENOG comprises Laboratoire de Géochimie, IFP, Rueil-Malmaison, France; Institute of Petroleum and Organic Geochemistry, KFA, Jülich, Germany; Geologisches Institut der Universität Köln, Germany; Laboratoire de Chimie Organique des Substances Naturelles associé au CNRS, Université Louis Pasteur, Strasbourg, France; Netherlands Institute for Sea Research, Department of Marine Biogeochemistry, Texel, the Netherlands; Department of Environmental Chemistry, CID-CSIC, Barcelona, Spain; Organic Geochemistry Unit, University of Bristol, UK and receives funding from the European Community (EC contract # CHRX-CT94-0474). This work was partly supported by a PIONIER grant to JSSD from the Netherlands Organisation for Scientific Research (NWO). We thank Gian Batissta Vai, B.C. Schreiber, Brendan Keely, Peter Hofmann, Jan Ebbing, Stefan Schouten, other members of the ENOG group and the management of the gypsum mine for advice and assistance during sampling. We acknowledge R. Kloosterhuis (NIOZ) for elemental analysis of the isolated kerogens.

References

- van Aarssen B. G. K., Cox H. C., Hoogendoorn P. and de Leeuw J. W. (1990) A cadinene biopolymer in fossil and extant dammar resins as a source for cadinanes and bicadinanes in crude oils from South East Asia. *Geochim. Cosmochim. Acta* **54**, 3021-3031.
- van Aarssen B. G. K., Horsfield B. and de Leeuw J. W. (1991) A comparative study of three different pyrolysis methods used to characterise a biopolymer isolated from fossil and extant dammar resins. *J. Anal. Appl. Pyrolysis* **20**, 125-139.
- Allan J., Bjørøy M. and Douglas A. G. (1980) A geochemical study of the exinite group maceral alginite, selected from three Permo-Carboniferous Torbanites. In *Advances in Organic Geochemistry 1979* (ed. A. G. Douglas and J. R. Maxwell); 599-618.
- Behar F., Derenne S. and Largeau C. (1995) Closed pyrolyses of the isoprenoid algaenan of *Botryococcus braunii*, L race: Geochemical implications for derived kerogens. *Geochim. Cosmochim. Acta* **59**, 2983-2997.
- van Bergen P. F., Collinson M. E., Sinninghe Damsté J. S. and de Leeuw J. W. (1991) A novel polyphenol biopolymer isolated from fossil seeds: An alternative source for (alkyl) phenol moieties in coals. *Amer. Chem. Soc.-Dic. Fuel Chem.* **36**, 698-701 (preprint).
- van Bergen P. F., Collinson M. E., Sinninghe Damsté J. S. and de Leeuw J. W. (1994) Chemical and microscopical characterization of inner seed coats of fossil water plants. *Geochim. Cosmochim. Acta* **58**, 231-239.
- Berkaloff C., Casadevall E., Largeau C., Metzger P., Peracca S. and Virlet J. (1983) The resistant polymer of the walls of the hydrocarbon-rich alga *Botryococcus braunii*. *Phytochemistry* **22**, 389-397.
- Berner R. A. (1989) Biogeochemical cycles of carbon and sulfur and their effect on atmospheric oxygen over Phanerozoic time. *Palaeogeograph. Palaeoclimatol. Palaeoecol.* **73**, 97-122.
- Bertrand P. and Lallier-Vergès E. (1993) Past sedimentary organic matter accumulation and degradation controlled by productivity. *Nature* **364**, 786-788.
- Bertrand P., Lallier-Vergès E., Martinez L., Pradier B., Tremblay P., Huc A., Jouhannel R. and Tricart J.-P. (1990) Examples of spatial relationships between organic matter and mineral groundmass in the microstructure of the organic-rich Dorset Formation rocks (Great Britain). *Org. Geochem.* **16**, 661-675.
- Bertrand P., Lallier-Vergès E. and Boussafir M. (1994). Enhancement of both accumulation and anoxic degradation of organic carbon controlled by cyclic productivity: a model. *Org. Geochem.* **22**, 511-520.
- Bhatt M. V. and Kulkarni S. U. (1983) Cleavage of ethers. *Synthesis*, 249-282.
- Bishop A. N. and Philp R. P. (1994) The potential for amorphous kerogen formation via adsorption of organic material at mineral surfaces. 207th American chemical Society 1994, National Meeting, March 13-18, San Diego, CA, USA.
- Boon J. J., Pouwels A. D. and Eijkel G. B. (1987) Pyrolysis high-resolution gas chromatography-mass spectrometry studies on beech wood: capillary high-resolution mass spectrometry of a beech lignin fraction. *Biochem. Soc. Trans.* **15**, 170-174.
- Boreham C. J., Summons R. E., Roksandic Z., Dowling L. M. and Hutton C. (1994) Chemical, molecular and isotopic differentiation of organic facies in the tertiary

- lacustrine Durling oil shale deposit, Queensland, Australia. *Org. Geochem.* **21**, 685-712.
- Boucher R. J., Standen G., Patience R. L. and Eglinton G. (1990) Molecular characterization of kerogen from Kimmeridge clay formation by mild selective chemical degradation and solid state ^{13}C -NMR. In *Advances in Organic Geochemistry 1989* (ed. B. Durand and F. Behar); *Org. Geochem.* **16**, 951-958.
- Boussafir M., Lallier-Vergès E., Bertrand P. and Badaut-Trauth D. (1994a) Etude ultrastructurale de matières organiques micro-prélevées dans les roches de la "Kimmeridge Clay Formation" (Yorkshire, UK). *Bull. Centres Rech. Explor. Prod. Elf-Aquitaine*, pp. 275-277.
- Boussafir M., Lallier-Vergès E., Bertrand P. and Badaut-Trauth D. (1994b) Structure ultrafine de la matière organique des roches mères du kimmeridgien du Yorkshire (UK). *Bull. de la Soc. Géol. de Fr.* **165**, 355-363.
- Boussafir M., Lallier-Vergès E., Bertrand P. and Badaut-Trauth D. (1995a) SEM and TEM studies on isolated organic matter and rock microfacies from a short-term organic cycle of the Kimmeridge Clay Formation (Yorkshire, G.B.). *Lecture Notes in Earth Science Series* **57**, pp. 15-30. Springer-Verlag.
- Boussafir M., Gelin F., Lallier-Vergès E., Derenne S., Bertrand P. and Largeau C. (1995b) Electron microscopy and pyrolysis of kerogens from the Kimmeridge Clay Formation, UK: Source organisms, preservation processes, and origin of microcycles. *Geochim. Cosmochim. Acta.* **59**, 3731-3747.
- Bray E. E. and Evans E. D. (1961) Distribution of *n*-paraffins as a clue to recognition of source beds. *Geochim. Cosmochim. Acta* **22**, 2-15.
- Carlson D. A., Roan C.-S., Yost R. A. and Hector J. (1989) Dimethyl disulfide derivatives of long chain alkenes, alkadienes and alkatrienes for gas chromatography/mass spectrometry. *Anal. Chem.* **61**, 1564-1571.
- Chrétiennot-Dinet M.-J. (1990) *Atlas du Phytoplankton Marin, Vol. 3*. p.18. Centre de la Recherche Scientifique. Paris.
- Collinson M. E., van Bergen P. F., Scott A. C. and de Leeuw J. W. (1994) In *Coal and Coal-bearing Strata as Oil-prone Source Rocks?* (ed. A. C. Scott and A. J. Fleet); *Geol. Soc. Special Publ.* **77**, 31-70.
- Collister J. W., Lichtfouse E., Hieshima G. and Hayes J. M. (1994) Partial resolution of sources of *n*-alkanes in the saline portion of the Parachute Creek Member, Green River Formation (Piceance Creek Basin, Colorado) *Org. Geochem.* **21**, 645-659.
- Cranfield D. E., Raiswell R., Westrich J. T., Reaves C. M. and Berner R. A. (1986) The use of chromium reduction in the analysis of reduced inorganic sulphur in sediments and shales. *Chem. Geol.* **54**, 149-155.
- Cranwell P. A., Eglinton G. and Robinson N. (1987) Lipids of aquatic organisms as potential contributions to lacustrine sediments. II. *Org. Geochem.* **11**, 513-527.
- Derenne S., Largeau C., Casadevall E. and Connan J. (1988) Comparison of torbanites of various origins and evolutionary stages. Bacterial contribution to their formation. Cause of the lack of botryococcane in bitumens. *Org. Geochem.* **12**, 43-59.
- Derenne S., Largeau C., Casadevall E. and Berkaloff C. (1989) Occurrence of a resistant biopolymer in the L race of *Botryococcus braunii*. *Phytochemistry* **28**, 1137-1142.
- Derenne S., Largeau C., Casadevall E. and Sellier N. (1990a) Direct relationship between the resistant biopolymer and the tetraterpene hydrocarbon in the lycopadiene race of *Botryococcus braunii*. *Phytochemistry* **29**, 2187-2192.
- Derenne S., Largeau C., Casadevall E., Sinninghe Damsté J. S., Tegelaar E. W. and de Leeuw J. W. (1990b) Characterization of Estonian Kukersite by spectroscopy and

- pyrolysis: Evidence for abundant alkyl phenolic moieties in an Ordovician, marine, type II/I kerogen. In *Advances in Organic Geochemistry 1989* (ed. B. Durand and F. Behar); *Org. Geochem.* **16**, 873-888.
- Derenne S., Largeau C. and Casadevall E. (1991a) Occurrence of tightly bound isoprenoid acids in an algal, resistant biomacromolecule: possible geochemical implications. *Org. Geochem.* **17**, 597-602.
- Derenne S., Largeau C., Casadevall E., Berkaloff C. and Rousseau B. (1991b) Chemical evidence of kerogen formation in source rocks and oil shales via selective preservation of thin resistant outer walls of microalgae: origin of ultralaminae. *Geochim. Cosmochim. Acta* **55**, 1041-1050.
- Derenne S., Largeau C., Berkaloff C., Rousseau B, Wilhelm C. and Hatcher P. G. (1992a) Non-hydrolysable macromolecular constituents from outer walls of *Chlorella fusca* and *Nanochlorum eucaryotum*. *Phytochemistry* **31**, 1923-1929.
- Derenne S., Largeau C. and Hatcher P. G. (1992b) Structure of *Chlorella fusca* algaenan. Relationships with ultralaminae in lacustrine kerogens. Species- environment-dependant variations in the composition of fossil ultralaminae. *Org. Geochem.* **18**, 417-422.
- Derenne S., Le Berre F., Largeau C., Hatcher P., Connan J. and Raynaud J. F. (1992c) Formation of ultralaminae in marine kerogens via selective preservation of thin resistant outer walls of microalgae. In *Advances in Organic Geochemistry 1991* (ed. C. Eckhart and J. R. Maxwell); *Org. Geochem.* **19**, 345-350.
- Derenne S., Metzger P., Largeau C., van Bergen P. F., Gatellier J.-P., Sinninghe Damsté J. S., de Leeuw J. W. and Berkaloff C. (1992d) Similar morphological and chemical variations of *Gloeocapsomorpha prisca* in Ordovician sediments and cultured *Botryococcus braunii* as a response to changes in salinity. In *Advances in Organic Geochemistry 1991* (ed. C. Eckhart and J. R. Maxwell); *Org. Geochem.* **19**, 299-231.
- Derenne S., Largeau C. and Taulelle F. (1993) Elucidation, via solid-state ^{15}N NMR, of the origin of the alkylnitriles generated upon pyrolysis of ultralaminae-containing kerogens. In *Organic Geochemistry* (ed. K. Øygard); pp. 766-770. Falch Hurtigtrykk.
- Derenne S., Largeau C. and Berkaloff C. (1995) Chemical composition of the non-hydrolysable macromolecular constituent of *Chlorella marina* cell wall. First evidence of the occurrence of an aromatic-rich algaenan. *Organic Geochemistry: Developments and Applications to energy, Climate, Environment and Human History* (ed. J. O. Grimalt and C. Dorronsoro); pp. 948-950.
- Desprairies A., Bachaoui M., Ramdani A. and Tribovillard N. P. (1995) Clay diagenesis in organic-rich cycles from the Kimmeridge Clay Formation of Yorkshire (G.B.): implication for palaeoclimatic interpretations. In *Lecture notes in Earth Sciences* **57**, pp. 63-91. Springer-Verlag.
- Dong J.-Z., Vorkink W. P. and Lee M. L. (1993) Origin of long-chain alkylcyclohexanes and alkylbenzenes in a coal-bed wax. *Geochim. Cosmochim. Acta* **57**, 837-849.
- Douglas A. G., Sinninghe Damsté J. S., Fowler M. G., Eglinton T. I. and de Leeuw J. W. (1991) Unique distributions of hydrocarbons and sulphur compounds released by flash pyrolysis from the fossilised alga *Gloeocapsomorpha prisca*, a major constituent in one of four Ordovician kerogens. *Geochim. Cosmochim. Acta* **55**, 275-291.
- Dubreuil C., Derenne S., Largeau C., Berkaloff C. and Rousseau B. (1989) Mechanism of formation and chemical structure of Coorongite-I. Role of the resistant biopolymer and of the hydrocarbons of *Botryococcus braunii*. Ultrastructure of Coorongite and its relationship with Torbanite. *Org. Geochem.* **14**, 543-553.

- Durand B. (ed.) (1980) *Kerogen-insoluble organic matter from sedimentary rock*. Technip, Paris.
- Eglinton G., Gonzales A. G., Hamilton R. J. and Raphael R. A. (1962) Hydrocarbon constituents of the wax coatings of plant leaves: A taxonomic survey. *Phytochemistry* **1**, 89-102.
- Eglinton T. I. (1994) Carbon isotopic evidence for the origin of macromolecular aliphatic structures in kerogen. *Org. Geochem.* **21**, 721-735.
- Eglinton T. I., Rowland S. J., Curtis C. D. and Douglas A. G. (1986) Kerogen-mineral reactions at raised temperatures in the presence of water. *Org. Geochem.* **10**, 1041-1052.
- Eglinton T. I., Douglas A. G. and Rowland S. J. (1988a) Release of aliphatic, aromatic and sulphur compounds from Kimmeridge kerogen by hydrous pyrolysis: A quantitative study. *Org. Geochem.* **13**, 655-663.
- Eglinton T. I., Philp R. P. and Rowland S. J. (1988b) Flash pyrolysis of artificially matured kerogens from the Kimmeridge Clay (U.K.). *Org. Geochem.* **12**, 33-41.
- Eglinton T. I., Sinninghe-Damsté J. S., Kohnen M. E. L., de Leeuw J. W., Larter S. R. and Patience R. L. (1989) Analysis of maturity-related changes in the organic sulfur composition of kerogens by flash pyrolysis-gas chromatography. In *Geochemistry of sulfur in fossil fuels* (ed. W. L. Orr and C. M. White); *ACS Symposium Series* **429**, pp. 529-565. Amer. Chem. Soc.
- Eglinton T. I., Sinninghe Damsté J. S., Kohnen M. E. L. and de Leeuw J. W. (1990) Rapid estimation of the organic sulphur content of kerogens, coals and asphaltenes by pyrolysis-gas chromatography. *Fuel* **69**, 1394-1404.
- Eglinton T. I., Irvine J. E., Vairavamurthy A., Zhou W. and Manowitz B. (1994) Formation and diagenesis of macromolecular organic sulphur in Peru margin sediments. In *Advances in Organic Geochemistry 1993* (ed. N. Telnæs, van G. Graas and K. Øygard); *Org. Geochem.* **22**, 781-799.
- Elsgaard L., Isaksen M. F., Jørgensen B. B., Alayse A.-M. and Jannasch H. W. (1994) Microbial sulfate reduction in deep-sea sediments at the Guaymas Basin hydrothermal vent area: Influence of temperature and substrates. *Geochim. Cosmochim. Acta* **58**, 3335-3343.
- Espitalié J., Madec M. and Tissot B. (1980) Role of mineral matrix in kerogen pyrolysis : influence on petroleum generation and migration. *AAPG Bull.* **64**, 59-66.
- Farrimond P., Comet P., Eglinton G., Evershed R. P., Hall M. A., Park D. W. and Wardroper A. M. K. (1984) Organic geochemical study of the Upper Kimmeridge Clay of the Dorset type area. *Mar. Petrol. Geol.* **1**, 340-354.
- Flaviano C., Le Berre F., Derenne S., Largeau C. and Connan J. (1994) First indications of the formation of kerogen amorphous fractions by Selective Preservation. Role of non-hydrolysable macromolecular constituents of Eubacterial cell walls. *Org. Geochem.* **22**, 759-771.
- François R. (1987) A study of sulphur enrichment in the humic fraction of marine sediments during early diagenesis. *Geochim. Cosmochim. Acta* **51**, 17-27.
- Freeman K. H., Hayes J. M., Trendel J.-M. and Albrecht P. (1990) evidence from carbon isotope measurements for diverse origins of sedimentary hydrocarbons. *Nature* **343**, 254-256.
- Fukushima K. and Ishiwatari R. (1988) Geochemical significance of lipids and lipid-derived substructures interlaced in kerogen. *Org. Geochem.* **12**, 509-518.
- Gallois R. W. (1976) Coccolith blooms in the Kimmeridge Clay and origin of the North Sea oil. *Nature* **259**, 473-475.

- Gatellier J.-P. L. A., de Leeuw J. W., Sinninghe Damsté J. S., Derenne S., Largeau C. and Metzger P. (1993) Very early diagenesis of a resistant cell wall biomacromolecule of the green alga *Botryococcus braunii* (Race A) as revealed by spectroscopic and pyrolysis investigations of a Coorongite. *Geochim. Cosmochim. Acta* **57**, 2053-2068.
- Gelin F., Gatellier J.-P. L. A., Sinninghe Damsté J. S., Derenne S., Largeau C., Metzger P. and de Leeuw J. W. (1993) Mechanisms of flash pyrolysis of ether lipids isolated from the green microalga *Botryococcus braunii*. *J. Anal. Appl. Pyrolysis* **27**, 155-168.
- Gelin F., Sinninghe Damsté J. S., Derenne S., Largeau C., Metzger P. and de Leeuw J. W. (1994a) Scope and limitations of flash pyrolysis-gas chromatography/mass spectrometry as revealed by the thermal behaviour of high-molecular-weight lipids derived from the green microalga *Botryococcus braunii*. *J. Anal. Appl. Pyrolysis* **28**, 183-204.
- Gelin F., de Leeuw J. W., Sinninghe Damsté J. S., Derenne S., Largeau C. and Metzger P. (1994b) Similarity of chemical structures of soluble aliphatic polyaldehyde and insoluble algaenan in the green microalga *Botryococcus braunii* race A as revealed by analytical pyrolysis. *Org. Geochem.* **21**, 423-435.
- Gelin F., Sinninghe Damsté J. S., Harrison W. N., Maxwell J. R. and de Leeuw J. W. (1995) Molecular indicators for palaeoenvironmental change in a Messinian evaporitic sequence (Vena del Gesso, Italy): III. Stratigraphic changes in the molecular structure of kerogen in a single marl bed as revealed by flash pyrolysis. *Org. Geochem.* **23**, 555-566.
- Gelin F., Boogers I., Noordeloos A. A. M., Hatcher P. G., Sinninghe Damsté J. S. and de Leeuw J. W. (1996a) Novel, resistant microalgal polyethers: An important sink of organic carbon in the marine environments? Accepted in *Geochim. Cosmochim. Acta*.
- Gelin F., Sinninghe Damsté J. S., Harrison W. N., Reiss C., Maxwell J. R. and de Leeuw J. W. (1996b) Variations in origin and composition of kerogen constituents as revealed by analytical pyrolysis of immature kerogens before and after desulphurization. Submitted to *Org. Geochem.*
- Given P. H., Spackman W., Painter P. C., Rhoads C. A., Ryan N., Alemany L. and Pugmire R. J. (1984) The fate of cellulose and lignin in peats: an exploratory study of the input to coalification. In *Advances in Organic Geochemistry 1983* (ed. P. A. Schenck, J. W. de Leeuw and G. W. M. Lijmbach); pp. 399-407. Pergamon.
- Goossens H., de Leeuw J. W., Schenck P. A. and Brassell S. C. (1984) Tocopherols as likely precursors of pristane in ancient sediments and crude oils. *Nature* **312**, 440-442.
- Goossens H., de Leeuw J. W., Rijpstra W. I. C., Meyburg G. J. and Schenck P. A. (1989) Lipids and their mode of occurrence in bacteria and sediments - I. A methodological study of the lipid composition of *Acinetobacter calcoaceticus* LMD 79-41. *Org. Geochem.* **14**, 15-25.
- Goth K., de Leeuw J. W., Püttman W. and Tegelaar E. W. (1988) Origin of Messel Oil Shale kerogen. *Nature* **336**, 759-761.
- Guilford W. J., Schneider D. M., Labovitz J. and Opella S. J. (1988) High resolution solid state ^{13}C NMR spectroscopy of sporopollenin from different plant taxa. *Plant. Physiol.* **86**, 134-136.
- Hartgers W. A., Sinninghe Damsté J. S. and de Leeuw J. W. (1991a) Mechanisms of hydrocarbon formation during flash pyrolysis of kerogen. *Prep. Am. Chem. Soc. - Div. Fuel Chem.* **36**, 790-795.
- Hartgers W. A., Sinninghe Damsté J. S. and de Leeuw J. W. (1991b) Flash pyrolysis of silicon-bound hydrocarbons. *J. Anal. Appl. Pyrolysis* **20**, 141-150.

- Hartgers W. A., Sinninghe Damsté J. S. and de Leeuw J. W. (1992) Identification of C2-C4 alkylated benzenes in flash pyrolysates of kerogens, coals and asphaltenes. *J. Chromatogr.* **606**, 211-220.
- Hartgers W. A., Sinninghe Damsté J. S., Koopmans M. P. and de Leeuw J. W. (1993) Sedimentary evidence for a diaromatic carotenoid with an unprecedented aromatic substitution pattern. *J. Chem. Soc., Chem Comm.* **23**, 1715-1716.
- Hartgers W. A., Sinninghe Damsté J. S., Requejo A. G., Allan J., Hayes J. M. and de Leeuw J. W. (1994a) Evidence for only minor contributions from bacteria to sedimentary organic carbon. *Nature* **369**, 224-227.
- Hartgers W. A., Sinninghe Damsté J. S., Requejo A. G., Allan J., Hayes J. M., Ling Y., Xie T.-M., Primack J. and de Leeuw J. W. (1994b) A molecular and carbon isotopic study towards the origin and diagenetic fate of diaromatic carotenoids. In *Advances in Organic Geochemistry 1993* (ed. N. Telnæs, G. van Graas and K. Øygaard); *Org. Geochem.* **22**, 703-725.
- Harvey G. R., Sinninghe Damsté J. S. and de Leeuw J. W. (1985) On the origin of alkylbenzenes in geological samples. *Mar. Chem.* **16**, 187-188.
- Hatcher P. G., Spiker E. C., Szeverenyi N. M. and Maciel G. E. (1983) Selective preservation and origin of petroleum-forming aquatic kerogen. *Nature* **305**, 498-501.
- ten Haven H. L., Baas M., de Leeuw J. W. and Schenck P. A. (1987a) Late Quaternary Mediterranean sapropels, I- On the origin of organic matter in sapropel S₇. *Mar. Geol.* **75**, 137-156.
- ten Haven H. L., Baas M., de Leeuw J. W., Schenck P. A. and Brinkhuis H. (1987b) Late Quaternary Mediterranean sapropels II. Organic geochemistry and palynology of S₁ sapropels and associated sediments. *Chem. Geol.* **64**, 149-167.
- ten Haven H. L., Baas M., Kroot M., de Leeuw J. W., Schenck P. A. and Ebbing J. (1987c) Late Quaternary Mediterranean sapropels. III: Assessment of source of input and palaeotemperature as derived from biological markers. *Geochim. Cosmochim. Acta* **51**, 803-810.
- ten Haven H. L., Eglinton G., Farrimond P., Kohnen M. E. L., Poynter J. G., Rullkötter J. and Welte D. H. (1992) Variations in the content and composition of organic matter in sediments underlying active upwelling regimes: a study from ODP Legs 108, 112 and 117. In *Upwelling Systems: Evolution Since the Early Miocene* (ed. C. P. Summerhayes, W. L. Prell and K. C. Emeis); pp. 229-246. *Geol. Soc. Special Publ. No 64*.
- Hedges J. I. and Keil R. G. (1995) Sedimentary organic matter preservation: an assessment and speculative synthesis. *Mar. Chem.* **49**, 81-115.
- Hedges J. I., Cowie G. L., Ertel J. R., Barbour R. J. and Hatcher P. G. (1985) Degradation of carbohydrates and lignins in buried woods. *Geochim. Cosmochim. Acta* **49**, 701-711.
- van Heemst J. D. H., Peulvé S., de Leeuw J. W., Sicre M.-A. and Saliot A. (1995) Algal polyphenolic resistant macromolecules in marine dissolved and particulate organic matter. In *Organic Geochemistry: Developments and Applications to energy, Climate, Environment and Human History* (ed. J. O. Grimalt and C. Dorronsoro); pp. 940-942.
- Hemsley A. R., Barrie P. J., Chaloner W. G. and Scott A. C. (1993) The composition of sporopollenin: its contribution to living and fossil spore systematics. *Grana suppl.* **1**, 2-11.
- Herbin J. P., Geyssant J. R., Müller C., Mélières F., le groupe YORKIM and Penn I. E. (1991). Hétérogénéité quantitative et qualitative de la matière organique dans les

- argiles du Kimméridgien du val de Pickering (Yorkshire, U.K). Cadre sédimentologique et stratigraphique. *Rev. Inst. Fr. Pétrol.* **46**, 1-39.
- Herbin J. P., Müller C., Geysant J. R., Mélières F. and Penn I. E. (1993) Variation of the Distribution of organic matter within a transgressive system tract: Kimmeridge Clay (Jurassic), England. In *AAPG 1993 "Petroleum source rocks in a sequence stratigraphic framework* (ed. B. Katz and L. Pratt); pp. 67-100.
- Hibberd D. J. (1979) The structure and phylogenetic significance of the flagellar transition region in the chlorophyll *c*-containing algae. *BioSystems* **11**, 243-261.
- Hibberd D. J. (1981) Notes on the taxonomy and nomenclature of the algal classes Eustigmatophyceae and Tribophyceae (synonym Xanthophyceae). *Bot. J. Linn. Soc.* **82**, 93-119.
- Hobbie J. E., Daley R. J. and Jasper S. (1977) Use of Nuclepore filters for counting bacteria by fluorescence microscopy. *Appl. Environm. Microbiol.* **33**, 1225-1228.
- Hoefs M. J. L., Sinninghe Damsté J. S. and de Leeuw J. W. (1995a) Organic geochemistry of Arabian Sea surface sediments: paleoenvironmental implications. In *Organic Geochemistry: Developments and Applications to energy, Climate, Environment and Human History* (ed. J. O. Grimalt and C. Dorronsoro); pp. 158-160.
- Hoefs M. J. L., van Heemst J. D. H., Gelin F., Koopmans M. P., de Leeuw J. W. and Sinninghe Damsté J. S. (1995b) Alternative biological sources for 1,2,3,4-tetramethylbenzene in flash pyrolysates of kerogen. *Org. Geochem.* Accepted.
- Hofmann I. C., Hutchinson J., Robson J. N., Chicarelli M. I. and Maxwell J. R. (1992) Evidence for sulphide links in a crude oil asphaltene and kerogens from reductive cleavage by lithium in ethylamine. In *Advances in Organic Geochemistry 1991* (ed. C. B. Eckardt *et al.*); *Org. Geochem.* **19**, 371-387.
- Horsfield B. (1989) Practical criteria for classifying kerogens: Some observations from pyrolysis-gas chromatography. *Geochim. Cosmochim. Acta* **53**, 891-901.
- Horsfield B., Curry D. J., Bohacs K., Littke R., Rullkötter J., Schenk H. J., Radke M., Schaefer R. G., Carroll A. R., Isaksen G. and Witte E. G. (1994) Organic geochemistry of freshwater and alkaline lacustrine sediments in the Green River Formation of the Washakie Basin, Wyoming, U.S.A. In *Advances in Organic Geochemistry 1993* (ed. N. Telnæs, G. van Graas and K. Øygard); *Org. Geochem.* **22**, 415-440.
- Huc A. Y., Lallier-Vergès E., Bertrand P., Carpentier B. and Hollander D. J. (1992) Organic matter response to change of depositional environment in Kimmeridgian shales, Dorset, U.K. In *Organic matter: productivity, accumulation and preservation of organic matter in recent and ancient sediments.* (ed. J. Whelan and J. Farrington); pp. 469-486. Columbia Univ. Press.
- Jackson G. A. (1990) A model of the formation of marine algal flocs by physical coagulation processes. *Deep-Sea Res.* **37**, 1197-1211.
- Kadouri A., Derenne S., Largeau C., Casadevall E. and Berkaloff C. (1988) Resistant biopolymer in the outer walls of *Botryococcus braunii*, B race. *Phytochemistry* **27**, 551-557.
- Katz B. J. (1983) Limitations of "Rock-Eval" pyrolysis for typing organic matter. *Org. Geochem.* **4**, 195-199.
- Kawamura K., Tannenbaum E., Huizinga B. J. and Kaplan I. R. (1986) Long-chain carboxylic acids in pyrolysates of Green River kerogen. In *Advances in Organic Geochemistry 1985* (ed. D. Leythaeuser and J. Rullkötter); *Org. Geochem.* **10**, 1059-1065.

- Keely B. J., Blake S. R. and Maxwell J. R. (1995) Variations in pigment distributions in marls from a Miocene evaporitic sequence (Vena del Gesso, N. Italy). *Org. Geochem.* **23**, 527-539.
- Kenig F., Sinninghe Damsté J. S., Frewin N., Hayes J. M. and de Leeuw J. W. (1995) Molecular indicators for palaeoenvironmental change in a Messinian evaporitic sequence (Vena del Gesso, Italy). II. Stratigraphic variations in abundances and ^{13}C contents of free and sulphur-bound skeletons in a single marl bed. *Org. Geochem.* **23**, 485-526.
- Klok J., Cox H. C., Baas M., de Leeuw J. W. and Schenck P. A. (1984a) Carbohydrates in recent marine sediments II. Occurrence and fate of carbohydrates in a recent stromatolitic deposit: Solar Lake, Sinai. *Org. Geochem.* **7**, 101-109.
- Klok J., Baas M., Cox H. C., de Leeuw J. W., Rijpstra W. I. C. and Schenck P. A. (1984b) Qualitative and quantitative characterization of the total organic matter in a recent sediment (Part II). In *Advances in Organic Geochemistry 1983* (ed. P. A. Schenck *et al.*); *Org. Geochem.* **6**, 265-278.
- Kohnen M. E. L., Sinninghe Damsté J. S., Baas M., Kock-van Dalen A. C. and de Leeuw J. W. (1993) Sulphur-bound steroids and phytane carbon skeletons in geomacromolecules: Implications for mechanism of incorporation of sulphur into organic matter. *Geochim. Cosmochim. Acta* **57**, 2515-2528.
- Koopmans M. P., Sinninghe Damsté J. S., Lewan M. D. and de Leeuw J. W. (1995) Thermal stability of thiophene biomarkers as studied by hydrous pyrolysis. *Org. Geochem.* **23**, 583-596.
- Krein E. B. and Aizenshtat Z. (1994) The formation of isoprenoid sulfur compounds during diagenesis: simulated sulfur incorporation and thermal transformation. *Org. Geochem.* **21**, 1015-1025.
- Lallier-Vergès E., Boussafir M., Bertrand P. and Badaut-Trauth D. (1993a) Selective preservation of various organic matter types as assessed by STEM studies on a cyclic productivity-controlled sedimentary series (Kimmeridge Clay Formation). In *Organic Geochemistry: Poster sessions from the 16th International Meeting on Organic Geochemistry, Stavanger, 1993*. (ed. K. Øygard); pp. 384-386. Falch Hurtigtrykk.
- Lallier-Vergès E., Bertrand P., Bückel D., Huc A. Y. and Tremblay P. (1993b) Control of the preservation of organic matter by productivity and sulphate reduction in Kimmeridgian shales from Dorset (U.K.). *Mar. and Petrol. Geol.*, **10**, 600-605.
- Lallier-Vergès E., Bertrand P., Tribouillard N. P., Hayes J. M., Boussafir M., Zaback D. A. and Connan J. (1994) Productivity-induced sulfur enrichment of organic-rich sediments. 207th American Chemical Society 1994, National Meeting, March 13-18, San Diego, CA, USA.
- Largeau C. and de Leeuw J. W. (1995) Insoluble, non-hydrolysable, aliphatic macromolecular constituents of microbial cell walls. In *Advances in Microbial Ecology*, Vol. 14 (ed. J. Gwynfryn Jones); Plenum press. New-York.
- Largeau C., Casadevall E., Kadouri A. and Metzger P. (1984) Formation of Botryococcus-derived kerogens. Comparative study of immature torbanites and of the extant alga *Botryococcus braunii*. In *Advances in Organic Geochemistry 1983* (ed. P. A. Schenck, J. W. de Leeuw and G. M. M. Lijmbach); *Org. Geochem.* **6**, 327-332.
- Largeau C., Derenne S., Casadevall E., Kadouri A. and Sellier N. (1986) Pyrolysis of immature torbanite and of the resistant biopolymer (PRB A) isolated from extant alga *Botryococcus braunii*. Mechanism for the formation and structure of torbanite. In *Advances in Organic Geochemistry 1985* (ed. D. Leythaeuser and J. Rullkötter); *Org. Geochem.* **10**, 1023-1032.

- Largeau C., Derenne S., Casadevall E., Berkaloff C., Corolleur M., Lugardon B., Raynaud J.-F. and Connan J. (1990a) Occurrence and origin of ultralaminar structures in "amorphous" kerogens from various source-rocks and oil-shales. In *Advances in Organic Geochemistry 1989* (ed. B. Durand and F. Behar); *Org. Geochem.* **16**, 889-896.
- Largeau C., Derenne S., Clairay C., Casadevall E., Raynaud J.-F., Lugardon B., Berkaloff C., Corolleur M. and Rousseau B. (1990b) Characterization of various kerogens by scanning electron microscopy (SEM) and transmission electron microscopy (TEM)-Morphological relationships with resistant outer walls in extant micro-organisms. *Meded. Rijks Geol. Dienst.* **45**, 91-101.
- Larter S. R. (1984) Application of analytical pyrolysis techniques to kerogen characterisation and fossil fuel exploration/exploitation. In *Analytical Pyrolysis* (ed. Voorhees K. J.); pp. 212-275. Butterworth.
- Larter S. R. and Horsfield B. (1993) Determination of structural components of kerogens by the use of analytical pyrolysis methods. In *Organic Geochemistry, principles and applications* (ed. M. H. Engel and S. A. Macko); pp. 271-287. Plenum Press.
- Lattimer R. P. (1995) Pyrolysis field ionization mass spectrometry (Py-FI-MS) of polyolefins. *J. Anal. Appl. Pyrolysis* **31**, 203-226.
- Laureillard J., Largeau C., Waeghmaecker F. and Casadevall E. (1986) Biosynthesis of the resistant polymer in the alga *Botryococcus braunii*. Studies on the possible direct precursors. *J. Natural Product* **49**, 794-799.
- Laureillard J., Largeau C. and Casadevall E. (1988) Oleic acid in the biosynthesis of the resistant biopolymer of *Botryococcus braunii*. *Phytochemistry* **27**, 2095-2098.
- Le Berre F., Derenne S., Largeau C., Connan J. and Berkaloff C. (1991) Occurrence of non-hydrolysable, macromolecular, wall constituents in bacteria. Geochemical implications. In *Organic Geochemistry Advances and applications in energy and the natural environment* (ed. D. A. C. Manning); pp.428-431. Manchester Univ. Press.
- de Leeuw J. W. and Largeau C. (1993) A review of macromolecular organic compounds that comprise living organisms and their role in kerogen, coal and petroleum formation. In *Organic Geochemistry, principles and applications* (ed. M. H. Engel and S. A. Macko); pp. 23-72. Plenum Press.
- de Leeuw J. W., Rijpstra W. I. C. and Schenck P. A. (1981) The occurrence and identifications of C₃₀, C₃₁ and C₃₂ alkan-1,15-diols and alkan-15-one-1-ols in Unit I and Unit II Black Sea sediments. *Geochim. Cosmochim. Acta* **45**, 2281-2285.
- de Leeuw J. W., van Bergen P. F., van Aarssen B. G. K., Gatellier J.-P. L. A., Sinnighe Damsté J. S. and Collinson M. E. (1991) Resistant biomacromolecules as major contributors to kerogen. *Phil. Trans. R. Soc. Lond. B* **333**, 329-337.
- Liaaen-Jensen S. (1978) Chemistry of Carotenoid Pigments. In *Photosynthetic Bacteria* (ed. R. K. Clayton and W. R. Sistrom); pp. 233-248. Plenum Press.
- Lugardon B., Raynaud J.-F. and Husson P. (1991) Données ultrastructurales sur la matière organique amorphe des kérogènes. *Palynoscience* **1**, 69-88.
- McCaffrey M. A., Farrington J. W. and Repeta D. J. (1991) The organic geochemistry of Peru margin surface sediments: II. Paleoenvironmental implications of hydrocarbon and alcohol profiles. *Geochim. Cosmochim. Acta* **55**, 483-498.
- van de Meent D., Brown S. C., Philip R. P. and Simoneit B. R. T. (1980) Pyrolysis-High Resolution Gas Chromatography and Pyrolysis Gas Chromatography-Mass Spectrometry of Kerogens and Kerogen Precursors. *Geochim. Cosmochim. Acta* **44**, 999-1013.

- Metzger P. and Casadevall E. (1987) Lycopadiene, a tetraterpenoid hydrocarbon from new strains of the green alga *Botryococcus braunii*. *Tetrahedron Lett.*, **28**, 3931-3934.
- Metzger P. and Casadevall E. (1989) Aldehydes, very long chain alkenylphenols, epoxides and other lipids from an alkadiene-producing strain of *Botryococcus braunii*. *Phytochemistry* **28**, 2097-2104.
- Metzger P. and Casadevall E. (1991) Botryococcoid ethers, ether lipids from *Botryococcus braunii*. *Phytochemistry* **30**, 1439-1444.
- Metzger P. and Casadevall E. (1992) Ether lipids from *Botryococcus braunii* and their biosynthesis. *Phytochemistry* **31**, 2341.
- Metzger P., Berkaloff C., Casadevall E. and Couté A. (1985) Alkadiene- and botryococcene-producing races of wild strains of *Botryococcus braunii*. *Phytochemistry* **24**, 2305-2312.
- Metzger P., Templier J., Largeau C. and Casadevall E. (1986) A *n*-alkatriene and some *n*-alkadienes from the A race of the green alga *Botryococcus braunii*. *Phytochemistry* **25**, 1869.
- Metzger P., Largeau C. and Casadevall E. (1991) Lipids and macromolecular lipids of the hydrocarbon-rich microalga *Botryococcus braunii*. Chemical structure and biosynthesis. Geochemical and biotechnological importance. In *Prog. Chem. Org. Nat. Prod.* (ed. W. Herz *et al.*); vol. 57, pp. 1-70. Springer Verlag.
- Metzger P., Pouet Y., Bischoff R. and Casadevall E. (1993) An aliphatic polyaldehyde from *Botryococcus braunii* (A race). *Phytochemistry* **32**, 875-883.
- Meuzelaar H. L. C., Haverkamp J. and Hileman F. D. (1982) *Pyrolysis Mass Spectrometry of Recent and Fossil Biomaterials, Techniques and Instrumentation in Analytical Chemistry*, Vol. 3, Elsevier.
- Moers M. E. C., de Leeuw J. W., Cox H. C. and Schenck P. A. (1988) Interaction of glucose and cellulose with hydrogen sulphide and polysulphides. In *Advances in Organic Geochemistry 1987* (ed. L. Matavelli and L. Novelli); *Org. Geochem.* **13**, 1087-1091.
- Moers M. E. C., Baas M., de Leeuw J. W., Boon J. J. and Schenck P. A. (1990) Occurrence and origin of carbohydrates in peat samples from a red mangrove environment as reflected by abundances of neutral monosaccharides. *Geochim. Cosmochim. Acta* **54**, 2463-2472.
- Morris R. J. and Brassell S. C. (1988) Long-chain alkanediols: biological markers for cyanobacterial contributions to sediments. *Lipids* **23**, 256-258.
- Nip M., Tegelaar E. W., Brinkhuis H., de Leeuw J. W., Schenk P. A. and Holloway P. J. (1986) Analysis of modern and fossil plant cuticles by Curie point Py-GC and Curie point Py-GC-MS: Recognition of a new, highly aliphatic and resistant biopolymer. In *Advances in Organic Geochemistry 1985* (ed. D. Leythaeuser and J. Rullkötter); *Org. Geochem.* **10**, 769-778.
- Nip M., de Leeuw J. W. and Schenck P. A. (1987) Structural characterization of coals, coal macerals and their precursors by pyrolysis-gas chromatography and pyrolysis-gas chromatography-mass spectrometry. *Coal Sci. Technol.* **11**, 89-92.
- Nip M., de Leeuw J. W. and Schenck P. A. (1988) The characterisation of eight maceral concentrates by means of Curie-point pyrolysis gas chromatography and Curie-point pyrolysis gas chromatography-mass spectrometry. *Geochim. Cosmochim. Acta.* **52**, 637-648.

- Nip M., de Leeuw J. W., Schenck P. A., Windig W., Meuzelaar H. L. C. and Crelling J. C. (1989) A flash pyrolysis and petrographic study of cutinite from the Indiana paper coal. *Geochim. Cosmochim. Acta* **53**, 671-683.
- Orr W. L. (1986) Kerogen/asphaltene/sulphur relationships in sulphur-rich Monterey oils. In *Advances in Organic Geochemistry 1985* (ed. D. Leythausser and J. Rullkötter); *Org. Geochem.* **10**, 499-516.
- Panganamala R. V., Sievert C. F. and Cornwell D. G. (1971) Quantitative estimation and identification of O-glycerol as alkyl iodides and their hydrocarbon derivatives. *Chem. Phys. Lipids* **7**, 336-344.
- Pfendt P. A. (1984) Comparison of the general chemical nature of various kerogens based on their reactivities towards bromine. *Org. Geochem.* **6**, 383-390.
- Philp R. P. and Calvin M. (1976) Possible origin for insoluble organic (kerogen) debris in sediments from insoluble cell-wall materials of algae and bacteria. *Nature* **262**, 134-136.
- Philp R. P., Suzuki N. and Galvez-Sinibaldi A. (1992) Early-stage incorporation of sulfur into protokerogens and possible kerogen precursors. In *Organic matter: productivity, accumulation, and preservation in recent and ancient sediments*. (ed. J. K. Whelan and J. W. Farrington); pp. 264-282. Columbia. New-York.
- Poutsma M. L. (1990) Free-radical thermolysis and hydrogenolysis of model hydrocarbons relevant to processing of coal. *Energy and Fuel* **4**, 113-131.
- Pradier B. and Bertrand P. (1992) Etude à haute résolution d'un cycle de carbone organique des argiles du Kimméridgien du Yorkshire (GB): relation entre composition pétrographique du contenu organique observé in-situ, teneur en carbone organique et qualité pétrolière. *C. R. Acad. Sc. Paris* **315**, 187-192.
- Ramanampisoa L. and Disnar J. R. (1994) Primary control of paleoproduction on organic matter preservation and accumulation in the Kimmeridge rocks of Yorkshire (U.K.). *Org. Geochem.* **21**, 1153-1167.
- Ramanampisoa L., Bertrand P., Disnar J. R., Lallier-Vergès E., Pradier B. and Tribouvillard N. P. (1992) Etude à haute résolution d'un cycle de carbone organique des argiles du Kimméridgien du Yorkshire (GB): résultats préliminaires de géochimie et de pétrographie organique. *C. R. Acad. Sc. Paris* **314**, 1493-1498.
- Raynaud J.-F., Lugardon B. and Lacrampe-Couloume G. (1988) Observation de membranes fossiles dans la matière organique "amorphe" de roches-mères de pétrole. *C. R. Acad. Sci. Paris* **307**, 1703-1709.
- Requejo A. G., Allan J., Creaney S., Gray N. R. and Cole K. S. (1992) Aryl isoprenoids and diaromatic carotenoids in paleozoic source rocks and oils from the western Canada and Williston basins. *Org. Geochem.* **19**, 245-264.
- Robinson N., Cranwell P. A., Eglinton G., Brassel S. C., Sharp C. L., Gophen M. and Pollinger U. (1987) Lipid geochemistry of Lake Kinneret. *Org. Geochem.* **10**, 733-742.
- Schaeffer P., Ocampo R., Callot H. J. and Albrecht P. (1993) Extraction of bound porphyrins from sulphur-rich sediments and their use for reconstruction of palaeoenvironments. *Nature* **364**, 133-136.
- Schaeffer P., Harrison W. H., Keely B. J. and Maxwell J. R. (1995) Product distributions from chemical degradations of kerogens from a marl from a Miocene evaporitic sequence (Vena del Gesso, N. Italy) *Org. Geochem.* **23**, 541-554.
- Schouten S., van Driel G. B., Sinninghe Damsté J. S. and de Leeuw J. W. (1993) Natural sulphurisation of ketones and aldehydes: a key reaction in the formation of organic sulphur compounds. *Geochim. Cosmochim. Acta.* **57**, 5111-5116.

- Schouten S., Moerkerken P., Sinninghe Damsté J. S., Gelin F., Baas M., Ahmed M., van Bergen P. F. and de Leeuw J. W. (1996) Ruthenium tetroxide degradation of biopolymers and kerogens. In preparation.
- Sharpless K. B., Carlsen P. H. J., Katsuki T. and Martin V. S. (1981) A greatly improved procedure for ruthenium tetroxide catalysed oxidations of organic compounds. *J. Org. Chem.* **46**, 3936-3938.
- Sinninghe Damsté J. S. and de Leeuw J. W. (1990) Analysis, structure and geochemical significance of organically-bound sulphur in the geosphere: State of the art and future research. In *Advances in Organic Geochemistry 1989* (ed. B. Durand and F. Behar); *Org. Geochem.* **16**, 1077-1101.
- Sinninghe Damsté J. S., Kock-van-Dalen A. C., de Leeuw J. W. and Schenck P. A. (1987) The identification of 2,3-dimethyl-5-(2,6,19-trimethylundecyl)-thiophene, a novel sulphur-containing biological marker. *Tetrahedron Lett.* **28**, 957-960.
- Sinninghe Damsté J. S., Eglinton T. I., de Leeuw J. W. and Schenck P. A. (1989) Organic sulphur in macromolecular sedimentary organic matter: I. Structure and origin of sulphur-containing moieties in kerogens, asphaltenes and coals as revealed by flash pyrolysis. *Geochim. Cosmochim. Acta* **53**, 873-889.
- Sinninghe Damsté J. S., Eglinton T. I. and de Leeuw J. W. (1992) Alkylpyrroles in a kerogen pyrolysate: Evidence for abundant tetrapyrrole pigments. *Geochim. Cosmochim. Acta* **56**, 1743-1751.
- Sinninghe Damsté J. S., Wakeham S. G., Kohnen M. E. L., Hayes J. M. and de Leeuw J. W. (1993a) A 6000-year sedimentary molecular record of chemocline excursions in the Black Sea. *Nature* **362**, 827-829.
- Sinninghe Damsté J. S., De Las Heras F. X. C., van Bergen P. F. and de Leeuw J. W. (1993b) Characterization of Tertiary Catalan lacustrine oil shales: Discovery of extremely organic sulphur-rich Type I kerogens. *Geochim. Cosmochim. Acta* **57**, 389-415.
- Sinninghe Damsté J. S., Frewin N., Kenig F. and de Leeuw J. W. (1995) Molecular indicators for palaeoenvironmental change in a Messinian evaporitic sequence (Vena del Gesso, Italy). I: Variations in extractable organic matter of ten cyclically deposited marl beds. *Org. Geochem.* **23**, 471-483.
- Smith P. M. R. (1984) The use of fluorescence microscopy in the characterisation of amorphous organic matter. *Org. Geochem.* **6**, 839-845.
- Smith D. J., Eglinton G. and Morris R. J. (1983) Occurrence of long-chain alkan-diols and alkan-15-one-1-ols in a Quaternary Sapropel from the Eastern Mediterranean. *Lipids* **18**, 902-905.
- Sundararaman P., Biggs W. R., Reynolds G. J. and Fetzer J. C. (1988) Vanadylporphyrins, indicators of kerogen breakdown and generation of petroleum. *Geochim. Cosmochim. Acta* **52**, 2337-2341.
- Tegelaar E. W. (1990) *Resistant biomacromolecules in morphologically characterized constituents of kerogens: a key to the relationship between biomass and fossil fuels*. PhD thesis, University of Utrecht, The Netherlands.
- Tegelaar E. W., de Leeuw J. W., Largeau C., Derenne S., Schulten H.-R., Müller R., Boon J. J., Nip M. and Sprenkels J. C. M. (1989a) Scope and limitations of several pyrolysis methods in the structural elucidation of a macromolecular plant constituent in the leaf cuticle of *Agave Americana* L. *J. Anal. Appl. Pyrolysis* **15**, 29-54.
- Tegelaar E. W., Mattheizing R. M., Jansen J. B. H., Horsfield B. and de Leeuw J. W. (1989b) Possible origin of *n*-alkanes in high-wax crude oils. *Nature* **342**, 529-531.

- Tegelaar E. W., de Leeuw J. W., Derenne S. and Largeau C. (1989c) A reappraisal of kerogen formation. *Geochim. Cosmochim. Acta* **53**, 3103-3106.
- Templier J., Largeau C., Casadevall E. and Berkaloff C. (1992a) Chemical inhibition of resistant biopolymers in outer walls of the A and B races of *Botryococcus braunii*. *Phytochemistry* **31**, 4097-4104.
- Templier J., Diesendorf C, Largeau C. and Casadevall E. (1992b) Metabolism of *n*-alkadienes in the A race of *Botryococcus braunii*. *Phytochemistry* **31**, 113-120.
- Templier J., Largeau C. and Casadevall E. (1993) Variations in external and internal lipids associated with inhibition of the resistant biopolymer from the A race of *Botryococcus braunii*. *Phytochemistry* **33**, 1079-1086.
- Tissot B. P. and Welte D. H. (1984) *Petroleum formation and occurrence*, 2nd edition. Springer.
- Tribovillard N. P., Desprairies A., Bertrand P., Lallier-Vergès E., Disnar J.-R. and Pradier B. (1992) Etude à haute résolution d'un cycle du carbone organique de roches kimméridgiennes du Yorkshire (Grande-Bretagne): minéralogie et géochimie (résultats préliminaires). *C.R. Acad. Sci. Paris* **314** (II), 923-930.
- Tribovillard N. P., Desprairies A., Lallier-Vergès E., Bertrand P., Moureau N., Ramdani A. and Ramanampisoa L. (1994) Geochemical study of organic matter rich cycles from the Kimmeridge Clay Formation of Yorkshire (UK): productivity versus anoxia. *Palaeogeogr. Palaeoclim. Palaeoecol.* **108**, 165-181.
- Trudinger P. A. (1992) Bacteria sulfate reduction: Current status and possible origin. In *Early Organic Evolution: Implications for Mineral and Energy Resources* (ed. M. Schidlowski *et al.*); pp. 367-377. Springer-Verlag.
- Tyson R. V., Wilson R. C. L. and Downie C. (1979) A stratified water column environmental model for the type Kimmeridge Clay. *Nature* **277**, 377-380.
- Vai G. B. and Ricci Lucchi F. (1977) Algal crust, autochthonous and clastic gypsum in a cannibalistic evaporite basin: a case history from the Messinian of Northern Apennines. *Sedimentology* **24**, 211-244.
- Veldhuis M. J. W. and Admiraal W. (1987). The influence of phosphate depletion on the growth and colony formation of *Phaeocystis pouchetii* (Hariot) Lagerheim. *Mar. Biol.* **95**, 47-54.
- Verardo D. J., Froelich P. N. and McIntyre A. (1990) Determination of organic carbon and nitrogen in marine sediments using the Carlo Erba NA-1500 analyser. *Deep-Sea Res.* **37**, 157-165.
- Vincenti M., Guglielmetti G., Cassani G and Tonini C. (1987) Determination of double bond position in diunsaturated compounds by mass spectrometry of dimethyl disulphide derivatives. *Anal. Chem.* **59**, 694-699.
- Volkman J. K., Barrett S. M., Dunstan G. A. and Jeffrey S. W. (1992) C₃₀-C₃₂ alkyl diols and unsaturated alcohols in microalgae of the class Eustigmatophyceae. *Org. Geochem.* **18**, 131-138.
- Wampler T. P. and Levy E. J. (1986) Effects of slow heating rates on products of polyethylene pyrolysis. *Analyst* **111**, 1065-1067.
- Wefer G. (1989) Particles flux in the Oceans: effects of episodic production. In *Report of the Dahlem Workshop on Productivity of the Oceans: Present and Past*. (ed. W. H. Berger, V. S. Smetacek and G. Wefer); pp. 139-154, Wiley, Chichester.
- Whelan J. K. and Emeis K.-C. (1992) Sedimentation and preservation of amino compounds and carbohydrates in marine sediments. In *Organic matter: productivity, accumulation, and preservation in recent and ancient sediments*. (ed. J. K. Whelan and J. W. Farrington); pp. 177-200. Columbia. New-York.

REFERENCES

- Widdel F. (1988) Microbiology and ecology of sulfate- and sulfur-reducing bacteria. In *Biology of anaerobic organisms* (ed. J. B. Zehnder); pp. 469-585. Wiley.
- Williams P. F. V. (1986) Petroleum Geochemistry of the Kimmeridge Clay of onshore southern and eastern England. *Mar. Petrol. Geol.* **3**, 258-281.
- Williams P. F. V. and Douglas A. G. (1980) A preliminary organic geochemical investigation of the Kimmeridgian oil shales. In *Advances in Organic Geochemistry 1979* (ed. A. G. Douglas and J. R. Maxwell); pp. 531-545.
- Williams P. F. V. and Douglas A. G. (1983) The effect of lithologic variation on organic geochemistry in the Kimmeridge Clay, Britain. In *Advances in Organic Geochemistry 1981* (ed. M. Bjorøy *et al.*); pp. 568-575.
- Zeliber J. L., Romankiw L., Hatcher P. G. and Colwell R. R. (1988) Comparative analysis of the chemical composition of mixed and pure cultures of green algae and their decomposed residues by ^{13}C nuclear magnetic resonance spectroscopy. *Appl. Environm. Microbiol.* **54**, 1051-1060.
- Zeng Y. B., Eglinton G., Robinson N. and Cassani F. M. (1988) Long-chain alkane-diol and alkan-keto-1-ol components of the Messel kerogen. *Cour. Forsch. Inst. Senckenberg* **107**, 37-51.

Acknowledgments

The number of co-authors cited in the publications assembled in this thesis manuscript clearly indicates that this work would not have been carried out without the help of many people. Therefore, many thanks go to those, from Delft, Paris, Orléans and Texel, who directly collaborated with me and consequently helped in the conception of the chapters in this thesis. They are, of course, many more people who, to a lesser extent, participated in the work presented here. I would like to thank all of them for both their help and their forgiveness for not mentioning them personally due to my fear of being disrespectful to those I would inevitably forget.

Samenvatting

De onoplosbare, macromoleculaire fractie van sedimentair organisch materiaal, kerogeen genaamd, vormt het grootste organisch koolstofreservoir op aarde. Om deze reden is kerogeen in de laatste decennia, nadat de benodigde onderzoekstechnieken waren ontwikkeld, uitvoerig bestudeerd. De oorsprong van kerogenen, in het bijzonder mariene kerogenen, staat echter nog steeds ter discussie. Het onderzoek dat beschreven wordt in dit proefschrift is gewijd aan dit probleem. Gepoogd werd de chemische structuur van kerogeen te onderzoeken, voornamelijk met behulp van analytische pyrolyse methodes, teneinde de vorming ervan te kunnen begrijpen. Dientengevolge was het eerste deel van het onderzoek gericht op de pyrolysemechanismen van bekende hoogmoleculaire verbindingen (hoofdstuk 2 tot en met 4).

Etherlipiden die waren geïsoleerd uit de groene microalg *Botryococcus braunii* werden gepyrolyseerd (hoofdstuk 2). De pyrolyseproducten werden geïdentificeerd als alkenen, alkanen en ketonen. De positie van de carbonyl groep in de ketonen kwam overeen met de positie van de etherbinding in de etherlipiden. Dit gaf duidelijk aan dat pyrolytische verbreking van secundaire etherbindingen zowel ketonen als alkanen of alkenen genereert. Bovendien bleek dat verbreking van de etherbinding de eerste stap was die leidde tot de vorming van andere pyrolyseproducten. Dit onderzoek resulteerde in gedetailleerde kennis van pyrolysemechanismen van polyethers.

Enkele andere complexe non-etherlipiden die waren geïsoleerd uit *B. braunii* werden ook aan flash-pyrolyse onderworpen, en hun thermisch gedrag wordt besproken in hoofdstuk 3. Specifieke lipiden die tot 64 koolstofatomen en lange alkylketens bevatten bleken niet te worden gepyrolyseerd, maar simpelweg te verdampen. Een aanzienlijk deel van het verdampte materiaal bereikte de gaschromatografische kolom die was gekoppeld aan de pyrolyse eenheid niet, maar condenseerde op het glazen buisje waarbinnen het pyrolysedraadje zich bevond. Aangenomen werd dat dit verschijnsel zich ook voordoet bij hoogmoleculair materiaal dat losgemaakt wordt na de pyrolyse van macromoleculen, hetgeen een nadeel van de gebruikte methode betekent. Echter, aangetoond werd dat andere lipiden die ethergebonden alifatische structuren bevatten wel werden gepyrolyseerd. De pyrolysemechanismen waren vergelijkbaar met die beschreven in hoofdstuk 2. Op basis van deze kennis werd de structuur van het uit *B. braunii* ras L geïsoleerde algaenan geïdentificeerd als een macromolecuul bestaande uit C_{40} isoprenoïde eenheden die voornamelijk ethergebonden zijn op de C-14 en C-15 posities.

Meer informatie over de pyrolyse van biomacromoleculen wordt gegeven in hoofdstuk 4. Een oplosbaar biopolymeer (gedefinieerd als een alifatische polyaldehyde) dat was geïsoleerd uit *B. braunii* ras A, werd onderworpen aan flash-pyrolyse. Het zeer complexe pyrolysaat, bestaande uit verzadigde en (meervoudig) onverzadigde *n*-koolwaterstoffen van C_6 tot C_{31} , *n*-alkyl cyclohexanen en *n*-alkylbenzenen, werd vergeleken met het pyrolysaat van het onoplosbare algaenan van dezelfde alg. Gedetailleerd onderzoek van de twee pyrolysatens onthulde zeer nauwe structurele overeenkomsten. Er werd daarom geconcludeerd dat het onoplosbare algaenan een meer gecondenseerde en/of vertakte vorm van het oplosbare alifatische polyaldehyde was.

Bewijzen voor het bestaan van zulke alifatische algaenanen in het mariene milieu worden gepresenteerd in hoofdstuk 5. Vijf van de zeven onderzochte mariene

microalgen bleken resistente biomacromoleculen te bevatten. De chemische structuur van het algaenan dat gebiosynthetiseerd wordt door de eustigmatofyt *Nannochloropsis salina* werd bestudeerd met behulp van vaste stof ^{13}C NMR, chemische degradatie met HI en RuO_4 , en flash-pyrolyse. Uit dit onderzoek bleek dat het algaenan van *Nannochloropsis* bestaat uit C_{28} tot C_{34} lineaire alkylketens die zijn verbonden via etherbindingen. Op basis van de aanwezigheid van vergelijkbare algaenanen in andere mariene algen werd geconcludeerd dat een aanzienlijk deel van mariene kerogenen uit selectief gepreserveerde algaenanen bestaat. Aangenomen wordt derhalve dat deze biomacromoleculen de voorlopers van mariene olie zijn. In hoofdstuk 6 wordt het chemische karakter van de geïsoleerde algaenanen in detail beschreven. Er werd aangetoond dat een tweede eustigmatofyt, *Nannochloropsis* sp., een algaenan biosynthetiseert dat sterk lijkt op dat van *N. salina*. Verder onderzoek van de vrije en estergebonden lipiden van de eustigmatofyten onthulde de aanwezigheid van C_{28} - C_{36} diolen en C_{30} - C_{32} alkenolen. De posities van de alcoholgroep en de dubbele bindingen kwamen nauw overeen met de positie van de etherbindingen in de algaenanen. Voorgesteld werd dat deze diolen en alkenolen de biosynthetische voorlopers en bouwstenen van de algaenanen zijn. Voor de algaenanen van de algaenan producerende chlorofyten *Chlorella spaerckii*, *Chlorococcum* sp. en *Nannochloris* sp. kon geen duidelijke voorloper worden vastgesteld. Deze algaenanen bestaan uit mengsels van macromoleculen met verschillende structuren, deels alifatisch wat betreft de eerste twee algen, en geheel aromatisch wat betreft de laatste alg. De geochemische implicaties van het voorkomen van algaenan producerende soorten in het mariene milieu worden ook besproken.

Het belang van algaenanen in het mariene ecosysteem wordt besproken in hoofdstuk 7, waarin de aard en de heterogene samenstelling van kerogenen die zijn geïsoleerd uit Kimmeridge sedimenten (Yorkshire, Verenigd Koninkrijk) centraal staan. In dit onderzoek werd pyrolyse uitgevoerd in samenhang met electronenmicroscopie. Tussen de verschillende morfologische en chemische eigenschappen van deze kerogenen werden nauwe verwantschappen waargenomen. Er werden drie verschillende, herkenbare typen organisch materiaal geïdentificeerd: materiaal afkomstig van landplanten, microscopisch amorfe, zwavelbevattende (macro)lipiden, en gepreserveerde algaenanen. Relaties tussen de relatieve hoeveelheden van deze typen organisch materiaal en zowel de waterstof index als de hoeveelheid totaal organisch koolstof werden vastgesteld.

Kerogenen die waren geïsoleerd uit meer recente sedimenten (Vena del Gesso, Messinien, Italië) werden uitvoerig bestudeerd met behulp van flash-pyrolyse (hoofdstuk 8). De aard, hoeveelheid en oorsprong van de pyrolyseproducten wordt besproken. De negen bestudeerde kerogenen bleken hoofdzakelijk te bestaan uit homogene macromoleculaire componenten, naar wordt aangenomen algaenanen, en zwavelgebonden lipiden die tijdens de vroege diagenese zijn ingebouwd in de onoplosbare matrix. In hoofdstuk 9 wordt de pyrolyse beschreven van de residuen van dezelfde kerogenen na behandeling met CrCl_2 en Li/EtNH_2 . Door deze behandeling werden de meeste (meervoudig) zwavelgebonden componenten verwijderd uit het macromoleculaire netwerk, hetgeen resulteerde in een fractie die was geconcentreerd in alifatische macromoleculen, *i.e.* algaenanen.

Aangetoond is dat algaenanen die worden geproduceerd door levende mariene algensoorten ook in het verleden gebiosynthetiseerd werden en via selectieve preservatie in sedimenten zijn aangerijkt zodat ze belangrijke componenten vormen van kerogenen van mariene sedimenten.

Résumé

La fraction insoluble et macromoléculaire de la matière organique sédimentaire, appelée kérogène, constitue le plus large réservoir de carbone organique terrestre. Pour cette raison, elle a été étudiée intensivement durant les trente dernières années en fonction du développement des techniques appropriées à son étude. Cependant, l'origine des kérogènes, et plus particulièrement des kérogènes marins, demeurent sources de controverses. En conséquence, l'essentiel du contenu de ce mémoire a pour but d'apporter des éléments de réponse à ces questions, l'approche ayant été l'étude de la formation et de l'évolution des kérogènes par l'examen de leur structure chimique, principalement par des techniques de pyrolyse analytique. Les premiers chapitres sont donc consacrés à la compréhension des mécanismes de pyrolyse par l'étude de composés à haut poids moléculaire donc la structure chimique était préalablement connue (Chapitre 2-4).

Des éthers lipidiques isolés de la microalgue verte *Botryococcus braunii* ont été pyrolysés (chapitre 2). Les pyrolysats sont principalement composés d'alcènes, alcanes et cétones. La position du groupement carbonyle de ces dernières correspond à celle de la liaison éther dans les éthers lipidiques. Ceci indique que la rupture des liaisons éthers secondaires est l'étape initiale et engendre la production de cétones et d'alcènes ou alcanes. En conséquence, des mécanismes de pyrolyse détaillés ont pu être établis à partir de ces études.

Des lipides complexes, ne contenant pas de liaisons éthers, isolés de *B. braunii* ont aussi été dégradés par pyrolyse "flash" afin d'analyser leur comportement thermique (chapitre 3). Ces études ont révélé que certains lipides contenant jusqu'à 64 atomes de carbone et possédant de longues chaînes hydrocarbonées ne subissent aucune rupture pyrolytique mais évaporent et se condensent sur le tube de verre qui entoure la zone de pyrolyse. On peut donc considérer que ce phénomène se produise aussi pour les composés à haut poids moléculaire libérés lors de la pyrolyse de macromolécules et constitue ainsi l'un des inconvénients majeur de la méthode. L'étude d'autres lipides constitués de longues chaînes hydrocarbonées liées par des ponts éthers a cependant permis de mettre en valeur des mécanismes de pyrolyse similaires à ceux décrits dans le chapitre 2. Enfin, grâce aux connaissances ainsi acquises, une structure chimique du biopolymère insoluble (algaenane) isolé de *B. braunii*, race L, a pu être déterminée. Elle est composée d'unités isoprénoides comprenant 40 atomes de carbone et liées par des ponts éthers principalement en C-14 et C-15.

Dans le chapitre 4, un biopolymère soluble (défini comme polyaldéhyde aliphatique) isolé de *B. braunii*, race A, a aussi été étudié par pyrolyse analytique. Le pyrolysats ainsi obtenu, extrêmement complexe et majoritairement composé de *n*-hydrocarbures saturés et (poly)insaturés, alkylcyclohexanes et alkylbenzènes, est comparé avec celui de l'algaenane insoluble biosynthétisé par la même espèce d'algue. Les deux pyrolysats sont fortement analogues démontrant ainsi que la structure chimique de l'algaenane est une forme plus condensée et/ou réticulée du polyaldéhyde aliphatique.

Le chapitre 5 montre l'existence d'algaenanes similaires dans le milieu marin. Cinq des sept microalgues marines étudiées produisent ces biomacromolécules résistantes. L'algue *Nannochloropsis salina* de la classe des Eustigmatophyceae biosynthétise un algaenane dont les caractéristiques moléculaires furent observées par RMN du carbone, dégradations chimiques par HI et RuO₄ et pyrolyse "flash". La

découverte de plusieurs espèces de microalgues marines produisant des algaenanes permet d'envisager que le kérogène marin soit, en partie, composé d'algaenanes préservés sélectivement au cours de la diagenèse. En conséquence, ces biomacromolécules peuvent être considérées comme précurseurs de certains pétroles marins. L'algaenane produit par une seconde algue eustigmatophyte (*Nannochloropsis* sp.) possède une structure chimique similaire à celle de *N. salina* : des chaînes hydrocarbonées linéaires ayant 28 à 34 atomes de carbone liées par plusieurs ponts éthers (chapitre 6). L'étude des fractions lipidiques de ces deux espèces a aussi révélé la présence d'alcanediols et d'alcénols possédant les mêmes caractéristiques structurales que les monomères des algaenanes et sont donc vraisemblablement les précurseurs biosynthétiques de ces derniers. Trois microalgues marines de la classe Chlorophyceae (*Chlorella spaerckii*, *Chlorococcum* sp. et *Nannochloris* sp.) produisent aussi des algaenanes. Cependant, contrairement à ceux identifiés dans les eustigmatophytes, leur nature chimique est plus complexe et est en partie constituée d'unités aromatiques. Le chapitre 6 présente aussi les implications géologiques engendrées par l'existence de ces algaenanes marines.

Le chapitre 7 souligne l'importance des algaenanes sélectivement préservés, dans la formation de kérogènes isolés de sédiments du Kimméridgien (Yorkshire, G.B.). Cette étude montre que des techniques de pyrolyse associées à la microscopie électronique permettent d'observer d'importantes corrélations entre les différentes caractéristiques morphologiques et chimiques de ces kérogènes. Il est aussi montré que l'abondance relative de certains types de matières organiques dans ces kérogènes hétérogènes est corrélée à la fois avec l'indice d'hydrogène et la teneur en carbone organique des sédiments correspondants.

Les kérogènes isolés d'un sédiment plus récent (Vena del Gesso, Messinien, Italie) ont été étudiés en détail par pyrolyse "flash" (chapitres 8 et 9). La nature, l'abondance et l'origine des produits de pyrolyse y sont analysés en détail et révèlent que les 9 kérogènes sont essentiellement constitués de composants macromoléculaires homogènes, probablement algaenanes, ainsi que de lipides incorporés au réseau macromoléculaire par des liaisons (poly)soufrées lors de la diagenèse précoce. Le chapitre 9 démontre qu'il est possible d'éliminer une grande partie de cette fraction organo-soufrée en traitant chimiquement les kérogènes avec CrCl_2 et Li/EtNH_2 . Les résidus ainsi obtenus sont enrichis en algaenanes préservés sélectivement.

En conclusion générale, les travaux entrepris lors de cette thèse ont permis de montrer que des algaenanes similaires à ceux biosynthétisés par des algues marines contemporaines, ont certainement aussi été produits à l'époque de la déposition de sédiments marins anciens et représentent une fraction importante des kérogènes marins.

Curriculum Vitae

François Gelin was born on the 8th January, 1966 in Nantes (France). After he passed the "baccalauréat" in 1984, he dedicated his studies to chemistry, first as an undergraduate student at the "Ecole Supérieure de Chimie Organique et Minérale" (ESCOM) and at the University Pierre et Marie Curie in Paris until 1989. He received his degree of "Ingénieur chimiste" in September 1991. In August 1989, he left France to Texas (USA) to follow graduate studies at the Department of Chemistry of the University of Houston. His research investigations focused on the chemical and physical properties of substituted ferrocenes. In the meantime, he was a teaching-assistant in Organic and General Chemistry. He obtained the "Master of Science" degree in December 1991.

His research fellowship in Organic Geochemistry started in May 1992 at the Delft University of Technology in the Organic Geochemistry Unit, supervised by Prof. Dr. Jan W. de Leeuw. In 1993, he joined a C.N.R.S. research network (GdR 942) to study Kimmeridgian sediments at the University of Orléans (Dr. Philippe Bertrand) and at the "Ecole Nationale Supérieure de Chimie de Paris" (Dr. Claude Largeau). Since April 1994, his PhD investigations have continued, under the auspices of the European Network of Organic Geochemists (ENOG), at the department of Marine Biogeochemistry and Toxicology of the Netherlands Institute for Sea Research (NIOZ) in Texel.